# The Role of Claudin-CD81 Co-Receptor Interaction(s)

# In Hepatitis C Virus Entry

**By**

**Christopher Davis**

A thesis submitted to The University of Birmingham for the degree of doctor of philosophy.

College of Medical & Dental Sciences
Division of Immunity and Infection
The University of Birmingham
Supervisors: Professor Jane McKeating and Dr. Peter Balfe.
May 2011

UNIVERSITY OF
BIRMINGHAM

## University of Birmingham Research Archive

### e-theses repository

This unpublished thesis/dissertation is copyright of the author and/or third parties. The intellectual property rights of the author or third parties in respect of this work are as defined by The Copyright Designs and Patents Act 1988 or as modified by any successor legislation.

Any use made of information contained in this thesis/dissertation must be in accordance with that legislation and must be properly acknowledged. Further distribution or reproduction in any format is prohibited without the permission of the copyright holder.

**Abstract**

Hepatitis C Virus (HCV) infection is a hepatotropic, enveloped virus with a positive sense RNA genome. The prevalence rate of the virus has been shown to be 2.9% of the world population, equating to around 170 million infected individuals. Due to the high level of chronic infection and progressive nature of the liver disease, HCV is a major health concern.

Four host proteins have so far been indicated as viral receptors; scavenger receptor BI, CD81, Claudin1 and Occludin. The interaction of CD81 and Claudin1 has been previously demonstrated which lead us to determine whether specific interactions are essential for HCV entry.

Using a combination of imaging and biochemical methods we were able to demonstrate that only receptor active Claudins specifically interacted with CD81. We also evaluated the ability of previously published Claudin1 mutants to interact with CD81 and demonstrated that receptor inactive mutants no longer form an association with CD81. A bioinformatic model predicted the association of the T149, E152 and T153 residues of CD81 EC2 with the 62-66 region of Claudin1. Mutation of these residues lead to an ablation of Claudin1 association and a reduction in on HCV entry, further indicating the requirement of the Claudin1-CD81 complex in the entry process.

**Acknowledgments**

I would like to thank Prof. Jane McKeating and Dr. Peter Balfe for providing me with a challenging and enjoyable project and for all the supervision I have received. I am also very grateful to Helen Harris for her development and patient teaching of the FIR and FRET analysis. I would also like to acknowledge Michelle Farquhar and Christopher Mee for all their guidance and unwearied assistance with all the random ideas I pestered them with. I would also like to thank Claire Brimacombe, Nicola Fletcher, Joe Grove, Ke Hu, Adam Jennings, Luke Meredith, Ian Rowe, Anne Schwarz, Zania Stamataki, Sam Tilakaratne, Jennifer Timpe and Garrick Wilson, the remaining members of the Mckeating group, past and present, for providing an enjoyable environment in which to study.

I would also like to acknowledge the help and support from the collaborators that made many aspects of my project possible. Firstly I would like to thank Jonathan Mullins for the bioinfomatic modelling and for the long conversations that were invaluable. I would like to thank Steve Young for his teaching and guidance through the world of Biacore. Finally I would like to thank both Kitty McCaffrey and Heidi Drummer for supplying the recombinant proteins used in the Biacore experiments.

**Publications**

**Davis, C.**, Harris, H.J., Balfe, P., Mullins, J.G.L., McKeating, J.A. (2011) Identification of amino acid residues that are essential in CD81-Claudin-1 receptor complex formation and hepatitis C virus entry. *In preparation for J. Biol Chem.*

Farquhar, M.J., Hu, K., **Davis, C.,** Boo, I., Mee, C.J., Tomlinson, M.G., Rappoport, J.Z., Drummer, H.E., Balfe, P., McKeating, J.A. (2011) A Role for Tetraspanin CD81 Endocytosis in Hepatitis C Virus Entry. *Submitted J. Biol Chem.*

Lupberger, J., Zeisel, M.B., Xiao, F., Thumann, C., Fischer, B., Mee, C., **Davis, C.,** Fofana, I., Gorke, S., Soulier, E., Lavillette, D., Cosset, F.L., Patel, A.H., Wolf, P., Doffoël, M., Raffelsberger, W., Poch, O., McKeating, J.A., Brino, L., Baumert, T.F. (2011) RNAi screen identifies epidermal growth factor receptor and ephrin receptor A2 as host factors for hepatitis C virus entry and targets for antiviral therapy. *Nature Medicine:* May;17(5):589-95

Harris, H.J.*, **Davis, C**.*, Mullins, J.G.L., Hu, K., Goodhall, M., Farquhar, M.J., Mee, C.J., Balfe, P., McKeating, J.A. (2010) Claudin association with CD81 defines hepatitis C virus entry. *J Biol Chem* 285: 21092-102. *Authors contributed equally to this study.

**Davis, C.,** Harris, H.J., McKeating, J.A. (2010). The involvement of tight junction protein Claudin-1 in Hepatitis C Virus entry. *Current Topics in Membranes,* 65:273-292

Fletcher NF, Yang JP, Farquhar MJ, Hu K, **Davis C**, He Q, Dowd K, Ray SC, Krieger SE, Neyts J, Baumert TF, Balfe P, McKeating JA, Wong-Staal F. (2010) Hepatitis C Virus Infection of Neuroepithelioma Cell Lines. *Gastroenterology*, 139(4): 1365-1374.

Krieger, S.E., Zeisel, M.B., **Davis, C.,** Thumann, C., Harris, H.J., Grunert, F., Thi, V.L.D., Cosset, F-L., McKeating, J.A., Schuster, C., Baumert, T.F (2010) Inhibition of hepatitis C virus infection by anti-CLDN1 antibodies is mediated by inhibition of E2-CD81-CLDN1 association. *Hepatology* 51(4): 1144-1157.

Mee, C.J., Harris, H.J., Farquhar, M.J., Wilson, G., Reynolds, G.M., **Davis, C.,** van IJzendoorn, S.C.D., Balfe, P., McKeating, J.A. (2009) Polarization restricts hepatitis C virus entry into HepG2 hepatoma cells. *J. Virol* 83: 6211-6221.

Harris, H.J., Farquhar, M.J., Mee, C.J., **Davis, C.,** Reynolds, G.M., Jennings, A., Hu, K., Yuan, F., Deng, H., Hubscher, S.G., Han, J.H., Balfe, P., McKeating, J.A. (2008) CD81 and claudin 1 coreceptor association: role in hepatitis C virus entry. *J Virol.* 82: 5007-20

**Table of Contents**

**List of Figures**

**List of Tables**

# Chapter 1:

# Introduction

## 1.1 Discovery of HCV and the disease

By the mid 1970's two distinct forms of hepatitis, termed infectious and serum, had been shown to have viral etiology (1-2). Feinstone et al demonstrated that infectious hepatitis was caused by a virus they termed Hepatitis A (HAV) (2). This virus belongs to the picornaviridae family of viruses which consists of non-enveloped particles containing positive single stranded RNA. HAV is transmitted via the Faecal-Oral route and usually only produces an acute infection (3). Serum hepatitis was shown by Bayer et al to be caused by Hepatitis B virus (HBV) (1). The discovery of the so called Australia antigen and the subsequent production of antibodies enabled investigators to determine the viral particle; HBV belongs to the Hepadnavirus family and consists of an enveloped particle containing a DNA genome. The transmission route of the virus is known to be via contact with infected blood or bodily fluids. The ability of the virus to integrate into the host genome enables the virus to persist in the host, leading to a chronic infection (4).

The discovery of these two viruses enabled the creation of screening tools that led to the discovery that the majority of post-transfusion hepatitis was caused by an as yet unknown factor (5). The ability to infect chimpanzees despite filtration up to 80nM and the ability of organic solvents to inactivate the particle, suggested a small enveloped virus was the etiological agent, later termed viral non-A, Non-B (NANB) (5-10)

The first identification of the causative agent of NANB post transfusion hepatitis by *Choo et al* used a blind recombinant immunoscreening approach (11). Briefly, the approach involved producing cDNA fragments of nucleic acid purified from experimentally infected chimpanzee serum. This cDNA library was for binding to sera from NANB-infected individuals and from an experimentally infected chimpanzee. This approach yielded one clone of the NANB

agent, which allowed hybridisation assays to be performed. This led to the determination of the genome and allowed for further characterisation of the causative agent (12). The clone was expressed in a yeast expression system and the proteins used to develop an assay for detecting circulating antibodies against the infectious agent. This assay allowed researchers to accurately study samples for the presence of the newly discovered agent and quickly established that a very high fraction of NANB hepatitis could be ascribed to this new agent, which was termed Hepatitis C virus (HCV) (12-13).

Since its identification HCV has been shown to be a major health issue worldwide, infecting around 2-3% of the worlds' population (14). HCV establishes a chronic infection in around 75% of cases; with an estimated 123 million persistently infected individuals (15). Chronic infection by HCV leads to a progressive disease of the liver. Infection is often asymptomatic but can progress to hepatic fibrosis with 20-30% of individuals developing liver cirrhosis within 20-25 years of infection. The cumulative 5 year incidence of hepatocellular carcinoma in these individuals is 10-15%. Extra-hepatic conditions such as cryoglobulinemia, glomerulonephritis, pophryia cutanea tarda and sicca syndrome have been documented (16-17). It is estimated that between 40-74% of chronically infected individuals will develop at least one of these conditions (18).

## 1.2 Basic virology

HCV has been classified as part of the *Flaviviridae* family, prototype of the genus *Hepacviridae*, although it differs in specific details of its genome organisation and the absence of an insect vector as part of its viral life cycle. The virus has a positive stranded RNA genome of around 9.4 Kb in length, encapsulated within an envelope. The RNA can directly interact with the 40s ribosomal subunit, via an Internal Ribosomal Entry site (IRES) at the 5' end of the genome, allowing translation of the viral RNA into a single polyprotein and circumventing the usual translation process of cellular messenger RNA (figure 1.1) (19-20). The polyprotein is co- and post-translationally cleaved by cellular and viral proteases into the 10 individual viral proteins. There are three designated structural proteins; Core (C), envelope glycoprotein 1 (E1) and envelope glycoprotein 2 (E2). Processing of the polyprotein releases the further viral proteins p7 and the six non-structural proteins (NS2-NS5B), which are necessary for replicating the viral RNA and immune evasion.

The core protein of HCV is believed to form the viral nucleocapsid (21). The HCV capsid is an icosahedral shaped particle of around 33nm (22), with the expression of recombinant core protein leading to the formation of nucleocapsid-like particles of between 30-40nm (23-24). The core protein requires signal peptidase and signal peptide peptidase cleavage to form the mature protein (25). The mature core exists as a dimeric α-helical structure that associates with lipid droplets within the cytosol of the cell. Lipid droplets are stores of triacylglycerol and cholesterol ester, which are surrounded by a phospholipid leaflet and a protein layer (27-28). Although it is not fully known how the core assembles to form the viral capsid, it has been demonstrated that the association with the lipid droplets is essential for the production of infective viral particles (25, 27, 29-30).

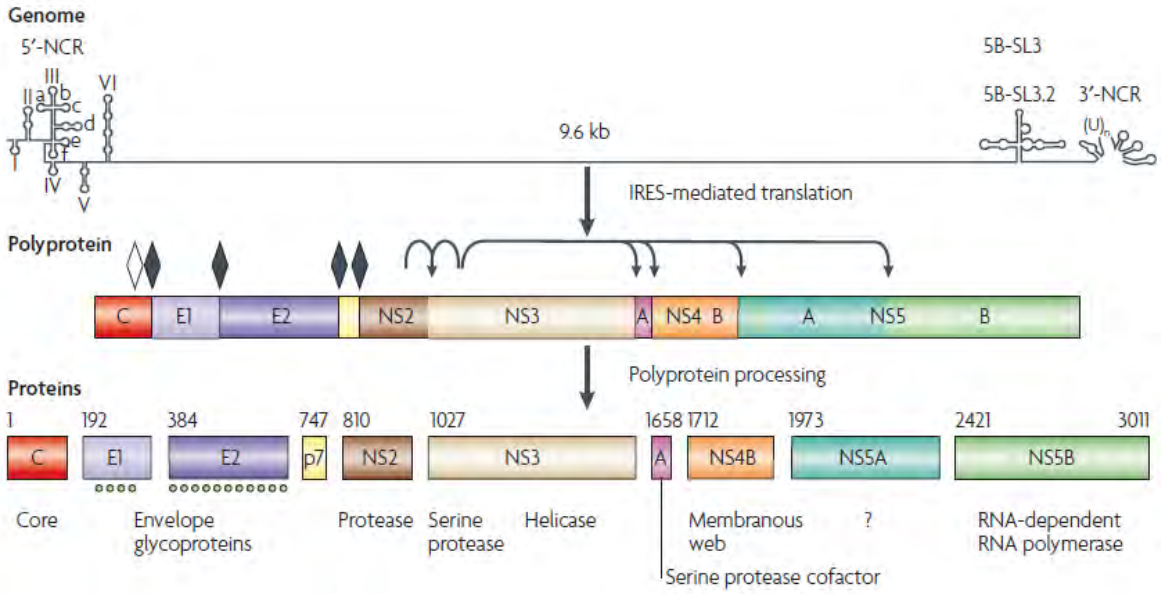


**Figure 1.1: Schematic of the HCV polyprotein processing.** The individual proteins are produced by cleavage of a polyprotein precursor by either the host or viral protease. The structural protein core (C), two Envelope Proteins (E1 and E2) and p7 are cleaved by host proteins. The non-structural proteins (NS2-NS5B) are cleaved by the encoded viral proteases. Taken from (26).

The E1 and E2 proteins of HCV are responsible for the interaction with the cellular receptors and internalisation of the viral particle. As with the core protein host signal peptidases are responsible for the cleavage of the proteins from the HCV polyprotein. E1 and E2 are classified as type I integral transmembrane proteins with C-terminal transmembrane domains. The N-terminus of the E1 and E2 proteins contains 6 and 11 N-glycosylation sites, respectively. The ectodomain is targeted to the lumen endoplasmic reticulum where the proteins are N-linked glycosolated (31). The HCV envelope proteins form a non-covalently linked heterodimer that is retained in the ER membrane. During the folding process the glycoproteins have been shown to interact with a lectin-like ER chaperone calnexin. Whether the interaction is essential for the correct folding of the heterodimer still needs to be determined (32-34).

The p7 belongs to a group of ion channel forming viral proteins called viroporins (35). Although the isolated protein has been shown to act very similarly to influenza encoded M2, in forming an ion channel that is sensitive to amantadine, it is still debated whether p7 is a structural protein (36). It has been demonstrated that p7 is required for the replication of HCV in chimpanzees (37). The protein has also been shown to be required for efficient particle release, with p7 inhibitors preventing viral release (38-41).

NS2 protein is essential for viral replication in vitro and in vivo by cleaving the polyprotein between the NS2 and NS3 proteins (42-44). In addition the NS2 has also been implicated in viral assembly. Although the exact mechanism has not been fully determined the direct interaction to the p7 and E2 proteins is essential in the production of viral particles (45-46) NS2 has also been shown to associate with the NS3-NS4A enzyme complex, which is also required for viral assembly (46-47).

The NS3 protein has been shown to have serine protease and NTPase/helicase activity (48). The enzymatic activity has been shown to require the NS4A protein as a cofactor (49-50). The NS3/4A complex is responsible for cleaving the polyprotein to release the NS3, NS4A, NS4B, NS5A and NS5B proteins (50-51). The helicase activity of the NS3 is required for replication and, although the exact function is not known, it may be required to eliminate RNA secondary structures or unwind double stranded RNA intermediates created during replication (52-53). In addition to its role in polyprotein processing the NS3/4A complex is involved in subverting the host immune response. The Toll-like recptor-3 and retinoic acid-inducible gene I (RIG-I) pathways detect the presence of extracellular and intreacellular double stranded RNA (dsRNA), respectively. Upon dsRNA detection these pathways lead to the induction of interferon-β, which in turn can induce an anti-viral state in the host (reviewed in (54)). The NS3/4A protease disrupts the cellular RIG-I pathway through proteolysis of Cardiff an interferon regulatory factor-3 (IRF-3) activator. NS3/4A cleavage of Cardiff, also referred to as MAVS, IPS-1 and VISA, results in its dissociation from the mitochondrial membrane and disruption of signaling to the antiviral immune response (55-57). The disruption of the TLR-3 pathway is achieved by the cleavage of TRIF (also called TICAM-1) adaptor protein, which also activates IRF-3 (58).

The NS4B protein has been shown to induce morphological changes in the endoplasmic reticulum. The structure formed is known as the membranous web and is believed to be the site of genome replication (59-61). In addition to the formation of the membranous web NS4B has also been shown to contain a nucleotide binding domain. This domain has been shown to bind and hydrolyze GTP with the mutation of the domain affecting HCV RNA replication (62). It has also been suggested that NS4B could be involved in viral assembly. A

mutation of the N216 residue in the C-terminus enhances HCVcc production without affecting RNA replication. Although NS4B is required for assembly the role it plays still remains unknown (63).

The NS5B protein contains the GDD polymerase motif and has therefore been identified as the RNA dependent RNA polymerase (64-66). The crystal structure of the catalytic domain of NS5B shows the palm, finger and thumb subdomains as seen in other polymerases (67-69). The fingers and thumb modulate the RNA interaction with the active site located in the thumb domain. The finger and thumb domains encircle the active site forming a tunnel that the single-stranded RNA is guided along. The NTPs required for the RNA synthesis gain access to the active site by another positively charged tunnel in the protein structure (70).

Finally the NS5A protein is thought to be important for replication due to its interactions with the other NS proteins, but its main function is believed to be involved in immune evasion as it can modulate the interferon response (71-74). The binding of PKR by NS5A has been shown to down regulate the induction and transduction of the interferon-dependent antiviral response (74-75). The interaction with cellular proteins, such as PI3K, p53, Raf-1, Grb2, indicate the role NS5A could play in regulating the cell cycle check points (76-79).

The current treatment for HCV infection consists of Pegylated Interferon α-2a and Ribavirin. The rates of sustained virological response in those treated with dual therapy are 46% for individuals infected with genotype 1, 76% for those infected with genotypes 2 or 3 and 77% for those infected with genotype 4 (80). Due to these low response rates, the toxicity and cost of the treatment, the development of new therapies is urgently required. Two protease inhibitors Boceprevir (Merck) & Telaprevir (Vertex) have recently been approved by the FDA for the treatment of HCV, with other antiviral compounds targeting the viral lifecycle at various stages of development. The virus is found within individuals as a quasispecies, which

is developed over the course of their infection through neutral and adaptive evolution (81-82). The ability of the virus to quickly develop resistance is a major concern for any potential therapies.

### 1.3 Tools for viral research

For reasons that have not fully been determined, the direct culture of virus from infected patients is extremely difficult, with few reports of successful attempts. The use of primary viruses or clinical strains of HCV to study entry therefore are limited. For this reason a number of molecular biology based approaches have been created to study the entry of HCV and have proved to be invaluable. These include soluble forms of the HCV glycoproteins, pseudotypic retroviruses encoding the HCV glycoproteins and, most recently, a cell culture attenuated virus that shows robust in vitro replication and virus production.

#### 1.3.1 Soluble HCV glycoprotein E2

One of the earliest tools developed to study the interaction of HCV envelope proteins and cellular receptors was a soluble form of E2 (sE2). The removal of the transmembrane region after amino acid 661 of the protein led to the secretion of E2 from the cell (83). Soluble E2 was used as a surrogate model to study virus cell surface interactions. The protein can be produced in large quantities and was used to discover of cellular receptors for HCV. sE2 has also been shown inhibit cell culture derived HCV entry into cells and is recognised by antibodies derived from chronically infected individuals (84). It must be noted, however, that the HCV E1 and E2 proteins are believed to exist as a heterodimer on the particle

surface and any interactions of the E2 protein alone may not mimic the true interactions and function(s) of HCV glycoproteins. Measuring internalisation events is also not possible, which has led to the development of other experimental systems (85-88).

### 1.3.2 HCV pseudoparticles

To address the possible shortcomings of sE2 and reconstitute the HCV glycoprotein, a system was developed using retroviral particles that incorporated both HCV glycoproteins, so called HCV pseudoparticles (HCVpp) (89-91). Retrovirus particles egress from the cell by budding from the plasma membrane of cells, in doing so they incorporate envelope proteins derived from the plasma membrane. Consequently, heterologous proteins expressed at the cell surface can be incorporated into particles. HCVpp are generated by co-transfecting 293-T cells with plasmids encoding the HCV glycoproteins, a reporter gene, usually luciferase or a fluorophore, and a packaging construct encoding the gag-pol genes of HIV or Murine Leukaemia virus. The HCV glycoproteins can be the E1 and E2 from any of the HCV genotypes. Entry of these pseudoparticles into cells is defined by the HCV glycoproteins, which deliver the retrovirus particle into the cytosol of the target cell. The genes delivered by the retroviral particle undergo reverse transcription and are integrated into the cellular genome. After the integration event the reporter gene is expressed, allowing the detection of successful viral entry (92). The development of this system allowed investigators to discover the cellular proteins involved in the internalisation of the HCV (88, 90-91, 93).

### 1.3.3 The JFH-1 strain of HCV

One of the biggest milestones in HCV research was the development of a HCV strain that has the ability to replicate, assemble and release infectious particles from cultured hepatoma cells (HCVcc) (94-96). A HCV RNA clone derived from a Japanese patient suffering fulminant hepatitis replicates efficiently and supports secretion of viral particles when transfected into Huh7 cells. This strain was termed Japanese Fulminant Hepatitis-1 (JFH-1cc). JFH-1cc particles are infectious for chimpanzees as well as UpA-SCID chimeric mice, which contain transplanted human hepatocytes. Virus can be recovered from the JFH-1cc-infected animals and will replicate in cell culture (94). Subsequently chimeras of JFH-1cc have been produced that have improved many aspects of the system. Chimeras have also been produced which express glycoproteins from different structural proteins (97-100). As a consequence of the development of these systems the full viral life cycle, from entry to egress, can be studied not only in hepatocyte derived cell lines but also primary cultures of human hepatocytes (94-96, 98, 101).

**1.4 Discovery of receptors or entry factors.**

All viruses are intracellular parasites and, with the exception of yeast and fungal viruses that have no extracellular part to their life cycle, must traverse the barrier of the cellular membrane. The means by which viruses other than plant viruses achieve this is by interacting with specific factors on the cell surface which mediate their binding and entry into the cell. These factors can be highly specific and can define virus host and cellular tropism. The initial interaction of the HCV with the cell is thought to be via the low Density Lipoprotein Receptor (LDL-R) and Glycosoaminoglycans (GAGs), in particularly Heparin Sulphate. Interfering with interaction of the viral particles to these proteins by enzyme treatments does prevent infection (102). One point that has to be made at this stage is that the usage of heparin sulphate as an entry factor has been shown to be a cell culture attenuation in other viruses and therefore the observations related to heparin sulphate may not hold true *in vivo* (103-104).

More specific protein interactions have been shown between the HCV particle, which are considered the specific receptor proteins, and the tetraspanin CD81 (88, 91, 93, 105-106), scavenger receptor class B membrane I (SR-BI) (107-109), three members of the Claudin family Claudin1, 6 and 9 (110-113) and Occludin (figure 1.2) (114-115).

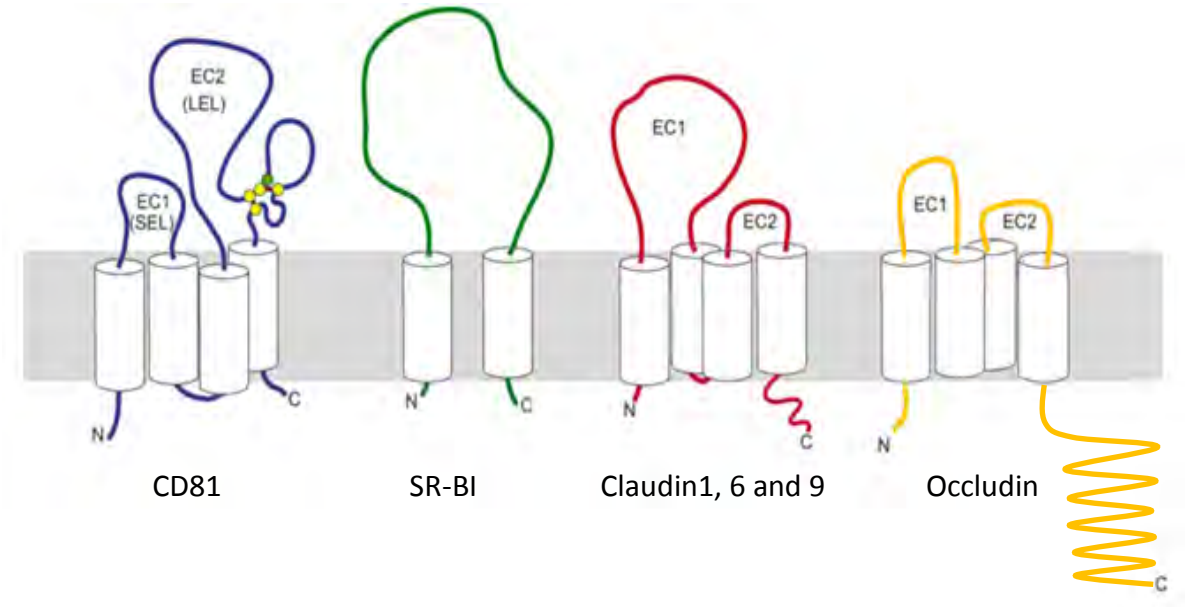


**Figure 1.2: Hepatitis C Virus entry factors.** The diagram shows a schematic representation of the known entry factors for HCV. CD81, Claudin1, 6 and 9 and Occludin share a similar overall topology of four transmembrane domains with two extracellular loop regions, denoted as EC1 and EC2. SR-BI has two transmembrane domains and a single extracellular loop. The EC2 of CD81 contains cysteine residues that are known to form disulphide bridges, denoted by yellow circles, with the conserved glycine depicted by the Green circle

### 1.4.1 CD81

The first protein to be identified as a potential entry factor for HCV was CD81 (106). CD81 belongs to a group of proteins called tetraspanins. In humans there are around 33 identified tetraspanin proteins, 36 in *Drosophila melanogaster*, and 20 in *Caenorhabditis elegans.* Tetraspanins have also been shown to be extensively expressed in plants, fungi, and protozoan amoebae (116). Tetraspanins have been shown to be involved in many biological processes, including fertilisation of oocytes and a wide variety of cell to cell interactions, they are also involved in the immune system (reviewed in (117)). There is also evidence for their involvement in metastasis of cancer cells and infection by malaria (reviewed in (117-119)). Tetraspanins share a common structure, depicted in figure 1.2, of four transmembrane domains, a conserved Cysteine-Cysteine-Glycine motif and at least two more Cysteine residues that are critical for forming two disulphide bridges within the second or large extracellular loop (120-121). The first extracellular loop (EC1) is generally small and, due to a lack of specific antibodies or structural information, very little is known about its biological importance (122). The large or second extracellular loop (EC2) has been reported to be involved in protein-protein interactions. The region responsible for the majority of the interactions is thought to be the conserved disulphide bridge region of EC2 (122).

It has been demonstrated that members of the tetraspanin superfamily form a network, referred to as a tetraspanin web, that interact with and organise other cell surface proteins (122, 123). The tetraspanin proteins can form homodimers, trimers and tetramers and have been suggested as the fundamental building blocks of the tetraspanin web. In addition to the tetraspanin-tetraspanin associations further binding partners have been demonstrated.

The best characterised tetraspanin-partner pairs include CD151–integrin $\alpha_3\beta_1$, CD151–integrin $\alpha_6\beta_1$ and CD81–CD19. CD9 and CD81 share two partners, EWI-2 and CD9P-1–EWI-F–FPRP (119, 122, 126-127). The association of these partners with the tetraspanin have been shown to be important in the regulation of these proteins and their functions. The regulation and cell surface expression of CD19 is reliant on its tetraspanin partner CD81. CD81 deficient mice have demonstrated a reduced level of CD19 cell surface expression. The reduced level of CD19 leads to impaired B cell activation and antibody production in response to T cell (128-130). In contrast the integrin does not rely on CD151 for its surface localisation but the association is essential for integrin $\alpha_3\beta_1$ to interact with the basal lamina (122, 131). Mutations within CD151, which ablate its interaction with integrin $\alpha_3\beta_1$ and integrin $\alpha_6\beta_1$, have been associated with a number of conditions such as hereditary nephritis, pretibial epidermolysis bullosa, platelet malfunctions, deafness and β-thalassemia minor (132-133). Knockout mice models also show disorders in platelet clotting, keratinocyte migration and lymphocyte proliferation (134-135). The use of knockout mouse models has also shown a variety of tetraspanin functions. CD9 deletion leads to defects in sperm–egg fusion, monocyte fusion with brain and peripheral nerve defects also observed (136-139). CD37, CD151 and TSSC6 knockout mice showed abnormal lymphocyte activation with Peripherin/RDS and ROM deletions leading to retinal degeneration (reviewed in (122, 126)).

Tetraspanins have also been essential for the life cycles of a number of viruses. The tetraspanin Tspan7 was shown to interact with the VP26 of Herpes Simplex Virus-1. The siRNA knockdown of Tspan7 leads to a reduction in viral replication (140). Human papillomaviruses localises with CD63 and CD151 on the cell surface following cell attachment. The antibody targeting or siRNA knockdown of CD63 has been shown to

prevent viral entry (141). The egress of HIV-1 has been shown to proceed through tetraspanin enriched microdomains containing CD9, CD63, CD81 and CD82 in dendritic cells, T-cells and macrophages (142-146).

The first evidence demonstrating the involvement of CD81 in HCV entry was gained by screening a human cDNA library expressed in mouse fibroblasts with sE2, from which it was shown that E2 interacted with CD81 (106). Further studies have demonstrated the importance of the E2 interaction with CD81 as monoclonal antibodies against both E2 and CD81 inhibit HCVpp and HCVcc entry (147-148). siRNA silencing of CD81 expression in Huh-7 cells prevented HCVpp and HCVcc entry whilst the introduction of CD81 into HepG2 cells, a non permissive CD81 negative hepatocyte cell line, enabled HCVpp and HCVcc entry, demonstrating the requirement of CD81 for viral entry (94, 147, 149). Infection of HepG2-CD81 cells with HCVpp virus expressing glycoproteins from different genotypes demonstrated the universal requirement of CD81 by all HCV genotypes (147, 150). Additionally CD81 from various species also render HepG2 cells permissive to entry, indicating that CD81 is not responsible for HCV being a human specific pathogen (88).

A soluble form of the second extracellular loop of CD81 (CD81-EC2) has proven to be an extremely useful reagent in determining aspects of the viral interactions with CD81. The CD81-EC2 has been shown to neutralise both HCVpp and HCVcc infection (149). The binding of E2 has also been demonstrated to purified full length CD81 produced in the yeast *Pichia pastoris (151).* Crystallographic analysis of CD81-EC2 demonstrated that the protein forms dimers (120). The disruption of the ability of the CD81-EC2 to form dimers, via specific mutations, correlated with a reduction in E2 binding (152). The kinetics of the interaction of E2 and E1/E2 to CD81-EC2 were studied using surface plasma resonance, which showed that

the E1/E2-CD81-EC2 dissociation rate was much lower than that of E2-CD81-EC2. Furthermore, dimeric forms of CD81-EC2 have been show to have a 10-fold more efficient binding of E2 compared to monomeric CD81-EC2 (153).

Although CD81 is a highly specific receptor for the HCV E1/E2, its ubiquitous expression throughout the body (122) and the variability of genotype binding efficiency to CD81 (154-155), led investigators to look for additional entry factors.

### 1.4.2 Scavenger receptor class B type I

The initial evidence for the role of Scavenger receptor class B type 1 (SR-BI) came from the observation that HepG2 cells, which lack CD81, bind sE2. This was shown to be mediated via a specific interaction with SR-BI (109). SR-BI is a member of the CD36 superfamily and plays an essential role in lipoprotein metabolism. Lipoproteins comprise a cholesterol ester core surrounded by lipids and apoproteins. These structures transport triglycerides and cholesterol around the body and are categorised by their density, as High density (HDL), low density (LDL) or very low density lipoproteins (VLDL) (156-157). SR-BI is a membrane protein of 509 amino acids in length. The structure is compromised of two transmembrane domains with a single large extracellular loop of around 403 amino acids. It has been shown to interact with a variety of ligands including VLDL, LDL, HDL and naturally occurring modified forms of LDL such as oxidised LDL (oxLDL) and acetylated LDL (158-160). A major role of SR-BI is the selective uptake of cholesterol from HDL particles. Firstly HDL is bound to SR-BI, via the apoprotein ApoAI, before cholesterol is selectively transferred to the membrane of the cell or the HDL holoparticle is endocytosed (161). Movement of unesterified cholesterol can

also occur from the cell to the HDL particle, known as cholesterol efflux (157). The role of SR-BI in HCV infection has been shown by the inhibition of HCV infection by SR-BI ligands oxLDL and serum amyloid-α (162-164). HDL has been shown to enhance HCV entry, as well as reducing the efficacy of neutralising antibodies (165-166). This enhancement by HDL can be prevented by blocking the movement of cholesterol from bound HDL to the cell using drug treatment, indicating that the cholesterol content of the membrane may be important for HCV entry (162, 166-167). SR-BI has been shown to interact with the hypervariable region of HCV E2, as deletion of this region ablated binding (109). Silencing of SR-BI expression and treating cells with antibodies specific to SR-BI reduces HCV entry (89, 108, 162, 166-169). Overexpression of SR-BI in Huh-7 cells enhances HCV entry, suggesting its expression in Huh7 cells is limiting (108, 169). Taken together these facts demonstrate a role for SR-BI in HCV infection and show that SR-BI expression levels have a direct impact on viral entry.

### 1.4.3 Claudin1

As many cell lines that express both CD81 and SR-BI were not permissive to HCVpp infection, other factors were predicted to be required for HCV entry into cells, (91, 93). Subsequently, three members of the Claudin family were shown to mediate HCV entry (110, 113). Claudins are a family of integral membrane proteins of around 23kDa, which are constituents of tight junctions (170). Claudin proteins form strands, via homotypic or heterotypic cis-interactions, within the plasma membrane of the cell. These strands can then interact with Claudins in an opposing cell closing the intercellular gap formation of the tight junction (170-171). Tight Junctions are mainly involved in the maintenance of epithelial and endothelial barrier function. The Claudin involved in the formation of the junction determines the permeability to solutes and the movement of ions between the apical and basal surface of the cell. Hence, Claudin expression in various tissues is highly specific for the function of those tissues (170, 172). It is also believed that expression of certain Claudins is dependent on the stage of development, for example Claudin6 is detected in embryonic epithelia, showing reduced expression over time (173). The organisation of Claudin proteins within the tight junctions of epithelial cells has been shown to be dependent upon their association with the scaffolding proteins zonula occludens (ZO)-1 and 2 (174). However, this association is not required for localisation in nonpolarized cells (175). Claudin association with ZO-1 and ZO-2 is dependent on a PDZ binding domain at its C-terminus. The Claudin proteins have also been shown to bind to the PDZ domains of various proteins, most notably Claudin1 which can associate with not only ZO-1, -2 and -3 but multi PDZ domain protein and Pals1-associated tight junction protein PATJ (176-178). Recent work using liver sections has shown that Claudin 1 not only localises to the tight junction but also exists at the basal

and lateral surfaces (179). The existence of these pools of Claudin may be related to the trafficking of newly synthesised proteins to the plasma membrane before translocating into the tight junction.

The discovery of Claudin1 as a mediator of HCV entry came from work performed by Evans et al who used a cDNA expression screening approach. They introduced a library of proteins found in the permissive hepatocellular carcinoma cell line, Huh7.5, into the non-permissive 293-T cell line, which expresses both CD81 and SR-BI. The resultant screen demonstrated that Claudin1 could render 293-T cells permissive for HCVpp entry (110). Reducing Claudin1 expression with siRNA ablated HCVcc entry into Huh7.5 cells. Further work performed by Zheng et al demonstrated that the permissive nature of the Claudin1 negative cell line Bel7402 was due to Claudin9. Silencing of Claudin9 in Bel7402 ablated HCVpp entry. This group also demonstrated that Claudin9, as well as the closely related Claudin6, could mediate HCVpp entry into 293-T cells, whilst other members of the Claudin family members were not functional receptors (113). The relevance of Claudin6 and 9 in entry of HCV into the hepatocyte is unlikely to be high, as neither protein is expressed in the liver. We demonstrated that the Huh7.5 cell line has a small mRNA signal for Claudin6 but a complete lack of Claudin9 mRNA (180) whilst a complete lack of expression of the two proteins was shown in the liver (181). It must be highlighted at this point that the role of both SR-BI and CD81 in HCV entry was defined by their direct interaction with sE2, as of yet the role of Claudins has been shown in the gain of entry to non-permissive cell lines and not through a defined direct interaction with the virus (110, 182-183).

Several groups have created Claudin mutants in order to determine specific residues that are required for receptor activity. Evans et al first demonstrated that the N-terminal third of

the EC1 of Claudin1 is essential for its function by creating chimeric proteins with the receptor inactive Claudin7. By swapping this region between Claudin1 and Claudin7 the authors were able to produce a receptor inactive Claudin1 and a receptor active Claudin7. Within the N-terminal third of the EC1 there are five amino acid differences, which the authors mutated to define the critical residues for receptor activity. Exchanging residues in the Claudin1 and Claudin7 EC1 at positions 32 and 48 showed a loss and gain of receptor activity, respectively (figure 1.3) (110). These positions were also demonstrated by Liu et al, with the addition of two further positions in the EC2 of Claudin1, F148 and R158 (114). A more extensive mutational analysis was performed by Cukierman et al, where they demonstrated that mutating a motif conserved among all Claudins, W30-GLW51-C54-C64, as well as D38 also created a receptor inactive Claudin1 (183). Mutational analysis of Claudin9 demonstrated that residues S38 and V45 are essential for its receptor activity (113). Unfortunately no clear mechanism was shown in these publications, although there are suggestions by the authors that the mutations may affect cell-cell contacts and the ability of the Claudin to form trans interactions which may be required for function. Liu et al reported that the localisation of the Claudin1 was defined at cell-cell contacts, with the receptor inactive Claudin1 mutants having a more diffuse localisation. Reseeding of 293-T cells expressing Claudin1, to break cell-cell contacts also lowers the infection efficiency, although how the experiment was performed was not detailed in the publication (114).

In addition to the requirement of the EC1 of Claudin1 it was also demonstrated that the C-terminal and the putative palmitoylation sites are not required for its receptor activity. The deletion of the C-terminal tail has no affect on HCVpp entry (110, 184), indeed the production of an Occludin-Claudin1 chimeric protein where only the EC1 of Claudin1 was

present demonstrates that the EC1 alone is required for receptor activity (114). Together these data indicate that the interaction of Claudin1 with the actin cytoskeleton is not essential for receptor activity.

To date a direct interaction of Claudin1, 6 or 9 with the HCV particle has not been demonstrated and the involvement of the Claudins in entry may be due to their ability to interact with CD81. It has been demonstrated previously that Claudin1 can associate with CD81 (125, 183-184). Experiments using a Claudin1 bearing a F10x3 tag, which allowed inhibition of infection using an M2 anti-FLAG antibody, allowed the time at which the virus escaped neutralisation to be determined. The results demonstrated that an anti-CD81 (JS81) and M2 anti-FLAG reached their half-maximal inhibition level at 18 and 73 minutes after addition of the virus, respectively. This suggests that the function of Claudin1 occurs at a later stage than that of CD81 (110). However, a rat polyclonal anti-Claudin1 antibody was shown to have a half-maximal inhibition time of 33±6 minutes, compared with anti-CD81 JS81 with a time of 30±10 minutes (182). These two sets of results were not produced on the same cell lines or using the same virus, Evans et al used 293-T cells and HCVpp virus whilst Krieger et al used Huh7.5 cells and HCVcc virus, however the differences question the relative timings of the post-attachment receptor interactions.

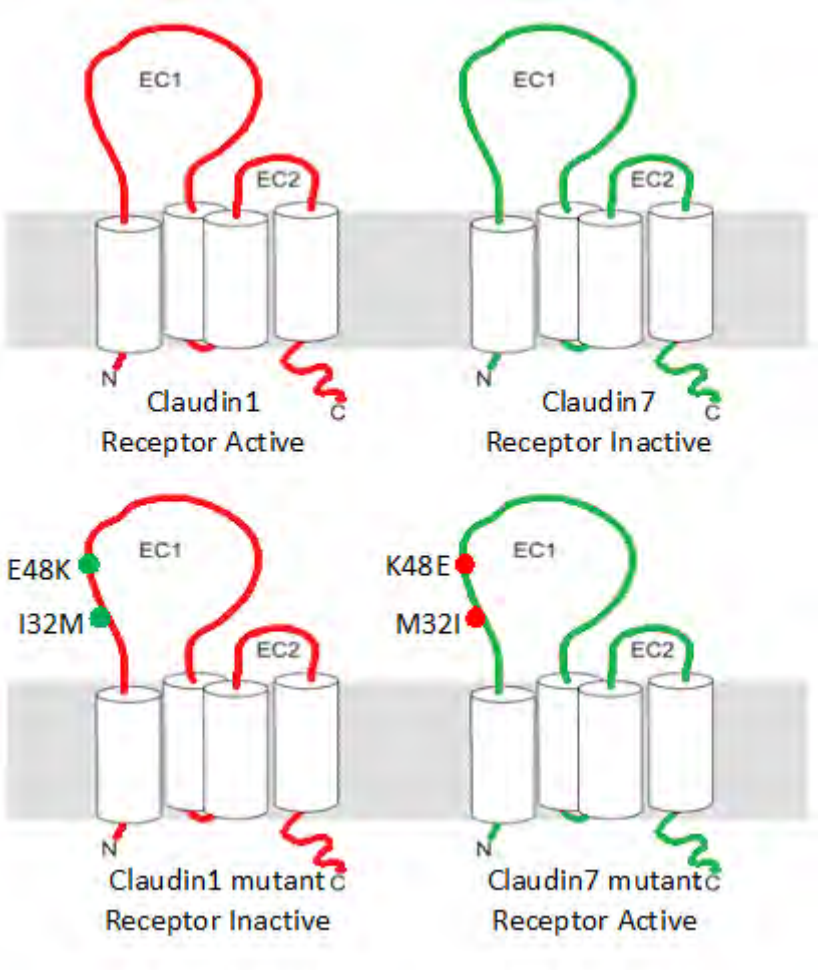


**Figure 1.3: Schematic representation of receptor active and inactive Claudin proteins.** The diagrams show a representation of the Claudin1 and Claudin7 constructs created by Evans *et al,* with their receptor activities detailed. The upper row shows the wild type Claudin1 and 7, the lower row shows their reciprocal mutations, with the amino acid changes and their positions highlighted.

### 1.4.4 Occludin

Recently two reports published almost simultaneously implicated Occludin as the fourth HCV entry factor (114-115). The rationale and experimental approaches of the 2 groups were quite independent and very different, which taken together strengthens the evidence for a specific role of Occludin in the HCV entry process.

Ploss et al sought to address the question of why cell lines that encode CD81, SR-BI and Claudin1 were resistant to viral entry. They therefore repeated the process that enabled them to show Claudin1 as a HCV entry factor by expressing genes from the highly permissive Huh7.5 cell line in a non-permissive cell line using a cyclic lentivirus based repackaging screen (110). The cell line in question was a mouse embryonic fibroblast cell line, NIH3T3 overexpressing CD81, SR-BI and Claudin1. From this screen Occludin was identified. The authors then proceeded to show that expressing Occludin in a renal carcinoma cell line, 786-O, or in TZM cells, a Hela cell derivative that has low levels of endogenous Occludin, permitted HCVpp entry into cells which are naturally non-permissive. In addition to overexpressing Occludin to render cells permissive, the authors demonstrated that siRNA silencing Occludin expression in Huh7.5 cells, led to a significant reduction in entry of both HCVcc and HCVpp. Finally the authors demonstrated that HCVpp entry into NIH3T3 and CHO cells requires human CD81 and Occludin, whereas SR-BI and Claudin 1 could be of mouse origin (115).

Lui et al wanted to determine whether HCV entry mimicked Coxsackie B Virus entry, which enters cells via tight junction interactions. The authors therefore performed both siRNA and shRNA knockdown of tight junction proteins Claudin1, Occludin, ZO-1, JAM-A and the Coxsackie and Adenovirus Receptor (CAR) in Huh7.5.1 cells. Their results showed that

Claudin1, Occludin and ZO-1 knockdown resulted in a reduced viral entry. Claudin1 and Occludin knockdown did not alter the expression of the other HCV receptors, however the ZO-1 knockdown resulted in a reduction in Claudin1 expression. The authors also produced chimeric proteins of Claudin1 and Occludin and determined their receptor activity in 293T cells, only those proteins containing the EC1 of Claudin1 showed receptor activity. This result is somewhat expected as Claudin1 lacking a C-terminus is still receptor active (184) and 293-T cells express endogenous Occludin (115).

Occludin was first identified by Furuse et al as an integral membrane protein located in tight junctions. Structurally it is very similar to Claudins, with four transmembrane domains and two cytoplasmic regions at the N- and C- termini (185). The role of Occludin seems to be related to the maintenance of tight junctions. Knockout mice studies demonstrated that tight junctions could still form in the absence of Occludin with no gross phenotype (186), indicating that Occludin is not absolutely required for tight junction formation. However the treatment of polarised Caco-2 cells with peptides of the first extracellular loop of Occludin caused an increase in tight junction permeability (187-188). The function of Occludin is related to its ability to interact with the cytoskeleton. Occludin is anchored to the cytoskeleton by interacting with the guanylate kinase region of ZO-1 via the Domain E region of its C-terminus, termed the coiled-coil region (189-191). As part of the regulation of tight junctions Occludin, as well as Claudin, are readily internalised (192). Occludin has been shown to co-internalise with Claudin1 via Clathrin-mediated processes (193) as well as being induced to internalise by stress in a Caveolae mediated process (194).

## 1.5 Tight junction proteins and viral entry

Tight junctions are responsible for the regulation of movement of solutes, ions and water across the endothelia or epithelia. They also form a barrier preventing the access of pathogens to the underlying tissue (172, 195-196). Some 30 proteins have been identified which serve distinct functions in maintaining the barrier function of the tight junction (192). Some viruses have evolved to exploit tight junction proteins in order to enter and infect the target cell. Examples include Adenovirus, Coxsackievirus-B (CVB), Feline Calicivirus (FCV), Swine vesicular disease virus (SVD), Reovirus as well as HCV (195). Another virus that has been shown to interact with tight junction proteins is Rotavirus, a major cause of gastroenteritis in mammals. Unlike the other viruses, that use tight junction proteins as co-receptors, Rotavirus disrupts tight junctions, via the interaction of VP8 protein with JAM-A, to gain access to the "deeper" membrane-associated integrins that act as its entry factors (195, 197).

The entry process of FCV and Reovirus also utilise JAM-A. The entry process of FCV is poorly understood but it appears to internalise upon receptor binding via clathrin mediated endocytosis (198-199). JAM-A has been implicated as a receptor along with α2,6-Linked sialic acid, the latter has been suggested to determine the typical oral and upper respiratory tract pattern of infection. Due to its broad expression, JAM-A may be responsible for systemic febrile diseases relating to specific highly viral strains (198-200). The stages in Reovirus entry are better defined than those of FCV. First the virus interacts with the cell surface via α2,3-linked sialic acid (α2,6-linked for serotype 3 reoviruses). The virus then forms a high affinity interaction with JAM-A. This virus-JAM-A complex then interacts with

β1 integrin, which mediates the internalisation of the virus via clathrin mediated endocytosis (201).

Two further examples of viruses that utilise tight junction components are Adenovirus and CVB. Entry of both viruses was shown to be via a shared protein referred to as the Coxsackie and Adeno Receptor (CAR) (10, 202). Binding of Adenovirus to the cell occurs via a high affinity interaction of the fibre protein of the virus with the D1 domain of the CAR receptor (203-204). The virus then interacts via an argine-glycine-aspartate motif in its Penton base with $\alpha_v\beta_3$ and $\alpha_v\beta_5$integrins, which leads to the internalisation of the virus (205). This internalisation has been shown to be via clathrin-mediated endocytosis, although subpopulations of virions have been reported to associate with a Lipid Raft/Caveolae mediated endocytosis pathway (206-207).

Since CVB and HCV both utilise Occludin in their entry process, CVB has become a model for many researchers of how HCV enters the cell. The process for the entry of CVB has been shown by Coyne and Bergleson to be facilitated by Decay-Accelerating Factor (DAF), CAR and Occludin (figure 1.4) (208-209). CVB engagement with DAF activates the non-receptor tyrosine kinase, AbI, which in turn induces Rac GTPase and causes the relocalisation of the virus to the tight junction. Once relocated to the tight junction the virus can interact with TJ resident CAR protein, which causes a conformational change in the virus. The activation of Fyn kinase, a tyrosine specific phospho-transferase, induced by the engagement of DAF allows the internalisation of the virus in a caveola-dependent manner (208). The evidence for the involvement of Occludin was shown by the effects of siRNA treatment on cells, which caused a reduction in viral entry by trapping virus at the tight junction.

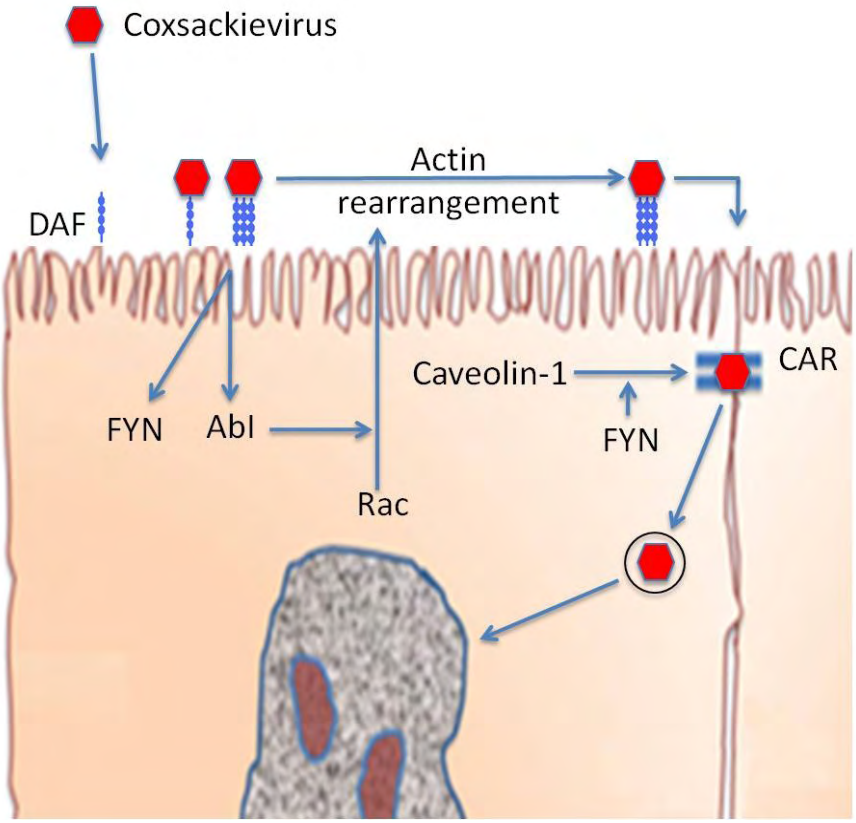


**Figure1.4: Coxsackievirus (CVB) entry into polarized cells.** CVB binds to Decay-Accelerating Factor (DAF). The binding activates the non-receptor tyrosine kinase, AbI, which in turn induces Rac GTPase and causes the relocalisation of the virus to the tight junction. Once relocated to the tight junction the virus can interact with TJ resident CAR protein, which leads to a conformational change in the virus. The virus then enters the cell by a caveola-dependent manner (208).

The role of Occludin in CVB entry has thus far been shown to be associated with the entry of the virus after it has relocated to the tight junction. Additionally the entry of Occludin and viral particles were caveolin dependent and required the activation of the GTPases Rab34, Ras, and Rab5, which are associated with macropinocytosis (209). An intriguing development in CBV entry has been the demonstration that in non-polarised Hela cells both DAF-dependent and DAF-independent viruses enter via a Dynamin- and lipid raft-dependent process. In these cells the internalisation of the virus was also shown to be clathrin, caveolae and endosomal acidification independent (210). This demonstrates two different entry methods depending on whether the virus is interacting with a polarised or non-polarised cell target.

Parallels between aspects of CVB and HCV entry are evident in the use of two tight junction proteins as well as the interaction with an initial factor on the cell surface. HCV entry has also been shown to be reduced by inhibiting PKA (211). PKA has been shown to activate Ras as part of cAMP-PKA pathway, which has been shown to be involved in proliferation, differentiation, metabolism, immune response and, more specifically, viral entry cytoskeletal reorganisation (212). Whereas DAF has been shown to re-localise the virion to the cell junction, the same has not been shown for CD81. Although several similarities exist between aspects of the entry process, more work is required to demonstrate if HCV can enter in a CVB-like manner and not by a distinct mechanism.

### 1.6 Effects of polarisation on viral entry

The interface between the lumen and the various organs is lined by a polarised cell layer. Within the respiratory and the gastrointestinal tract this cell layer consists of epithelial cells that exhibit a simple polarity. These cells compose of an apical and basal surface that faces the lumen and lamina surfaces respectively. The cells in the layer are joined laterally together by tight junctions, Adhesion Junction, gap junctions and desmosome (figure 1.5) (170, 195, 213-215). Using the human colon carcinoma cell line, Caco-2 cells, it was demonstrated that HCV could entry non-polarised and polarised with equal efficiency (180). However the use of this simple polarised cell line does not reconstitute the type of polarity found within the liver. Hepatocytes, the target of HCV, have a more complex polarity, with at least two basal surfaces and their apical surface forming a channel or bile canaliculi (figure 1.6) (216). The more complex polarity of hepatocyes may lead to a restricted access to proteins associated with the tight junction. In order to better define the effects of polarity on HCV entry a hepatocyte in vitro model is required. The cell line that demonstrates this polarity is the HepG2 cell line, which with the introduction of CD81 becomes permissive for HCV entry (149, 216). It has been demonstrated HepG2 become more resistant to viral entry with polarisation. Expression of a fluorophore labelled Claudin1 protein within HepG2 cells demonstrated that, as cells develop into a hepatocyte type polarity, discrete pools of Claudin1 appear at both the tight junction and basal/lateral surface from an initially more diffuse localisation around the plasma membrane (figure 1.7) (179). Expression of fluorescent labelled Occludin also demonstrates a diffuse expression of the protein around the plasma membrane, with enriched domains at the tight junction. Both of these staining patterns can be seen in figure 1.7. In vitro staining of polarized

HepG2, WIFB9 cells and human liver tissue with a commercial anti-Occludin antibody only showed the protein at the tight junctions (179). The different staining patterns could be due to the over expression of the fluorescent protein or it could also indicate the levels of protein at the basal surface may be below the detection threshold for the available occludin antibody. Flourescence resonance energy transfer (FRET) analysis of non-polarised HepG2 cells showed a similar level of interaction of CD81 and Claudin1 as previously reported in Huh7.5 and 293-T cells (184). Although the levels of FRET between CD81 and Claudin1 were comparable between polarised and non-polarised HepG2 cells, there was no detectable FRET occurring in the tight junction regions (179, 217). This along with the ability of non-polarised cells such as Huh7.5 and 293-T cells to support infection suggests that non-tight junction associated forms of Claudin1 are involved in the entry process and polarisation affects the access to the co-receptor.

A.

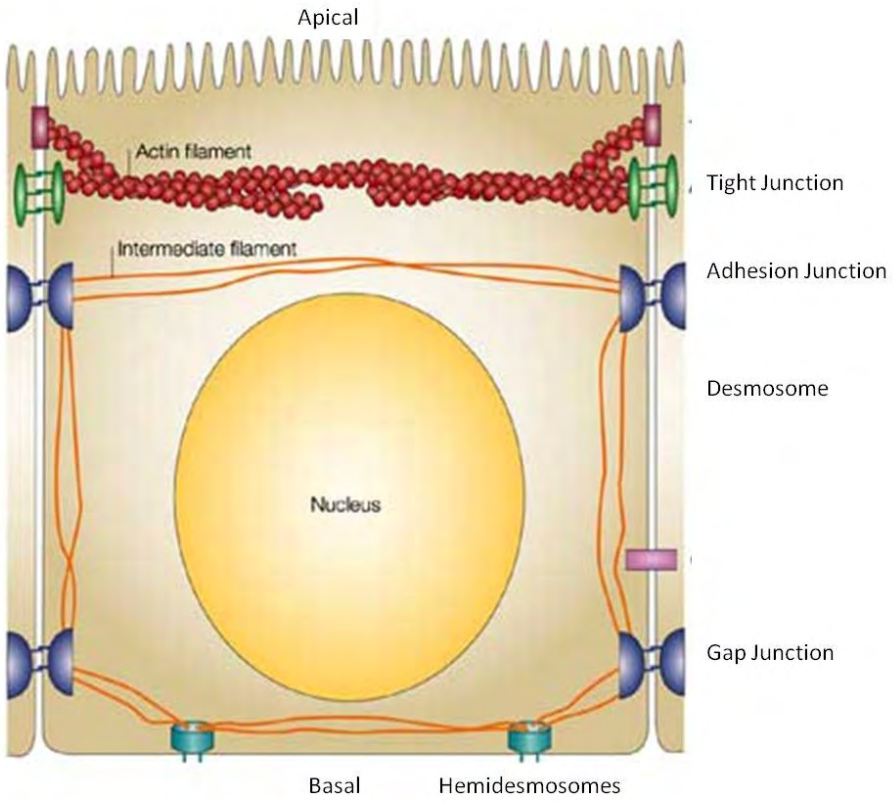
Apical
Actin filament
Intermediate filament
Nucleus
Basal
Hemidesmosomes
Tight Junction
Adhesion Junction
Desmosome
Gap Junction

B.

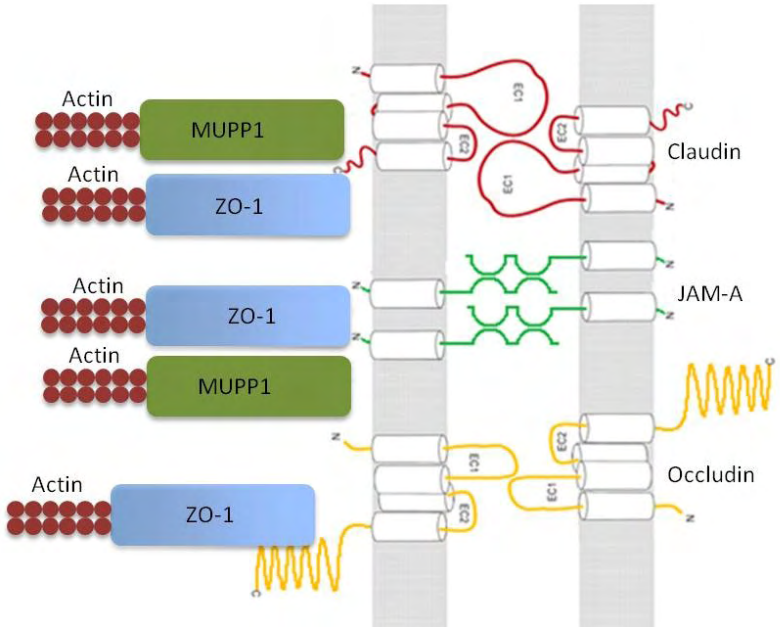
Actin
MUPP1
Actin
ZO-1
Actin
ZO-1
Actin
MUPP1
Actin
ZO-1
Claudin
JAM-A
Occludin

**Figure 1.5: Schematic representation of lateral cell-cell junction regions.** A) Depicts the location of the different complexes that close the gap between two adjacent cells in an epithelial layer. The most apical complex is the tight junction followed by the adhesion junction, desmosome and the most basal complex the Gap junction. B) Shows an enlarged view of the tight junction. The main tight junctions proteins are members of the Claudin protein family, Junction adhesion molecule-A (JAM-A) and Occludin. Claudin, JAM-A and Occludin interacts with the Actin cytoskeleton of the cell via associates with Zona Occludin-1 (ZO-1). Claudin and JAM-A also associate with multi-PDZ domain protein 1 (MUPP1), which can also interact with actin (174, 176, 213, 215, 218). The image shown is modified from (213).

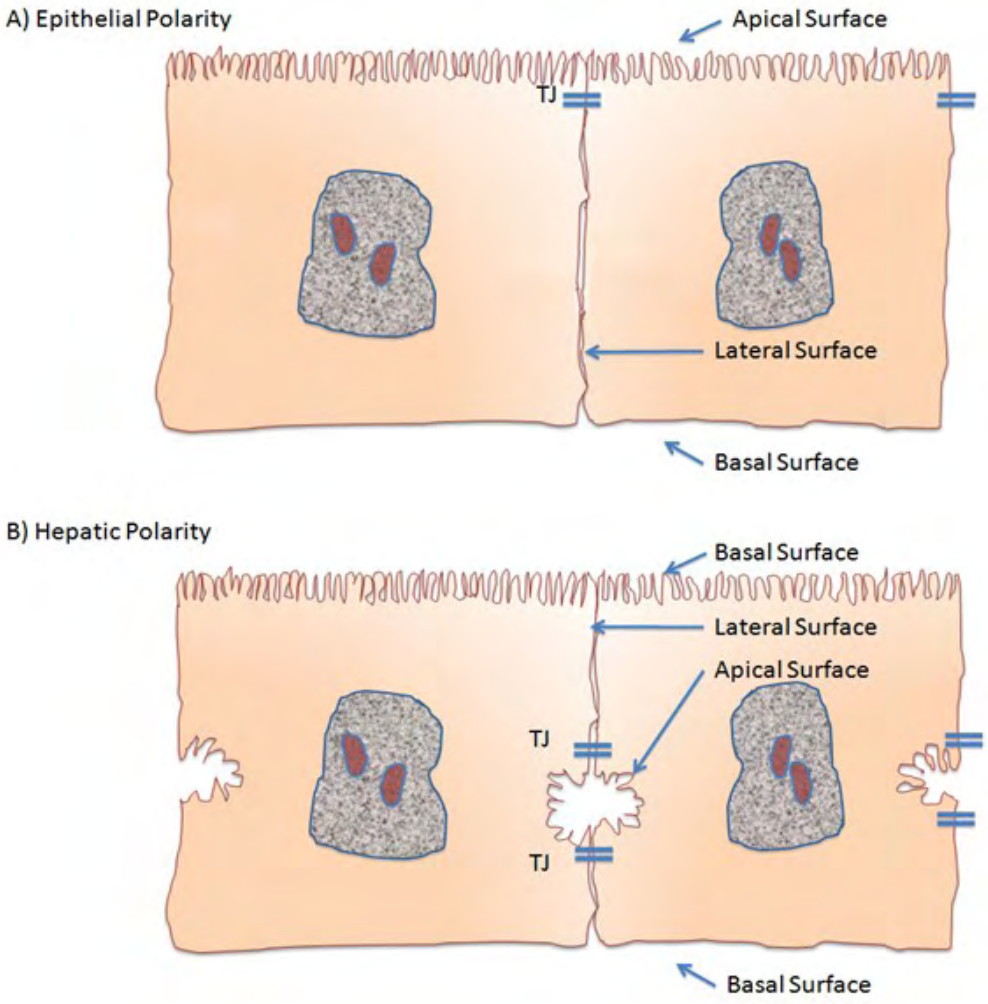


**Figure 1.6: Schematic representation of polarised epithelial and hepatic cells.** Two types of polarisation are shown A) shows simple epithelial polarity, epithelial cells form a polarised continuous apical surface providing a barrier between the extracellular environment and the deeper tissues of the body. The tight junctions that form between neighbouring cells are in close proximity to the apical surface. B) Hepatic polarity, Hepatocytes form an apical surface between cells which generates a tubular structure, the bile caniliculus. The tight junctions seal this tube and isolate its contents.

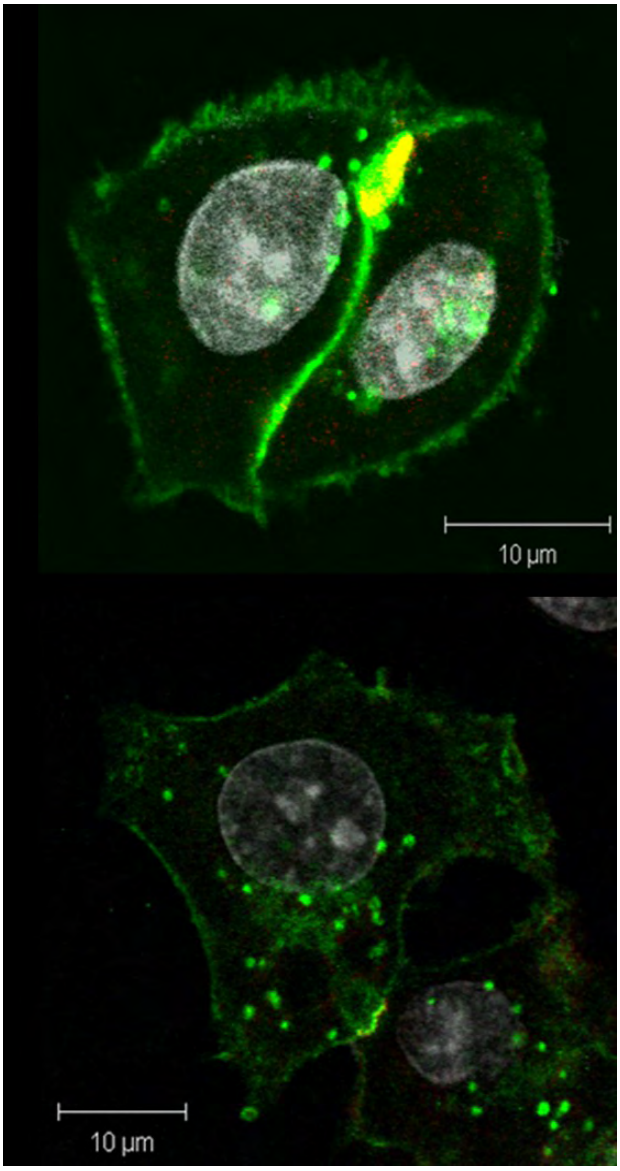


**Figure 1.7: Confocal images of polarised HepG2 cells expressing fluorophore-labelled Claudin1.** HepG2 cells engineered to express AcGFP labelled Claudin1 or Occludin (A and B respectively) and allowed to polarise. The cells were fixed and stained for ZO-1, using and anti-Zo-1 primary antibody and a Alexa Fluor 594 anti IgG (H+L), to indicate the position of the tight junction. A) shows that Claudin1 co-localizes with ZO-1 at the tight junction (yellow region) and is also present at the basal and lateral surfaces of the plasma membrane. B) shows Occludin has a similar pattern as Claudin1 with expression at both the tight junction, basal and lateral surfaces. Images provided by Helen Harris and Chris Mee.

### 1.7 Project aims

The work presented here shows that the interaction of Claudin1 with CD81 seems to be required for viral entry, although it still remains to be determined whether the virus requires binding to a CD81-Claudin1 complex in order to gain entry. The aims of this project are to confirm whether the interaction with CD81 defines the receptor activity of Claudins, whether this is perturbed by antiviral treatments and to identify the regions of interaction between the two proteins. The aims of this project were achieved using a combination of biochemical and imaging analysis of the Claudin-CD81 interaction.

# Chapter 2:

# Materials and Methods

## 2.1 Cell lines

The cell lines utilised were 293-T, HepG2 and Huh7.5 (provided by Charles Rice Rockefeller University, New York, US). Cell lines were maintained in Dulbecco's modified Eagles Medium (DMEM) supplemented with 10% foetal bovine serum, 1% L-Glutamine and 1% non-essential amino acids.

## 2.2 Claudin and fluorophore plasmids

The various Claudin cDNA were obtained on a pBABEpuro backbone from Hongkui Deng (Peking University, Beijing, China). Plasmid stocks were expanded by incubating 25ng of plasmid DNA with 10µl of silver efficiency competent cells (Bioline, UK) for 45 minutes on ice. The mixture was heat shocked for 45 seconds at 42$^{o}$C before returning to ice for an additional 2 minutes. The contents were spread onto LB Broth 2% Agarose plates (10mls deionised $H_2O$ ($dH_2O$), 0.2g LB Broth base powder (Lennox L Broth Base, Invitrogen, UK), 0.2g Agarose) containing Ampicillin (100µg/ml) and incubated at 37$^{o}$C overnight. Colonies were selected from the plate and cultured in 5ml LB broth shaking at 350rpm at 37$^{o}$C overnight. Plasmid DNA was recovered from the bacterial cultures using a QIAprep Spin Miniprep kit (Qiagen, UK) performed in accordance with the manufacturer's instructions.

## 2.3 Generation of fluorophore tagged Claudin

The region coding the fluorophore from the pAcGFP-c1 or DsRED-monomer-c1 plasmids (Clontech) was excised by incubating the plasmid for 1 hour in the presence of restriction enzymes BamHI and AgeI (2µg Plasmid DNA, 2µl NEB 2 10x Restriction Enzyme Buffer, 0.5 µl (5 units) BamHI, 0.5 µl (5u) AgeI, 14µl $dH_2O$) . The pBABEpuro-Claudin6 was linearised, with the correct overhanging ends to accept the fluorophore insert, using BamHI and NgoMIV restriction enzymes for 1 hour at 37$^{o}$C (2µl Plasmid DNA, 2µl Promega B 10x Restriction Enzyme Buffer, 0.5 µl (5u) BamHI, 0.5 µl (5u) NgoMIV, 14µl $dH_2O$). Plasmid maps showing the positions of the restriction enzyme sites relative to the coding regions can be seen in figure 2.1. The products were loaded onto a 2% Agarose gel in TAE buffer (4.84g/L 2-Amino-2(hydroxymethyl)propane-1,3-diol, 1.09g/L Glacial Acetic Acid, 0.29g/L ethlenediaminetetraactic acid in $dH_2O$, pH8.3, Invitrogen), containing 0.05% Ethidium Bromide(EtBr), and electrophoresis performed at 100 volts for 30 minutes. The gel was photographed using a Bio-Rad GelQuant imaging system and bands measured against a 1Kbp+ DNA ladder (Invitrogen, UK) (figure2.2). Bands of the correct size, 700bp for the liberated fluorophore and 5.9kbp for the linerised pBABEpuro Claudin6, were excised with a scalpel and the DNA recovered using a MinElute Gel Extraction Kit (Qiagen, UK) performed in accordance with the manufacturer's instructions. The Fluorophore insert was ligated into the linerised pBABE-Claudin6 vector by incubating 1.5µl of the vector (100ng), 1µl of the insert (50ng), 1µl (0.5 Units) T4 DNA Ligase, 5µl 2x T4 Ligase reaction buffer (Promega, UK) and 2.5µl $dH_2O$ for 20 minutes at room temperature. 5µl of the mixture was removed and added directly to Gold efficiency competent cells (Bioline, UK) and incubated on ice for 45 minutes.

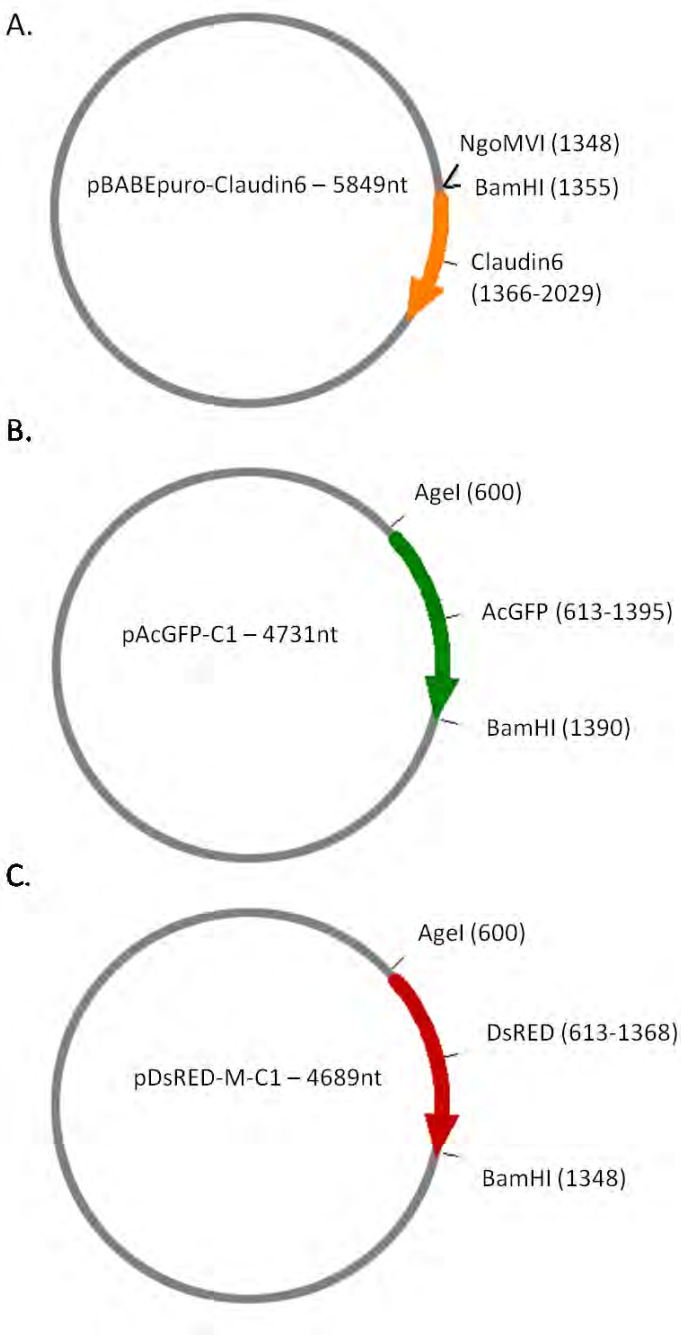


**Figure 2.1: Plasmid maps for pBABEpuro-Claudin6, pAcGFP-C1 and pDsRED-M-C1.** The plasmids maps for A) pBABEpuro-Claudin6, B) pAcGFP-C1 and C) pDsRED-M-C1 with the protein coding regions for Claudin6 (Yellow arrow), AcGFP (green arrow) and DsRED (red arrow) labelled with the positions of the coding region in the plasmid indicated in the brackets. The positions of the restriction enzymes used to digest the various plasmids are also listed with the position noted in the brackets.

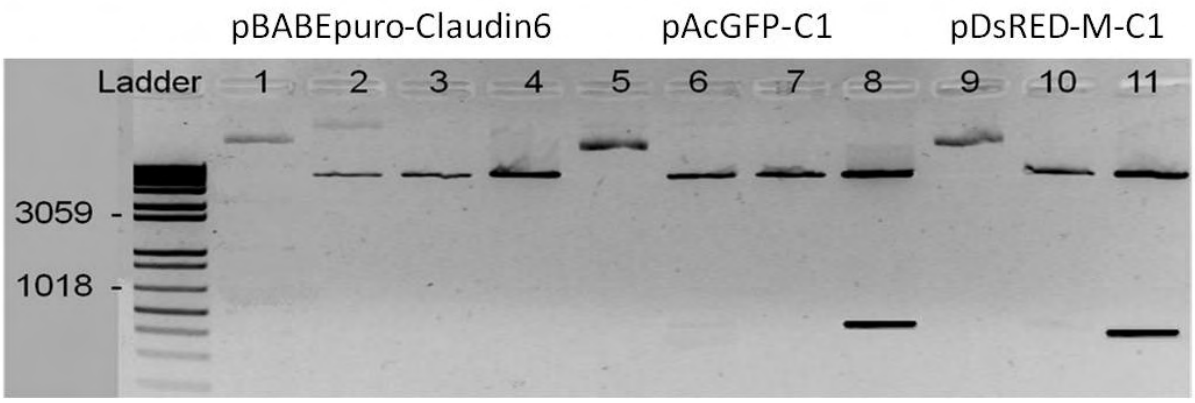


**Figure 2.2: Products of restriction digests on pAcGFP-C1, DsRED-Monomer-C1 and Claudin6.** Lane 4 shows the pBABEpuro-Claudin6 BamHI and NgoMIV double digest, with lanes 1, 2 and 3 showing the undigested, BamHI and NgoMIV digest respectively. Lanes 8 and 11 shows the AgeI and BamHI double digest of pAcGFP-C1 ad DsRED-Monomer-C1, with the insert released present at 790bp for AcGFP and 748bp for DsRED. Lanes 5 and 9 are undigested plasmids, 6 and 10 are AgeI digested plasmids and lane 7 is a BamHI digested Plasmid.

The cells were heated shocked at 42$^{o}$C for 45 seconds and returned to ice for 2 minutes. The cells were plated on LB Broth Agarose plates overnight at 37$^{o}$C. Colonies were then subjected to PCR analysis to identify plasmids containing the correct insert.

The PCR reaction mixture contained 11µl $dH_2O$, 1µl MgCl (25mM, Promega, UK), 3µl 5x GoTaq Buffer (Promega, UK), 0.3µl dNTPs (100nM, Invitrogen, UK), 0.03µl Forward Primer (DsRED+SalI 5'-CTCAGATGTCGACCTCAAGA-3', 10 µM, Invitrogen, UK), 0.03µl Reverse Primer (GGTA6 Claudin6 5'-CGCGCGGCCGTCGACTCAGACGTAATTCTTGGTAG-3', 10 µM, Invitrogen, UK) and 0.15µl Taq Polymerase (5u/µl, Promega, UK). The samples were subjected to the following thermal conditions: denaturing 95$^{o}$C at 5 minutes followed by 30 cycles of denaturing at 94$^{o}$C for 15 seconds, annealing at 50$^{0}$C for 15 seconds and polymerisation at 72$^{o}$C for 1 minute, followed by a 4$^{o}$C hold. The PCR product was loaded onto a 2% Agarose gel in TAE buffer, containing 0.05% EtBr, and electrophoresis performed at 100 volts for 15 minutes and examined under Long-wave Ultra violet light and compared to 1Kbp+ DNA ladder (invitrogen, UK). Clones that were positive by PCR were grown in liquid culture (5ml) (see *Plasmids* section for details) and the purified plasmid further tested using a SalI restriction digest, as plasmids containing the fluorophores will have gained a second SalI restriction site.

Subsequent Claudin clones were produced by performing a BamHI and SpeI double digest on the pBABEpuro AcGFP-Claudin6 or pBABEpuro-DsRED-Claudin6 plasmid to release the promoter and fluorophore encoding region and replacing with the corresponding region from other pBABEpuro-Claudin plasmids. This strategy was chosen as it allowed the largest number of plasmids to be modified, however 3 Claudin constructs (Claudin2, Claudin3 and

Claudin23) have internal NotI sites and could not be cloned in this way. The AcGFP/DsRED-Claudin1 was also transferred into the pTRIP vector using an NdeI/XhoI digest of pBABEpuro-AcGFP/DsRED-Claudin1 and the pTRIP-CD81 short provided by Michele Farquhar (University of Birmingham).

**2.4 Fluorophore tagging of Claudin1 and Claudin 7 mutants, Tetraspanin and Tetraspanin like proteins.**

Plasmid constructs encoding Tetraspanins CD81, CD82 and CD9 were selected to fluorophore label, the proteins were provided by Michel Farquhar (University of Birmingham), Heidi Drummer (Barnet institute, Australia) and Mike Tomlinson (University of Birmingham), respectively. A tetraspanin like protein, which is not localised within Tetraspanin webs, called T-cell differentiation protein (MAL), also referred to as T-lymphocyte maturation-associated protein was obtained from Dr. Mike Tomlinson (University of Birmingham).

The open reading frames were amplified using Phusion™ High-Fidelity DNA Polymerase (New England Biolabs) using the primers listed in table 2.1. The reaction mixture consisted of 32.5µl $dH_2O$, 10µl 5x HF Reaction Buffer, 1µl dNTPs (100nM, Fermentas, UK), 2.5µl Forward and Reverse primers (10 µM, Invitrogen, UK), 0.5µl Phusion polymerase. For each reaction 10ng of plasmid DNA was added to the reaction mixture and the following thermal cycle performed; denaturing at 98$^{o}$C for 2 minutes followed by 25 cycles of denaturing at 98$^{o}$C for 15 seconds, annealing and polymerisation at 72$^{o}$C for 90 seconds. The PCR product was loaded onto a 2% Agarose gel in TAE buffer, containing 0.05% EtBr, and electrophoresis

performed at 100 volts for 15 minutes and examined under Long-wave Ultra violet light and compared to a 1Kbp+ DNA ladder (invitrogen, UK). Bands of the correct size were excised from the gel and purified using a Gel Extraction Kit (Qiagen, UK). The recovered PCR products were ligated into pJET1.2/blunt Cloning Vector (Fermentas, UK) using the following reaction mixture: 10µl 2x Reaction Buffer, 6 µl $dH_2O$, 1 µl Ligase, 1µl pJET1.2/blunt Cloning Vector and 2 µl recovered PCR product. 5µl of the mixture was removed and added directly to Gold efficiency competent cells (Bioline, UK) and incubated on ice for 45 minutes. The cells were heated shocked at 42$^{o}$C for 45 seconds and returned to ice for 2mins.

Colonies produced from the transformation were PCR screened using primers specific to the regions either side of the cloning site of the pJET1.2/blunt cloning vector (Forward Primer 5'-CGACTCACTATAGGGAGAGCGGC-3', Reverse Primer 5' -AAGAACATCGATTTTCCATGGCAG-3'). The PCR reaction mixture contained 11µl $dH_2O$, 1µl MgCl, (25mM, Promega, UK), 3µl 5x GoTaq Buffer (Promega, UK), 0.3µl dNTPs (100nM, Invitrogen, UK), 0.3µl Forward Primer (10 µM, Invitrogen, UK), 0.3µl Reverse Primer (10 µM, Invitrogen) and 0.15µl Taq Polymerase (5u/µl, Promega, UK). The samples were subjected to the following thermal conditions: denaturing at 95$^{o}$C for 5 minutes followed by 30 cycles of denaturing at 94$^{o}$C for 15 seconds, annealing at 50$^{o}$C for 15 seconds and polymerisation at 72$^{o}$C for 1 minute, followed by a 4$^{o}$C hold. The PCR product was loaded onto a 2% Agarose gel in TAE buffer, containing 0.05% EtBr, and electrophoresis performed at 100 volts for 15 minutes and examined under Long-wave Ultra violet light and compared to a 1Kbp+ DNA ladder (invitrogen, UK). Colonies positive for an inserted fragment were cultured overnight and the plasmids purified as previously described. Claudin1 mutants, CD81, CD9 and MAL were digested with BamHI/XhoI and ligated into pBABEpuro- Claudin1 digested with BamHI/SalI. The

fluorophore coding region from a pBABEpuro-AcGFP-DsRED-Claudin1 was inserted using the BamHI and SpeI digest as described previously. CD82 was digested with XhoI and ligated into pBABE-AcGFP/DsRED-Claudin1 digested with SalI. The Claudin7 mutants were digested with a BamHI/HindIII and ligated into pBABE-AcGFP/DsRED-Claudin1 digested with BamHI/HindIII. The fragments were ligated as previously described and the colonies produced by transforming Gold Efficiency competent cells were screened using the GoTaq screening protocol using the forward primer DsRED+SalI (5'-CTCAGATGTCGACCTCAAGA-3') and the Reverse primer for the specific protein. Positive colonies were cultured overnight and purified plasmids sequenced to ensure the correct coding region is present in the clone.

**Table 2.1: Tetraspanin and tetraspanin like protein PCR primers**

| | |
|---|---|
| *Forward Primer:* | |
| CD81 | TCTAGAGGATCCGCCACCATGGGAGTGGAGGGCTGCAC |
| CD82 | GAGCGCTCGAGGGAATTCTGCAGATC |
| CD9 | GATCAGGGATCCACCATGCC |
| MAL | GAGATCTGCCGTCATGGCCCCCGCAGC |
| Claudin1 | GGATCCGCCACCATGGCCAACGCGGGGCTG |
| Claudin7 | GGATCCGCCACCATGGCCAATTCGGGCCTGCA |
| *Reverse Primer:* | |
| CD81 | TAGAAGGCACAGTCGAGG |
| CD82 | TAGAAGGCACAGTCGAGG |
| CD9 | TTCTAGGTGTCGACATTCCTAGACCATC |
| MAL | GCTCTCGAGGGCTTATGAAGACTTCCATC |
| Claudin1 | CTCGAGTCACACGTAGTCTTTCCCGCTGG |
| Claudin7 | AAGCTTTCACACATACTCCTTGGAAGAGTTGG |

Primers noted in a 5’ to 3’ direction

## 2.5 Stable cell lines

A 6 well plate, pre-treated with poly-l-lysine, was seeded with 293-T Phoenix cells at a density of $7x10^5$ cells per well in 3% serum in DMEM (without antibiotics). After 24hrs the cells were transfected, using lipofectamine2000 protocol, with 4ug of plasmid DNA. The supernatant was harvested at 48 and 72hrs post transfection. The supernatant from the phoenix cells was clarified by centrifuging at 1500rpm for 3mins. The clarified supernatant was passed through a 0.22µm filter. The supernantent was diluted 1:2 in 3% DMEM supplemented with 8µg/ml Polybrene and 10mM HEPES and incubated at room temperature for 30mins. The mixture was applied to 293-T cells and the cells centrifuged at 2500rpm for 1hr at $37^0$C. The cells were then incubated for 48hrs. The cells were treated with 10µg/ml Puromycin (Sigma, UK) to select for the transduced cells.

## 2.6 HCV pseudoparticle production genesis and infection

To generate the pseudoparticles, 293-T cells were seeded in a 6 well plate, pre-treated with Poly-L-Lysine (Sigma) for 5 minutes, at a cell density of $7x10^5$ cells per well in 3% antibiotic free DMEM. When the cells are ~60% confluent, the cells were co-transfected with a plasmid encoding the Gag-pol gene of HIV, the luciferase reporter gene, (NL4.3R$^-$E-Luc) and a plasmid encoding either HCV strain H77 E1E2 envelope glycoprotein, an empty vector control (Env$^-$pp) or Murine Leukemia Virus (MLV) envelope protein. The transfection was performed by incubating 6µl Fugene (Roche) in 100µl Optimem for five minutes. This was added to 10µl solution containing 800ng of NL4.3R$^-$E-Luc and 800ng envelope protein

plasmid and incubated at room temperature for 20 minutes. The DNA/Fugene mix was applied to cells and incubated for 6 hours, after which the media was replace with fresh 3% FBS, antibiotic free, DMEM. 48 hours post transfection the media was removed and clarified at 1500 rpm for 5 minutes in a centrifuge and passed through a .45µm filter. The media was stored at 4$^{o}$C prior to use in the pseudoparticle entry assay for up to 1 week.

Transfected 293-T or Huh-7.5 cells were seeded into a 96 well plate at a concentration of 1.7x10$^{4}$ cells per well, 100µl of media per well. When the cells were ~60% confluent either 100µl of H77pp, Env$^{-}$pp, media or MLVpp, 2µl of MLV stock diluted in 98µl of media, was applied to three wells (i.e. triplicate infections). Unless otherwise stated the virus was not removed from the cells. After the 72 hour incubation the media was replaced with 40µl Cell Lysis buffer (12.5 ml 1M Tris$PO_4$ solution pH7.8, 5ml CDTA, 50ml Glycerol, 5ml Triton-X-100, 1ml 1M DTT, adjusted to 500ml with $dH_2O$) and incubated at 4$^{o}$C for 1 hour. The luciferase activity of the lysate was assessed using the Luciferase Assay System Kit (E1501, Promega, Madison, USA) by adding 40µl of lysate to 35µl of Luciferase Assay Substrate (reconstituted in the Lucifase Assay Buffer) and measuring light output with a luminometer (Berthold 960). The neutralisation assay was performed in the same way, with the exception of pre-treating the cells prior to the addition of the pseudoparticles for 1hr with the concentration of the specified antibody. Data is presented as specific infectivity.

## 2.7 HCVpp entry after cholesterol depletion

293-T cells were seeded as previously described (2.6 HCV Pseudo Particle Entry and Neutralisation Assay) with the infection carried out as before. Cells were treated with a cyclic oligosaccharide that depletes cholesterol from the plasma membrane (methyl-β-cyclodextrin, MβCD) (219). Cells were treated for 1 hour prior to addition of H77pp, Env-pp or MLVpp. For the restoration of cholesterol the cells were treated for 1hr with 10mM MβCD, which depletes the cholesterol and cholesterol replenished by incubating with 10mM MβCD–1mM cholesterol complexes. The effects of the treatment(s) on the level of cholesterol was determined by measuring the total cholesterol after the various treatments using an Amplex Red assay kit according to the manufacturer's instructions (Invitrogen),

## 2.8 Fluorescence intensity profiling and FRET analysis

Transfected 293-T cells were grown on 22mm diameter borosilicate glass coverslips and imaged using a Zeiss MetaHead confocal system. The samples were photobleached at 561nm to prevent the energy transfer from the AcGFP fluorophore to DsRED fluorophore with images being taken before and after the photobleach. Using the profile function from the LSM software, the fluorescence intensities of the two fluorophores, before photobleaching, from several hundred pixels around the plasma membrane were determined and used to generate a scatter plot. The stoichiometry of the labelled proteins was inferred by fitting a linear regression to the data, with the correlation coefficient, $R^2$, describing how close the data fits to the linear regression. The gradient of this linear

regression determines the stoichiometry of the labelled proteins as shown previously and is termed a FIR plot (220-221).

The occurrence of FRET within the pixels from the FIR plot was determined using the gradual acceptor photobleaching methodology (222). FRET was determined by measuring the fluorescence intensity of the donor fluorophore over a gradual photobleaching of the acceptor fluorophore. The fluorescence intensity of the AcGFP fluorophore (the donor fluorophore) before photobleaching was subtracted from the fluoroecence intensity after photobleaching on a pixel by pixel basis, with FRET being indicated by a positive value. The proportion of plasma membrane where FRET occurs gives a measure of interaction, recorded as the percentage FRET (%FRET) between the two fluorophores. Further details of experimental procedures, such as fluorophore cross-talk corrections are detailed in (184).

**2.9 Surface plasmon resonance.**

The interaction of recombinant forms of Claudin1 with CD81 and the Anti-CD81 monoclonal antibodies with the large extracellular loops of CD81 were assessed using the Biacore 3000 system (Biacore AB). MBP-CD81 EC2 (Drummer 2002) was immobilised to a CM5 chip using the standard amine coupling method (Biacore, GE Healthcare). To limit the possibility of steric hindrance caused by oversaturation of the biacore chip the protein coupling was limited to 1000 response units. To control for nonspecific protein interactions all recombinant proteins were flowed over an “empty” (activated 1M ethanolamine blocked) channel and any response unit(s) observed subtracted from test channels. All interactions were performed in HBS-EP buffer (Biacore, GE Healthcare) at 25°C at a flow rate of

5µl/minute. In addition to the MBP-CD81 purified proteins we also obtained the EC1 of Claudin1 and Claudin7 fused to MBP (MBP-Claudin1 and 7) from the Drummer lab.

The interaction of MBP-CD81, MBP-Claudin1 and MBP-Claudin7 was performed by injecting the proteins at a concentration of 750µg/ml for 10mins and measuring the dissociation time over 20mins. The affinity of MBP-Claudin1 interaction with the immobilised MBP-CD81 was determined by flowing the MBP-Claudin1 over the chip surface for 10mins and measuring the dissociation time for 20mins at three concentrations (125, 250 and 500µg/ml). The affinity was calculated using the 1:1 drifting baseline model provided by the BIAevaluation software (Biacore) (102, 153, 204).

To determine the affinity of the anti-CD81 monoclonals the antibodies were injected for 1hr and dissociation recorded over 50 minutes. Each antibody was titrated in doubling dilutions starting at 0.5mM with the lowest concentration of 0.0036mM being injected first. The affinity antibody was determined by plotting the maximal level of binding for each concentration on an X,Y scatter plot and fitting a non-linear regression. The linear regression produced values for the theoretical binding capacity (Bmax, Response Units (RU)) and affinity (KD, µM).

To determine if MBP-CD81 and MBP-Claudin1 could still interact with the immobilised MBP-CD81 in the presence of anti-CD81 antibodies a competition assay was performed. The antibody was injected at a concentration of 500µM followed immediately by MBP, MBP-CD81 or MBP-Claudin1 at a concentration of 750µg/ml. The level of specific binding of the MBP-CD81 or MBP-Clauidn1 was determined by subtracting the change in response unit for the MBP protein form the change in response unit for the fusion proteins, if the value is positive then specific binding is occurring. A commercial anti-MBP was used for a positive

control of protein binding, this antibody should bind to the MBP moiety immobilized on the chip surface without interfering with the binding region of the CD81. In order to determine a value of affinity (KD) the response unit reached after one hour of injection, binding late, for each concentration was plotted and a non-linear regression fitted to the plots from which the KD is determined.

**2.10 Mammalian two hybrid system**

This technique allows for the accurate measurement of protein-protein interactions and is derived from familiar yeast 2-hybrid designs, optimised for use in mammalian systems. The system uses three plasmids, the first of which is the pG5luc plasmid, a reporter plasmid containing a GAL4 binding domain can be induced to express Firefly Luciferase via the transcriptional activation domain of herpes virus VP16 protein. Secondly the pBind vector which encodes the GAL4 fused protein which will associate to the GAL4 binding domain on the pG5luc. The third plasmid is the pACT vector, which expresses a second protein fused to a transcriptional activation domain of VP16. An interaction between the two fusion proteins fused to the GAL4 and VP16 domains will induce of the expression of Firefly Luciferase. The measurement of luciferase therefore gives a measure of protein interactions.

To measure the interaction of the various wild type and mutant CD81, Claudin1 and Claudin7 proteins the coding region of these proteins were cloned into the pBind and pACT plasmids. The parental proteins were cloned into both pBind and pACT vectors with the mutant proteins being cloned only into the pACT vector. The ORFs were amplified using Phusion™ High-Fidelity DNA Polymerase (New England Biolabs) using primers listed in table

2.2 using the same procedure as previously described (2.4 Fluorophore Tagging of Claudin1 and Claudin 7 mutants, Tetraspanin and Tetraspanin like proteins). The coding regions for the various proteins were digested with AsiSI/PmfI and ligated into pBind and pACT digested with the same enzymes. Colonies were screened and sequenced using the primers listed in table 2.2 using the protocol described previously (section 2.4).

The assay was performed to the manufacturers instructions with some small alterations. Briefly, 293-T cells were seeded in a 24 well plate pre-coated with poly-l-lysine at a density of $1x10^5$ cells/ml. 24hrs after seeding the cells were transfected with 1µg of the pG5luc, pBind and pACT plasmids using the lipofectamine2000 method. 48hrs post transfection the cells were lysed and tested for the presence of Firefly and Renilla luciferase activity using the Dual-Luciferase Reporter Assay System (Promega). Briefly the cells were incubated for 30mins, followed by one freeze thaw cycle, in 100ul of the passive lysis substrate provided. The cell lysates were then transferred to a single well of a 96well luminometer plate and loaded in to the luminometer (Bertholt 960) to measure the two different luciferase activities. Firstly 15ul of the Luciferase Assay Buffer II, which measures the firefly luciferase activity, was injected into each well and the light output measured for 2secs, then The Stop & Glo® Buffer, which measures the renilla luciferase activity, was injected and light output again measured for 2secs. Each different protein combination was tested in triplicate with all firefly luciferase levels corrected using the level of renilla activity.

**Table 2.2: Mammalian two hybrid system PCR primers**

| | |
|---|---|
| *Forward Primer:* | |
| *CD81* | gcgatcgccATGGGAGTGGAGGGCTGCA |
| *Claudin1* | gcgatcgccATGGCCAACGCGGGGCT |
| *Claudin7* | gcgatcgccATGGCCAATTCGGGCCTGCA |
| | |
| *Reverse Primer:* | |
| *CD81* | gtttaaactcaGTACACGGAGCTGTTCCGGATG |
| *Claudin1* | gtttaaacTCACACGTAGTCTTTCCCGCTGG |
| *Claudin7* | gtttaaacTCACACATACTCCTTGGAAGAGTTG |

Primers noted in a 5’ to 3’ direction, lower case indicates cloning “tags”

**2.11 Site directed mutagenesis of CD81.**

In order to produce the CD81 mutants the "Phusion polymerase and into pJET1.2/blunt Cloning Vector method" was used as previously described (2.4 Fluorophore Tagging of Claudin1 and Claudin 7 mutants, Tetraspanin and Tetraspanin like proteins). A schematic representation of the mutagenesis procedure is shown in figure 2.3. Firstly using the CD81 BamHI and the CD81 mutant reverse primers, listed in table 2.3, PCR fragments were created with a BamHI on the 5' end, site specific mutation and a SacI site on the 3' end of the CD81K201 fragment or a SalI site for the remaining mutants. A second CD81 fragment was created using the CD81 155-166 and CD81 184-207 forward primers with the CD81 XhoI reverse primer, these fragments encoded a BamHI separated by a small polylinker to a SalI site in the CD81 155-166 fragment and a SacI site in the CD81 184-207 fragment at the 5' end. The two different fragments were digested with BamHI and ScaI digest of the CD81 184-207 and K201A Fragments with the remaining fragments digested with BamHI and SalI. These digested fragments were then ligated to produce full length CD81 ORFs containing the desired mutation. The mutants were then transferred into a pTRIP-AcGFP/DsRED-Claudin1 plasmid using a BamHI/XhoI digest to replace the Claudin1 with the CD81 mutants. The correct introduction of the CD81 was confirmed by sequencing using the CD81 BamHI and XhoI primers.

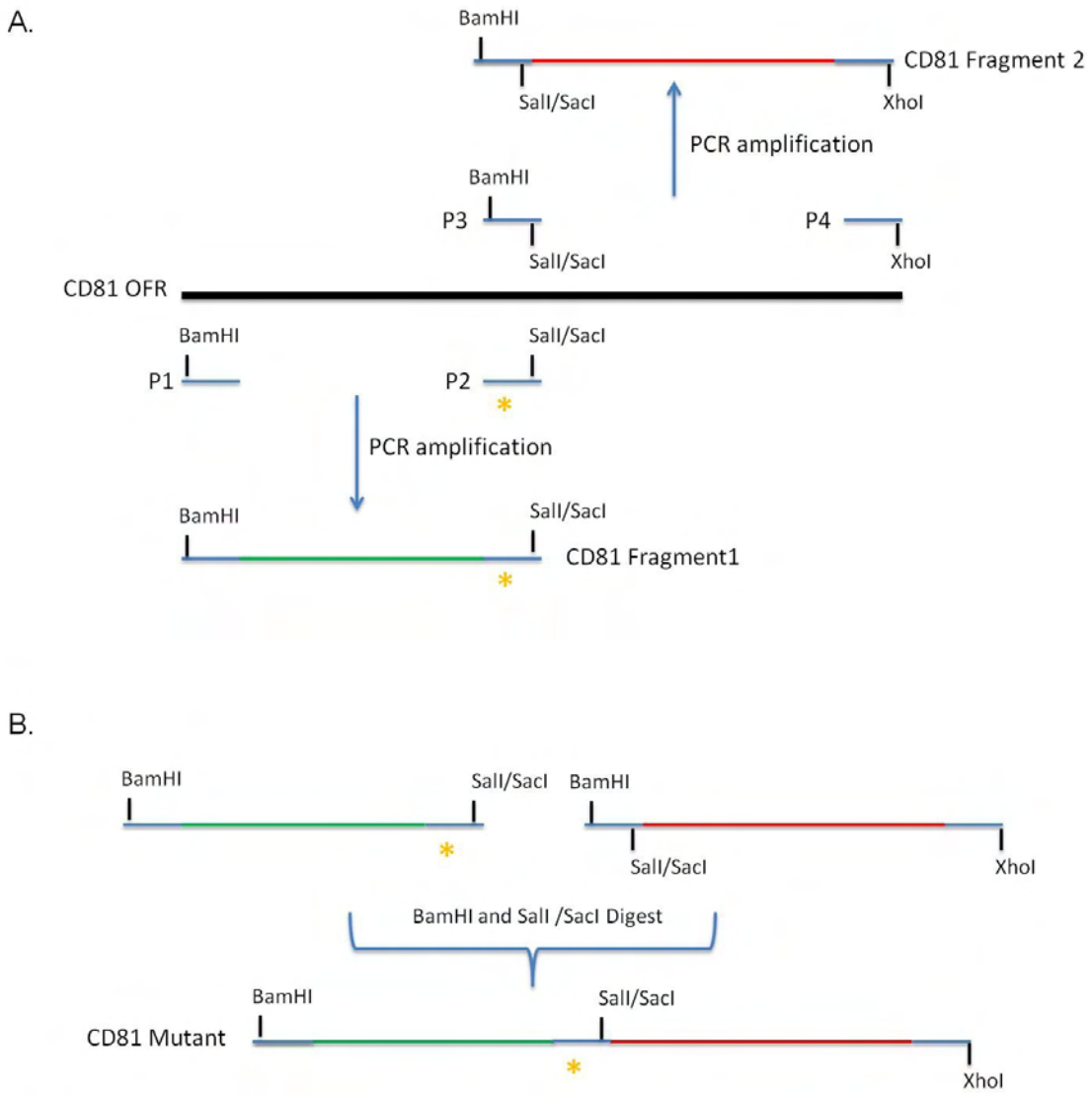


**Figure 2.3: Site directed mutagenesis of CD81.** A) Two fragments of CD81 were amplified using the Phusion polymerase. Fragement1 was amplified using the CD81 BamHI forward primer (P1) and CD81 mutant reverse primer (P2), which introduce a BamHI site to the 5' end with the specific mutation (yellow asterisk) and SalI or SacI site at the 3' end of the fragment. The fragment 2 is amplified using the CD81 155-166 or 184-207 forward primer (P3) and the CD81 XhoI reverse primer (P4) which introduces a BamHI and SalI or SacI site at the 5' end and a XhoI site at the 3' end of the fragment. B) A BamHI/SalI (SacI) digest is performed on the two Fragments, which are then ligated to produce a full length CD81 ORF containing a 5' BamHI site, the specific mutation and a 3' XhoI site.

**Table 2.3 Site directed mutagenesis PCR primers**

*Forward Primers:*

| | |
|---|---|
| CD81 BamHI | TCTAGAGGATCCGCCACCATGGGAGTGGAGGGCTGCAC |
| CD81 184-207 | ggatccCCTCTTCTCCGGAGCTCTGTACCTCATCGGCAT |
| CD81 155-166 | ggatccTGCTGTGGCTCgtcgACACTGACTGCTTTGAC |

*Reverse Primers:*

| | |
|---|---|
| CD81 XhoI | TTTCTAGGTctcgagTCAGTACACGGAGCTGTTCCGG |
| CD81 K148A | TCAGTGTcgacGAGCCACAGCAGTCAAGCGTCTCGTGGAAGGTCgcCACCAC |
| CD81 T149A | TCAGTGTcgacGAGCCACAGCAGTCAAGCGTCTCGTGGAAGGcCTTCACCAC |
| CD81 K148A/T149A | TCAGTGTcgacGAGCCACAGCAGTCAAGCGTCTCGTGGAAGGcCgcCACCAC |
| CD81 E152A | CAGTGTcgacGAGCCACAGCAGTCAAGCGTCgCGTGGAA |
| CD81 T153A | CAGTGTcgacGAGCCACAGCAGTCAAGCGcCTCGTGGAA |
| CD81 E152A/T153A | CAGTGTcgacGAGCCACAGCAGTCAAGCGcCgCGTGGAA |
| CD81 K201A | TGCCGATGAGGTACAgagctcCGGAGAAGAGG |

Primers noted in a 5’ to 3’ direction, lower case indicates cloning “tags”

### 2.12 Protein expression in mammalian cells by pTRIP gene delivery system

The pTRIP expression system allows the transduction of proteins within cells of interest and was developed by Zennou et al. 293-T cells are seeded onto a 6 well plate, pre-coated with poly-l-lysine, at a density of $6x10^5$ cells/well. 600ng of the pTRIP plasmid containing the target gene was transfected into 293-T cells along with 600ng of a plasmid encoded a replication deficient HIV gag-pol core and 400ng of a plasmid encoding the G envelope glycoprotein of vesicular stomatitis virus using fugene (Roche). 48hrs post transfection the media was removed from the cells and passed through a 0.25µm filter. The media was then applied to the target cells diluted 1:2 in fresh cell culture media.

### 2.13 sE2 binding quantification

To determine the effect of mutations within CD81 on E2 binding, wild type and various CD81 mutants were expressed in CHO cells using the pTRIP expression system. The cells were incubated in a 96 U bottomed well plate at a cell density of $2x10^5$ cells per well in 100ul of PBS containing 0.5%BSA and 0.01% sodium azide (Sigma) at room temperature for 20 mins. The sodium azide treatment ensures the minimal movement of proteins to and from the cell surface by inhibiting cell metabolism. The cells were incubated with 100µl of sE2 diluted 1:4 in the above buffer and incubated for 45mins at $37^oC$. The cells were washed and incubated with 5ug/ml of the mAb 10/76b, which recognises the HIV gp120 epitope tag (STSIRGKVQ) on the sE2, for 45mins at $37^oC$. Finally the cells are washed incubated in a 1:1000 dilution of an alexafluor 633 ant-Rat IgG for 45mins at $37^oC$. The cells are then washed and fixed with

4%paraformaldehyde for 10mins before detecting the level of E2 binding detected by flow cytometry.

**2.14 Statistics**

All tests were calculated using the Prism 4 package (GraphPad Software, CA). The majority of the statistical tests performed were non-parametric as these would allow test levels of significance without assuming a particular distribution for the data. The relevant tests are noted in the figure legends with the level of significance.

# Chapter 3:

# FIR and FRET methodologies to study CD81 and Claudin1 interaction

The entry of HCV into cells is a multi-step process culminating in a pH and Clathrin dependent internalisation (223-224). It has been demonstrated that the virus can directly interact, via the viral envelope glycoproteins, with CD81 (88, 91, 93, 105-106) and SR-BI (107-109). In contrast there is limited evidence showing a direct interaction with Claudin1 or Occludin, suggesting that their role in the entry process is downstream of the initial attachment of the virus to the cell surface. As described earlier, CVB entry has been suggested as a possible model of how HCV could enter the cell. CVB enters polarized Caco-2 cells via interactions with DAF, CAR and Occludin (208-209). The engagement of DAF leads to a relocalisation of the virus-DAF complex to the tight junction. There it interacts with CAR, which induces a conformational change in the virus that primes particle internalization via a caveola-dependent manner (208-209). CVB internalisation is dependent on Occludin, as siRNA specific knockdown of Occludin trapped virus particles at the tight junction. Occludin internalises with the virus, despite not directly interacting with the virus, leaving CAR at the plasma membrane. The role of Occludin seems to be in the recruitment of Caveolin-1 and other regulator molecules to the tight junction to promote virus internalisation (209). To date there is limited evidence to suggest or disprove CD81 or SR-BI acting in an analogous way to DA. Furthermore it is unknown whether Claudin1 is behaving in the same fashion as CAR, causing conformational changes to HCV after it is delivered to the tight junction. There is growing evidence that, in addition to interacting with the virus, CD81 interacts with Claudin1. The initial evidence of this interaction was reported by Kovalenko et al. who showed that Claudin1 co-precipitated with CD81 and other tetraspanin proteins after chemically cross-linking surface proteins (125). Subsequently other groups have shown this interaction using a Biomolecular fluorescence complementation BiFC assay (112, 183) and by FRET anlysis (184). These results suggest that, whatever the exact role of Claudin1 in the

entry process, an interaction with CD81 may be required. We therefore wanted to evaluate the role of the CD81-Claudin1 complex in HCV entry and define how the proteins interact using an imaging based approach previously developed within our group (184, 211) .

The imagining technique used is FRET, which can determine dynamic interactions between molecules. Conventional confocal fluorescence microscopy to study protein co-localisation is limited to a resolution of 232nm, which is too large a distance to determine whether a direct molecular interaction is occurring. FRET only occurs between two labelled proteins that are within 10nm of each other, thus enhancing the resolution to a workable value. Fluorophores absorb light energy at a particular wavelength, leading to their excitation, which is subsequently re-emitted at a longer wavelength. This absorbance (or excitation) and emission occurs over a range of wavelengths, referred to as spectra. When the emission and absorbance spectra of the two different fluorophores overlap, energy can be directly transferred between them by non-radiative energy transfer, this effect is illustrated by a Jablonski diagram (figure 3.1a). The fluorophore transferring its energy is referred to as the donor and the receiver is termed the acceptor. This loss of energy results in an apparent loss of overall fluorescence of the donor, referred to as donor quenching (figure 3.1d) (225).

Many methods of determining FRET have been developed, including two-colour ratio imaging or sensitised emission (226), spectral imaging (227-228), Fluorescence Lifetime Imaging Microscopy (FLIM) (229-231) and Polarised Anisotropy imaging (232). Each method has its advantages and disadvantages, ranging from natural excitation of the acceptor fluorophores being mistaken for FRET, to a general decrease in sensitivity due to a high background (the techniques are reviewed in (233)). We adopted an acceptor

photobleaching method, which utilises the targeted bleaching of the acceptor to block energy transfer from the donor (figure 3.1e). Preventing this energy transfer leads to an increase in the intensity of the donors fluorescence when FRET occurs. Recently developed tuneable lasers settings allow the gradual photobleaching of the acceptor, which make it possible to correct for the natural signal decay of the fluorophores.

There are several fluorophore pairs available for determining protein-protein interactions, we chose the AcGFP-C1 and DsRED-monomer-C1 fluors developed by Clontech. The original GFP and DsRED fluors required oligomerisation to yield high levels of fluorescence intensity. However, AcGFP-C1 and DsRED-monomer-C1 are mutant derivatives of GFP and DsRED, respectively, which have high level fluorescence as protein monomers (229). Using monomeric fluorophores means that single fluorophores can act as FRET pairs and enable us to measure and ensure an equimolar ratio which is required to infer FRET is occurring. We previously selected regions of protein co-localisation to determine whether FRET occurs (184, 211). However this approach may introduce some bias due to the selection of membrane regions with high 'local' concentrations of the proteins under study.

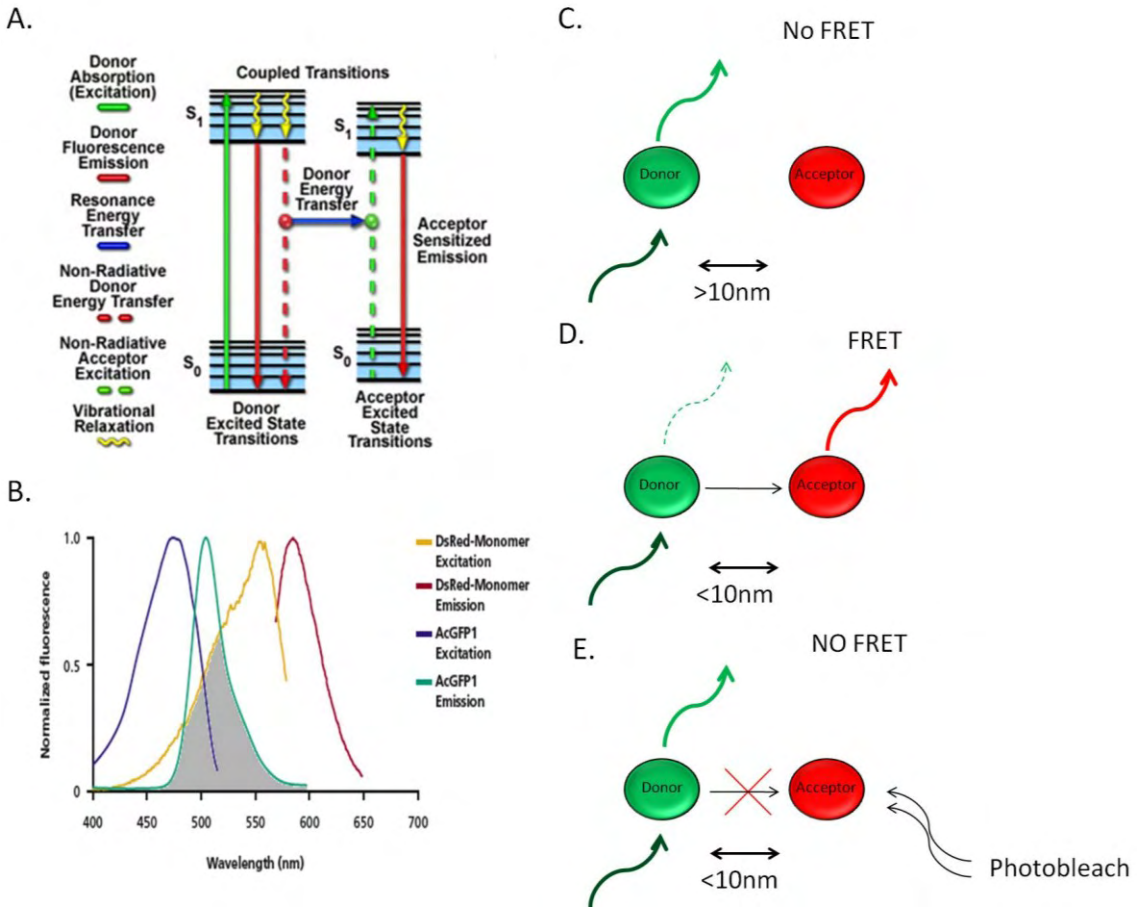


**Figure 3.1: Principles of FRET.** A) Shows a Jabolonski diagram of resonance energy transfer. The usual absorbance (Excitation) and Emission of energy by the donor are shown by solid green and red lines respectively. The blue line indicates the transfer of energy from the donor to the acceptor by resonance energy transfer (image taken from www.microscopy.fsu.edu). B) Shows the spectral overlap (grey area) between the emission spectrum of AcGFP (Green line) and excitation spectrum of DsRED (Yellow line), taken from www.clontech.com. The cartoons C-E depict the effect of distance on the interaction between two fluorophores, AcGFP (green circles) and DsRED (red circles). C) No FRET occurs between the two fluorophores due to the distance being above 10nm. D) FRET occurs when the fluorophores are close enough for energy transfer. Emission occurs from both fluorophores, with the AcGFP showing a reduced emission due to the loss of energy. E) Prevention of energy transfer by photobleaching of the DsRED fluorophore results in the AcGFP fluorophore emitting all of its energy as green fluorescence. Modified from (Rudolf, Mongillo et al. 2003).

To complement the FRET methodology we employed a technique known as Fluorescence Intensity Ratio (FIR) analysis that has previously been used to determine the subunit composition of the Cyclic nucleotide-gated (CNG) channels of olfactory neurons (220-221) and the epithelial $Na^+$ channel (ENaC) (220-221). Zheng and Zagotta used this method to show that the three subunits of the CNG assemble into a defined heteromeric structure (221). Staruschenko et al demonstrated that subunit assembly and stoichiometry are essential for normal physiological function of ENaC (220). In addition they found that heterotypic channel formation is favoured over homotypic channel formation when subunits are co-expressed. The FIR approach relies on labelling the desired proteins with different monomeric fluorophores, where the intensity of each fluorophore is directly related to protein concentration. An example of how the FIR works is shown in Figure 3.2a. The figure shows a confocal image of cells expressing AcGFP and DsRED labelled proteins; in this case DsRED-CD81 and AcGFP-CD81 protein. A profile line is drawn around the plasma membrane, indicated by the red line in figure 3.2b, which allows us to measure the intensity of the two fluorophores pixel-by-pixel along the membrane. These intensities are plotted on an X,Y scatter plot (figure 3.2c) and linear regression analysis performed (figure 3.2d). The gradient of the line defines the ratio the two proteins, or their stoichiometry, and is referred to as the FIR value. Along with the FIR value the regression analysis assesses how well the gradient fits the data through the correlation coefficient, noted as $R^2$.

If the $R^2$ value is too low the inferred FIR value produced is unreliable. We therefore do not assign a FIR value to data sets with an $R^2$ value which is less than the lowest value $R^2$ produced by a positive control. This method provides an accurate assessment of protein expression at the plasma membrane and shows whether the proteins are in a 1:1 ratio that

is required to interpret any FRET signals. Furthermore, profiling protein expression at the entire plasma membrane allows us to assess FRET across a wide range of protein expression levels, not only at areas of high protein expression. Distances between the two fluorophores can be determined by measuring the efficiency of energy transfer between the donor and acceptor fluorophores. But due to the large area we are measuring and the level of background “noise” within the assay we did not attempt to quantify the efficiency of energy transfer or to interpolate the spatial separation distance. We employed the method to determine whether FRET occurs or does not.

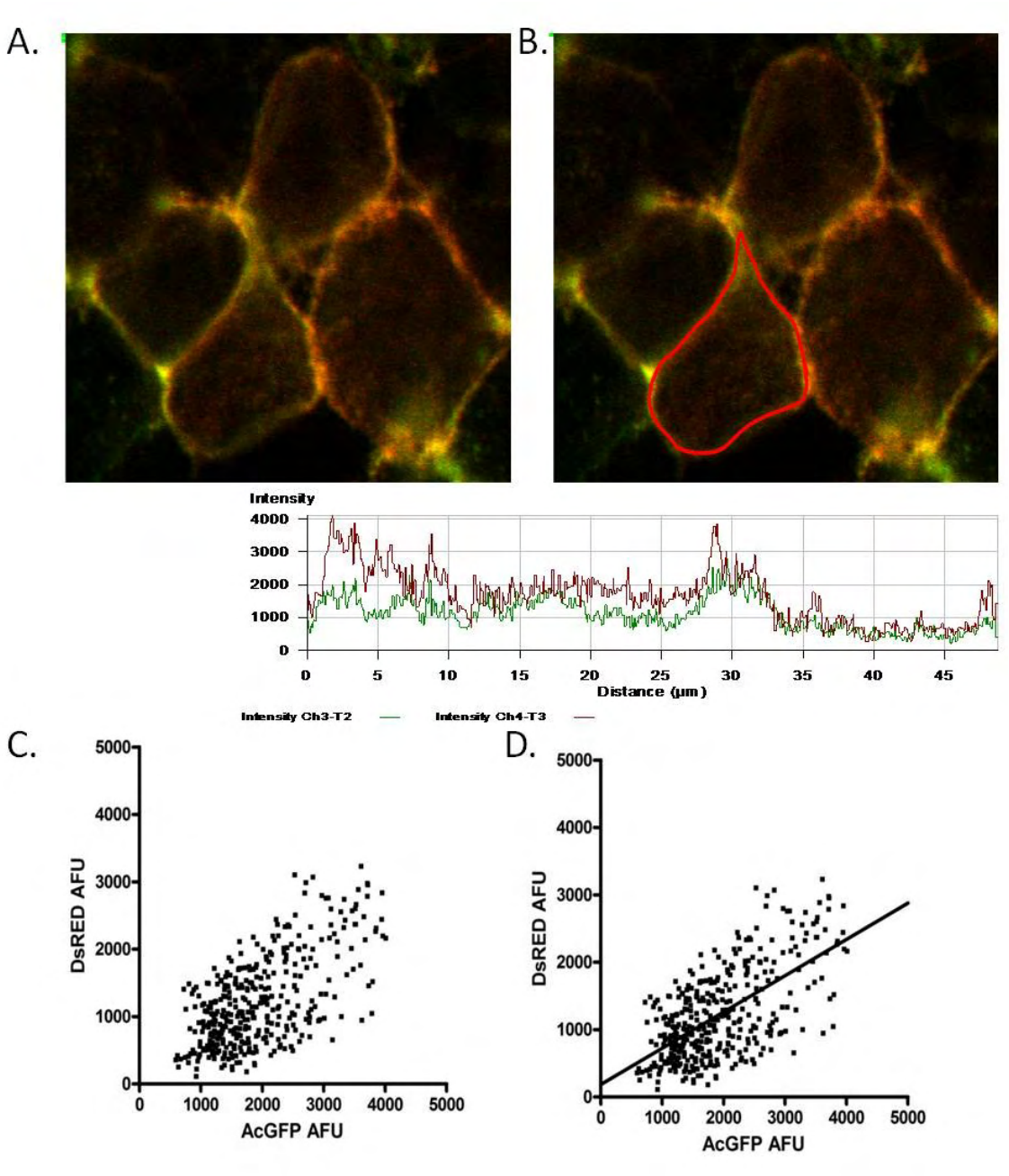


**Figure 3.2: FIR analysis method**. A) Images produced are laser scanning confocal images taken using the 63 x 1.2NA water immersion objectives and a meta head confocal microscope (Zeiss). B) The plasma membrane of the cell is traced using the profile function provided by the microscope software. The fluorescence intensities of the fluorophores are given on a pixel by pixel basis along the profile line. C) The fluorescence intensities of the two fluorophores are plotted on a scatter plot and D) a linear regression line is fitted to the data. The gradient of the linear regression line and the correlation of the data to the fitted line are recorded as the FIR value and $R^2$ value, respectively.

### 3.1 Use of FIR and FRET methodologies to study CD81 dimerisation.

To assess the suitability of FIR and FRET methodologies to study CD81 interaction with the various members of the Claudin family, we first looked at CD81 homodimerization. It is widely accepted that the CD81 EC2 forms dimers both when crystallized (Kitadokoro et al 2002) or when purified as a soluble protein (Drummer et al 2005). We therefore co-expressed CD81 labelled with AcGFP or DsRED in 293-T cells and performed FIR and FRET analysis on plasma membrane expressed CD81 (figure 3.3).

The images in figure 3.3 show the localisation of AcGFP-CD81 (figure 3.3a), DsRED-CD81 (figure 3.3b) and a merged image (figure 3.3c) showing their co-localisation at the plasma membrane. One of these cells (figure 3.3d) was used to produce the scatter plot and regression analysis performed to determine FIR (figure 3.3e). The Scatter plot has an $R^2$ value of 0.68 with a FIR value of 0.57. Since the DsRED fluorophore has intensity 60% of the AcGFP fluorophore with the camera system used we would expect to observe FIR values of 0.6 for proteins with a 1:1 stoichiometry. The observed FIR value for the CD81-CD81 association is therefore in agreement with 1:1 ratio expected for a CD81-CD81 homodimer. After photobleaching of this cell, those pixels where an increase in the donor signal was detected were re-analyzed (figure 3.3f). The scatter plot demonstrates that FRET can be detected across a wide range of protein expression, with 63.8% of pixels positive for FRET. The $R^2$ value and FIR values were 0.66 and 0.56, respectively, very similar to those of the entire data set (in figure 3.3e). The decrease in AcGFP fluorescence due to the FRET also appears across the entire range of protein expression, demonstrating the that data are not being biased due to variable expression levels.

In order to reduce the statistical errors in the experiment we chose to analyse at least 10 cells. Analysis of a further nine cells (figure 3.3G-I) gave an average $R^2$ of 0.49 (IQR 0.39 to 0.6) and a FIR value was 0.56 (Inter quartile range, IQR, 0.47 to 0.65). The proportion of pixels where FRET occurred (%FRET) was 64% (IQR 60%-69%), similar to the 69% FRET previously reported for CD81-CD81 interaction using acceptor photobleaching of selected regions of protein co-localisation (184). Overall these results demonstrate that the FIR methodology can quantify the ratio of proteins expressed at the plasma membrane and CD81-CD81 homotypic interactions can be measured by FRET.

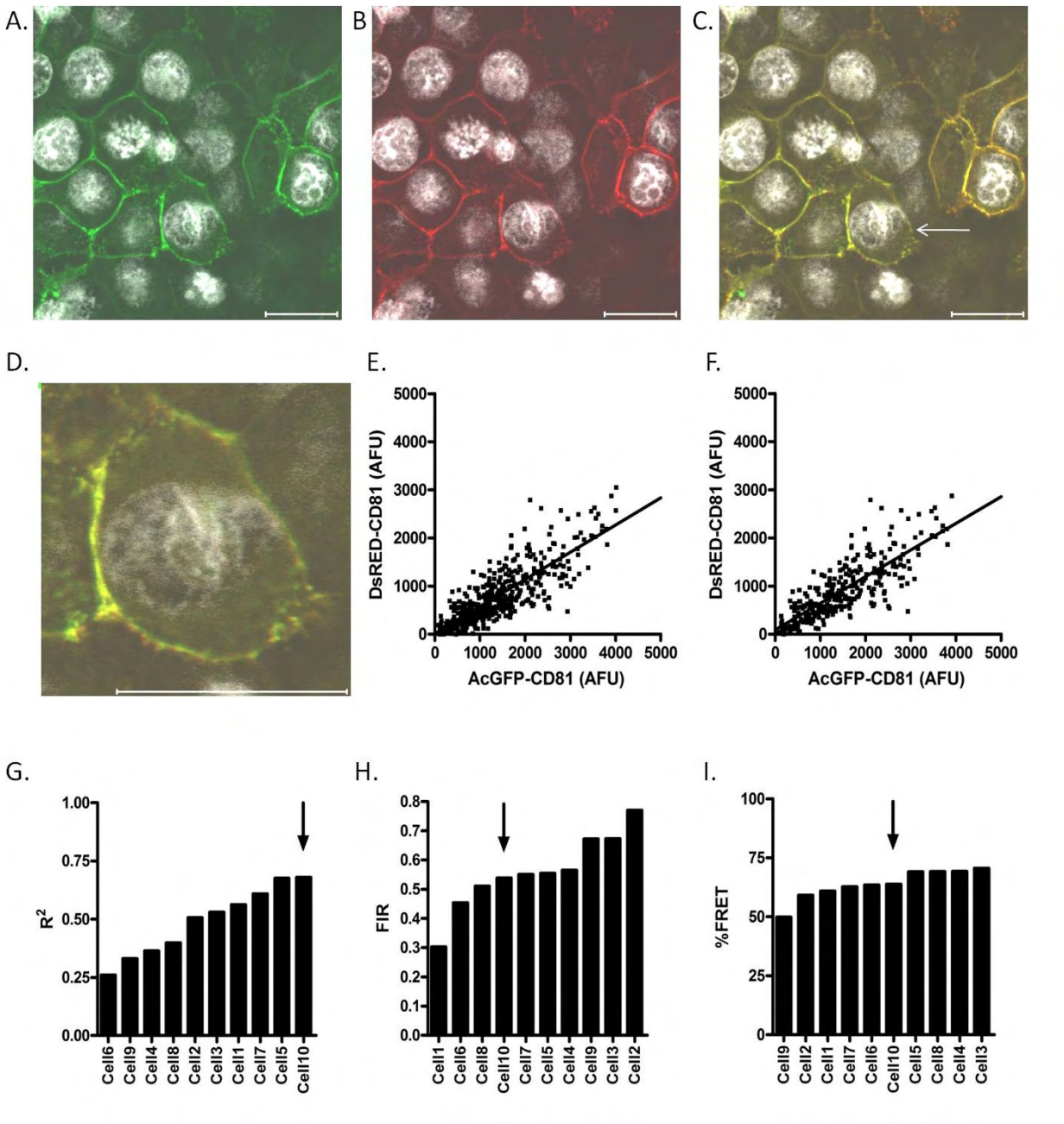


**Figure 3.3: Fluorescent Intensity Ratio in CD81 homotypic Interaction(s).** 293-T cells were co-transfected to express both AcGFP-CD81 and DsRED-CD81 to determine the FIR and FRET values for homodimer interaction. The figure shows images of A) AcGFP-CD81, B) DsRED-CD81 and C) a merged image. D) shows the cell (indicated with an arrow in C.), which produced E) the FIR plot with all the pixels represented and F) the FIR plot of only those pixels where FRET was detected. Summary graphs are shown for G) The correlation coefficient, $R^2$ , H) FIR values and I) %FRET values of 10 cells. The arrows present on plots G-H show the $R^2$, FIR values and %FRET of the cell shown in D.

### 3.2 Receptor activity of labelled Claudin proteins

Prior to studying Claudin1-CD81 association with FIR and FRET methodologies we first determined whether the fluoresecent tag affected the antigenicity or receptor activity of Claudin1. Firstly, we expressed unlabelled Claudin1, AcGFP-Claudin1 or DsRED-Claudin1 in 293-T cells, which do not express endogenous Claudin (110-111, 113), and stained the cells with a conformation-dependent anti-Claudin1 rat monoclonal antibody (MAB4618, R&D Systems). This antibody recognises the extracellular loop and, since the cells are stained live, only proteins expressed at the plasma membrane are labelled. Antibody staining and protein localisation is shown in figure 3.4. The images show that the staining pattern of both fluorophore labelled Claudin1 proteins was identical to the unlabelled protein. Finally, AcGFP-Claudin1 and DsRED-Claudin1 were equally well recognised by the antibody, leading us to conclude that the fluorophores fused to the N-terminus of Claudin1 had little or no affect on protein antigenicity or localisation.

Both fluorophore tagged fusion proteins were tested for their ability to support viral HCVpp infection (figure 3.5). Parental 293-T lack Claudin1 expression and failed to support HCVpp infection. Expression of tagged or non-tagged Claudin1 in 293-T cells supported similar levels of HCVpp entry. The overall level of entry in Claudin1 expressing 293T cells was lower than Huh7.5 cells infected with the same virus stock, this could be partially ascribed to the fact that the transfection efficiency was 30%, 35% and 37% for 293-T Claudin1, 293-T AcGFP-Claudin1 and 293-T DsRED-Claudin1 cells, respectively. All the cell types showed an equal level of MLVpp infection, ranging from 4.8 to 5.6 $x10^6$ RLU.

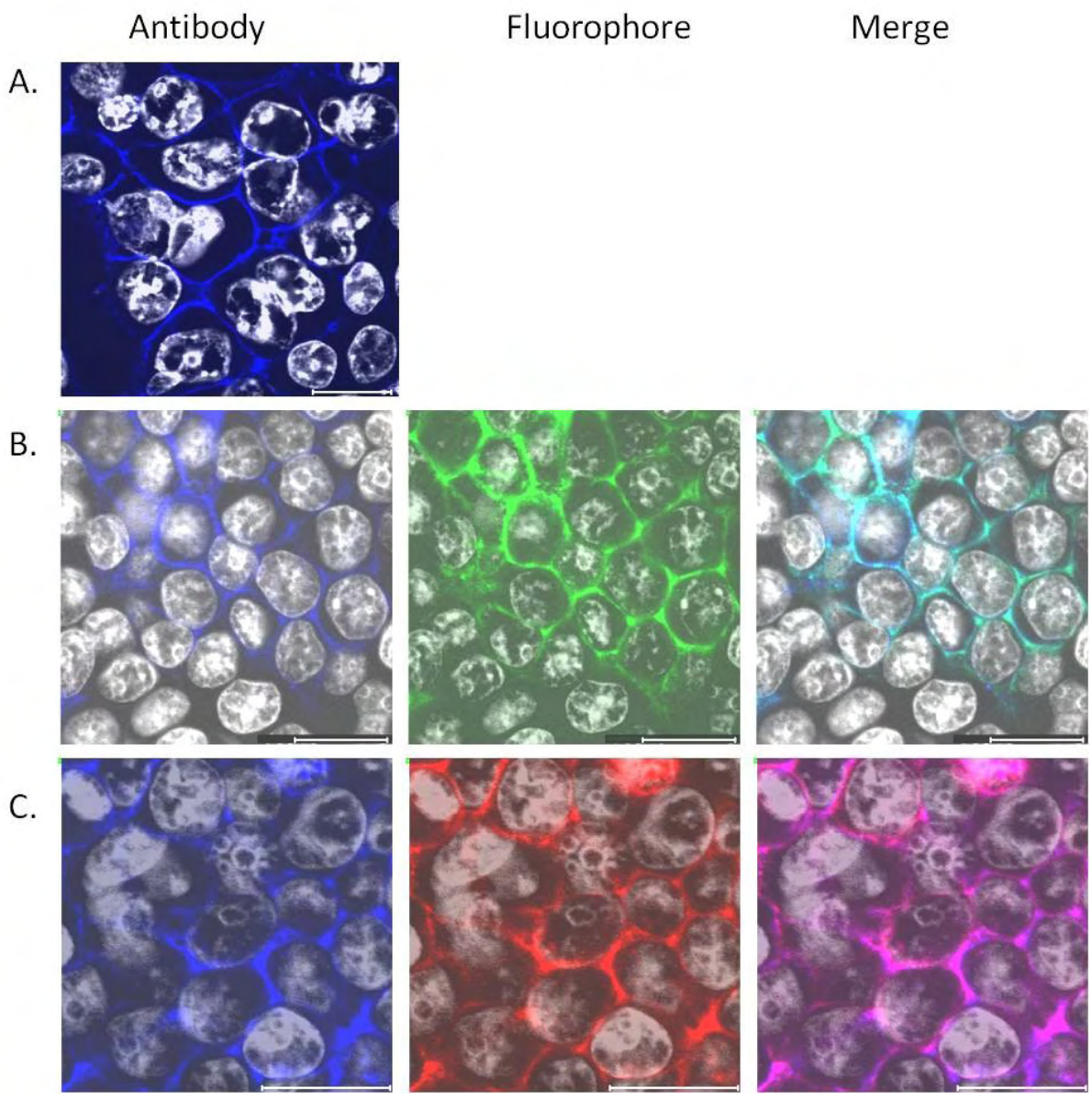


**Figure 3.4: Antigenicity of fluorophore tagged Claudin1**. 293-T cells were transfected to express Claudin1, DsRED-Claudin1 or AcGFP-Claudin1 (A, B and C respectively). The cells were stained with an anti-Claudin1 monoclonal antibody (R&D Systems), which recognises the extracellular loop of Claudin1 and a secondary Goat Alexa Fluor 633 anti anti Rat IgG (H+L) (Invitrogen). Cells were imaged using a 63 x 1.2NA water immersion objective and a meta head confocal microscope (Zeiss), Size bars are 20µm.

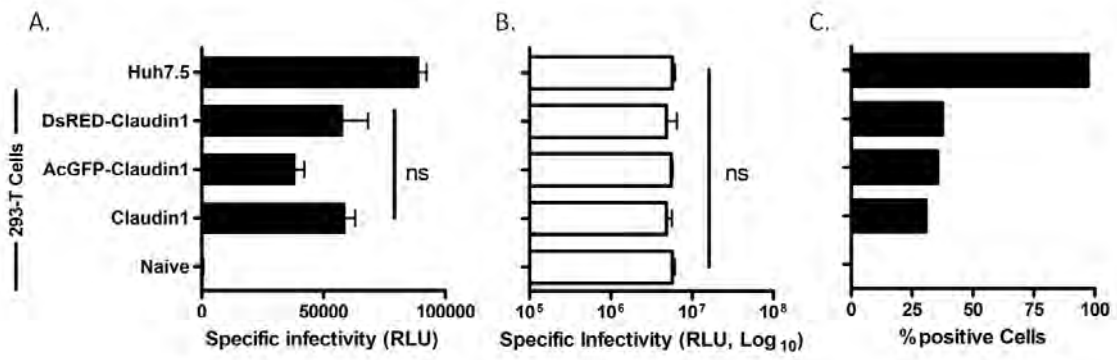


**Figure 3.5: Effect of N-terminal tagging Claudin1 on HCV receptor activity**. 293-T cells were transfected to express native or tagged versions of Claudin1 and evaluated for their ability to support HCVpp and MLVpp entry. Data is shown as specific infectivity (Relative Light Units, RLU) and represents the mean plus the standard error of three replicates. RLU signals were corrected for signal noise by subtracting the Env-RLU level. A) specific infectivity of HCVpp, B) specific infectivity of MLV and C) percentage of the cells expressing Claudin1 as determined by flow cytometry. A one way Analysis of Variance with Bonferroni's Multiple Comparison Test was used to assess the differences between the cells (ns = No Significant difference). This data is representative of three independent experiments

### 3.3 Heterotypic interaction of Claudin1 and CD81

Since fluorophore labelling had little effect on antigenicity or viral receptor activity of Claudin1 we chose to use these chimaeric molecules to study the interaction of AcGFP-Claudin1 or DsRED-Claudin1 with CD81 (figure 3.6). As before, 10 cells were analysed and the median values used to interpret FIR and FRET values. With DsRED-CD81, the AcGFP-CLDN1 showed an $R^2$ of 0.67 (Inter quartile range (IQR 0.6 – 0.72) and a FIR value of 0.64 (IQR 0.55 – 0.78). With AcGFP CD81 the DsRED-Claudin1 showed an $R^2$ of 0.68 (IQR 0.58 – 0.76) and a FIR value of 0.75 (IQR 0.67 – 0.9). These values are not significantly different from each other or from the CD81-CD81 values, of 0.62 (IQR 0.5 – 0.75) and 0.79 (0.59 – 0.97) for $R^2$ and FIR value respectively. From this we can conclude that Claudin1 is associating with CD81 with a 1:1 stoichiometry. The percentage FRET was also determined for each group, we found 36% ± 6.6%, 40% ± 15.9% and 40% ± 6.2% of pixels were positive for FRET for the AcGFP-CLDN1/DsRED-CD81, DsRED-Claudin1/AcGFP-CD81 and AcGFP-CD81/DsRED-CD81 pairs, respectively. Overall these data demonstrate that Claudin1 interacts with CD81 in a 1:1 stoichiometry at a similar level to the CD81 homotypic interaction. There was no significant difference between the values produced when the Claudin1 was labelled AcGFP or DsRED. The DsRED-Claudin1 did produce some intracellular staining in a subset of cells which may account for the higher level of variability in the %FRET value. The AcGFP-Claudin1 showed a more homologous staining pattern to that of the unlabelled Claudin1 and therefore this construct was used in the subsequent experiments.

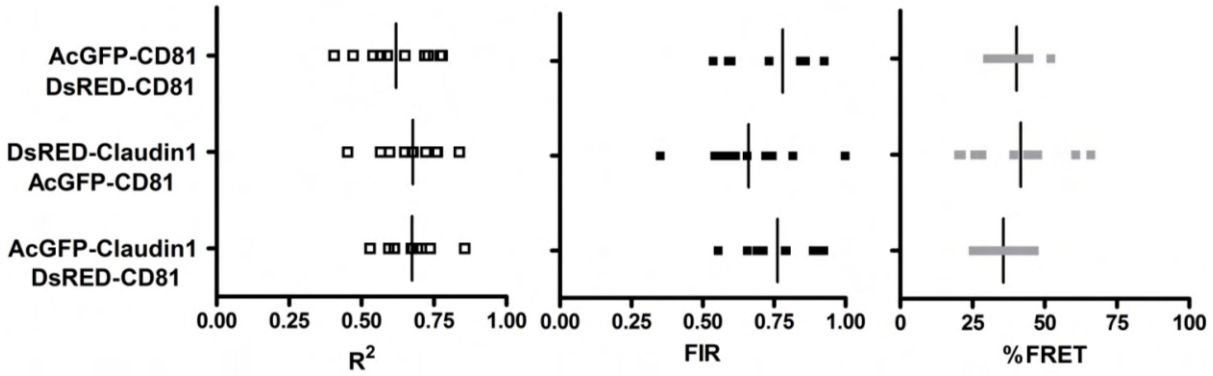


**Figure 3.6: FIR and FRET analysis of the Claudin1-CD81 heterotypic interaction.** 293-T cells were transfected to co-express AcGFP-Claudin1/DsRED-CD81, DsRED-Claudin1/AcGFP-CD81 or AcGFP-CD81/DsRED-CD81. The $R^2$, FIR and FRET were determined for 10 cells are shown in the dot plots. The median value is denoted by the solid line on each plot. This data is representative of two independent experiments

### 3.4 Association of Claudin1 with other tetraspanin proteins.

Heterotypic interactions have been demonstrated between CD81, CD9 and CD151 (125). These authors also showed that Claudin1 co-precipitated with these tetraspanin proteins. Given these observations we sought to determine whether Claudin1 interacts with other members of the tetraspanin family of proteins with a similar stoichiometry to CD81. We generated AcGFP fusion proteins of CD82, CD9 and tetraspanin like protein Myelin And Lymphocyte protein (MAL) to assess their interaction with Claudin1. MAL, also known as T-cell differentiation protein, has been shown to co-purify with glycosphingolipids in detergent insoluble domains but does not associate with tetraspanin proteins ((234), and Mike Tomlinson, personal communication) and provides an ideal control protein for FRET studies.

Transfection of 293-T cells to express AcGFP labelled CD82, CD9 and MAL demonstrated protein localisation at the plasma membrane (Figure 3.7a). We first assessed the interaction of the 3 tetraspanins and Claudin1 with MAL. The MAL-CD81 transfections showed an $R^2$ of 0.47 (IQR 0.16 -0.67), a FIR value of 0.9 (IQR 0.0 -1.42) and a %FRET of 9.6% ± 10.4. MAL-CD82 had an $R^2$ of 0.59 (IQR 0.47 - 0.66), a FIR value of 0.6 (IQR 0.38 - 0.72) and a %FRET of 9.3% ± 7.2. Finally, we found that MAL-CD9 had an $R^2$ of 0.52 (IQR 0.38 - 0.61), a FIR value of 0.91 (IQR0.37 - 1.24) and a %FRET of 13.8% ± 9.8. Since MAL has been reported not to interact with members of the tetraspanin family of proteins, these levels of %FRET can be considered non-specific interactions. In addition to assessing MAL association with tetraspanins, we measured MAL-Claudin1 interactions showed an $R^2$ of 0.32 (IQR 0.23 - 0.46), a FIR value of 0.31 (IQR 0.0 - 0.5) and a %FRET of 7.3% ± 8.6, again indicating non-specific interaction.

Next we determined the homotypic and heterotypic interactions between various tetraspanins. In this set of experiments the CD81-CD81 interaction showed an $R^2$ of 0.52 (IQR 0.35 - 0.64), a FIR value of 0.55 (IQR 0.48 - 0.67) and a %FRET of 63.8% ± 6.3. The CD82-CD82 and CD9-CD9 homotypic interactions were similar to the CD81-CD81 interaction (CD82-CD82 had an $R^2$ of 0.65 (IQR 0.57- 0.77), a FIR value of 0.8 (IQR 0.75 - 1.1) and a %FRET of 40.9% ± 7.4; CD9-CD9 had an $R^2$ of 0.55 (IQR 0.47 - 0.68), a FIR value of 0.45 (IQR 0.4 - 0.52) with a %FRET of 59.8% ± 9.2). The heterotypic interactions between tetraspanins were also similar to the CD81-CD81 interaction: the CD81-CD82 interaction had an $R^2$ of 0.74 (IQR0.64 - 0.77), a FIR value of 0.75 (IQR 0.63 - 0.92) and a %FRET of 39.4% ± 6.2; CD81-CD9 interaction resulted in an $R^2$ of 0.65 (IQR 0.55 - 0.73), a FIR value of 0.83 (IQR 0.6- 0.95) and a %FRET of 73.7% ± 14; finally CD82-CD9 association had an $R^2$ of 0.68 (IQR 0.58 - 0.82), a FIR value of 0.8 (IQR 0.75 - 1.07) and a %FRET of 31.1% ± 7.7.

In summary these interactions confirm the association of tetraspanins at the cell surface and provide a series of positive results against which to assess other datasets. The interactions of Claudin1 with CD81 or CD9 were not significantly different from the CD81-CD81 positive control: in these experiments Claudin1-CD81 had an $R^2$ of 0.66 (IQR 0.64 - 0.71), a FIR value of 0.64 (IQR 0.55 - 0.78) and a %FRET of 69.7% ± 7.7; whereas Claudin1-CD9 showed an $R^2$ 0.55 of (IQR 0.46 - 0.71), a FIR value of 0.92 (IQR 0.67 - 1.04) with a %FRET of 43.4% ± 20.1. Finally profiling Claudin1-CD82 cells gave an $R^2$ 0.56 of (IQR 0.45 - 0.67) and a FIR value of 1 (IQR 0.74 - 1.21), which was not significantly different to the CD81-CD81 FIR value. For these cells the %FRET between the fluorophores was significantly lower than for the other proteins studied (33.9% ± 12), however this value is still considerably higher than the FRET values observed for the non-specific interactions between tetraspanins and MAL (9 - 14%).

These results show that Claudin1 can associate with all of the tetraspanin proteins tested. It is unknown whether this is due to a direct association of Claudin1 with each protein or whether Claudin1 is anchored by CD81 into a larger Tetraspanin complex, bringing Claudin1 into close proximity with the tetraspanins but without any direct protein interactions. Our observation that the MAL protein showed low, non-specific, levels of interaction with Claudin1 allowed us to conclude that these results were specific and not an artefact of over expression of these fluorescent proteins at the plasma membrane.

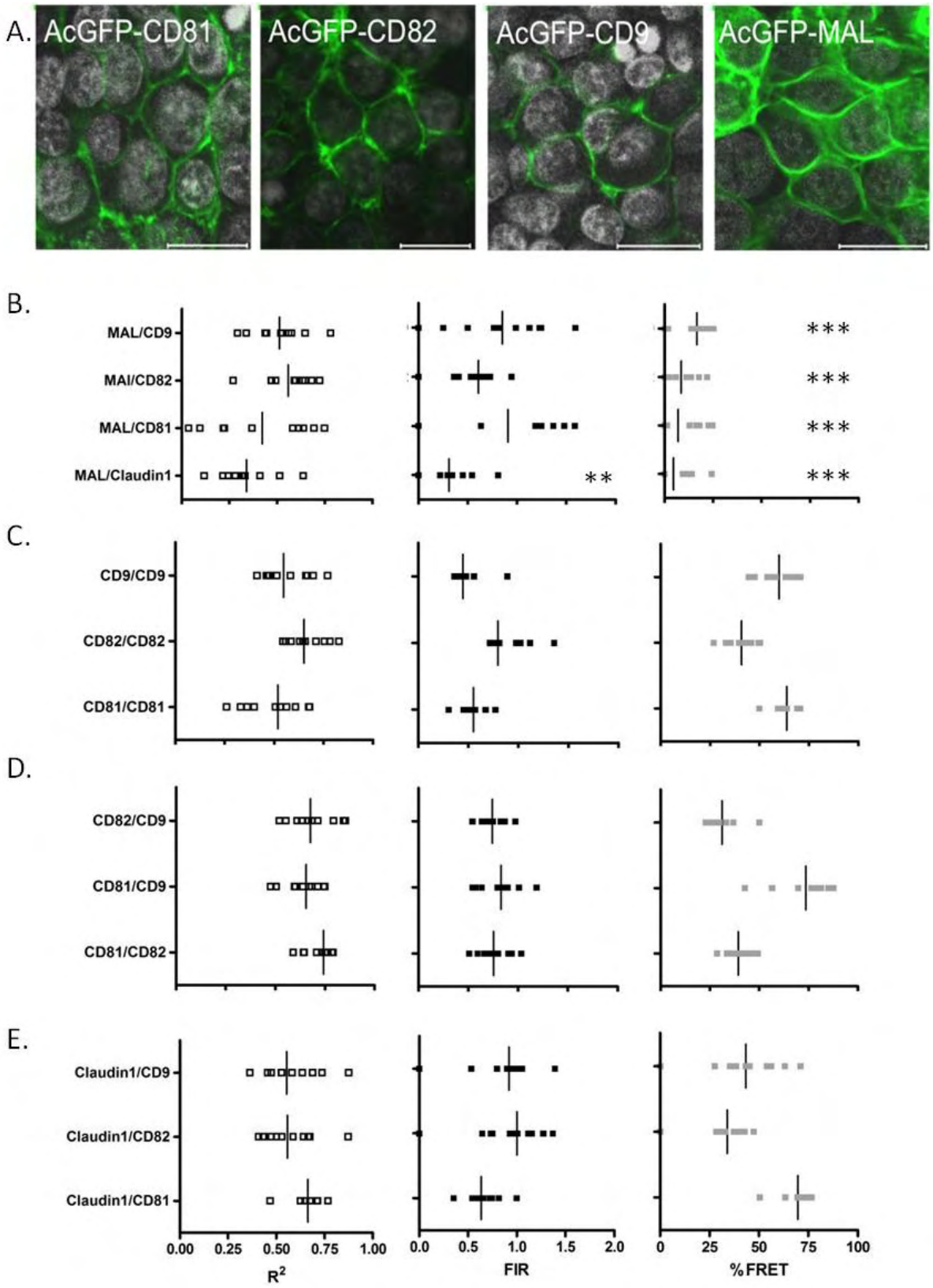
A.
AcGFP-CD81
AcGFP-CD82
AcGFP-CD9
AcGFP-MAL
B.
MAL/CD9
MAl/CD82
MAL/CD81
MAL/Claudin1
**
***
***
***
***
C.
CD9/CD9
CD82/CD82
CD81/CD81
D.
CD82/CD9
CD81/CD9
CD81/CD82
E.
Claudin1/CD9
Claudin1/CD82
Claudin1/CD81
0.00 0.25 0.50 0.75 1.00
R2
0.0 0.5 1.0 1.5 2.0
FIR
0 25 50 75 100
%FRET

**Figure 3.7: Interaction of Claudin1 with tetraspanins CD9, CD81 and CD82 and tetraspanin-like protein MAL**. A) AcGFP labelled CD81, CD82, CD9 and MAL were expressed in 293-T cells and their localisation assessed. Cells were imaged by laser scanning confocal microscopy using a 63 x 1.2NA water immersion objectives and a meta head confocal microscope (Zeiss), size bars are equal to 20µm. The proteins were co-expressed with DsRED labelled partners in various combinations to determine their interaction with one another and with Claudin1 or MAL. The mean correlation coefficient ($R^2$), fluorescent intensity ratio (FIR) and percentage FRET for ten cells is presented for B) MAL-protein Interactions C) Homotypic tetraspanin interactions, C) Heterotypic Tetraspanin Interactions and E) CLDN1-Tetraspanin interactions. One way Analysis of Variance and Bonferroni's Multiple Comparison Tests were used to determine the degree of significance (**p <0.01, ***p<0.001. This data is representative of two independent experiments.

### 3.5 Effects of CD9 over expression on Claudin1-CD81 association

Our laboratory reported that over expressing unlabelled Claudin1 in 293-T cells significantly reduced AcGFP-Claudin1/DsRED-CD81 FRET (184). Although 293-T cells are Claudin1 negative they do express endogenous CD81, which will result in a similar lowering of the %FRET value and potential underestimation of overall protein interaction(s). Since we found CD9 to have a similar FRET association with Claudin1 as CD81 (43.4% ± 20.1, figure 3.7) we sought to determine whether over expressing unlabelled CD9 could alter CD81-Claudin1 association and HCVpp infection. 293-T cells stably expressing AcGFP-Claudin1 and DsRED-CD81 were transduced to over express CD9 using the pTRIP lentiviral system. The cells were assessed for CD9 expression using an anti-CD9 antibody (SYB-1, Abcam, figure 3.8c), which showed a clear increase in the level of CD9 expression by flow cytometry.

Both naive and TRIP-CD9 cells were assessed for CD81/Claudin1 FIR and FRET analyses and HCVpp infection (Figure 3.8). Parental cells showed an $R^2$ of 0.51 (IQR 0.43 – 0.66) with a FIR value of 0.6 (IQR 0.48 – 0.92), whilst the pTRIP-CD9 cells had an $R^2$ of 0.73 (IQR 0.57 – 0.82) with a FIR value of 0.73 (IQR 0.63 – 0.83). The %FRET observed was 40.6% ± 12.8 and 40.3% ± 8.3 for the naive and pTRIP-CD9 cells respectively. These values are not significantly different and show that CD9 does not compete with CD81 for its interaction with Claudin1. Similarly, over expression of CD9 had no significant effect on HCVpp infection of 293-T cells expressing AcGFP-Claudin1. The level of entry was shown to be 44,853 ± 6,468 and 47,763 ± 1,583 RLU for the naive and CD9 over expressing cells, respectively.

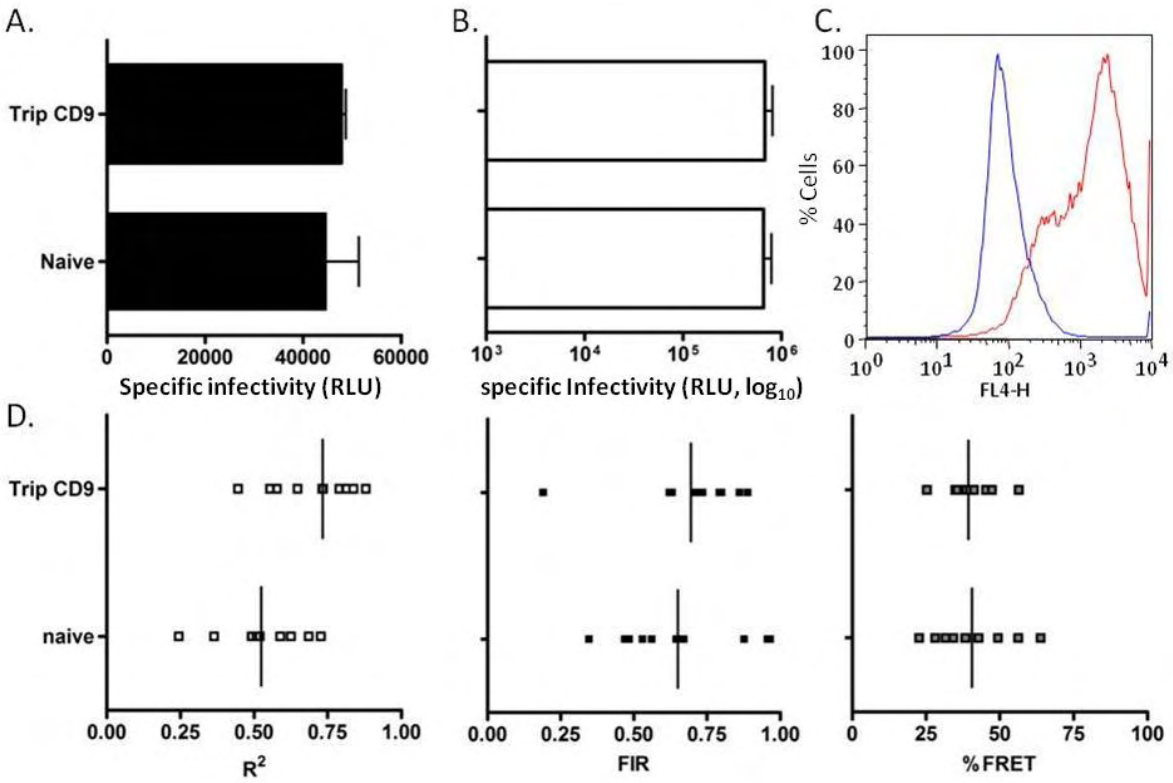


**Figure 3.8: Effects of CD9 over-expression on Claudin1-CD81 association and HCVpp infection.** AcGFP-Claudin1/DsRED-CD81 293-T cells were transduced to over express CD9 and compared to parental cells for their ability to support HCVpp and MLVpp entry. Data is shown as specific infectivity (Relative Light Units, RLU) and represents the mean plus the standard error of three replicates. A) specific infectivity of HCVpp. B) specific infectivity of MLVpp. C) levels of CD9 expression in parental cells (blue line) and cells over expressing CD9 (red line) as determined by FACS analysis. D) $R^2$, FIR and FRET values for the 2 cell lines are shown as dot plots for 10 cells. The median value is denoted by the solid line. This data is representative of two independent experiments.

### 3.6 Localisation and Receptor activity of fluorophore labelled Claudins.

To determine whether Claudin receptor activity is defined by its association with CD81, a panel of Claudin molecules representing classical (Claudin4, 7, 15 and 17) and non-classical (Claudin11 and 12) members of the Claudin superfamily were tagged with AcGFP to assess their association with CD81. As for Claudin1, it was important to ensure that the fluorophore labelling of these proteins did not perturb their localisation or receptor activity. Due to the lack of antibodies to the various Claudin proteins, localisation without a fluorophore label was assessed using a Flag epitope expressed at the C-terminus of the various unlabelled Claudins (constructs used were the kind gift of Hongkui Deng). All proteins were expressed in the Claudin negative 293-T cell line and were stained with an anti-FLAG antibody (Sigma). The staining patterns of the Claudin-FLAG clones are shown in figure 3.9. Claudin1, 4, 6, 12 and 17 localised at the plasma membrane, whilst Claudin15 showed an intracellular staining pattern. The remaining Claudin proteins, Claudin7, 9 and 11 were detected at both the plasma membrane and intracellular locations. The localisation of the fluorophore labelled Claudin proteins are shown in figure 3.10. Comparing their staining patterns to that of the Claudin-FLAG proteins shows that N-terminal tagging of the proteins with a flouorophore had little or no effect on their localisation. The fluorophore tagged fusion proteins were tested for their receptor activity using the HCVpp assay (figure 3.10). As expected the AcGFP-Claudin1 fusion protein showed receptor activity, as did Claudin6 and 9. The remaining Claudin proteins showed no receptor activity, in agreement with published reports (110, 113).

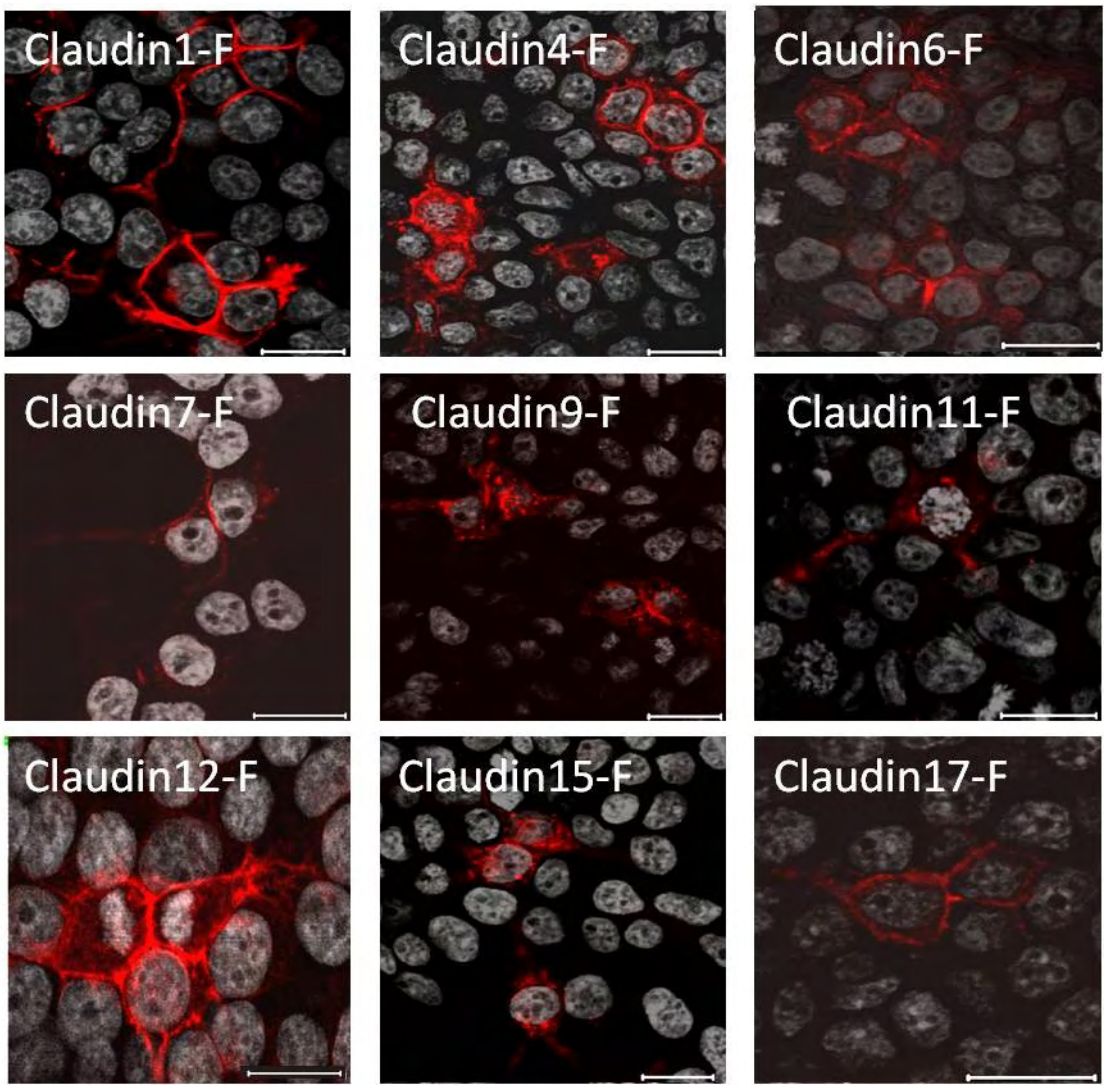


**Figure 3.9: Localisation FLAG-tagged Claudin proteins**. 293-T cells were transfected with various members of the Claudin family, which contained a FLAG epitope fused to their c-terminus. The cells were labelled with an anti-FLAG monoclonal and secondary labelled Alexa Fluor 633 anti IgG (H+L). Cells were imaged by laser scanning confocal microscopy using a 63 x 1.2NA water immersion objective and a meta head confocal microscope (Zeiss), Scale bars are equal to 20µm.

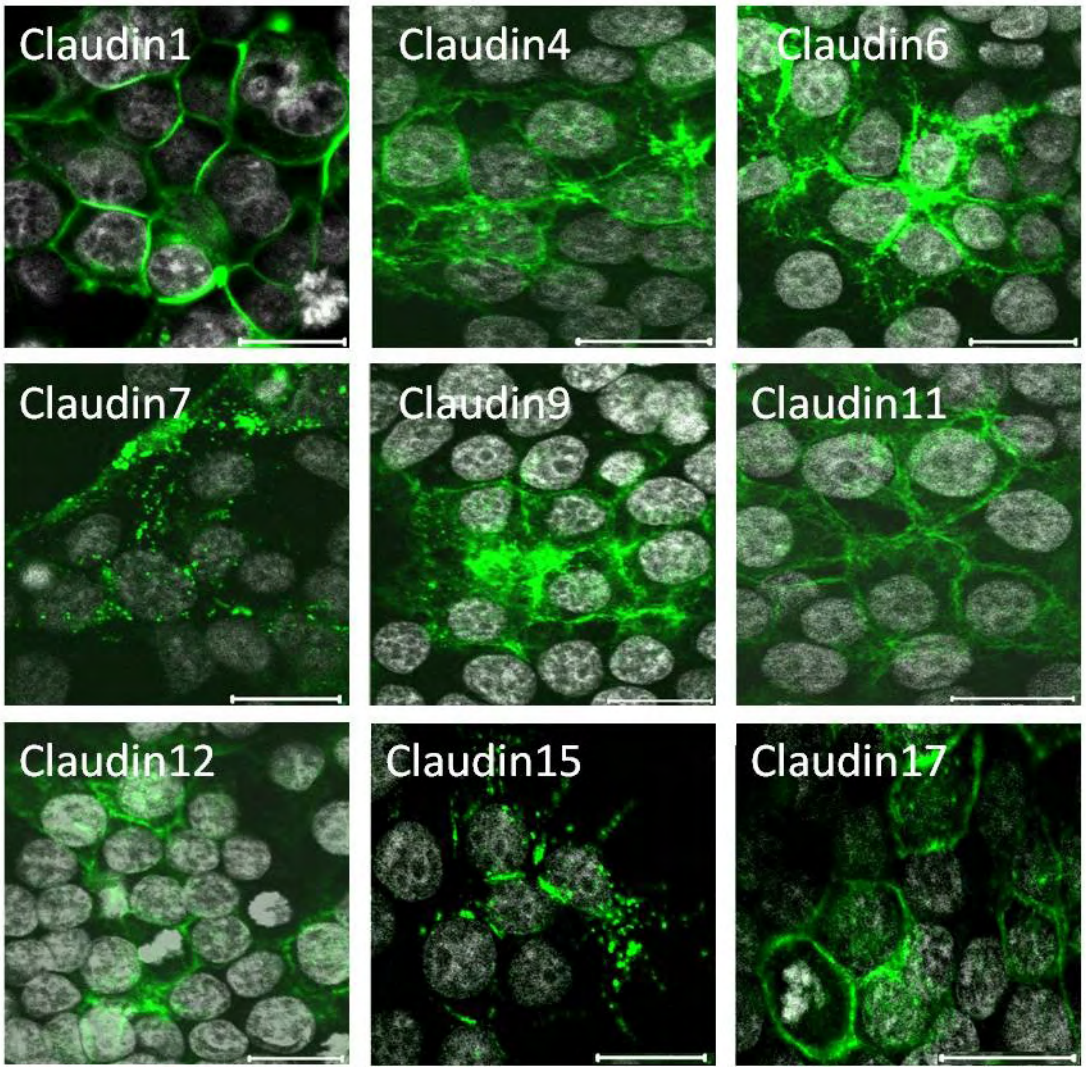


**Figure 3.10: Localisation of Fluorophore labelled Claudin proteins**. 293-T cells were transfected with various members of the Claudin family, which contained an AcGFP epitope fused to their N-terminus. Cells were imaged by laser scanning confocal microscopy using a 63 x 1.2NA water immersion objective and a meta head confocal microscope (Zeiss), Scale bars are equal to 20µm. Plasma membrane and intracellular patterns of staining are readily apparent.

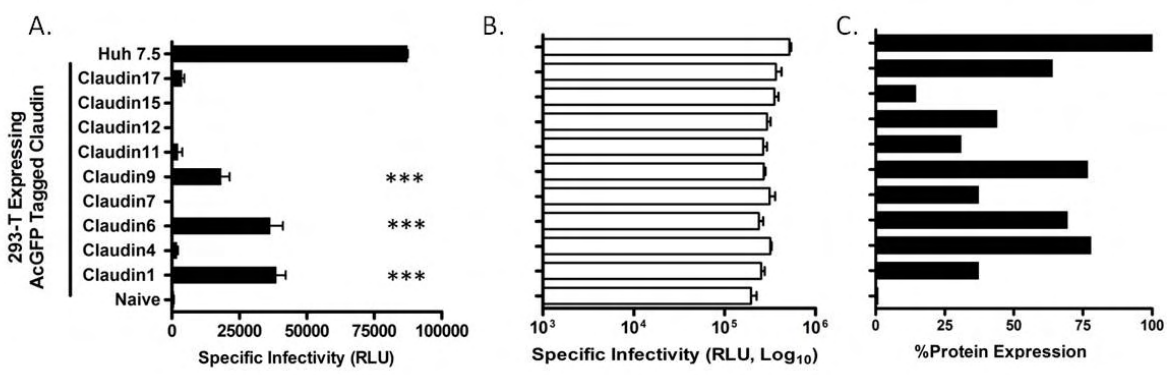


**Figure 3.11: Effect of N-terminal tagging various Claudin proteins on viral receptor activity**. 293-T cells were transfected to express AcGFP tagged versions of the Claudin family of proteins and evaluated for their ability to support HCVpp and MLVp entry. Data is represented as specific infectivity (Relative Light Units, RLU) and represents the mean plus the standard error of three replicates. HCVpp and MLVpp signals were corrected for signal noise by subtracting the Env-RLU level. A) Shows the specific infectivity of HCVpp into 293-T expressing AcGFP-CLDN fusion proteins. B) shows the MLVpp entry. C) shows the percentage of cells in Claudin expression as determined by flow cytometry. One way Analysis of Variance and Bonferroni's Multiple Comparison Test was used to determine the degree of significance (***p <0.01). This data is representative of three independent experiments.

To investigate which Claudin proteins could associate with CD81 the panel of AcGFP N-terminal tagged fusion proteins, representing both classical (Claudin1, 4, 6, 7, 9, 15 and 17) and non-classical (Claudin11 and 12) members of the Claudin family, were co-expressed with DsRED-CD81 in the Claudin negative 293-T cell line. A representative FIR plot for each Claudin is shown in figure 3.12. Only Claudin1, 6, 9 and 12 had an $R^2$ high enough to infer a FIR value (0.5, 0.6, 0.4 and 0.4 respectively). The FIR values for these Claudins with CD81 were 0.7 (IQR 0.67 – 0.74) for Claudin1, 1.0 (IQR 0.80 – 1.10) for Claudin6, 0.5 (IQR 0.40 – 0.67) for Claudin9 and 0.5 (IQR 0.26 – 0.83) for Claudin12 (table 1). As these values are not significantly different from that of the CD81-CD81, they suggest that the Claudins are associating with CD81 with a 1:1 stoichiometry. The levels of FRET were determined as 60% ± 4, 50% ± 6, 63% ± 7 and 15% ± 12 for Claudin1, 6, 9 and 12, respectively. The low %FRET value for Claudin12 with CD81 suggests there is negligible association between AcGFP-Claudin12 and DsRED-CD81. The %FRET value is around the level of non-specific interaction, set by the MAL-CD81 interaction, leading us to conclude that there is no specific interaction between Claudin12 and CD81. In contrast, the %FRET detected between CD81 and the receptor active Claudin1, 6 and 9 proteins are of a similar level to that observed for CD81-CD81 interaction. In summary, these results demonstrate that only receptor active Claudins showed a specific 1:1 stoichiometry with CD81, with the level of FRET interaction showing they are closely associated (<10nm).

Since Occludin is also important for HCV entry, we investigated the stoichiometry and association of AcGFP tagged Claudin molecules with Occludin. The majority of Claudins tested (-1, -6, -9, -11, -12 and -17) demonstrated a detectable association ($R^2$ 0.2-0.5), and FIR values of between 0.6 – 0.9 with variable levels of FRET, suggesting that receptor activity of the Claudin protein is unlikely to be defined by its ability to interact with Occludin (Table 1).

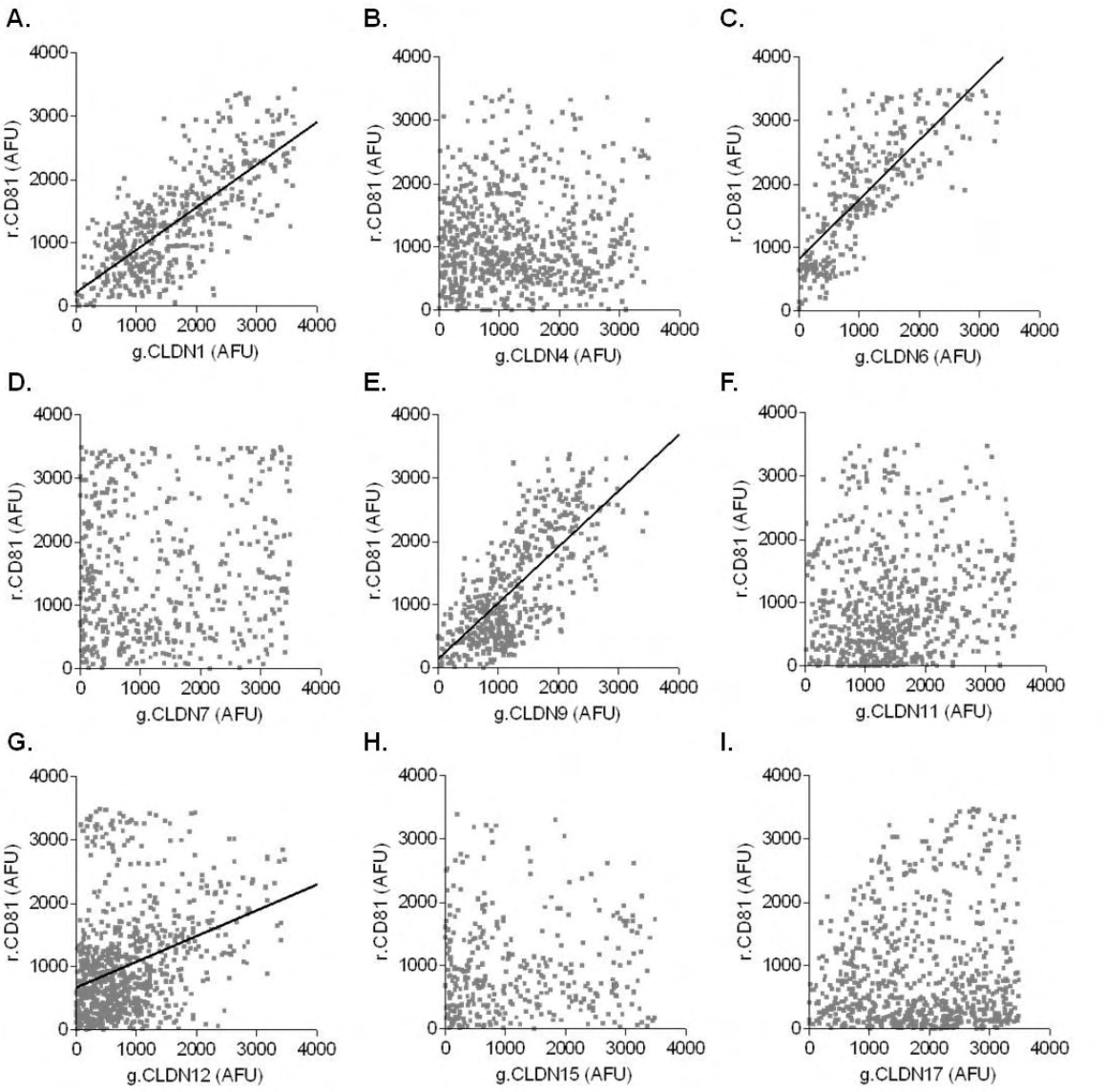


**Figure 3.12: Analysis of Claudin-CD81 interactions**. 293T cells were co-transfected to express DsRED-CD81 (r.CD81) and a panel of AcGFP-tagged Claudin (g.CLDN) constructs (CLDN1–17, panels A–I). Ten cells were imaged as described in Fiure 3.2, and estimates of g.Claudin association with r.CD81 association with evaluated by FIR analysis and summarized in Table 3.1. The images above represent the scatter plots closest to the median FIR for each g.Claudin- r.CD81 pair studied. This data is representative of two independent experiments.

Table 3.1: Fluorescent tagged Claudin protein associations with CD81 and Occludin

| | $r^2$ (IQR)* | FIR (IQR) | %FRET ± sd# |
|---|---|---|---|
| CD81 association with: | | | |
| Claudin1 | 0.5 (0.42 – 0.61) | 0.7 (0.67 – 0.74) | 60 ± 4 |
| Claudin4 | 0.2 (0.17 – 0.24) | 0.3 (0.21 – 0.41) | 5 ± 8 |
| Claudin6 | 0.6 (0.54 – 0.62) | 1.0 (0.80 – 1.10) | 50 ± 6 |
| Claudin7 | 0.0 (0.00 – 0.09) | ND† | ND |
| Claudin9 | 0.4 (0.36 – 0.50) | 0.5 (0.40 – 0.67) | 63 ± 7 |
| Claudin11 | 0.2 (0.16 – 0.23) | 0.3 (0.19 – 0.41) | 7 ± 4 |
| Claudin12 | 0.4 (0.28 – 0.48) | 0.5 (0.26 – 0.83) | 15 ± 12 |
| Claudin15 | 0.0 (0.00 – 0.04) | ND | ND |
| Claudin17 | 0.2 (0.17 – 0.30) | 0.3 (0.22 – 0.52) | 6 ± 8 |
| Occludin association with: | | | |
| Claudin1 | 0.4 (0.29 – 0.54) | 0.7 (0.60 – 0.82) | 48 ± 1 |
| Claudin4 | 0.2 (0.14 – 0.34) | 0.3 (0.29 – 0.53) | 30 ± 7 |
| Claudin6 | 0.2 (0.04 – 0.36) | 0.8 (0.57 – 0.53) | 27 ± 9 |
| Claudin7 | 0.1 (0.04 – 0.18) | ND† | ND |
| Claudin9 | 0.3 (0.13 – 0.48) | 0.7 (0.39 – 0.79) | 18 ± 8 |
| Claudin11 | 0.4 (0.12 – 0.45) | 0.7 (0.62 – 0.83) | 23 ± 7 |
| Claudin12 | 0.3 (0.19 – 0.37) | 0.6 (0.51 – 0.71) | 38 ± 6 |
| Claudin15 | 0.1 (0.08 – 0.21) | ND | ND |
| Claudin17 | 0.5 (0.28 – 0.51) | 0.9 (0.74 – 1.07) | 40 ± 5 |

* – Interquartile range

# – Standard deviation

† – Not Determined

**3.7 Analysis of Claudin1-CD81 interactions by surface plasmon resonance.**

The EC2 of CD81 has been reported to be the main region involved in protein-protein interactions (122). Nakajima et al were able to fuse the EC2 loop of CD81 to maltose binding protein (MBP-CD81), and the fusion proteins interacted with HCV sE2 by Surface Plasmon Resonance (SPR) (153). Evans et al identified regions of Claudin1 EC1 that were essential for HCV receptor activity (110). We therefore determined whether recombinant Claudin1 EC1 and CD81 EC2 loops could associate by SPR technique. We obtained recombinant MBP-CD81 from the Drummer lab (Burnet institute, Australia), and generated recombinant Claudin1 or Claudin7 fused to MBP (MBP-Claudin1 and MBP-Claudin7 respectively). MBP-CD81 or MBP-Claudin1 were immobilised onto SPR chips and the various recombinant proteins tested for interactions (figure 3.13). Homotypic Claudin1 and CD81 protein interactions were observed, with minimal detection of either recombinant loop protein interacting with MBP. MBP-CD81 demonstrated a specific interaction with MBP-Claudin1 and a minimal interaction with MBP or MBP-Claudin7 (Figure 3.13). The affinity of the Claudin1-CD81 interaction was determined by flowing MBP-CLDN1 over the MBP-CD81 chip surface at varying concentrations (figure 3.14). The association constant was determined to be $243M^{-1}s^{-1}$ with a dissociation constant of 0.0973 $s^{-1}$, which gives an approximate affinity (KD) of 40µM. These values were calculated using the 1:1 drifting baseline model provided by the BIAevaluation software (Biacore), which corrects for the signal due to movements in the response unit which are not attributed to the injection of an anylate.

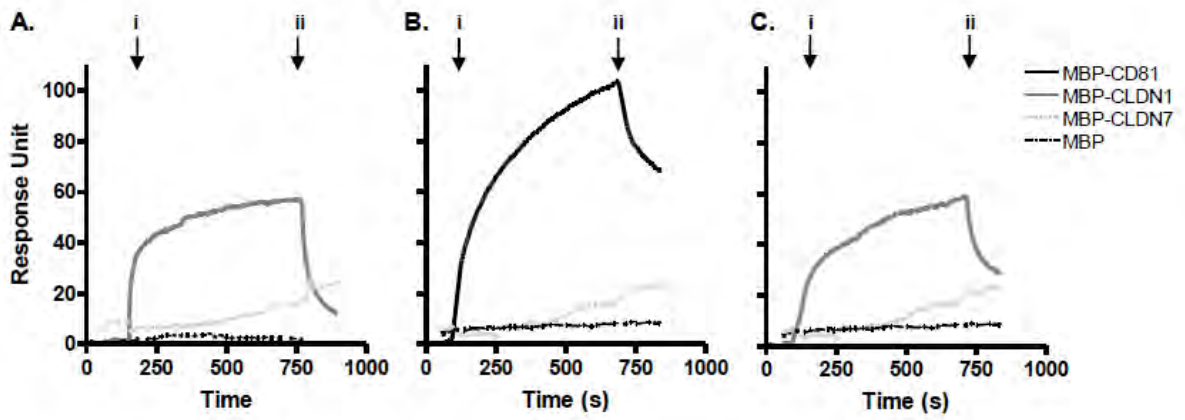


**Figure 3.13: Analysis of Claudin1-CD81 extracellular loop interactions by surface plasmon resonance.** MBP-Claudin1 EC1 (**A**) and MBP-CD81 EC2 (**B-C**) were immobilized onto the biosensor chip surface. Homotypic protein interactions were demonstrated by flowing MBP-Claudin1 EC1 (solid grey line) or MBP-CD81 EC2 (solid black line) over the respective chip surfaces (**A-B**), with either MBP-CLDN7 EC1 (dotted light grey line) or MBP (dotted black line) as negative controls at a concentration of 1mg/ml. Heterotypic interactions between MBP-Claudin1-EC1 and MBP-CD81 EC2 are depicted in (**C**). To control for non-specific interactions, all MBP fusion proteins were flowed over an activated and blocked 'empty' channel and these response unit(s) subtracted from test channels. The arrow indicates the 'association phase' **i** when proteins were flowed over the respective chip surfaces, the 'dissociation phase' begins at time **ii** when protein injection is stopped. Data is representative of two independent experiments.

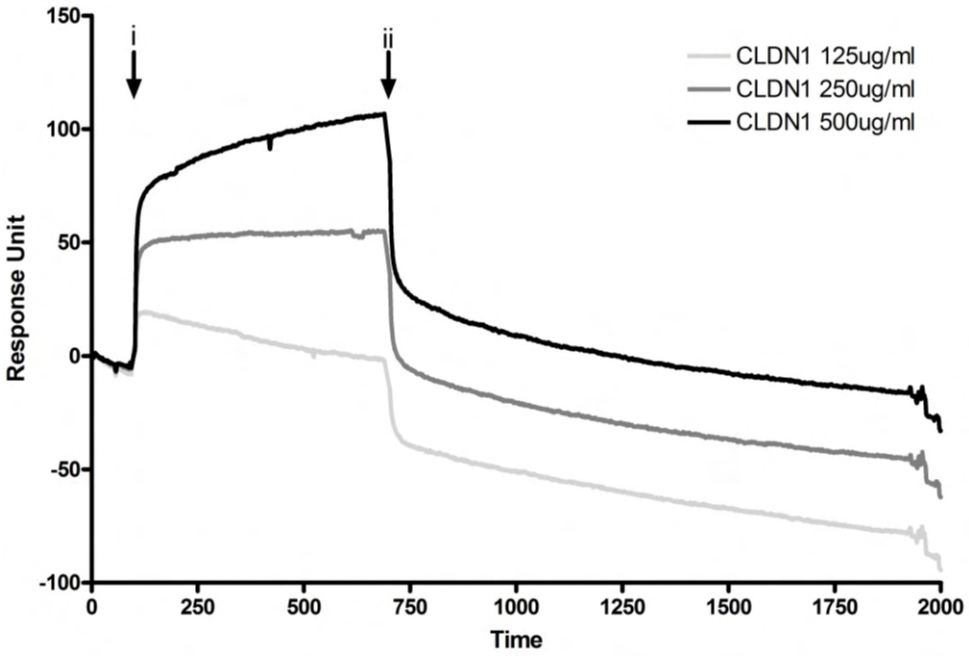


**Figure 3.14: Affinity of Claudin1-CD81 extracellular loop interactions by surface plasmon resonance.** MBP-CD81 EC2 was immobilized onto the biosensor chip surface. MBP-Claudin1 EC1 was flowed over the chip surface at a concentration of 125µg/ml (light grey line), 250µg/ml (grey line) or 500µg/ml (black line). The arrow indicates the 'association phase' **i** when proteins are flowed over the respective chip surfaces, the 'dissociation phase' begins at time **ii** when protein injection is stopped. This data is representative of two independent experiments.

### 3.8 Discussion

The interaction between the two HCV co-receptors Claudin1 and CD81 has been demonstrated by both biochemical (125) and imaged based approaches (183-184). Our previous publication, using a FRET based approach, found that receptor active Claudin1 associated with CD81, whereas the non-receptor active Claudin4 showed no interaction (184). A limitation of these previous approaches was the lack of information obtained about the Claudin1-CD81 complex. In the case of the FRET based approach regions of high protein co-localisation were selected for the analysis, which could introduce bias to the results. We therefore developed new methods for probing the Claudin1-CD81 complex and determining whether their specific interaction dictates HCV receptor activity.

We utilised an imaging based technique termed FIR measurement that has been previously used to determine the subunit composition of heterotypic olfactory channels and of the epithelial Na1 channel (220-221). This technique can be used to define the ratio of two fluorophore labelled proteins at a given location (such as the plasma membrane). Although this technique can define a gross stoichiometry it is limited by the resolution of the image. We therefore sought to measure FRET which can detect close associations, as this phenomena requires the two fluorophores to be within 10nm of one another. The accurate interpretation of the FRET signal requires an equal concentration of the two fluorophores. For this reason the presence of FRET can only be reliably inferred for proteins with a FIR value corresponding to a 1:1 stoichiometry.

We generated a panel of fluorescently labelled Claudin proteins and determined their interaction with CD81. These studies were performed in 293-T cells which lack any endogenously expressed Claudins. We found receptor active Claudins 1, 6 and 9, to have a

defined relationship with CD81, with the FIR analysis indicating a 1:1 stoichiometry. The receptor inactive Claudin12 also showed a 1:1 stoichiometry, the remaining Claudins showied no discernable pattern of association.

As these Claudin-CD81 complexes had a 1:1 stoichiometry the presence of FRET could be assessed to demonstrate whether the proteins are close enough to show energy transfer. FRET was only detected between the receptor active Claudins (Claudin1, 6 and 9) and CD81. In contrast the receptor inactive Claudin12 showed a low level of FRET that was comparable to non-specific protein interactions, as defined by the MAL-CD81 FRET analysis. Overall these results show that Claudin1, 6, 9, the receptor active Claudins, all form a heterodimer complex with CD81 at the plasma membrane. Using recombinant CD81 and Claudin1 proteins we have been able to demonstrate that this interaction occurs between the EC1 of Claudin1 with the EC2 of CD81 with an approximate affinity of 40μM. Nakajima et al have reported the affinity of CD81-HCV E2 to be 92 nM (153), which indicates that the Claudin1-CD81 interaction is weaker interaction. Transient protein interactions are typically thought to be short lived with weak binding values normally in the μM-mM KD range. The low KD values are usually a consequence of high association and dissociation rate constants (235-238). As the KD for the Claudin1-CD81 complex is within the range for transient protein interactions the proteins could be present in the membrane in a state of constant flux between single and complex forms. This has been observed in single particle trafficking experiments performed by Helen Harris, which demonstrated that the two proteins diffuse separately before coming together and co-diffusing as a complex and then dissociating (Helen Harris, unpublished data).

The relevance of Claudin6 and 9 to HCV infection is still to be determined. Our laboratory previously reported using qRT-PCR that Claudin6 has a lower level of expression than Claudin1, with Claudin9 mRNA being undetectable in Huh-7.5 cells (180). Zheng et al reported that Claudin6 was also expressed in HepG2 cells (113). Claudin6 is thought to be primarily expressed in embryonic epithelia, showing reduced expression over time (173), whilst Claudin9 is reported to be expressed exclusively in the ear (239). However it should be noted that expression of Claudins within tissues can be altered under certain conditions (240), and the majority of the research has been conducted on cancerous tissue (241-243). It is therefore possible that Claudin6 and 9 could be expressed in the liver under particular circumstances, such as liver damage. There is some evidence that peripheral blood mononuclear cells (PBMCs) could be involved in the HCV lifecycle (244-247). PBMCs have been shown to have high levels of Claudin6 and 9 with no detectable Claudin1 expression (113).

The direct interaction of Claudin1, 6 or 9 with the HCV particle has, so far, not been fully demonstrated. This could indicate that an alteration of the HCV glycoprotein conformation, possibly upon binding to CD81, maybe required for Claudin to directly interact with the HCV particle. Alternatively Claudin could function by facilitating the internalisation of the CD81-virus complex. To ascertain whether the interaction between Claudin1 and CD81 is essential for HCV infection we need to determine whether perturbation of the interaction purturbs particle internalisation.

In addition to the interaction of Claudin1 with CD81, other tetraspanin proteins appear to have an association, as indicated by our FIR and FRET analysis (CD81, CD82 and CD9). The presence of these interactions could be indirect due to ability of CD81 to interact with these

members of the tetraspanin family of proteins (125). It is known that tetraspanin webs, which are regions of high tetraspanin protein concentration, interact to organise other cell surface proteins and are involved in many biological processes (117, 122, 123 91). It is unlikely that the Claudin1-CD81 complex require localisation within tetraspanin webs to act as a receptor complex, since CD81 palmitoylation mutants, which do not interact with the tetraspanin web, are still receptor active (248).

# Chapter 4:

# Modulation of Claudin1-CD81 association

So far we have shown that an interaction exists between the receptor active Claudin proteins and CD81. In order to determine if the Claudin-CD81 interaction is essential for HCV entry we assessed the interaction under various conditions that have been shown to reduce or ablate viral entry. Firstly Hepatocytes, which are the major reservoir supporting HCV replication in the liver, are highly polarised (216). Since all of our previous Claudin1-CD81 FRET experiments utilised non-polarised 293T cells, we need to study receptor association in a polarised model system. As our group has previously published data demonstrating that polarisation reduces HCV entry it is important to determine the effects on the Claudin1-CD81 complex (179-180).

**4.1 Effects of cell polarisation on Claudin1-CD81 association.**

To assess the effect of polarisation on HCV entry our cell line of choice is the human HepG2 hepatoblastoma line (HepG2). The cell line polarizes in culture, forming spheroid structures at sites of cell-cell contact that resemble bile canaliculi in the liver. These structures contain tight junctions and express multiple membrane protein markers (reviewed in Ref. (216)). HepG2 cells were transduced to express AcGFP-Claudin1/DsRED-Claudin1 or AcGFP-Claudin1/DsRED-CD81 and allowed to proliferate for 72hrs, whereupon polarized cells were identified by staining for the apical tight junction marker ZO-1 (figure 4.1 a-c) (179). At the basolateral surface the Claudin1-CD81 association had an $R^2$ of 0.7 (0.56 – 0.81), a FIR value of 0.67 (0.56 - 0.74) and %FRET of 39% ± 13.6. These results are similar to those shown previously for the Claudin1-CD81 association in 293-T cells (see previous chapter). In contrast, receptor association at the tight junction region was very different, with Claudin1-CD81 showing an $R^2$ of 0.13 (0.03 – 0.33), a FIR value of 0.16 (0.6 - 0.25) and a %FRET of just

4.7% ± 6.4. This lack of association appears to be due to CD81 being largely excluded from tight junctions. Importantly, the association of Claudin1 homodimers was comparable at the basolateral and tight junction regions, demonstrating FRET values of 19.27% ± 14.78 at the basolateral surface and 16.35% ± 19.44 at the tight junctions. The %FRET for the Claudin1 homodimer at the two locations are low, which is likely due to pools of endogenous Claudin1 reducing the level of FRET detected, as previously reported (184). In summary, Claudin1 demonstrated comparable association(s) with Claudin1 at basolateral and tight junction locations in polarized HepG2 cells, similar to our observations in non-polarized 293T cells. However significant differences were noted for AcGFP-Claudin1 and DsRED-CD81 association at the basolateral and tight junction domains of HepG2 cells. These data are consistent with our previous report demonstrating a role for basolateral pools of Claudin1 in HCV infection (179).

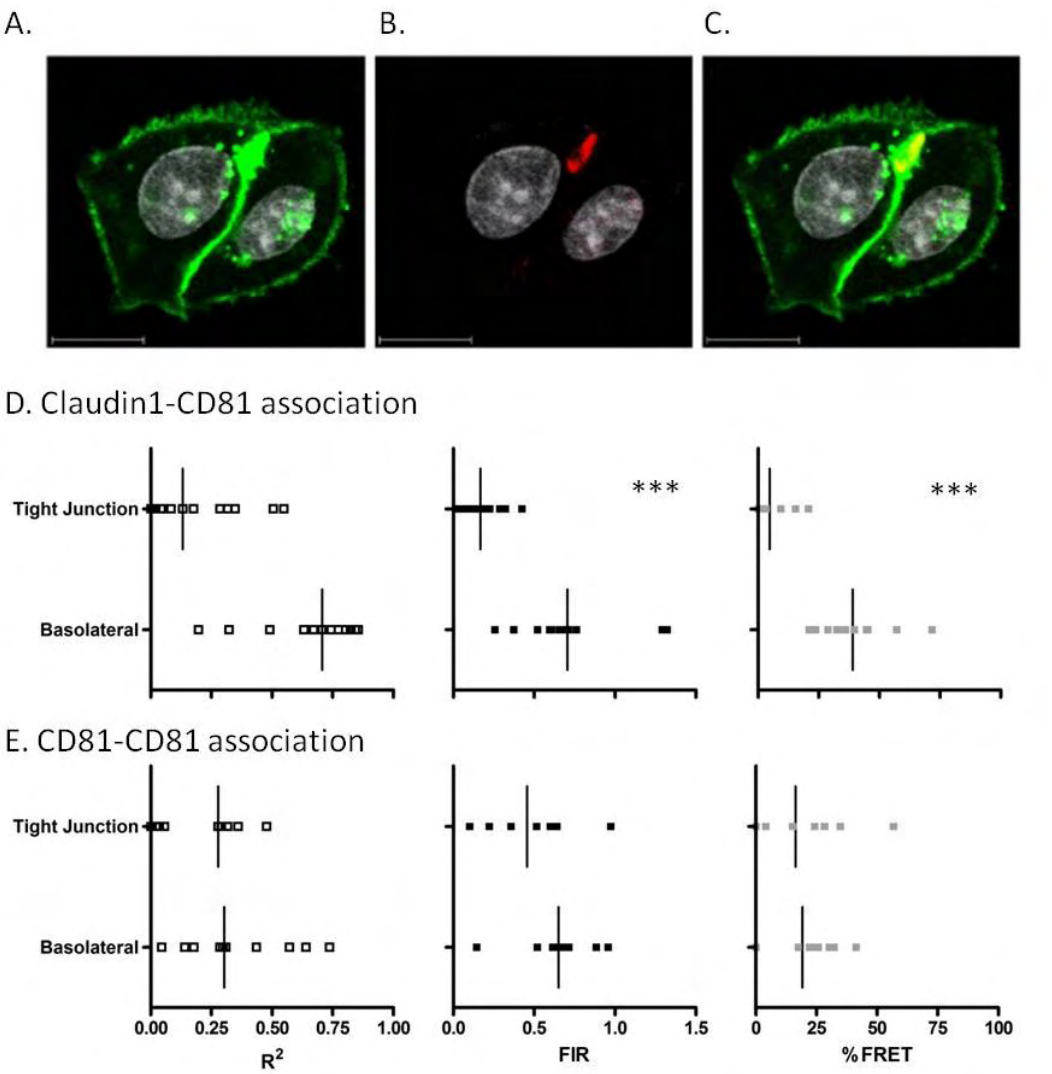


**Figure 4.1: Effect of cell polarization on Claudin1-CD81 and Claudin1-Claudin1 association.** HepG2 cells were transfected to express AcGFP-Claudin1/DsRED-CD81 and AcGFP-Claudin1/DsRED-Claudin1 and allowed to polarize over a period of 72hrs. Apical bile canalicular structures were identified by staining with anti-ZO-1 and visualized with an alexa-633-conjugated secondary anti-rabbit Ig. A) Represents two HepG2 cells showing AcGFP-Claudin1 staining, B) anti-ZO-1 staining, showing the location of the tight junction with C) showing the merged image. The $R^2$, FIR and %FRET values for Claudin1-CD81 and Claudin1/Claudin1 in 10 cells at junctional and basolateral areas are shown (D and E, respectively). A Kruskal-Wallis Anova with a Dunn's Multiple Comparison Test was used to assess differences between basolateral and tight junction regions of the cell (*** $p < 0.001$). This data is representative of two independent experiments. Images provided by Helen Harris and Chris Mee.

**4.2 The role of cholesterol in CD81-CD81 and Claudin1-CD81 association(s).**

Tetraspanin protein interactions are known to be modulated by cholesterol (249-251). Kapadia and colleagues reported that HCV entry is dependent on the cholesterol content of the host cell membrane, however, the underlying mechanism was not defined. To investigate a role of cholesterol in Claudin1-CD81 and CD81-CD81 association we used a cyclic oligosaccharide that depletes cholesterol from the plasma membrane (methyl-β-cyclodextrin, MβCD) (219). The removal of cholesterol can be reversed by treating cells with MβCD saturated with cholesterol. 293-T cells expressing AcGFP-Claudin1/DsRED-CD81 were treated with 10mM MβCD, that removed ~50% of total cholesterol as determined using an Amplex Red assay kit (Invitrogen), and cholesterol levels were partially restored to 75% of their initial value by treating with 10mM MβCD–1mM cholesterol complexes (figure 4.2c). Depleting cholesterol significantly reduced both HCVpp and MLVpp entry and partial restoration of cholesterol increased HCVpp and MLVpp infection (figure 4.2a and b respectively). The removal of cholesterol led to an increase in the FIR value as well as a reduction in Claudin1-CD81 FRET. Untreated cells showed a AcGFP-Claudin1/DsRED-CD81 FIR value of 0.79 (0.65-1.049) whereas cholesterol depleted cells had a FIR value of 1.28 (0.99-1.99). The FRET value for untreated cells was 45.63% ± 8.514, that was reduced to 22.14% ± 28.65 following cholesterol depletion (figure 4.2e). In contrast, MβCD treatment had no detectable effect on AcGFP-CD81/DsRED-CD81 FIR (figure 4.2d), with untreated cells showing a FIR value of 0.75 (0.69-0.87) compared to 0.62 (0.52-0.7) following cholesterol depletion. The frequency of pixels where FRET occurred between AcGFP-CD81 and DsRED-CD81 was reduced, from 63.2% ± 14.98 to 54.8% ± 5.83, although this was not significant. Restoring cholesterol after depletion led to a recovery of the Claudin1-CD81 association. The Claudin1-CD81 had a FIR value of 0.66 (0.59-0.7) with a %FRET of 50.12% ± 10.27,

similar to the untreated cell values. Overall these results demonstrate that Claudin1-CD81 association is cholesterol dependent, which may contribute to the reduced susceptibility of MβCD treated cells to HCV infection. Kapada et al demonstrated that the level of CD81 expressed at the cell surface was significantly reduced in MβCD treated cells, however we found that untreated and treated cells showed mean fluorescent intensities at the plasma membrane of DsRED-CD81 of 2111± 608.2 and 2317 ± 491.7 respectively. The Claudin1 however showed reduced fluorescence intensity levels from 1580 ± 605.9 to 821.7 ± 209.0, which explains the increase in the FIR value for MβCD treated cells. The discrepancy between these results and those published previously may be explained by the different cell types with Kapadia et al using Huh-7 cells, whereas with our experiments were performed using the 293-T cell line (249).

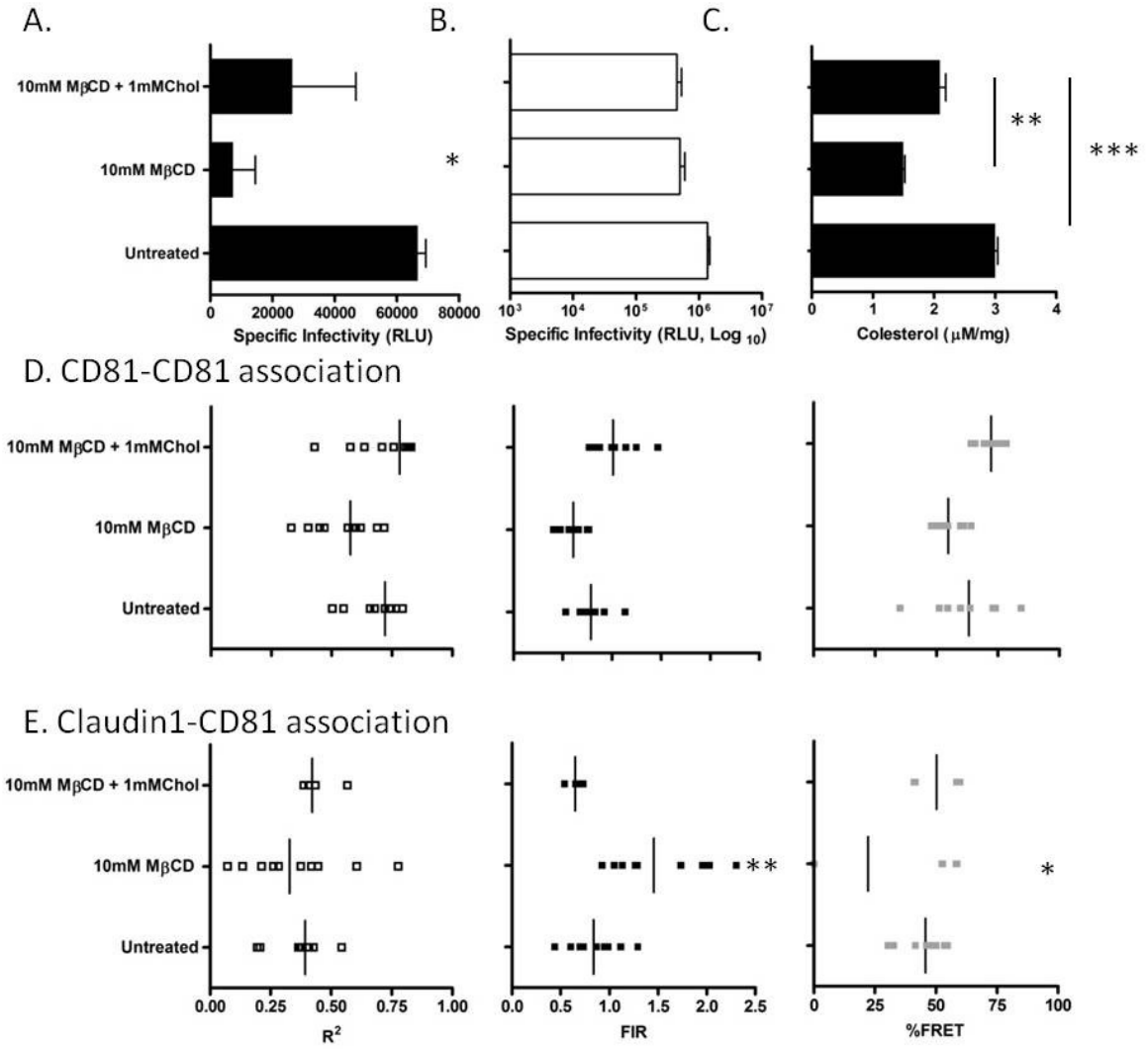


**Figure 4.2: The role of cholesterol in virus entry and CD81-CD81 and Claudin1-CD81 association(s).** 293-T cells were transfected to express AcGFP-Claudin1/DsRED-CD81 or AcGFP-CD81/DsRED-CD81. The cells were treated with 10mM Methyl-β-cyclodextrin (MβCD), 1mM Cholesterol (chol) or with 10mM MβCD followed by 10mM MβCD+1mM Cholesterol. The AcGFP-CLDN1/DsRED-CD81 expressing cells were assessed for HCVpp and MLVpp entry (a and b respectively). The association of the C) AcGFP-CD81/DsRED-CD81 homodimer and D) AcGFP-Claudin1/DsRED-CD81 were measured and the $R^2$, FIR and FRET values for 10 cells represented as dot plots. The median value is denoted by the solid vertical line on the plots. One way Analysis of Variance and Bonferroni's Multiple Comparison Test was used to determine the degree of significance (*p <0.05, **p <0.01). This data is representative of three independent experiments.

### 4.3 Perturbation of Claudin-CD81 association with anti-CD81 antibodies

It has been previously demonstrated that both the binding of recombinant HCV E2 (88-89, 91, 106) and viral infection can be inhibited by anti-CD81 monoclonal antibodies (252). Our group has produced a panel of anti-CD81 monoclonal antibodies which we were interested to determine if they have an effect on CD81-CD81 homodimer or Claudin1-CD81 heterodimer. The panel tested consisted of 7 monoclonal antibodies and one Fab fragment. The antibodies have previously been shown to inhibit HCV entry into Huh7.5 cells with $IC_{50}$ values ranging for 0.067 to 1.34μM (Michelle Farquhar, unpublished data). Before evaluating their effects, if any, on the interaction of Claudin1 with CD81 we first assessed their ability to inhibit HCVpp infection of 293-T cell line stably expressing AcGFP-CLDN1. The cells were pre-treated with the various antibodies at a concentration of 67μM, which is a saturating concentration for all the antibodies (Ke Hu, private communication), before the inoculating H77pp or MLVpp virus (figure 4.3). The results show that all the anti-CD81 antibodies reduce H77pp viral entry without effecting MLVpp entry. There was some variation in the inhibition levels at this concentration with the 2s66Fab showing the lowest level of inhibition of 69.4%, and 2s20 showing the greatest level of inhibition of 89.4%

The affinity of the antibodies for CD81 was assessed by surface plasmon resonance using the MBP-CD81 described earlier. The MBP-CD81 was immobilised on the BIAcore sensorschip surface and the antibodies passed over the chip surface at various concentrations to obtain a measure of affinity (Figure 4.4). The affinity of the antibodies was determined by plotting the maximal level of binding for each concentration on an X,Y scatter plot and fitting a non-linear regression line (figure 4.4b). The values of the theoretical binding capacity (Bmax, Response Units (RU)) and affinity (KD, μM) are shown in figure 4.3c.

The antibodies show different KD values, ranging from 1.22µM for 2s20 to 142.7µM for 1s135. The lowest Bmax value seen was 249.1 RU for 1s337 antibody, with the highest noted for 2s20 with a value of 2407 RU. The results show a wide range in the binding capacities of the various antibodies and the concentration of antibody required to saturate CD81. However, we found no correlations between the Bmax, the affinity, and level of viral inhibition. The antibodies were also tested by other members of our group for their binding capacity to Huh7.5 cells, which again showed no correlation to the Biacore results. The likely reason for the lack of correlation between the Biacore and cell based experiments is the context of the CD81 protein. The Biacore uses a recombinant form of the EC2 of CD81 that will immobalised to the chip surface via lysine residues and may therefore adopt various orientations. The full length CD81 on the cell surface is not only restricted to its orientation but will also be interacting with other membrane proteins, which may alter how the antibodies are interacting with the protein. However the Biacore result confirms that all antibodies bind to CD81 EC2.

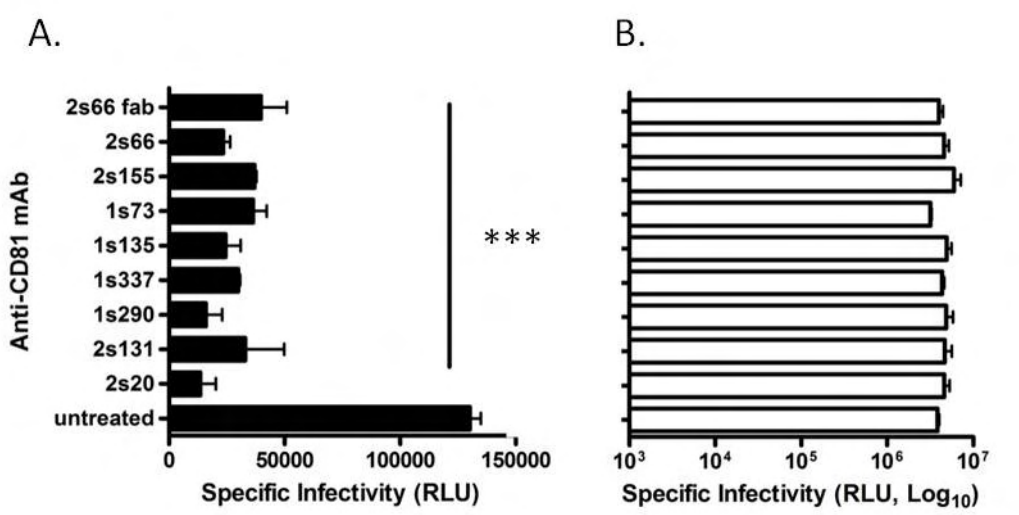


**Figure 4.3: Anti-CD81 inhibition of HCVpp infection**. A 293-T cell line stably expressing AcGFP-Clsudin1 was evaluated for its ability to support HCVpp and MLVpp entry in the presence of Anti-CD81 monoclonal antibodies. Data are represented as specific infectivity (Relative Light Units, RLU) and represent the mean plus the standard error of three replicates. A) Shows the specific infectivity of HCVpp. B) shows the specific infectivity of MLV. A One way Analysis of Variance with a Bonferroni's Multiple Comparison Test was used to determine the degree of significance (***$p<0.001$). This data is representative of two independent experiments.

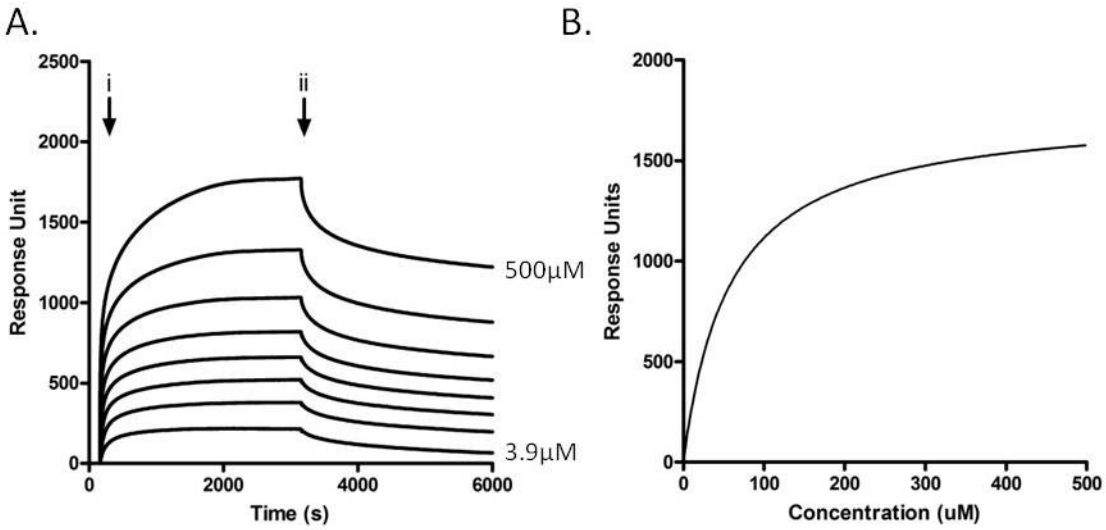


C.

| | Bmax (RU) | KD (µM) |
|---|---|---|
| 2s20 | 2407 ± 32.92 | 1.217 ± 0.19 |
| 2s131 | 595.4 ± 15.83 | 2.093 ± 0.46 |
| 1s290 | 986.4 ± 69.96 | 3.426 ± 1.6 |
| 1s337 | 249.1 ± 6.85 | 3.618 ± 0.64 |
| 1s135 | 1144 ± 28.92 | 142.7 ± 8.93 |
| 1s73 | 1755 ± 28.87 | 84.57 ± 4.01 |
| 2s155 | 1757 ± 179 | 57.54 ± 18.7 |
| 2s66 | 685.9 ± 12.82 | 3.32 ± 0.41 |
| 2s66 Fab | 564.4 ± 16.34 | 44.75 ± 4.4 |

**Figure 4.4: Determination of the anti-CD81 mAb affinity for MBP-CD81 by surface plasmon resonance.** MBP-CD81 was immobilized onto the bio-sensor chip surface and a panel of anti-CD81 antibodies flowed over the chip surface at various concentrations, ranging from 500µM to 3.9µM. A) shows the sensograms for 2s155 at the various concentrations, where the arrow indicates 'association time' (**i**) when antibodies are flowed over the respective chip surfaces and the 'dissociation phase' (**ii**), when antibody injection is stopped. B) shows the x,y scatter plot produced by plotting the response units (RU) at the end of the end of the association phase against the concentration. A non-linear regression line was fitted to produce the Bmax and affinity values shown C. This data is representative of two independent experiments.

**4.4 Anti-CD81 modulation of CD81-CD81 and Claudin1-CD81 association(s).**

The effect of the antibodies was assessed in cells co-expressing AcGFP-CD81/DsRED-CD81 or AcGFP-Claudin1/DsRED-CD81. All the antibodies showed a minimal perturbation of CD81 homodimers (figure 4.5a), with a range of FIR values of the antibody treated cells from 0.46 (0.39-0.57) to 0.71 (0.5-0.95), with no significant differences from untreated cells with a FIR value of 0.56 (0.46-0.68). There was also no difference between %FRET values, with untreated cells showing a %FRET of 34.4% ± 6.44 and antibody treated cells demonstrating a range of FRET values between 27% ± 13.7 to 41.5% ± 7.6. In contrast, Claudin1-CD81 association was significantly reduced by all of the anti-CD81 monoclonal antibodies, with the exception of 1s337 (figure 4.5b). Antibody treatments caused a large reduction in the $R^2$, which means that either a gradient or %FRET can be estimated. Antibody 1s337 showed an $R^2$ of 0.28 (0.077-0.35), a FIR value of 0.67 (0-0.870) and a %FRET of 43.97% ± 33.2. Although 1s337 reduced Claudin1-CD81 association, as shown by the FIR and FRET values, the difference was not significant compared to untreated cells ($R^2$ 0.5 (0.44-0.62), FIR value of 0.67 (0.55-0.77) and %FRET of 43.22% ± 6.4). In addition to the bivalent antibodies we studied the effect of a monovalent 2s66 FAb fragment on AcGFP-CD81/DsRED-CD81 and AcGFP-Claudin1/DsRED-CD81 association. The 2s66 FAb bound to CD81 with a lower affinity than the complete IgG molecule (44.75µM ± 4.39 compared to 3.33 µM ± 0.414), as shown in figure 4.4c, it also showed a lower level of inhibition at the single tested concentration (69.4% and 81.2% respectively). The 2s66 Fab had no detectable effect on AcGFP-CD81/DsRED-CD81 or AcGFP-Claudin1/DsRED-CD81 FIR or FRET values. This result suggests that bivalent engagement and possible cross-linking of CD81 is essential to modulate lateral protein interactions. In summary, bivalent antibody engagement of CD81 perturbs its interaction with Claudin1 and may contribute to the neutralizing activity of these mAbs.

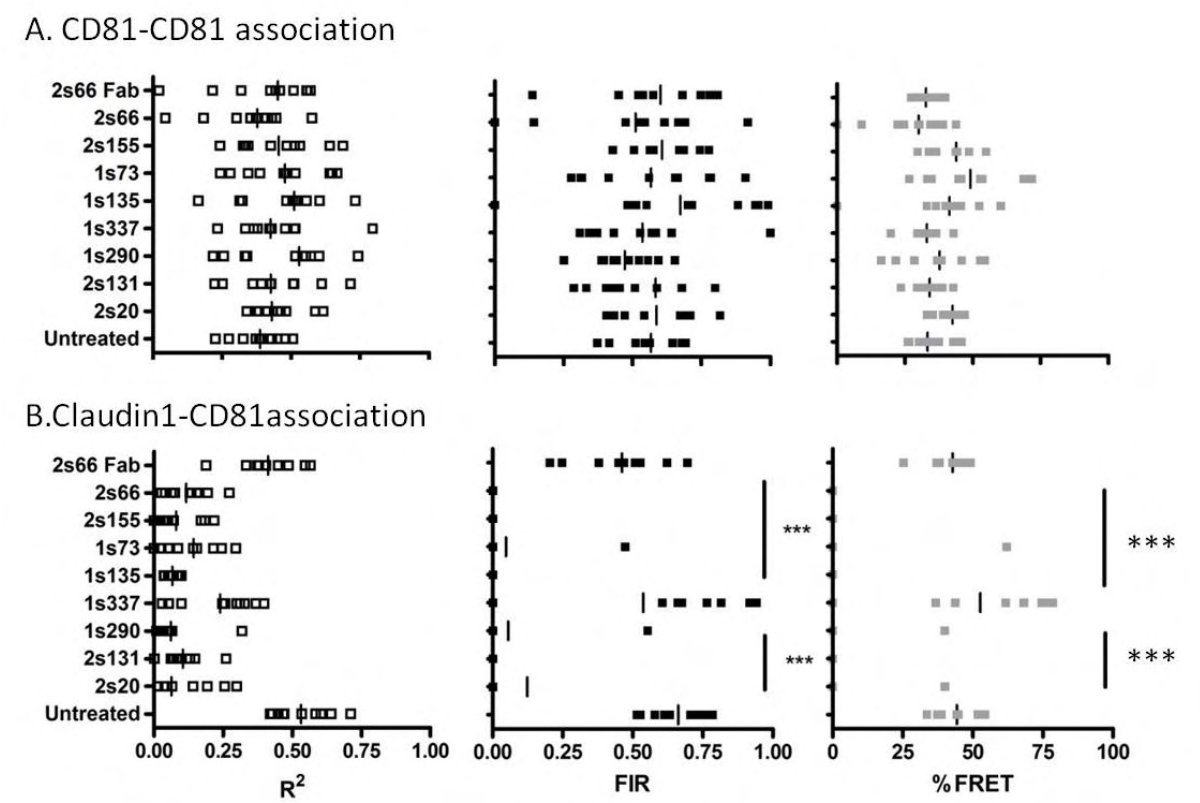


**Figure 4.5: Anti-CD81 modulation of CD81-CD81 and CLDN1-CD81 association(s).** 293T cells were transfected to express AcGFP-CD81/DsRED-CD81 or AcGFP-CLDN1/DsRED-CD81 and treated with a panel of anti-CD81 mAbs at equimolar concentrations (13µM) for 1h at 37$^{o}$C. The effects of mAb treatment on AcGFP-CD81/DsRED-CD81 (A) and AcGFP-CLDN1/DsRED-CD81 (B) $R^2$, FIR and %FRET of ten cells is presented. A Kruskal-Wallis anova with a Dunn's Multiple Comparison Test was used to determine if the treatments caused a significant alteration from an untreated control (***p <0.001). This data is representative of two independent experiments.

To confirm the results of anti-CD81 mAb perturbation of Claudin1-CD81 FRET association, we used an independent surface Plasmon resonance technique to measure the effect(s) of antibodies on recombinant MBP-CD81 and MBP-Claudin1 association. MBP-CD81 was bound to the chip surface and the panel of anti-CD81 mAbs injected at a concentration of 500μM followed immediately by MBP, MBP-CD81 or MBP-Claudin1 at a concentration of 750μg/ml. To define the level of specific binding of MBP-CD81 or MBP-Claudin1 to tethered MBP-CD81 in the presence of the panel of antibodies we determined the net change in response units compared to MBP alone. In short the final response unit reached after injecting the MBP was subtracted from the response unit shown for the MBP-CD81 or MBP-Claudin1 response unit (figure 4.6a and b). A positive value for the response unit indicates that binding has occurred between the MBP-CD81 of MBP-Claudin1 in the presence of the antibody, with a neutral or negative value indicating the antibody inhibiting the association of the proteins with the tethered MBP-CD81. As a positive control of MBP-CD81 and MBP-Claudin1 association was assessed in the presence of a commercial anti-MBP antibody (NEB, Clone No. E8032), which should bind to the tethered MBP-CD81 without interfering with the CD81 moiety. As shown in figure 4.6c although there was a reduction in most of the antibodies compared to the anti-MBP control, none could prevent the CD81-CD81 interaction, which mirrors the results shown previously. As predicted the majority of antibodies, with the exception of 1s337, 2s155 and 2s66Fab, reduced CD81-Claudin1 association as indicated by the negative change in response unit values. These results reflect the pattern shown in the imaging based techniques, with the exception of the mAb 2s155

which was unable to prevent CD81-Claudin1 association. It is possible that this discrepancy is due to subtle differences in the interactions of recombinant fusion proteins and full length membrane tethered molecules. One may hypothesise that the protein conformation is restrained in the membrane, whereas the purified loops may interact in ways that are not prevented by the 2s155 antibody.

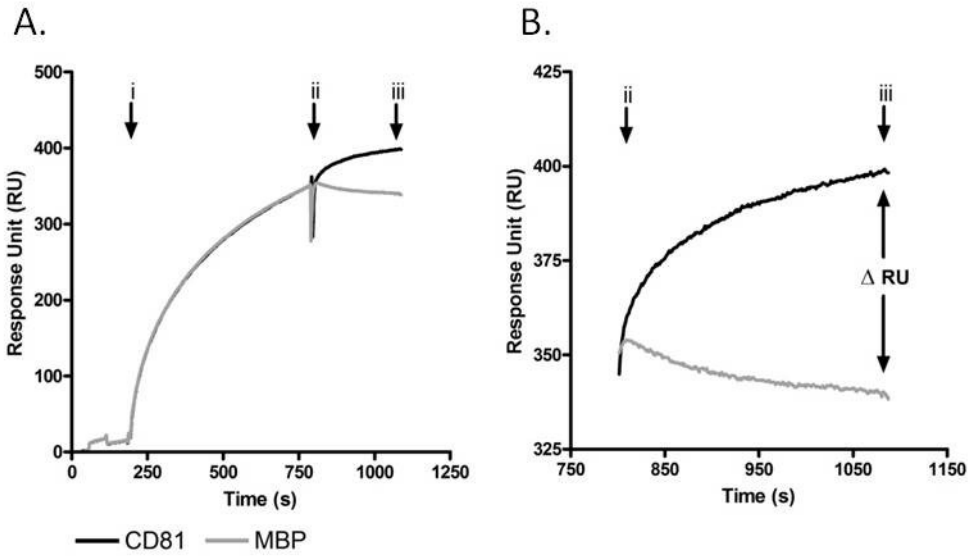


C.

| Antibody | Claudin1 | CD81 |
|---|---|---|
| MBP | 159.7 | 102.3 |
| 2s20 | -25.8 | 60.1 |
| 2s131 | -18.1 | 42 |
| 1s290 | -20.3 | 44 |
| 1s337 | 131.5 | 241.1 |
| 1s135 | -25.2 | 28.3 |
| 1s73 | -29.1 | 24 |
| 2s155 | 11.2 | 33.3 |
| 2s66 | -18.9 | 34.1 |
| 2s66 Fab | 43 | 89.6 |

**Figure 4.6: Determination of the ability of anti-CD81 antibodies to inhibit CD81-CD81 and Claudin1-CD81 interaction(s) by surface plasmon resonance.** MBP-CD81 was immobilized onto the bio-sensor chip surface. A panel of anti-CD81 antibodies and a commercial anti-MBP antibody were flowed over the chip surface at a concentration of 500µM then MBP, MBP-CD81 or MBP-Claudin1 was then injected at a concentration of 750ug/ml. A) Shows the sensogram for anti-MBP injected at the time point indicated by arrow **i**. At arrow **ii** the antibody injection is stopped and either MBP or MBP-CD81 injected. The amount of MBP-CD81 or MBP-Claudin1 bound is determined by subtracting the response units change (ΔRU) observed with MBP between time points **ii** and **iii** from MBP-CD81 or MBP-Claudin1 values. B) Shows an expanded view of the sensorgram between regions ii and iii. C) Shows a table of

the ΔRU for the MBP-CD81 and MBP-Claudin1 binding in the presence of various anti-CD81 antibodies. This data is representative of two independent experiments**.**

**4.5 Anti-Claudin1 modulation of Claudin1-CD81 association(s).**

The results obtained using the panel of anti-CD81 monoclonal antibodies led us to investigate the effects of anti-Claudin1 antibodies on receptor association. The first antibody we obtained was a polyclonal serum produced by the Thomas Baumert group (INSERM, Université de Strasbourg) (253). This polyclonal serum was raised in Wistar rats using a genetic immunisation method and post-immune sera were screened for reactivity with Bosc cells, an Adenovirus 5 transformed 293-T cell line, transduced to express Claudin1. The resulting antiserum recognised epitopes in the extracellular region of Claudin1 (253). We first sought to confirm the specificity of the anti-Claudin1 and to determine which region the antiserum may be binding. To achieve this we performed a FACS based screen using an AcGFP labelled panel of Claudin family members. To act as a negative control a pre-immune serum from the inoculated animal was used. The results, shown in figure 4.7d, show that the polyclonal anti-Claudin1 only recognises AcGFP-Claudin1. The other members of the Claudin family failed to bind the antibody above the background levels observed with the pre-immune serum, with the exception of Claudin17, which showed a low level staining. To assess the region of Claudin1 recognised by the anti-serum we characterised its reactivity with chimeric Claudin1/7 proteins (kind gift of Matt Evans (110)). These chimeric proteins are schematically shown in Figure 4.8 and consist of a Claudin7 backbone encoding the N-terminal third up to residue G49 (N1/3), half up to residue S58 (N1/2), or C-terminal EC1 (C1/2), residues S58 to R82, of Claudin1 (110). Overall the results show that the polyclonal serum specifically recognising the N-terminal third of the Claudin1 EC1 (figure 4.8g).

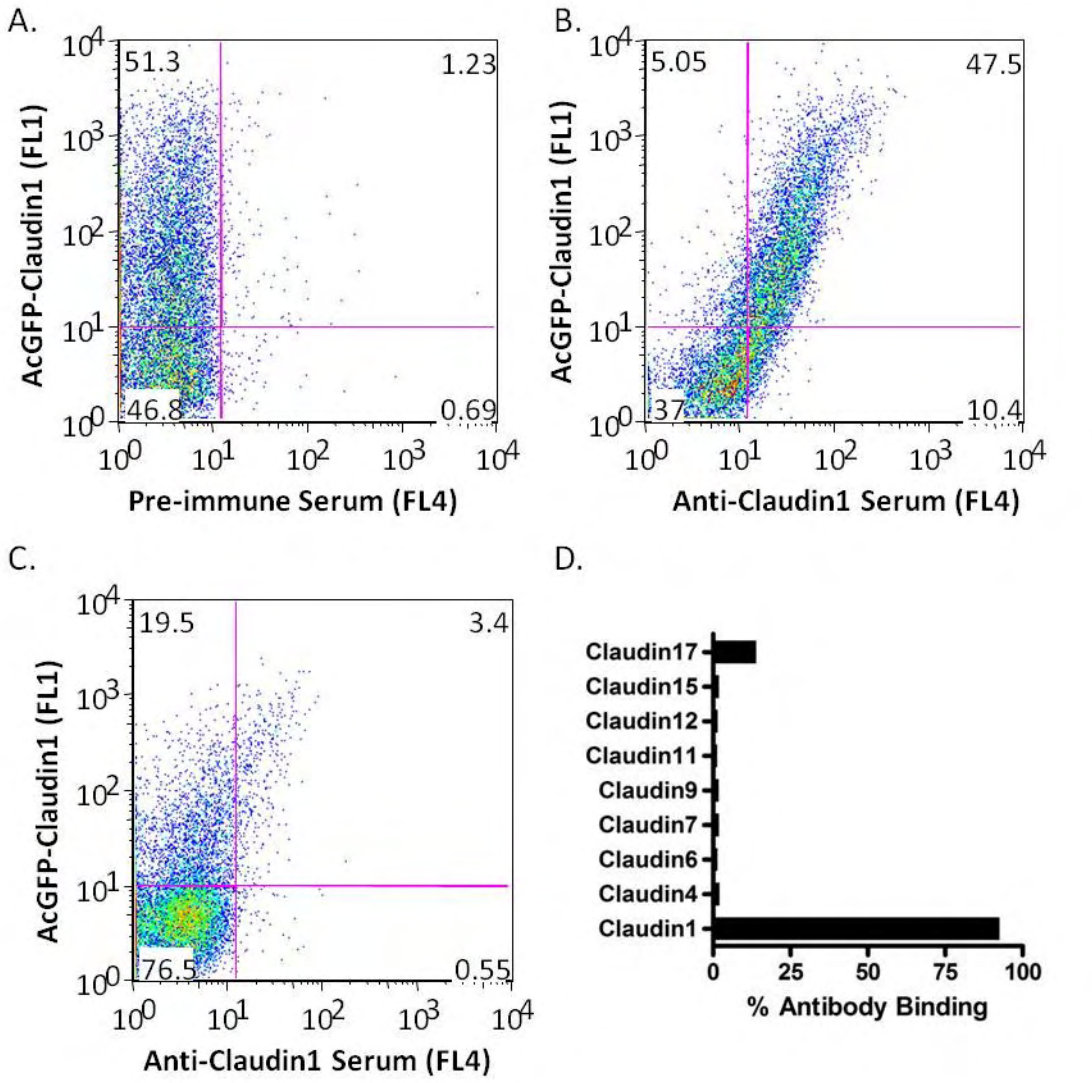


**Figure 4.7: Anti-Claudin1 polyclonal antibody specificity.** 293-T cells were transfected to express a panel of AcGFP labelled Claudin family members. The cells were incubated with a pre-immune serum or with anti-Claudin1 serum at a dilution of 1:100. A) Shows the FACS plot for AcGFP-Claudin1 cells stained with the pre-immune serum, B) the anti-Claudin1 anti-serum. C) shows a FACS plot for anti-serum reactivity with AcGFP-Claudin17 expressing 293T cells. D) Shows the percentage of antibody binding to Claudin positive cells with the thresholds being set by naive 293-T cells. This data is representative of three independent experiments.

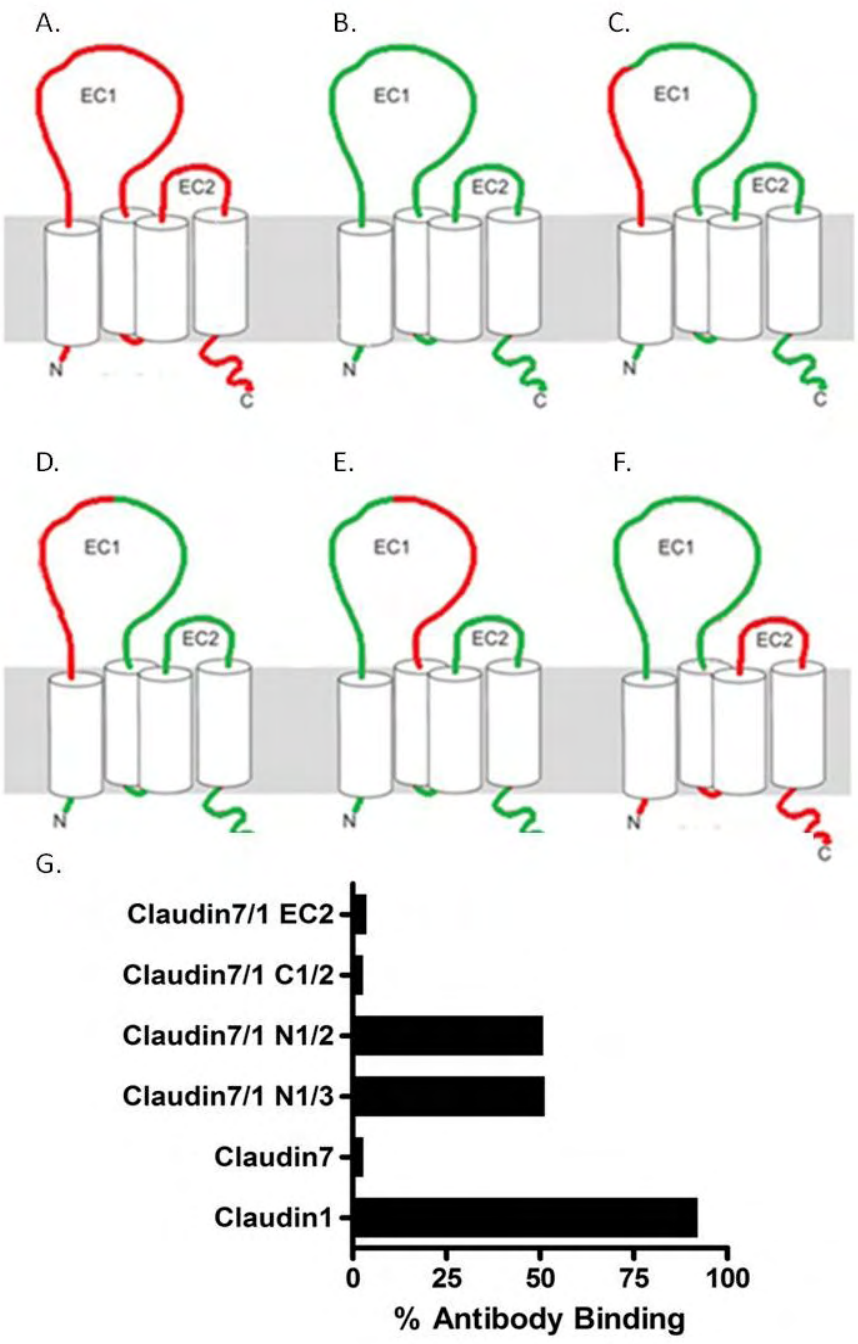


**Figure 4.8: Anti-Claudin1 polyclonal epitope mapping using chimeric Claudin1 and 7 proteins.** 293-T cells were transfected to express fluorophore labelled Claudin1, Claudin 7 or one of the Claudin7/1 chimeras. A schematic diagram of the different chimeras is shown in a-f. A) is Claudin1, B) Claudin 7, C) Claudin 7/1 N1/3, D) Claudin7/1 N1/2, E) Claudin 7/1 C1/2 and F) Claudin 7/1 EC2. G) Shows the level of antibody binding as determined by FACS analysis. This data is representative of two independent experiments.

The anti-Claudin1 antiserum was assessed for its ability to inhibit HCVpp entry and for its effect on Claudin1-CD81 association. The antiserum was incubated with the AcGFP-Claudin1 293-T stable cell line, co-expressing DsRED-CD81, at a dilution of 1:100 or 1:400 for 1hr prior to adding HCVpp of MLVpp. The results show that a 1:100 dilution of anti-Claudin1 reduced HCVpp infection by 87% of the pre-immune serum levels (figure 4.9a). The anti-Claudin1 also had a significant effect on Claudin1 with CD81 association (figure 4.9d). Although the antibody had no effect on FIR values there was a significant dose dependent reduction in Claudin1-CD81 FRET, where the 1:100 dilution reduced FRET from 41.72% ± 5.15 to 6.11% ± 5.37; and the 1:400 dilution reduced FRET to 26.29% ± 8.6. The anti-Claudin1 only affected Claudin1-CD81 association, there was no effect on CD81-CD81 or Claudin1-Claudin1 homodimer associations (figure 4.9c and e, respectively).

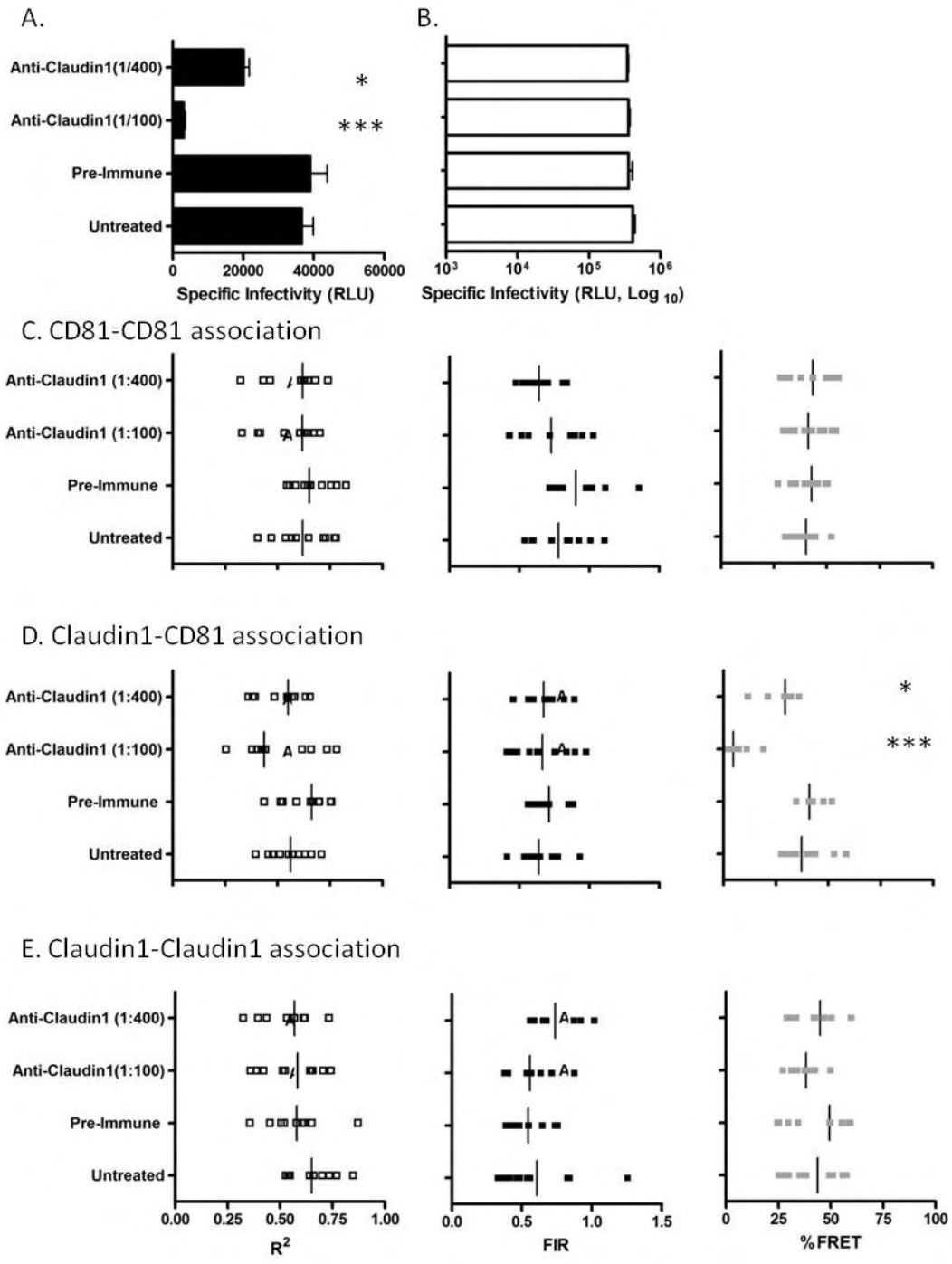
A.
Anti-Claudin1(1/400)
Anti-Claudin1(1/100)
Pre-Immune
Untreated
*
***
0
20000
40000
60000
Specific Infectivity (RLU)
B.
$10^3$
$10^4$
$10^5$
$10^6$
Specific Infectivity (RLU, Log $_{10}$)
C. CD81-CD81 association
Anti-Claudin1 (1:400)
Anti-Claudin1 (1:100)
Pre-Immune
Untreated
D. Claudin1-CD81 association
Anti-Claudin1 (1:400)
Anti-Claudin1 (1:100)
Pre-Immune
Untreated
*
***
E. Claudin1-Claudin1 association
Anti-Claudin1 (1:400)
Anti-Claudin1(1:100)
Pre-Immune
Untreated
0.00
0.25
0.50
0.75
1.00
$R^2$
0.0
0.5
1.0
1.5
FIR
0
25
50
75
100
%FRET

**Figure 4.9: The effect of an anti-Claudin1 serum on viral entry and CD81-CD81, Claudin1-CD81 and Claudin1-Claudin1 association(s).** 293-T cells were transfected to express AcGFP-CD81/DsRED-CD81, AcGFP-Claudin1/DsRED-CD81 or AcGFP-Claudin1/DsRED-Claudin1. These cells were treated with pre-immune serum, a 1:100 or a 1:400 Dilution of anti-CLDN1 polyclonal antibody. The AcGFP-CLDN1/DsRED-CD81 cells were assessed for HCVpp and MLVpp entry (a and b respectively). The association of the C) AcGFP-CD81/DsRED-CD81 homodimer, D) AcGFP-Claudin1/DsRED-CD81 and E) AcGFP-Claudin1/DsRED-Claudin1 were assessed in the presence of the anti-CLDN1 polyclonal. $R^2$, FIR and %FRET values for 10 cells are represented in the dot plots and the median value denoted by the solid vertical line. One way Analysis of Variance and Bonferroni's Multiple Comparison Test was used to determine the degree of significance (*p <0.05, **p <0.01, ***p<0.001). This data is representative of three independent experiments.

Following the production of the polyclonal serum the Baumert group went on to produce a panel of anti-Claudin1 mAbs, from which we were able to obtain 3 different clones (6E1, 7D3 and 8A9) (254). A commercial anti-Claudin1 monoclonal has also recently become available from R&D systems (R+D, Clone no. 421203). As with the polyclonal antibody, we tested the specificity of these clonal antibodies and determined the binding site for each (figure 4.10). All antibodies showed specificity for Claudin1 without binding to other Claudin proteins. As with the polyclonal serum, Claudin17 showed a low level binding of mAbs 6E1, 7D3, 8A9 and R&D. The Claudin7/1 chimeras indicate that all Claudin1 mAbs bind to the N-terminal third of the EC1 loop.

The anti-Claudin1 monoclonal antibodies were assessed for their ability to inhibit HCVpp entry and to perturb Claudin1-CD81 association. All of the antibodies significantly reduced HCV entry without affecting MLVpp infection at a final concentration of 67µM (figure 4.11a and b respectively), with mAbs 6E1, 7D3, 8A9 and R+D inhibiting HCVpp by 57%, 42%, 60%, and 41%, respectively. This level of reduction was similar to that published for the antibodies (254). The authors did show a further reduction in pseudoparticle entry at higher antibody concentrations of 670µM (254).

The anti-Claudin1 mAbs had no effect on CD81-CD81 homodimers but significantly disrupted Claudin1-CD81 association (figure 4.11c and d respectively). The FIR value for the mAbs 6E1, 7D3, 8A9 and the R+D was 0 (0-0.41), 0.2 (0-0.8), 0 (0-0.42) and 0.66 (0-1.18), respectively compared to an untreated control of 0.7248 (0.6 - 0.9). 6E1 and 8A9 showed a significant difference in the FIR value compared to the untreated control, there was also a reduction in the 7D3 gradient. The R+D antibody seemed to cause an increase in the inter-quartile range compared to the untreated cells, which although the median value was

similar the association is less well defined. All these results are in contrast to that shown for the polyclonal rat serum, which showed no effect on the FIR value. All of the antibodies led to a significant reduction in Claudin1-CD81 FRET of 7.3% ± 12.35, 9.28% ± 12.51, 9.6% ± 16.0 and 10.66% ± 14.08 for mAbs 6E1, 7D3, 8A9 and R+D, respectively).

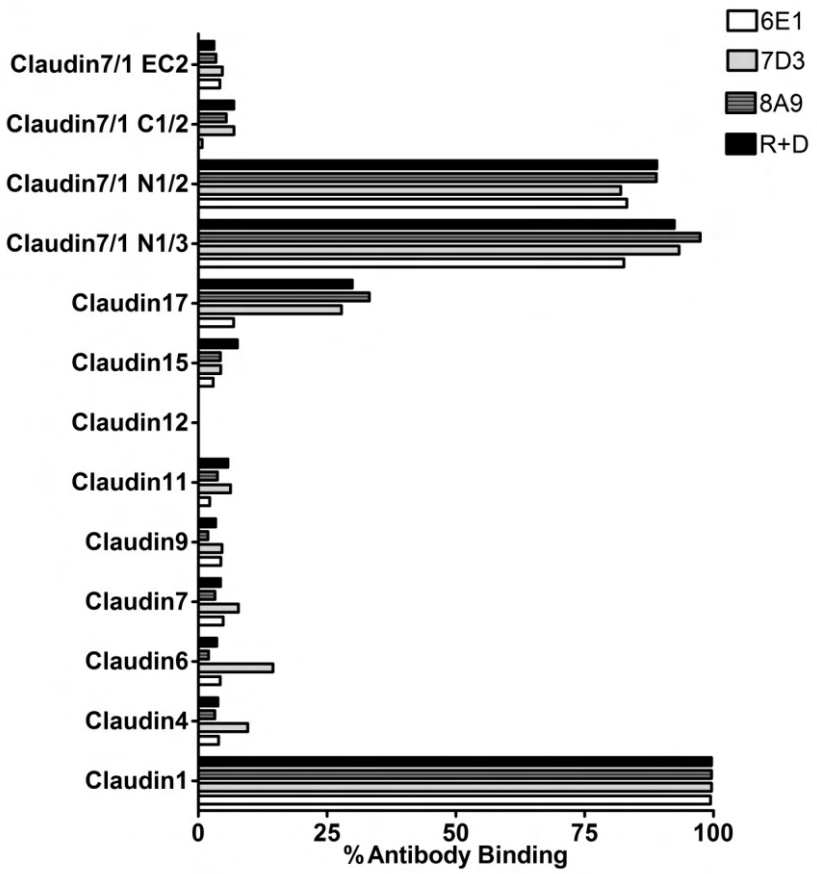


**Figure 4.10: Anti-Claudin1 mAb specificity.** 293-T cells were transfected to express a panel of AcGFP labelled Claudin family members and Claudin7/1 Chimeras. The cells were incubated with anti-Claudin1 monoclonal antibodies at a concentration 67µM. The bar chart shows the percentage of antibody binding,that is the percentage of cells positive for Claudin antibody binding, with the thresholds being set by naive 293-T cells. This data is representative of two independent experiments.

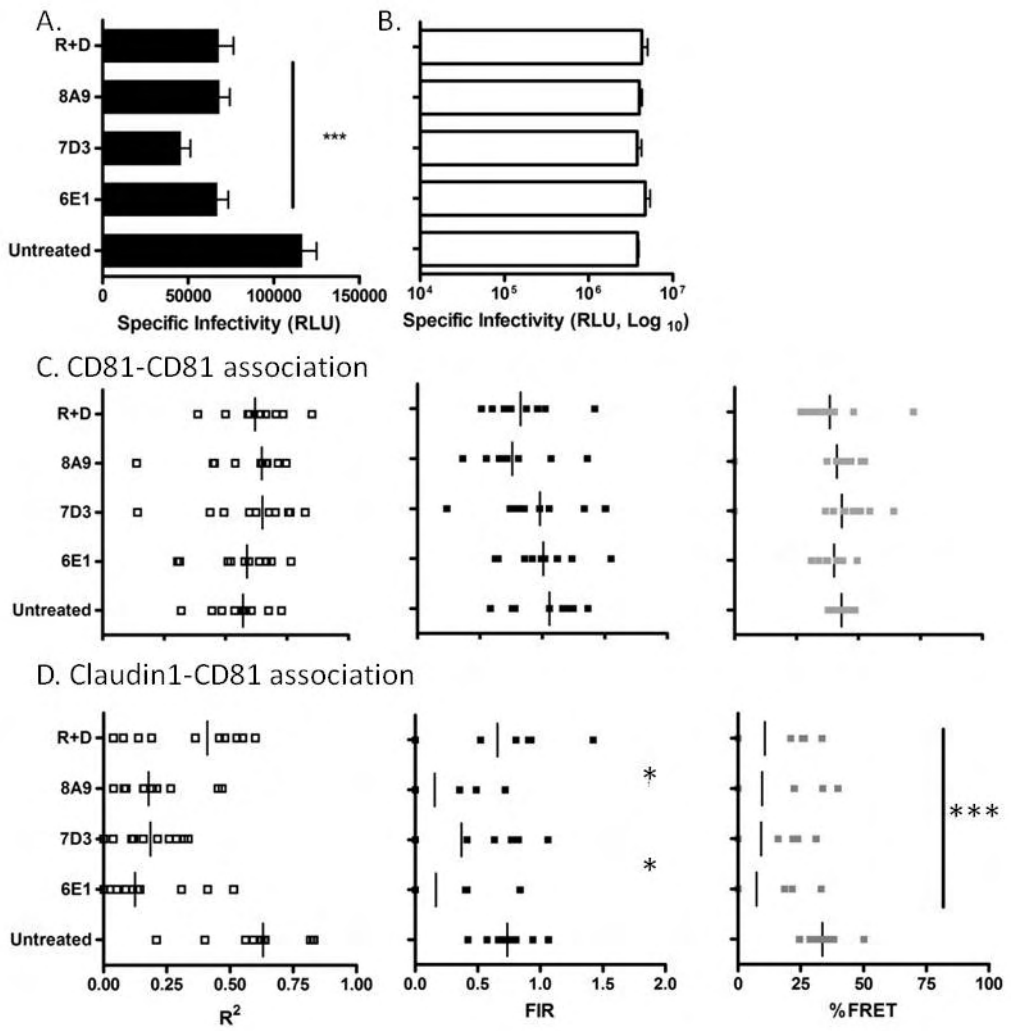


**Figure 4.11: The effect of anti-Claudin1 monoclonal antibodies on viral entry and CD81-CD81 and Claudin1-CD81 association(s).** 293-T cells were transfected to express AcGFP-CD81/DsRED-CD81, AcGFP-Claudin1/DsRED-CD81 or AcGFP-Claudin1/DsRED-Claudin1. The cells were treated with the various anti-CLDN1 mAbs at a concentration of 67µM for 1hr at 37$^{o}$C. AcGFP-CLDN1/DsRED-CD81 cells were assessed for HCVpp and MLVpp entry (A and B respectively). The association of the C) AcGFP-CD81/DsRED-CD81 homodimer and D) AcGFP-Claudin1/DsRED-CD81 heterodimer were assessed in the presence of the Anti-CLDN1 mAb. The $R^2$, FIR and FRET values for 10 cells are represented in the dot plots and the median value is denoted by a solid vertical line. One way Analysis of Variance and Bonferroni's Multiple Comparison Test was used to determine the degree of significance (*p <0.05, **p <0.01, ***p<0.001). This data is representative of two independent experiments.

## 4.6 Discussion

The observation that only receptor-active Claudins associate with CD81 provides supporting evidence for a role of these protein complexes in HCV entry. To further explore the conditions in which these complexes exist and whether disruption of the complexes limits HCV entry we studied the effects of cell polarization and receptor specific antibodies on receptor association. The major reservoir supporting HCV replication *in vivo* is thought to be hepatocytes in the liver. Hepatocytes are polarized and the results shown so far are for Claudin1-CD81 association in non-polarised 293-T cells. We therefore needed to extend our investigation to study Claudin1-CD81 association in a polarised cell.

Hepatocytes polarise with at least two basal surfaces facing the circulation and a branched network of grooves between adjacent cells that constitute the apical or bile canalicular surface (255). Tight junction strands encircle the apical region and comprise multiple transmembrane, scaffolding, and signalling proteins (reviewed in (191)). We recently reported Claudin1 expression at basolateral and apical hepatocyte membranes in normal liver tissue (256) and in polarized HepG2 cells, with an enrichment at tight junction associated apical sites (179). To investigate the presence and location of receptor complexes in the polarized HepG2 hepatoma cell line, we transduced HepG2 cells to stably express AcGFP- and DsRED-tagged versions of Claudin1 and CD81. Claudin1 was found to associate with basolateral pools of Claudin1 and CD81 with reduced FRET values (36 and 25%, respectively) compared with 293T cells, most likely representing competition from endogenous Claudins, as previously reported (184). The polarised cells have large pools of Claudin1 at the tight junction region, identified by ZO-1 staining, with CD81 being largely excluded from these apical sites and exhibiting a minimal association with Claudin1 (figure

1.7). HCV enters the liver via the sinusoidal blood, and so the virus is most likely to encounter receptors expressed on the sinusoidal or basal surface of the hepatocyte. Our current data, showing that Claudin1 receptor activity associates with the formation of Claudin1-CD81 complexes at the basolateral surface of polarized hepatoma cells, support a model where virus engagement of Claudin1-CD81 complexes at the basal membrane may initiate the particle internalization process (184). At present it is unknown whether any of the viral receptors, including CD81 and Claudin1, are endocytosed with HCV, and further research on the trafficking and endocytic routing of receptor complexes and virus particles in polarized hepatocytes is required to fully appreciate the entry process of HCV.

A previous publication reported that the level of host cell cholesterol directly impacted on HCV entry (249). As tetraspanin protein interactions are known to be modulated by cholesterol (249-251), we assessed whether depletion of cholesterol had any effect on Claudin1-CD81 association. Depleting cholesterol with methyl-β-cyclodextrin significantly reduced Claudin1-CD81 association (from 45.63% ±8.514 to 22.14% ± 28.65), whereas the CD81-CD81 association was unaffected. The Claudin1-CD81 association was restored when cholesterol was re-introduced into the cell. These results suggest that observations by Kapadia et al could be due to the removal of the Claudin1-CD81 complex preventing HCV entry. The authors showed that the level of expression of CD81 is lowered (249). Koutsoudakis et al have reported that there is a threshold level of CD81 required for entry to occur (257). We however found that the level of CD81 remains constant, with slight drop in the levels of Claudin1 at the cell surface. The use of different cell lines and detection methods may account for the different observations.

The observation that recombinant forms of MBP-Claudin1 EC1 and MBP-CD81 EC2 associate demonstrates a role for these domains in defining protein receptor complexes. Our group cloned a number of anti-CD81 mAbs that recognise conformational epitopes in EC2, providing tools to probe the domains of CD81 associating with Claudin1. All of the anti-CD81 monoclonal antibodies reduced FRET between CD81 and Claudin1 and yet had minimal impact on CD81-CD81 interactions (figure 4.4), which were verified by BIAcore (figure 4.6) The CD81 in both the FRET and Biacore are in an oligomeric form, CD81 is known to dimerise and this is required for HCV entry (120, 152). A Fab fragment of one antibody, 2s66, had minimal effects on the Claudin1-CD81 association suggesting that cross-linking of CD81 may be necessary to perturb the CD81 association with Claudin1 (figure 2.4 and 2.5). As the Fab fragment could still neutralise viral entry, albeit at a significantly lower titre, we can only suggest that disruption of the Claudin1-CD81 complex contributes but may not be the main mechanism of inhibition of viral entry for this antibody. Whether the cross linking of the CD81 dimers is required for the antibodies to prevent the interaction of Claudin1 with CD81 is unknown. Without a detailed idea of the antibody binding site it is unknown whether the steric hindrance is negated by the smaller size of the Fab fragment, whereas the larger IgG may be large enough to perturb the interaction. One would assume that the lack of effect on the homotypic interaction and the perturbation of the Claudin1-CD81 interaction demonstrate that the antibodies are directed to regions responsible for Claudin1 interactions. Using the BIAcore technology we are able to look at the interaction of Claudin1 with CD81 in isolation but this comes with a cost. The recombinant proteins are not full length proteins and are unlikely to be constrained by the same physical environment as the plasma membrane. The tethering of extracellular loops of the full length proteins by their transmembrane domains may lead to a different confirmation of the loops. The FRET allows

for the study of the interaction in the natural environment but with the unknown of other interacting proteins. The results from the two techniques have demonstrated the interaction of the two proteins.

In addition to the anti-CD81 antibodies we were also able to test a number of anti-Claudin1 antibodies. These antibodies could also inhibit viral entry and were shown to perturb the Claudin1-CD81 association. The binding of the anti-Claudin1 antibodies to the N-terminal 3$^{rd}$ of the Claudin1 EC1 indicate this is the region may be involved in interactions with the EC2 of CD81. The polyclonal anti-Claudin1 has been reported to inhibit E2 protein and HCV particle binding to Huh7.5.1 cells, with E1 still binding to the cell (253). Given the limited information supporting a role for Claudin1 to directly associate with virus these results are somewhat unexpected. The interaction of HCV with CD81 has been demonstrated to be independent of Claudin1 (153, 258) with the anti-Claudin1 mAbs causing a dissociation of the Claudin1-CD81 complex that would make it unlikely the antibodies are inhibiting the interaction of the virus with CD81.

Overall the results demonstrate that the perturbation of the Claudin1-CD81 complex by cholesterol depletion and specific antibodies prevents viral entry. We hypothesise that Claudin1 modulates CD81 interactions with the virus that promote virus internalization. The interaction of proteins may occur between the N-terminal 3$^{rd}$ of Claudin1 with specific regions on the CD81 EC2.

# Chapter 5:

# Identification of the Claudin-CD81 interface by site directed mutagenesis

In the previous chapter we demonstrated that Claudin1 association with CD81 was disrupted by various treatments which reduced HCV infection, supporting a role for the co-receptor complex in virus entry. To ascertain whether Claudin1 association with CD81 is essential for HCV infection we studied the interaction of several published and newly generated receptor inactive mutants. Evans et al reported that specific residues in the EC1 of Claudin1 and Claudin7 which, when interchanged, could alter the protein's ability to act as a co-receptor. Claudin 1 and 7 differ in 5 residues within the EC1 loop, with two of these residues being the determining factor for receptor activity (110). Claudin1 encodes an isoleucine and a glutamic acid at positions 32 and 48, respectively. A single change to methionine at position 32 or lysine at position 48, encoded in Claudin7, reduced the proteins ability to act as a co-receptor, with a double mutant rendering the protein receptor inactive. The reverse was observed when Claudin7 residues were mutated to encode the Claudin1 amino acids (110). Since Claudin1 EC1 interacts with CD81 and the anti-Claudin1 antibodies that perturb co-receptor association bind to the same region we hypothesized that these residues could play a direct role in Claudin1 association with CD81. We first sought to demonstrate the effect(s) of receptor inactivating mutations on Claudin1 association with CD81 and secondly to define the residues in the two proteins that are essential for this interaction.

**5.1 Localisation and antigenicity of fluorophore labelled Claudin1 and 7 mutants**

First we fluorophore labelled the mutant proteins and expressed them in 293-T cells to assess their localisation (figure 5.1). Wild type Claudin1 shows a strong staining pattern at the plasma membrane, whilst Claudin7 has a more punctuate appearance. The Claudin1 I32M/E48K mutation causes the protein to have a Claudin7-like phenotype with punctuate regions at the plasma membrane and increased intracellular pools. The single mutation of Claudin1 at the I32M or E48K positions induces an intermediate phenotype, although the I32M mutant appears to be closer to a Claudin7 phenotype. Mutation of Claudin7 caused the protein to localise in a more Claudin1 phenotype. The single mutations of M32I and K48E again produced an intermediate phenotype with the double mutant showing a more uniform localisation at the plasma membrane.

The antigenicity of the mutant proteins was assessed using the panel of anti-Claudin1 antibodies (figure 5.2). 293-T cells transduced to express wild type and mutant Claudin1 and Claudin7 proteins, were stained with anti-Claudin1 polyclonal and anti-Claudin1 6E1, 7D3, 8A9 and R+D monoclonal antibodies (figure 5.2). As shown in the previous chapter the antibodies showed a high level of binding to Claudin1 wild type protein. The Claudin1 I32M mutant also showed a high level of binding, equivalent to that of wild type. Mutating Claudin1 at position 48 from a glutamic acid to a lysine prevented the binding of the antibodies. As the antibodies are shown to bind within the N-terminal third of the protein, their inability to bind Claudin1 with this mutation could be due to this amino acid being part of the antibody epitope. The Claudin7 K48E mutant showed a low level of binding with two anti-Claudin 1 antibodies: 7D3 and 8A9 monoclonal antibodies bound 17% and 33% of cells. The Claudin7 M32I/K48E double mutant showed higher levels of binding for these two

antibodies, 32% for 7D3 and 50% for 8A9, with the polyclonal anti-Claudin1 binding to 33% of the cells. The ability of the M32I mutation in Claudin7 to increase the level of binding of the antibodies is a little unexpected as the corresponding mutation in Claudin1 had no effect on antibody binding. However, the amino acid sequence of Claudin1 and Claudin7 differ in the N-terminal third at five positions in total (residues 31, 32, 33, 41 and 48). The M32I change in the context of the flanking glutamine at position 31 and serine at position 33 could favourably alter the structure to improve the availability of this antibody epitope.

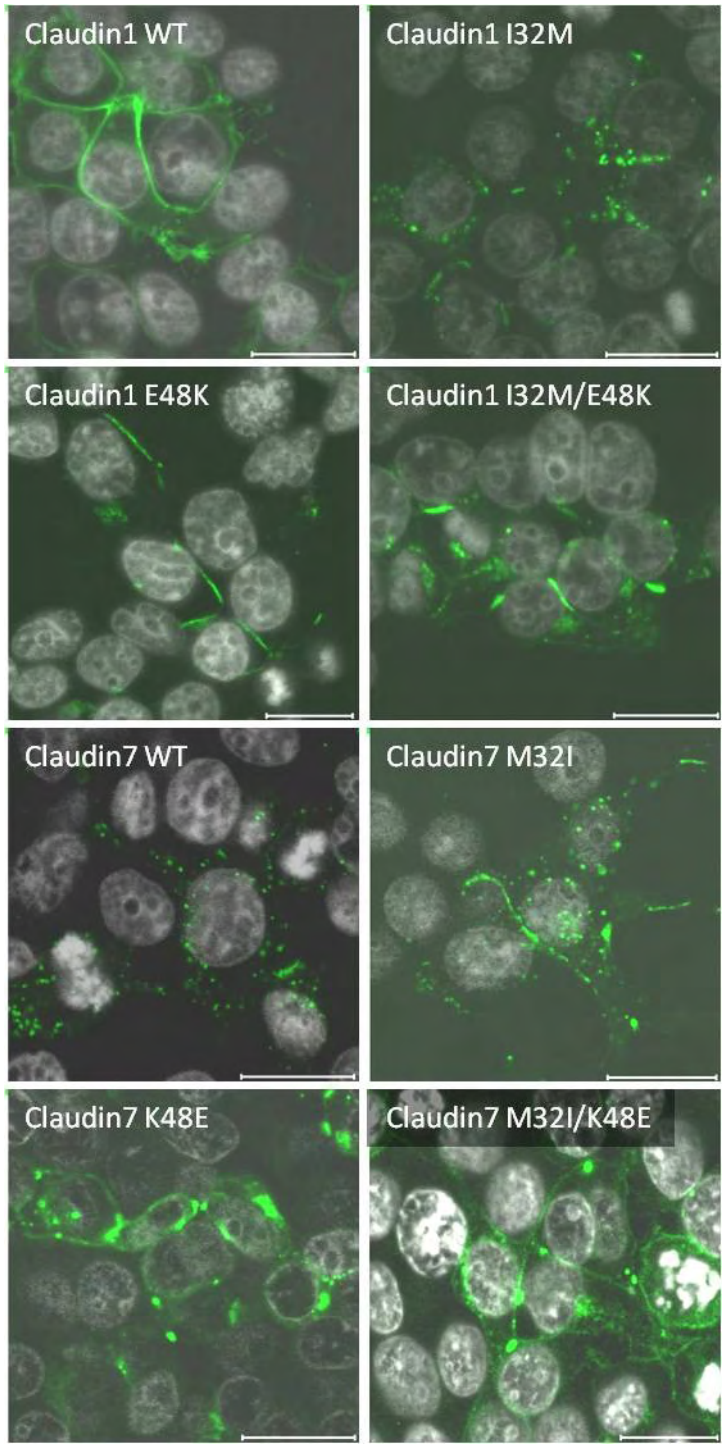


**Figure 5.1: Localisation of fluorophore labelled Claudin1 and 7 mutant proteins.** 293-T cells were transfected with the various Claudin1 and 7 mutants, which contain an AcGFP epitope fused to the N-terminus. Images produced are laser scanning confocal images taken using a 63 x 1.2NA water immersion objective and a meta head confocal microscope (Zeiss). Size bars are equal to 20µm**.** This data is representative of two independent experiments.

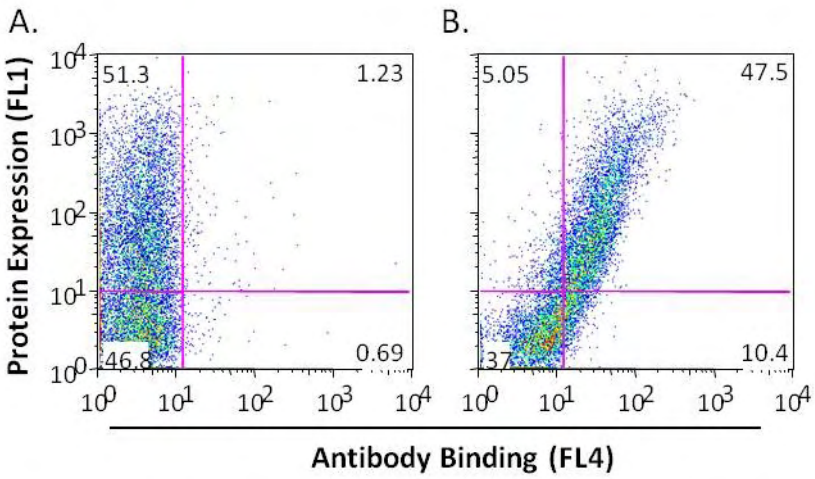


C.

| | Anti-Claudin1 (%Binding) | | | | |
|---|---|---|---|---|---|
| | Polyclonal | 6E1 | 7D3 | 8A9 | R+D |
| Claudin1 | 91 | 93 | 98 | 99 | 98 |
| Claudin1 I32M | 91 | 95 | 98 | 97 | 95 |
| Claudin1 E48K | 6 | 5 | 4 | 3 | 5 |
| Claudin1 I32M/E48K | 5 | 6 | 2 | 3 | 4 |
| Claudin7 | 1 | 9 | 6 | 6 | 7 |
| Claudin7 M32I | 1 | 7 | 5 | 3 | 4 |
| Claudin7 K48E | 3 | 4 | 17 | 33 | 4 |
| Claudin7 M32I/K48E | 32 | 5 | 32 | 50 | 4 |

**Figure 5.2: Antigenicity of Claudin1 and 7 mutants.** 293-T cells were transfected to express a panel of AcGFP labelled Claudin1 and Claudin7 mutants. The cells were incubated with the anti-Claudin1 polyclonal antibody at a concentration of 1:100, or with the panel of anti-Claudin1 monoclonal antibodies at a concentration 67µM. A) Shows the FACS plot of the AcGFP-Claudin1 wild type cells incubated with the Rat pre-immune serum, realized with an Alexaflour 633 anti-Rat IgG. B) shows the same cells stained with the anti-Claudin1 polyclonal serum, 51% of cells expressed AcGFP-Claudin1, the anti-Claudin1 polyclonal serum bound to 91% of these cells (47.5%/51.3%), similar pairs of FACS plots were obtained for each of the mutant expressing cell lines (data not shown) C) The table shows the percentage of antibody binding to cells that are expressing the Claudin protein. This data is representative of two independent experiments.

### 5.2 Receptor activity of labelled Claudin1 and Claudin7 mutant proteins

Having assessed protein localisation and antigencitiy we evaluated the ability of the mutant proteins to support HCVpp entry. The Claudin1 wild type demonstrated a robust level of entry with a mean RLU of 24013 ± 1794. All mutations in Claudin1 reduced HCVpp entry to the level observed for naive 293-T negative control. In contrast, mutations in Claudin7 showed a marked increase in receptor activity. The mutants showed entry levels of 49.9%, 62.7% and 68.2% for the M32I, K48E and M32I/K48E respectively, compared to the entry mediated by the wild type Claudin1. Interestingly the Claudin1 E48K and Claudin7 K48E have similar levels of entry, suggesting that mutation of this residue has a greater ability to change the receptor activity of Claudin7 than of Claudin1.

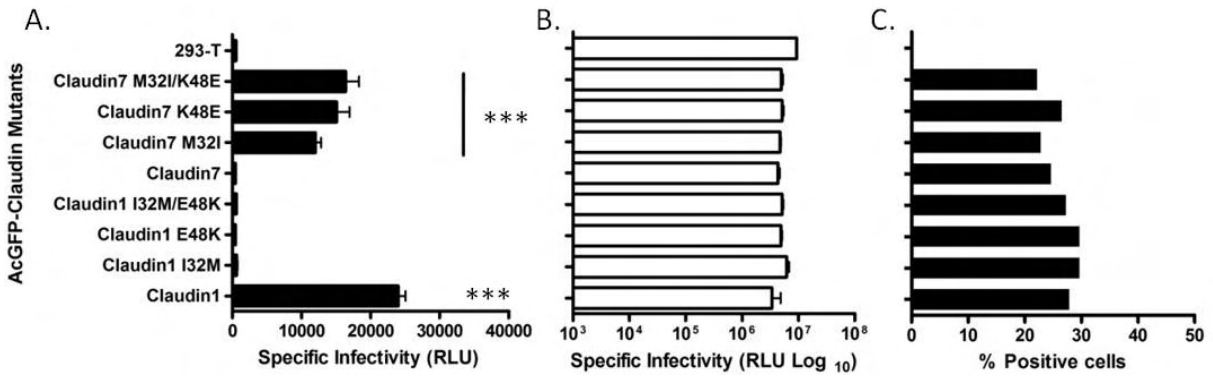


**Figure 5.3: Viral receptor activity of fluorophore labelled Claudin1 and Claudin7 mutants.** 293-T cells were transfected to express AcGFP-Claudin1 and Claudin7 mutants and their ability to support HCVpp and MLVpp entry assessed. Data is represented as specific infectivity (Relative Light Units, RLU) and represents the mean plus the standard error of three replicates. A) Shows the specific infectivity of HCVpp. B) shows the specific infectivity of MLV. C) Shows the percentage of the cells expressing Claudin as determined by FACS analysis. A One way Analysis of Variance with a Bonferroni's Multiple Comparison Test was used to determine the degree of significant difference from the naive 293-T negative control (***$p<0.001$). This data is representative of two independent experiments.

## 5.3 Homotypic association of Claudin mutants and their association with CD81 and Occludin

Analysis of the panel of AcGFP-Claudin mutants for their association with DsRED-CD81 and DsRED-Occludin was performed using the FIR and FRET methodologies. The results are shown in figure 5.3 and table 5.1. AcGFP-CLDN1 and AcGFP-CLDN7 wild-type proteins showed the expected high and low FIR values with CD81 and Occludin, as previously observed (Table 1). Interestingly, the two mutations in CLDN1 (I32M and E48K), either alone or in combination, abrogated any association with CD81 or Occludin. Consequently, no FIR value or %FRET could be assigned to the mutants for the CD81 or Occludin interaction. In contrast, both the single and double complementary changes in CLDN7 (M32I, K48E and M32I/K48E) resulted in a mutated molecule that showed a clear association with CD81 (17% ± 18.45, 25.32% ± 25.83 and 40.5% ± 16.62 %FRET for M32I, K48E and M32I/K48E, respectively). These %FRET values were not significantly different from those seen for Claudin1-CD81 association. Interestingly, the mutations did not promote Claudin7 association with Occludin, suggesting that direct Claudin-Occludin interactions are not required for Claudin receptor activity.

In order to perform their barrier function Claudins form strands within the plasma membrane of a cell. These *cis*-interactions occur in addition to the *trans*-interacts with Claudins on opposing cells (170, 172). To determine whether the mutations affect protein cis-interactions we assessed their ability to form homo-dimers. We found that both wild type Claudin1 and Claudin7 can form homodimers (figure 5.3 and table 5.1), with %FRET values ranging from 12 – 29%, with only Claudin1 I32M/E48K double mutant (12.38% ±

11.02) showing a significant reduction in %FRET relative to the wild type protein (29% ± 5.97).

Evans and colleagues reported that the interchange of amino acid residues at positions 32 (I/M) and 48 (E/K) rendered Claudin1 inactive and Claudin7 active for infection, however the authors did not attempt to elucidate the mechanism(s) by which this loss arose. The results obtained here demonstrate that mutations in Claudin1 abrogate CD81 association. In contrast, mutations in Claudin7 have the reverse effect promoting a Claudin7-CD81 receptor complex. Although the Claudin1 mutants lost their association with Occludin there was no equivalent gain of association for the Claudin7 mutants, leading us to suggest that direct Claudin-Occludin association is not essential for viral receptor function.

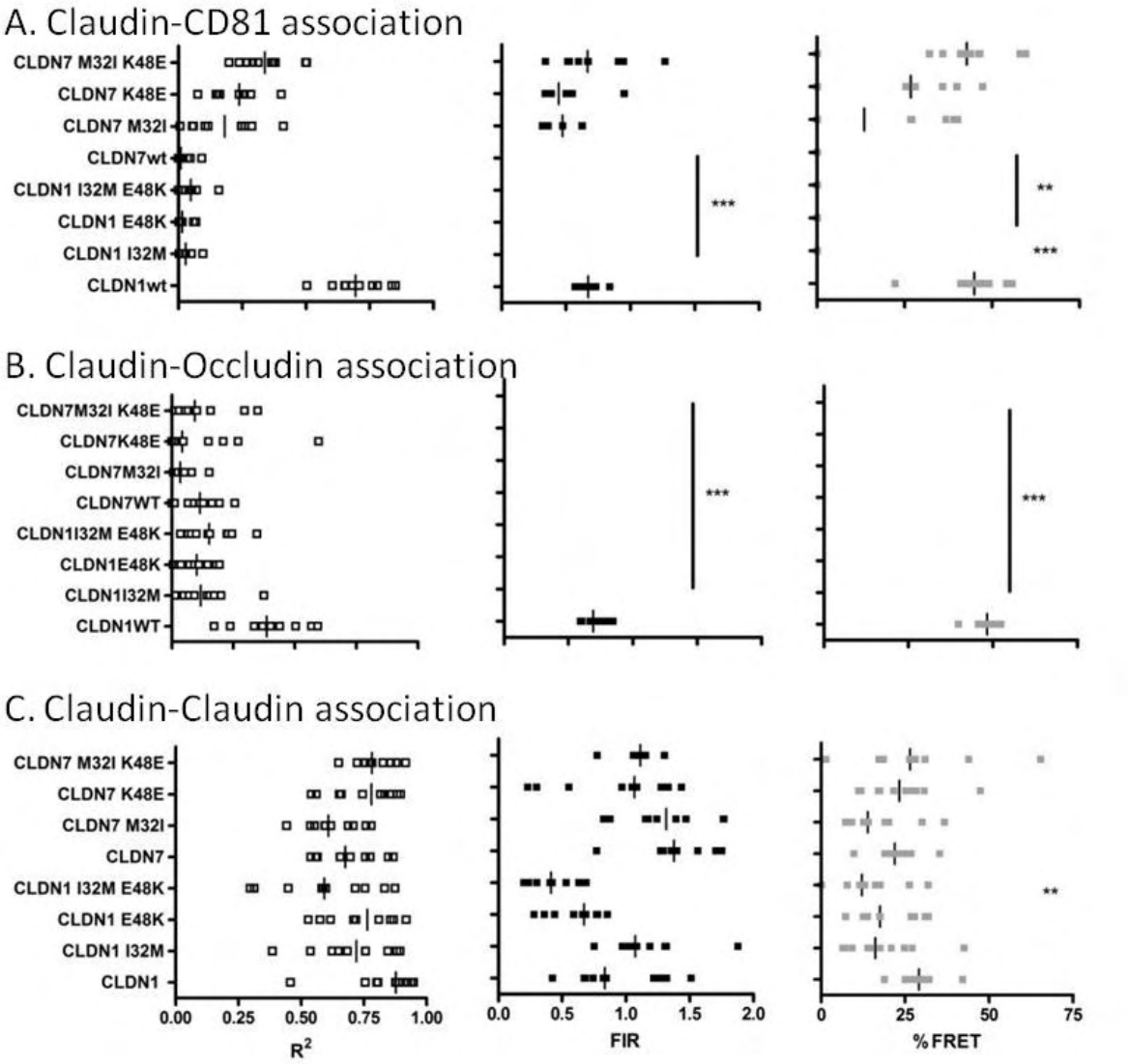


**Figure 5.4: Effect(s) of Claudin1 and Claudin7 EC1 mutations on CD81 and Occludin association.** 293T cells were transfected to express fluorescence-tagged mutant forms of AcGFP-Claudin and either DsRED-CD81 (A) or DsRED-Occludin (B), and the degree of association between fluorophore-tagged proteins assessed by FIR and FRET analysis. C) 293T cells were transfected with AcGFP- and DsRED-tagged versions of Claudin constructs to assess the effect of EC1 mutations on Claudin-Claudin cis-interactions. Median FIR and FRET values from ten individual cells are presented (*p<0.05, **p<0.01, ***p<0.001). This data is representative of two independent experiments.

Table 5.1 Fluorescent tagged Claudin mutant homotypic associations and heterotypic associations with CD81 and Occludin.

| | $R^2$ (IQR)* | FIR (IQR) | %FRET ± sd# |
|---|---|---|---|
| *CD81 association with:* | | | |
| Claudin1 | 0.695 (0.63 - 0.81) | 0.673(0.62 - 0.73) | 44.59 ± 9.18 |
| Claudin1 I32M | 0.029 (0.02 - 0.07) | ND | ND |
| Claudin1 E48K | 0.015 (0.01 - 0.06) | ND | ND |
| Claudin1 I32M/E48K | 0.049 (0.01 - 0.11) | ND | ND |
| Claudin7 | 0.009 (0.01 - 0.04) | ND | ND |
| Claudin7 M32I | 0.182 (0.05 - 0.28) | 0.475(0.34 - 0.63) | 17 ± 18.45 |
| Claudin7 K48E | 0.239 (0.15 - 0.27) | 0.444(0.36 - 0.75) | 25.32 ± 25.83 |
| Claudin7 M32I/K48E | 0.339 (0.26 - 0.44) | 0.668(0.52 - 0.93) | 40.5 ± 16.62 |
| *Occludin association with:* | | | |
| Claudin1 | 0.386 (0.29 - 0.54) | 0.692 (0.6 - 0.82) | 47.85 ± 3.41 |
| Claudin1 I32M | 0.117 (0.05 - 0.19) | ND | ND |
| Claudin1 E48K | 0.101 (0.03 - 0.16) | ND | ND |
| Claudin1 I32M/E48K | 0.151 (0.07 - 0.24) | ND | ND |
| Claudin7 | 0.114 (0.04 - 0.18) | ND | ND |
| Claudin7 M32I | 0.034 (0.01 - 0.07) | ND | ND |
| Claudin7 K48E | 0.043 (0.00 - 0.24) | ND | ND |
| Claudin7 M32I/K48E | 0.093 (0.04 - 0.23) | ND | ND |

| | | | |
|---|---|---|---|
| *Homotypic association with:* | | | |
| Claudin1 | 0.8771 (0.78 - 0.93) | 0.835(0.67 - 1.29) | 29 ± 5.97 |
| Claudin1 I32M | 0.7204 (0.58 - 0.86) | 1.076(0.98 - 1.31) | 18.39 ± 11.03 |
| Claudin1 E48K | 0.7642 (0.59 - 0.86) | 0.673(0.41 - 0.78) | 19.95 ± 8.68 |
| Claudin1 I32M/E48K | 0.5928 (0.38 - 0.79) | 0.413(0.22 - 0.58) | 12.38 ± 11.02 |
| Claudin7 | 0.6758 (0.56 - 0.81) | 1.379(1.28 - 1.73) | 22.31 ± 6.4 |
| Claudin7 M32I | 0.6078 (0.55 - 0.73) | 1.318(1.02 - 1.77) | 17.55 ± 9.29 |
| Claudin7 K48E | 0.7805 (0.61 - 0.87) | 1.067(0.43 - 1.31) | 23.74 ± 10.7 |
| Claudin7 M32I/K48E | 0.7822 (0.74 - 0.87) | 1.116(1.07 - 1.15) | 28.67 ± 17.93 |

* – Interquartile range

# – Standard deviation

ND – Not Determined

### 5.4 Mammalian two-Hybrid assessment of Claudin1 and Claudin7 interaction with CD81

To confirm the effect of Claudin1 and Claudin7 mutants on CD81 association we utilised a mammalian-two hybrid system (Checkmate mammalian two-hybrid system, Promega). This technique has been previously used to demonstrate the specific region of the cyclin-dependent kinase (CDK) CDK4 that binds human T-cell leukemia virus type 1 (HTLV-1) oncoprotein Tax (259). De Jong et al used the same system to demonstrate multimerisation of the 2B, 2C and 2BC proteins of coxsackievirus (260). Lwa et al demonstrated the interaction of the human guanine nucleotide binding protein beta subunit 5L (GNbeta5) and HBX protein of hepatitis B virus within HepG2 cells (261). Accurate measurement of protein interactions is derived from a familiar yeast 2-hybrid design, optimised for use in mammalian systems. In brief, a reporter plasmid containing a GAL4 binding domain can be induced to express Firefly Luciferase via the transcriptional activation domain of herpes virus VP16 protein. This reporter plasmid, pG5luc is co-transfected with plasmids encoding the two proteins of interest. The pBind plasmid will express one protein fused to the DNA-binding domain of GAL4 and pACT vector expresses a second protein fused to a transcriptional activation domain of VP16. An interaction between the two fusion proteins will result in the VP16 domain inducing the expression of Firefly Luciferase as a reporter for protein-protein interactions.

The CD81 protein was cloned into pBind plasmid with Claudin1 and Claudin7 mutants expressed in pACT plasmid. The pBind-CD81 and the pACT-Claudin1 or Claudin7 plasmids were co-transfected, along with the pG5luc, into 293-T cells and the firefly luciferase activity assessed after 48 hours. To assess the background noise, which could be caused by leaky

expression of the Firefly luciferase the pBind-CD81 was co-transfected with the pBind-MyoD plasmids for which no interaction should occur. The results for the various Claudin1 mutants are shown in figure 5.5b. Only Claudin1 showed a specific interaction with CD81 as indicated by a mean RLU of $3.86x10^7 \pm 0.079$, which was significantly above the RLU of $3.78x10^5 \pm 0.012$ for the pACT-MyoD negative control. The I32M, E48K and I32M/E48K Claudin1 mutants showed RLU levels of $1.225x10^6 \pm 0.108$, $1.334\ x10^6 \pm 0.012$ and $0.8095\ x10^6 \pm 0.053$, respectively, which are not significantly different for the negative control and therefore not interacting with the CD81. As shown in figure 5.5c, Claudin7 does not interact with CD81 as the RLU level of $6.5x10^5 \pm 0.133$ is not significantly different from the negative control. In contrast M32I, K48E and M32I/K48E mutants interact with the CD81 as the RLU levels are significantly above the negative control ($2.16x10^7 \pm 0.152$, $2.98\ x10^7 \pm 0.137$ and $3.52x10^7 \pm 0.075$, respectively). The results confirm that only Claudin1 and Claudin7 mutants interact directly with CD81. Overall these results are in agreement with the FIR and FRET imaging results (shown in figure 5.4 and table 5.1).

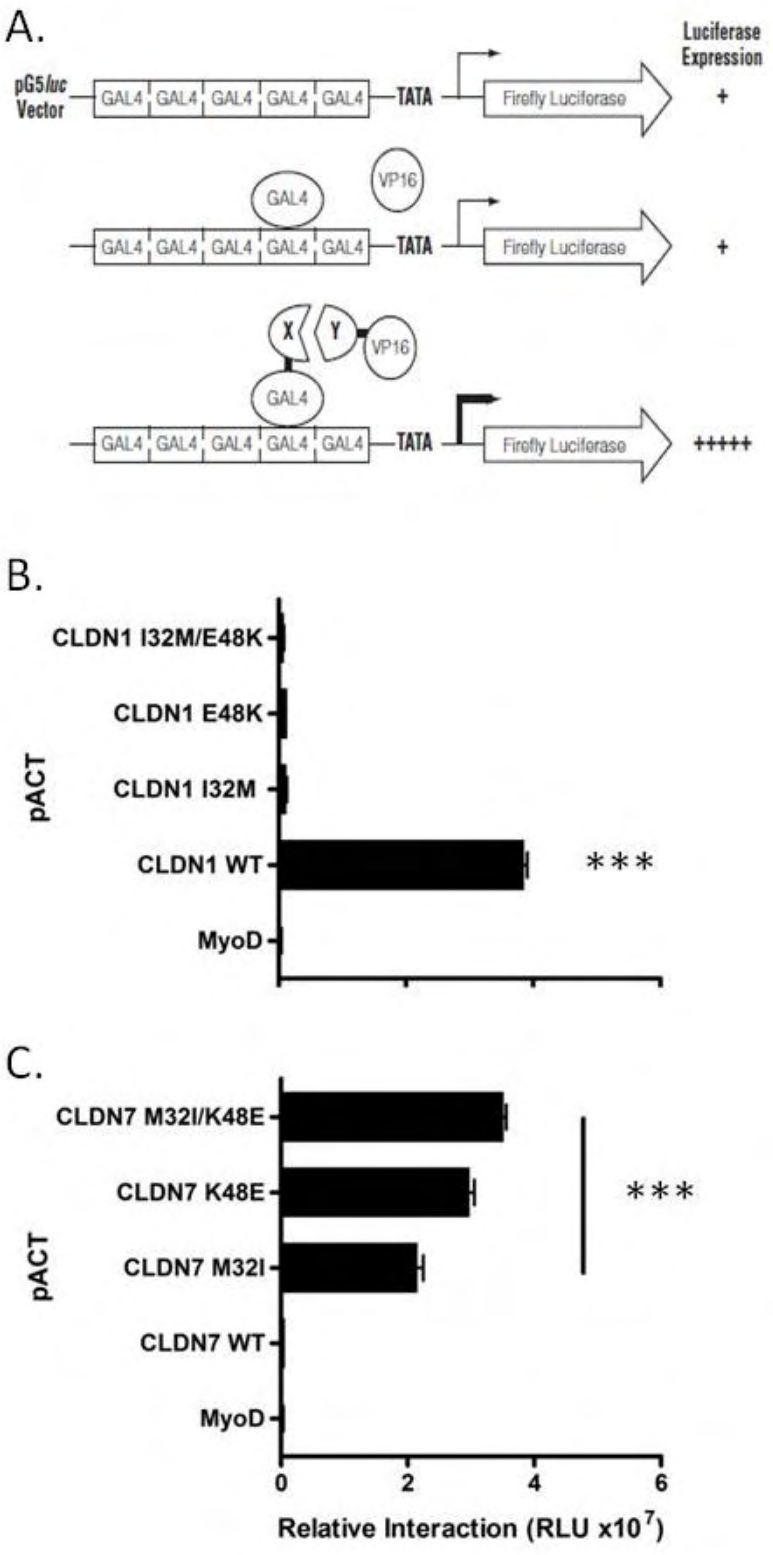
A.
Luciferase Expression
pG5luc Vector
GAL4
TATA
Firefly Luciferase
+
VP16
+
X
Y
+++++
B.
CLDN1 I32M/E48K
CLDN1 E48K
CLDN1 I32M
CLDN1 WT
MyoD
pACT
***
C.
CLDN7 M32I/K48E
CLDN7 K48E
CLDN7 M32I
CLDN7 WT
MyoD
pACT
***
0
2
4
6
Relative Interaction (RLU x10^7)

**Figure 5.5: Mammalian two-hybrid analysis of Claudin1 and Claudin7 EC1 mutations on protein association with CD81**. A) shows a schematic representation of the principles of the mammalian two-hybrid system (image taken from Promega technical manual TM049). A reporter plasmid (pG5luc), which contains a GAL4 binding domain, can be induced to express Firefly Luciferase by the transcriptional activation domain of VP16. This reporter plasmid is co-transfected into a mammalian cell line with the pBind and pACT plasmids, which express the two proteins of interest. The pBind plasmid co-expresses a protein fused to the DNA-binding domain of GAL4 and renilla luciferase, which can be used to correct for transfection efficiency. The pACT vector expresses a protein fused to a transcriptional activation domain of VP16. As the GAL4 fused protein will be associated to the GAL4 binding domain on pG5luc an interaction between the two fusion proteins will result in the VP16 domain inducing the expression of the Firefly luciferase. The activity of the firefly luciferase therefore gives a measure of protein association. 293-T cells were transfected to express the pG5luc and pBind-CD81 with B) the Claudin1 mutants and C) the Claudin7 mutants, cloned into the pACT vector, pACT-Myod was used as a negative control for non-specific interactions. A protein interaction was determined by showing an increase in luciferase activity above the negative controls. A One way Analysis of Variance with a Bonferroni's Multiple Comparison Test was used to determine the degree of difference from the wild type positive control (***$p<0.001$). This data is representative of three independent experiments.

**5.5 Bioinformatic modelling of Claudin1-CD81 interaction.**

To better understand the Claudin1-CD81 interaction we collaborated with Jonathan Mullins (Swansea University) to develop a theoretical model for the protein receptor complex. The crystal structure of CD81 EC2 is known (PDB 1G8Q) (120), however, no such structural information exists for any Claudin protein. The Claudin1 structure was modelled from homologous structures utilising a Biskit structural bioinformatics platform (Grunberg et al., 2007) that peruses the entire PDB for candidate homologues. The workflow incorporates the NCBI tools platform (Wheeler et al., 2008), including the BLAST program (Altschul et al., 1990) for similarity searching of sequence databases; T-COFFEE (Notredame et al., 2000) for alignment of the test sequence with the template; the MODELLER program (Eswar et al., 2003) for homology modelling, and the DSSP algorithm (Kabsch and Sander, 1983) for secondary structure validation. Protein-protein interactions were simulated between estimated Claudin1 and CD81 wild type or mutant structures and the known crystal structure of the human CD81 extracellular domain using Hex 5.0 (Mustard and Ritchie, 2005), fitting for shape and electrostatic interactions.

The structure of the Claudin1 EC1 is predicted to have few structural constraints, such as α helix, β sheet or disulphide bridging, and mainly consists of a coiled coil structure. The results suggest that the interaction between Claudin1 and CD81 relies on the orientation of two sets of contacts between parts of Claudin1 EC1 loop and the CD81 EC2 loop (Figure 5.6). The two regions of Claudin1 correspond to an early section of the EC1 loop that emerges from the first transmembrane domain (TM1), around residues 33-35; and another section approaching the re-entry to the membrane at the beginning of TM2, around residues 63-66. The T149, E152 and T153 residues of CD81 EC2 are predicted to interact with the 62-66

region of Claudin1. A further interaction between CD81 K148 residue and Claudin1 region 33-35 is also predicted, although this region may be more responsible for the general orientation of the loops rather than the formation of a stable, functionally viable complex.

Following the modelling of the wild type interaction the effects of single and double mutations at Claudin1 I32 and E48 residues were determined (figure 5.6, table 5.2 and 5.3). Substantial changes to the structure and orientation of the loop are predicted, with a short α helix being introduced into a structure which previously had a coiled coil structure. The introduction of this α helix removes the 63-66 region of Claudin1 from the CD81 residues at which either form electrostatic forces act or hydrogen bonding. Thus, single and double mutations at these residues are predicted to perturb the interaction with CD81.

To further explore this model, prior to testing the regions of CD81 predicted to interact with Claudin1, we evaluated the interaction(s) of an extensive panel of Claudin1 mutants reported by the Dragic laboratory (183). These mutants were created using an alanine scanning approach and involved residues that were putative sites for phosphorylation, palmitoylation, glycosylation or internalisation. Within this panel a number of receptor inactive mutants were produced, consisting of residues W30, I32, D38, G49, L50, W51, C54 and C64. We therefore evaluated the effect of all these mutations on Claudin1-CD81 interaction, as well as a number of mutants which had minimal effect on receptor activity (table 5.3). For the receptor active mutants, comprising T42A, M52A, S53A and N72A, the position(s) of the interfacing regions Y33-N39 and Q63-V66 are broadly maintained, with some minor alterations in the orientation of individual residues compared to wild type. CD81 binding was predicted to be maintained, with M52A and S53A predicted to have moderate binding whilst the T42A and N72A showed close to wild type binding to CD81. In

contrast, the receptor inactive mutants W30A, I32A, D38A, G49A and W51A are all predicted to cause substantial disruption to the interfacing regions Y33-N39 and Q63-V66. The interacting loop regions are either withdrawn beyond the range of interaction, for W30A, D38A and W51A, or the docking of the two regions to CD81 is precluded due to regions of the loop occupying the same spatially required areas as CD81, preventing the interaction region from associating with CD81. Overall these mutants are not predicted to associate with CD81. The modelling highlighted an interesting group of Claudin1 mutants, L50A, C54A and C64A, which show substantial alterations in their loop structure but maintain a CD81 interaction (figure 5.6). This interaction is not in the same conformation as wild type Claudin1 but the predicted E2 binding site of L162, I182, N184, F186 is positioned away from the Claudin1-CD81 association interface (258).

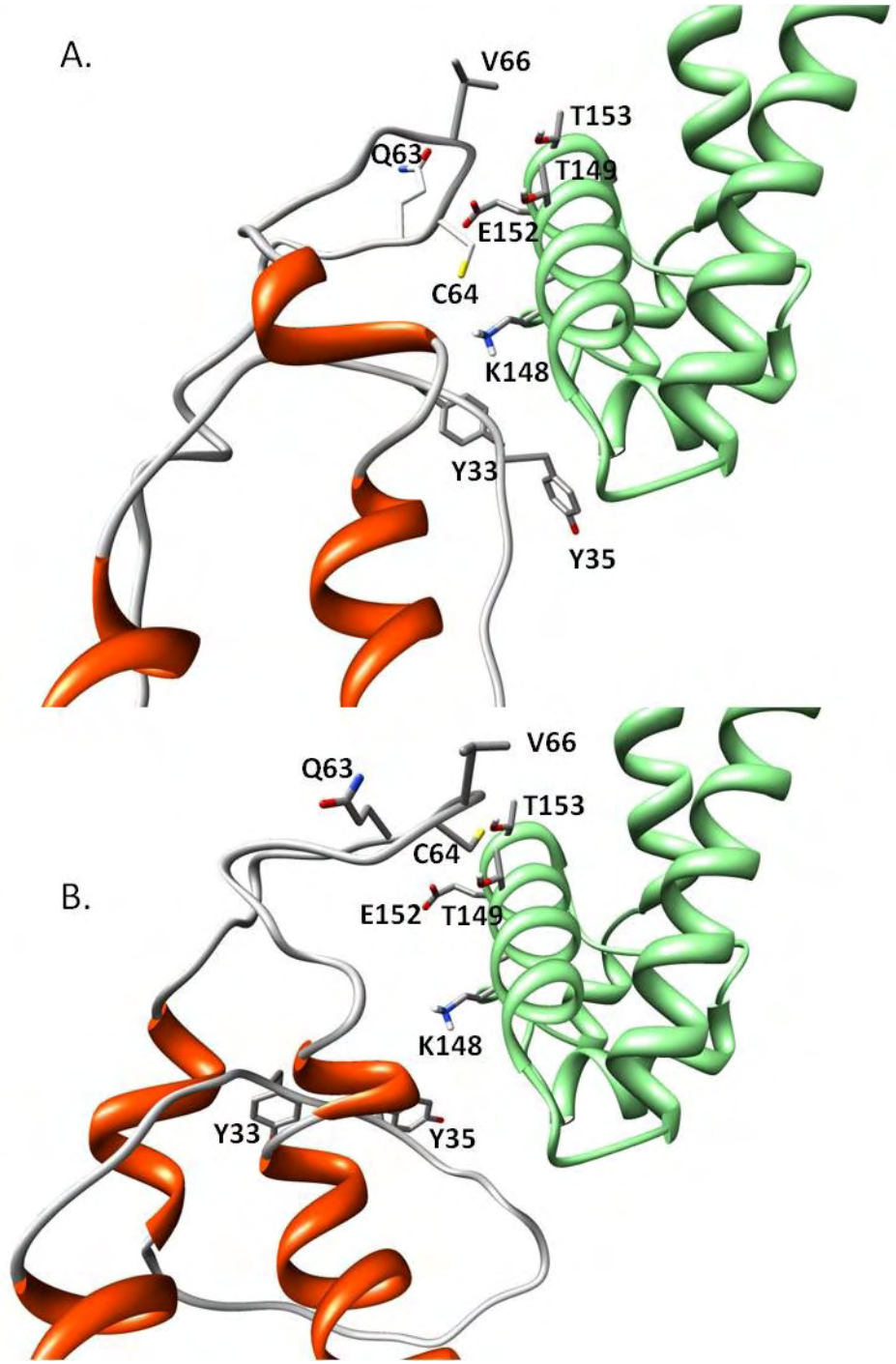
A.
V66
T153
Q63
T149
E152
C64
K148
Y33
Y35
B.
V66
Q63
T153
C64
E152
T149
K148
Y33
Y35

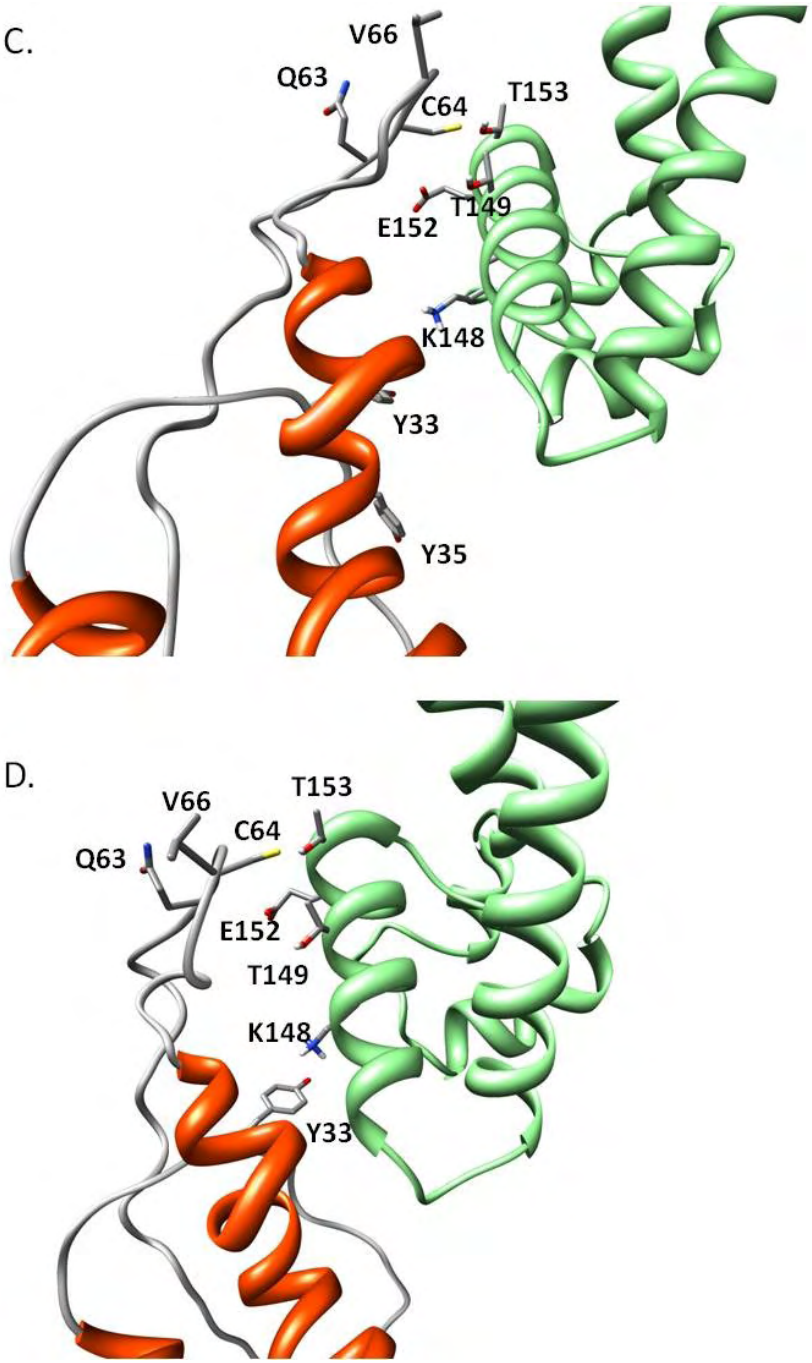


**Figure 5.5: Bioinformatic modelling of Claudin1-CD81 mutants association.** The image shows the A) Claudin 1, B) I32M, C) E48K and D) I32M/E48K Claudin1 mutants The image shows Claudin1 (white line), with the Transmembrane domain shown in orange, in association with CD81 (green line), with key interacting residues labelled. The major Claudin1 interactive regions include residues 33-35 and 63-66. The interacting residues of CD81 comprise residues K148, T149, E152 and T153. The main regions of association predicted for Claudin1 have been altered by the mutations to an extent where they are no longer within the spatial distance(s) to interact with CD81. Image produced using the Chimera program (University of San Francisco).

A.

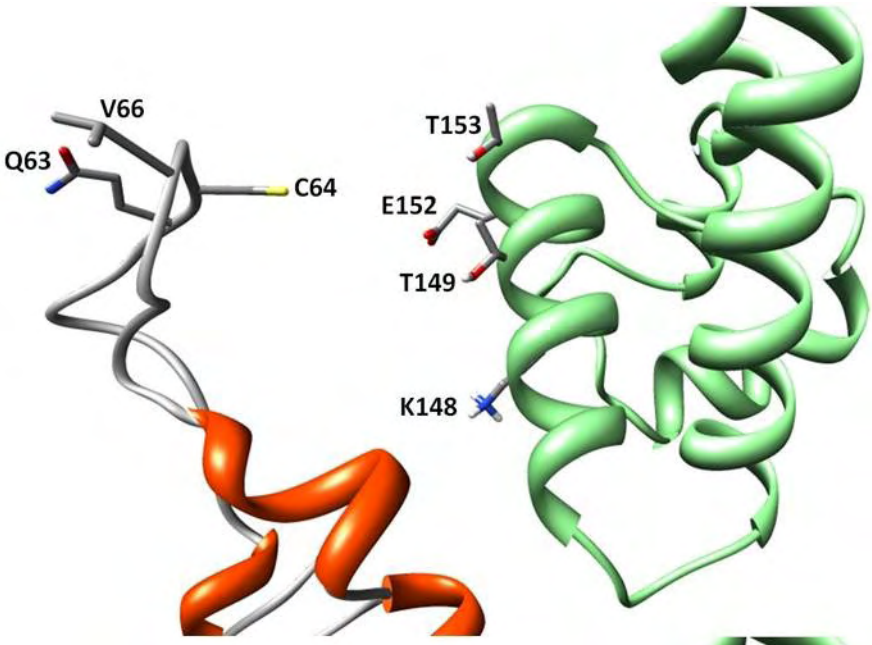
V66
Q63
C64
T153
E152
T149
K148

B.

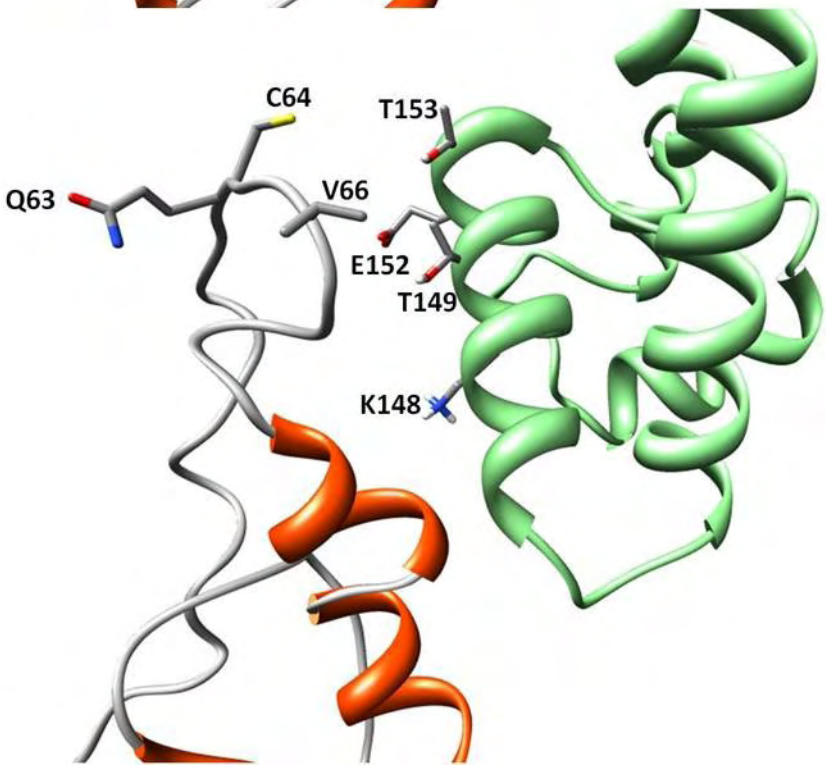
C64
T153
Q63
V66
E152
T149
K148

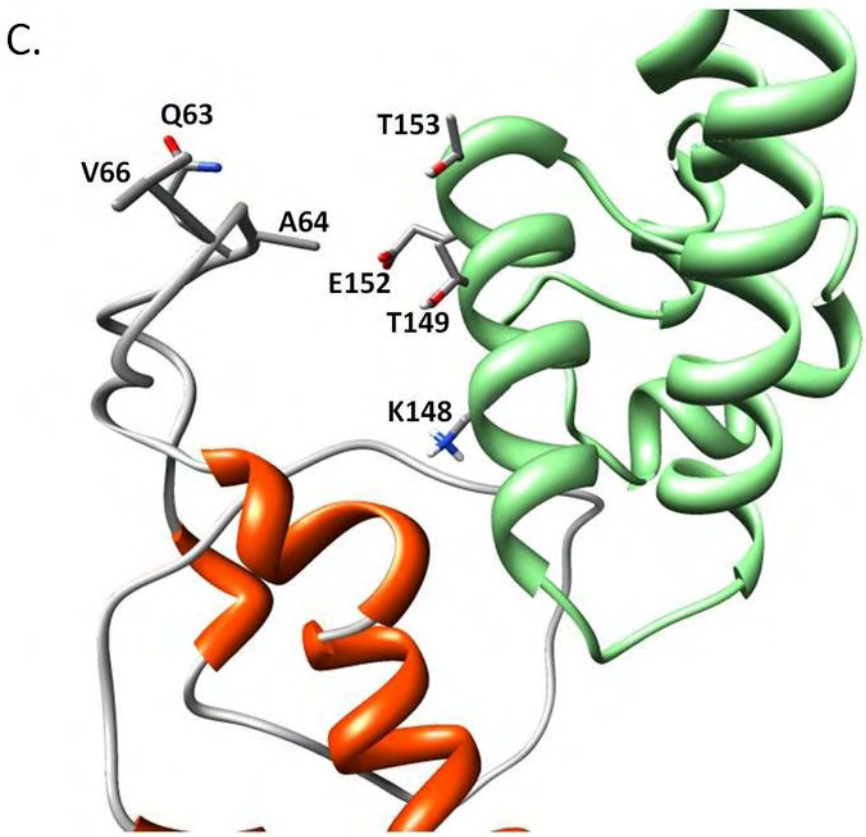


**5.6 Bioinformatic modelling of receptor inactive Claudin1-CD81 association.** Structural modelling of the Claudin1-CD81 association interface. The image shows the Claudin1 mutants A) L50A, B) C54A and C) C64A (white line), with the Transmembrane domain shown in orange, in association with wild type CD81 (green line), with key interacting residues labelled. The mutants are predicted to interact with CD81 although the orientation of the interaction and the structure of the EC1 loop are altered compared to wild type Claudin1. The distance between two of the Q63 residue of Claudin1 with the G152 residue of CD81 is increased from 3Å for the wild type Claudin1 to 13.64 Å, 11.81 Å and 8.29 Å for the L50A, C54A and C64A mutants respectively, which are beyond the range of intermolecular forces. Image produced using the Chimera program (university of San Francisco)

Table 5.2: Inferred atomic distances (Å) between residues of the interacting regions of Claudin1 and CD81

| | CD81 Residues | | | |
|---|---|---|---|---|
| *Claudin1* | K148 | T149 | E152 | T153 |
| Q63 | *11.42* | *8.12* | 3.00 | *6.05* |
| C64 | 3.43 | *5.80* | 3.55 | *6.65* |
| V66 | *12.14* | *4.51* | *7.14* | 3.79 |
| | | | | |
| *Claudin1 I32M* | | | | |
| Q63 | *11.66* | *8.13* | *10.88 (-)* | *11.21* |
| C64 | *9.46 (-)* | 2.53 (+) | *5.99 (-)* | *4.91* |
| V66 | *15.76* | *9.79* | *15.78* | *12.62 (-)* |
| | | | | |
| *Claudin1 E48K* | | | | |
| Q63 | 11.95 | 13.03 | 6.69 (-) | 12.13 |
| C64 | 4.85 (-) | 8.00 | 4.58 (-) | 10.15 |
| V66 | 10.08 | 4.09 | 3.12 (+) | 1.79 (*) |
| | | | | |
| *Claudin1 I32M/E48K* | | | | |
| Q63 | 12.86 | 9.63 | 5.99 (-) | 8.42 |
| C64 | 11.26 (-) | 5.14 | 3.50 (*) | 2.53 (+) |
| V66 | 15.50 | 7.84 | 10.66 | 6.79 (-) |

Distances based on closest end group. Comparisons to wild type shown; (-) Association Lost; (+) Association Gained; (*) Association Maintained

Table 5.3 Bioinformatic model predictions for the effect(s) of specific Claudin1 mutations on CD81 association

| Claudin1 | Disruption Y33-Y35 | Disruption Q63-V66 | Disruption of orientation of interacting residues | Predicted to interact with CD81 |
|---|---|---|---|---|
| WT | None | None | None | Yes |
| I32M | Withdrawn | Withdrawn from E152 | Yes | No |
| E48K | Withdrawn | Withdrawn from E152 | Yes | No |
| I32M/E48K | Withdrawn | Withdrawn from E152 | Yes | No |
| W30A | Projecting | Withdrawn from E152 | Yes | No |
| I32A | Projecting | Withdrawn from E152 | Yes | No |
| D38A | Withdrawn | Withdrawn from E152 | Yes | No |
| T42A | None | None | None | Yes |
| G49A | Projecting | Withdrawn from E152 | Yes | No |
| L50A | None | None | None | Yes |
| W51A | Projecting | Withdrawn from E152 | Yes | No |
| M52A | None | Withdrawn from E152 | Yes | Yes |
| S53A | None | None | Yes | Yes |
| C54A | Projecting | Withdrawn from E152 | Yes | Yes |
| C64A | Projecting | Withdrawn from E152 | Yes | Yes |
| N72A | None | None | None | Yes |

### 5.6 Localisation and antigenicity of Claudin1 mutants

To determine whether the predictions made by the Claudin1-CD81 interaction model were correct we studied a panel of Claudin1 mutants recently reported by the Dragic lab for their association with CD81 (183). Twelve Claudin1 mutants were fluorophore labelled and expressed in 293-T cells, which showed a variety of staining patterns (figure 5.7). Although all the mutant proteins had some level of plasma membrane expression, several showed a high level of intracellular staining (figure 3.4). The wild type protein can be visualized at the plasma membrane, which is also seen for T42A, G49A, L50A, M52A, C54A and C64A mutants. The W30A and W51A mutations showed plasma membrane but with some intracellular accumulation. The I32A mutant had the same staining pattern as the I32M mutant shown earlier (figure 5.1) with punctuate staining at both the plasma membrane intracellular sites and at the plasma membrane, this is also observed for D38A and N72A mutants. Finally, the mutation at position S53A induced a punctuate plasma membrane staining with no detectable intracellular staining.

The cells expressing these mutants were incubated with the panel of anti-Claudin1 antibodies used previously to determine the antigenicity of the various Claudin1 mutants (figure 5.8). Mutation at residues W30A and L50A abrogated the binding of all antibodies. Selected antibodies showed a low level of binding, between 15.5 to 31.5%, to G49A, W51A, C54A and C64A mutants. However, binding was only detected to cells expressing the highest levels of protein. The remaining mutants showed levels of antibody binding comparable to that of wild type Claudin1. In summary, our results demonstrate that several mutations affect protein localisation and conformation. Although there is evidence that all Claudin1 mutants localise to the plasma membrane they do so to varying levels, whether this is due to misfolded protein being retained within the cells is unknown.

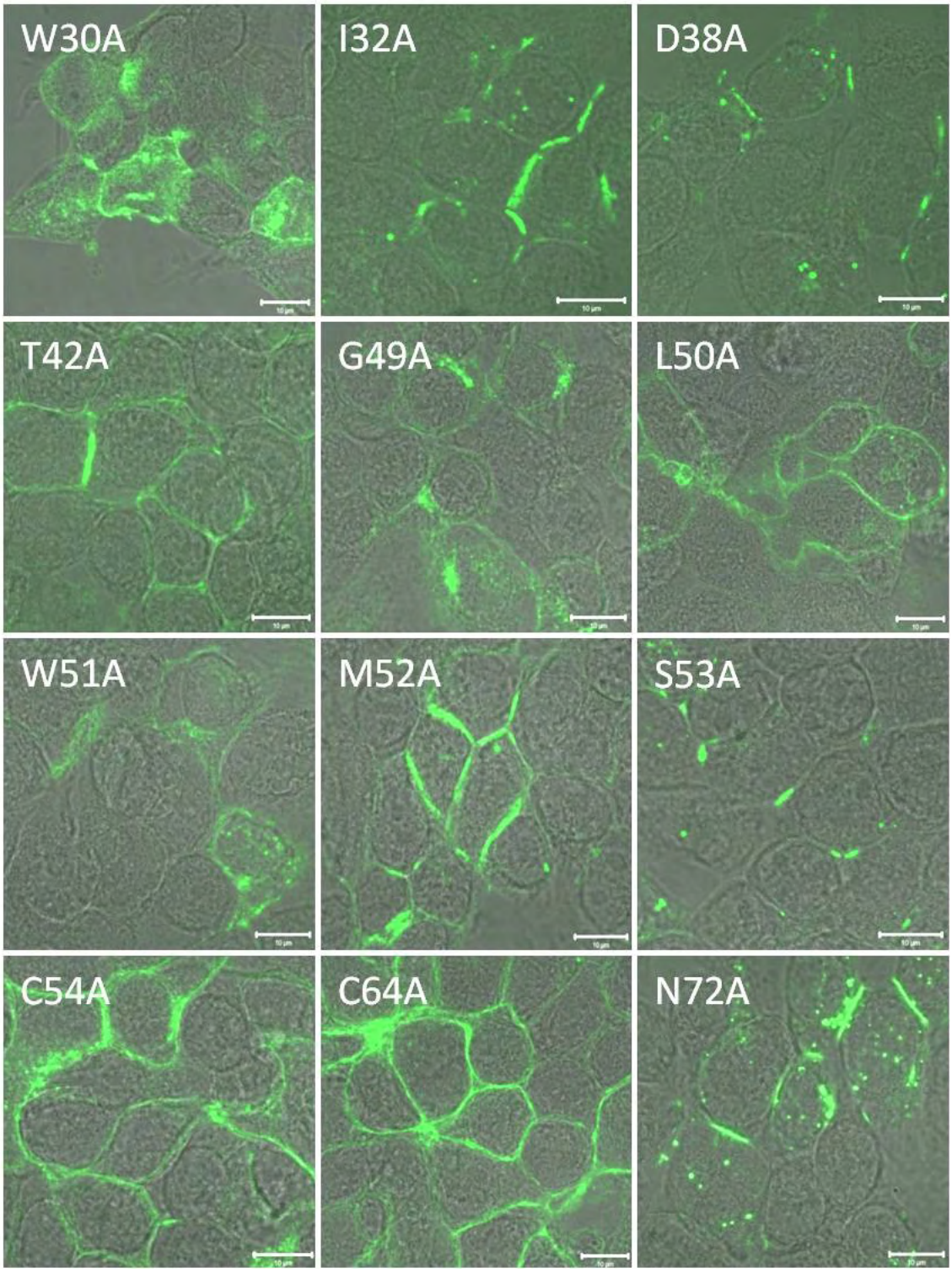


**Figure 5.7: Localisation of Fluorophore labelled Claudin1 mutants.** 293-T cells were transfected with the various Claudin1 mutants, which contain an AcGFP epitope fused to the N-terminus. Images produced are laser scanning confocal images taken using the 63 x 1.2NA water immersion objectives and a meta head confocal microscope (Zeiss). Size bars are equal to 10µm. This images are representative of two independent experiments.

A.

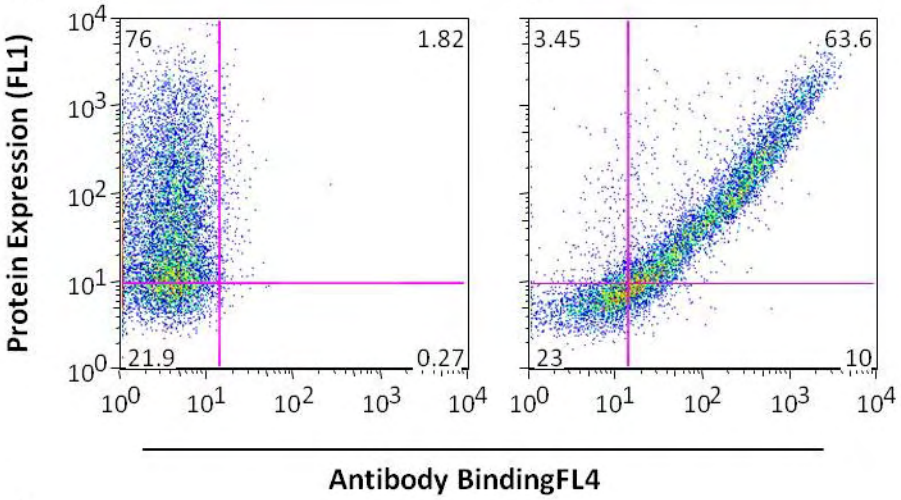


C.

| | Anti-Claudin1 (%Binding) | | | | |
|---|---|---|---|---|---|
| | Polyclonal | 6E1 | 7D3 | 8A9 | R+D |
| WT | 91 | 81 | 78 | 85 | 87 |
| W30A | 5 | 1 | 4 | 1 | 1 |
| I32A | 79 | 81 | 75 | 89 | 93 |
| D38A | 81 | 83 | 73 | 77 | 78 |
| T42A | 78 | 96 | 68 | 97 | 89 |
| G49A | 23 | 1 | 33 | 10 | 16 |
| L50A | 5 | 12 | 8 | 6 | 8 |
| W51A | 20 | 16 | 28 | 16 | 16 |
| M52A | 94 | 96 | 95 | 98 | 99 |
| S53A | 92 | 84 | 85 | 90 | 93 |
| C54A | 4 | 31 | 9 | 7 | 2 |
| C64A | 3 | 34 | 2 | 21 | 0.3 |
| N72A | 92 | 88 | 94 | 90 | 91 |

**Figure 5.8: Antigenicity of Claudin1 mutant proteins.** 293-T cells were transfected to express the panel of AcGFP labelled Claudin1 mutants. The cells were incubated with an anti-Claudin1 polyclonal antibody at a concentration of 1:100 or with a panel of anti-Claudin1 monoclonal antibodies at a concentration of 67µM. A) Shows the FACS plot of the AcGFP-Claudin1 incubated with rat pre-immune serum with Alexafluor 633 anti-Rat IgG. B) shows the same cells stained with anti-Claudin1 polyclonal serum. C) The table summarises the percentage of antibody binding (as defined previously), which is the percentage of cells positive for Claudin protein expression and antibody binding, with thresholds being set by naive 293-T cells. This data is representative of two independent experiments.

### 5.7 Receptor activity of labelled Claudin1 mutant proteins

As with the previous Claudin mutants, we wanted to confirm HCV receptor activity before using the proteins in the FIR and FRET analysis. The fluorophore labelled Claudin1 proteins were transfected into 293-T cells, with wild type Claudin1 as a positive control for HCVpp entry (figure 5.9). The wild type protein produced a mean RLU level (± standard deviation) of 157,186 ± 40662 with the T42A, M52A, S53A and N72A mutants showing levels of entry that were not significantly different from wild type protein (Mean RLU of 110,683 ± 48148, 93,016 ±56167, 88,036 ± 38876 and 117,326 ± 28411 respectively). All of the remaining mutants supported minimal entry equivalent to viral entry into parental 293-T cells, with RLU levels ranging from 3,600 ± 2788 to 7,396 ± 2287. The receptor activity of the mutant proteins is similar to those reported by Cukierman et al. (183).

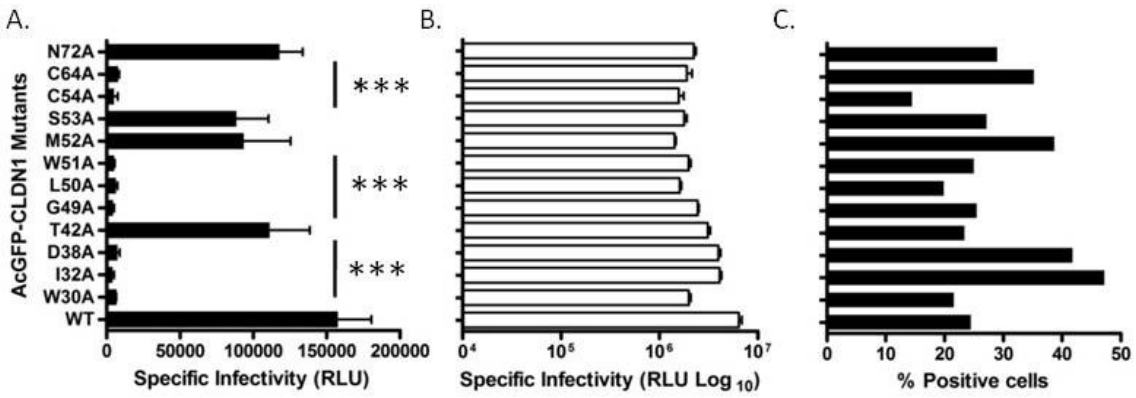


**Figure 5.9: Receptor activity of Claudin1 mutants**. 293-T cells were transfected to express AcGFP-Claudin1 mutants and evaluated for their ability to support HCVpp and MLVpp entry. Data is represented as specific infectivity (Relative Light Units, RLU) and represents the mean plus the standard error of three replicates. A) Shows the specific infectivity of HCVpp. B) shows the specific infectivity of MLVpp. C) Shows the percentage of cells expressing Claudin1 as determined by FACS analysis. A One way Analysis of Variance with a Bonferroni's Multiple Comparison Test was used to determine the significance of differences from wild type positive control (***$p<0.001$). This data is representative of three independent experiments.

### 5.8 Association of Claudin1 mutants with CD81

After confirming the effect(s) of the mutations on Claudin1 localisation, antigenicity and receptor activity we established their interaction with CD81. The mutants were first assessed for their ability to interact with CD81 using FIR and FRET analysis, which was independently confirmed using the mammalian two-hybrid system (figure5.10a and b respectively and Table 5.4). The results show that all receptor active mutants (T42A, M52A, S53A and N72A) were able to interact with CD81. The %FRET of these mutants and the wild type protein varied from 33.56 to 43.33% (no statistically significant differences noted). The mammalian two-hybrid system showed that all receptor active Claudin1 mutants were able to interact with CD81 whereas, the receptor inactive mutants W30, I32, D38, G49 and W51 showed a minimal interaction with CD81 in both assay systems. The FIR and FRET results showed that W30A, I32A, D38A and W51A had no determinable FRET values, due to the low $R^2$ value detected, whilst the G49A mutant produced a small FRET value equivalent to non-specific interactions (10.06% ±21.36). The mammalian two hybrid assay detected no interaction with CD81, as indicated by RLU levels indistinguishable from the negative control of $3.79x10^5$ ($1.24x10^6$, $1.25x10^6$, $2.62x10^5$, $1.04x10^6$ and $1.56x10^6$ respectively). As predicted from the bioinformatic modelling, mutation of Claudin1 residues L50, C54 or C64 did not perturb protein association with CD81. Overall these results have validated the accuracy of our model and enable us to predict and to evaluate the residues of CD81 which associate with Claudin1.

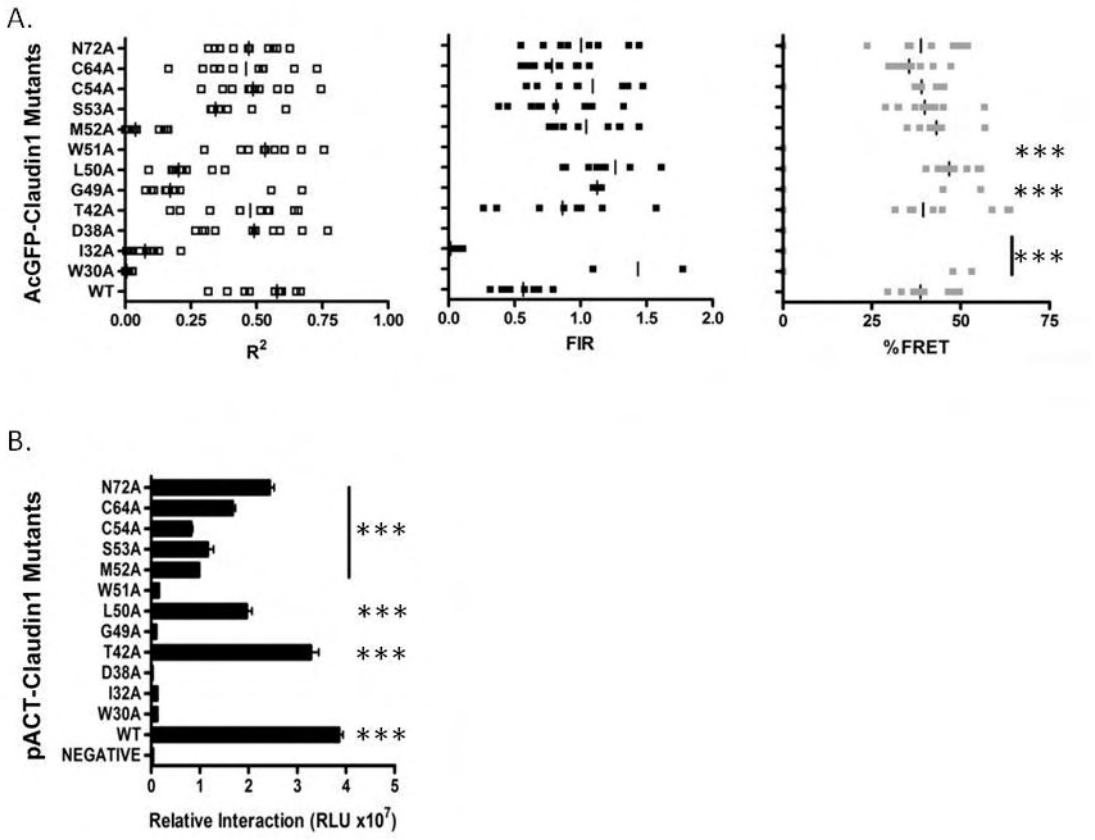


**Figure 5.10: Effect of Claudin1 EC1 loop mutations on protein association with CD81.** A) The $R^2$, FIR and %FRET of AcGFP-Claudin1 mutants with DsRED-CD81 were determined, where the median value is denoted by a solid line. A One way Analysis of Variance with a Bonferroni's Multiple Comparison Test was used to assess the degree of difference from the wild type positive control (***p<0.001). B) 293-T cells were transfected to express pG5luc and pBind-CD81 with the pACT-Claudin1 mutants, pACT-MyoD was used as a negative control for non-specific interactions. An interaction of the proteins is determined by showing a luciferase level significantly above the negative control using. A One way Analysis of Variance, Bonferroni's Multiple Comparison Test was used to assess the degree of difference from the wild type positive control (***p<0.001). This data is representative of two independent experiments.

Table 5.4: FIR and FRET analysis of fluorescent tagged Claudin1 mutants association with CD81

| | $R^2$ (IQR)* | FIR (IQR) | %FRET ± sd# |
|---|---|---|---|
| *CD81 association with:* | | | |
| WT | 0.577 (0.422 0.624) | 0.609 (0.427 - 0.6757) | 40.6 ± 6.864 |
| W30A | 0.006 (0.002 0.021) | ND | ND |
| I32A | 0.076 (0.010 0.119) | ND | ND |
| D38A | 0.490 (0.299 0.631) | ND | ND |
| T42A | 0.476 (0.266 0.596) | 0.924 (0.526 - 1.084) | 37.7 ± 22.95 |
| G49A | 0.171 (0.104 0.382) | 1.126 (1.094 - 1.158)† | 10.1 ± 21.36 |
| L50A | 0.532 (0.455 0.638) | 1.159 (0.974 - 1.493) | 43.3 ± 15.97 |
| W51A | 0.039 (0.003 0.154) | ND | ND |
| M52A | 0.344 (0.326 0.436) | 0.980 (0.794 - 1.296) | 43.0 ± 5.827 |
| S53A | 0.486 (0.389 0.601) | 0.757 (0.536 - 1.078) | 39.7 ± 7.89 |
| C54A | 0.460 (0.317 0.584) | 0.978 (0.630 - 1.415) | 36.7 ± 13.2 |
| C64A | 0.471 (0.350 0.571) | 0.794 (0.593 - 0.975) | 36.4 ± 5.451 |
| N72A | 0.476 (0.266 0.596) | 0.984 (0.783 - 1.249) | 33.6 ± 19.68 |

* – Interquartile range

† - Min. And Max values

# – Standard deviation

ND – Not Determined

### 5.9 Localisation and antigenicity of Fluorophore labelled CD81 Mutants

Our bioinformatic model predicts that CD81 residues K148, T149, E152 and T153 interact with Claudin1. The threonine (T) residues are likely to form hydrogen bonds with glutamic acid (E) and lysine (K) residues in Claudin1 EC1 forming electrostatic interactions, due to their overall negative and positive charges, respectively. In addition to these residues the K201 position was selected since our model predicted it to be involved in the CD81 dimerisation by interacting with the T149 residue. Although CD81 dimerisation is not essential for E2 binding it may prove to be essential for the Claudin1-CD81 complex formation (152-153).

To ascertain the role of these CD81 residues in protein localisation, antigenicity and receptor activity we mutated each of the selected residues to an alanine and expressed the mutant proteins in the CD81 negative HepG2 hepatoma cell line. All of the mutants expressed at comparable levels and localised to the plasma membrane, with minimal evidence for intracellular accumulation (figure 5.11). Cells were stained with the panel of anti-CD81 antibodies, used previously, to determine if the mutations affect protein antigenicity (figure 5.12). Overall the mutations had minimal effect on antibody reactivity, with a high level of binding occurring for each antibody.

Since CD81 has been shown to interact with the HCV E2 we performed an E2 binding assay to determine whether any of the mutations affected E2 binding. Since HepG2 cells express SR-BI, which can also interact with E2, we transduced Chinese hamster ovary cells (CHO cells) to express the various CD81 mutants as the E2 protein will not interact with naive CHO cells (figure 5.13). This assay showed that mutating the various selected regions of CD81 caused no significant reduction in the proteins ability to bind E2. In summary, these

experiements demonstrate that the selected mutations have minimal effect on the tertiary structure, as both conformational-dependent antibodies and HCV E2 interact at comparable levels to wild type CD81 protein. The staining pattern demonstrates the proteins are expressed at the plasma membrane and are in the correct location to interact with HCV particles.

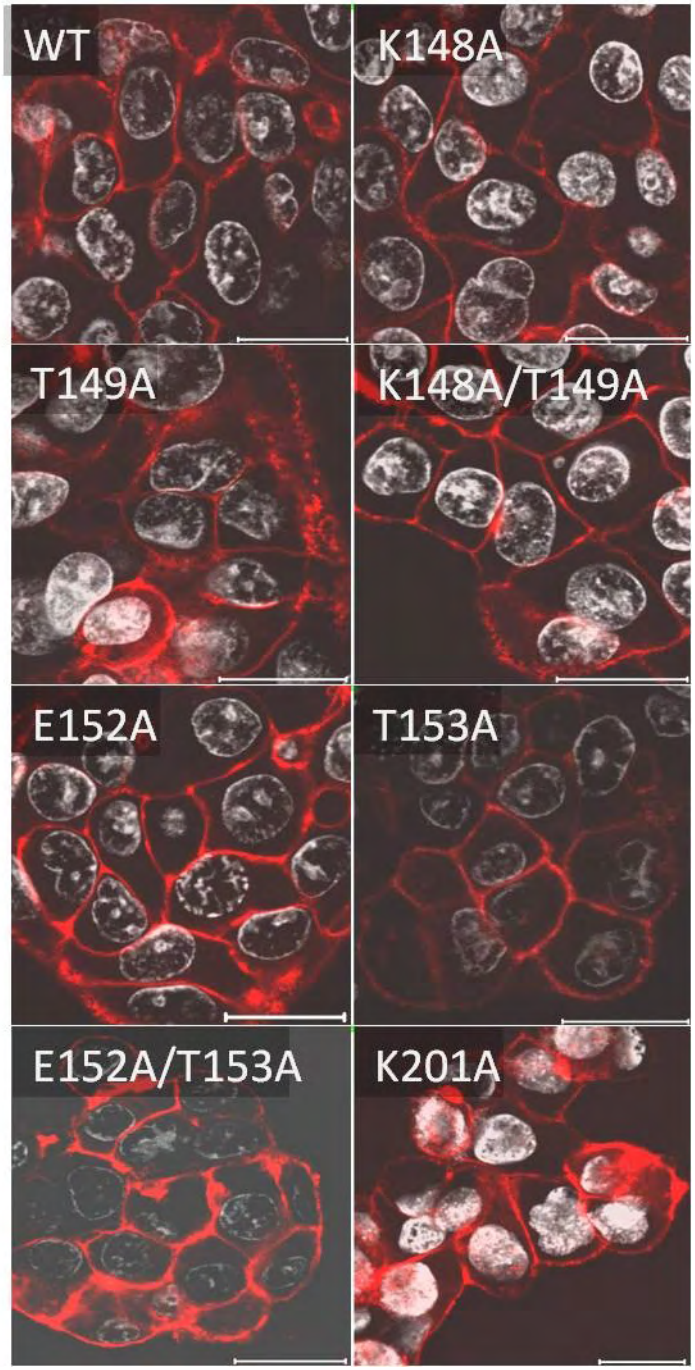


**Figure 5.11: Localisation of fluorophore labelled CD81 mutants.** HepG2 cells were transduced with the various CD81 mutants, which contained a DsRED epitope fused to the N-terminus. Images produced are laser scanning confocal images taken using the 63 x 1.2NA water immersion objectives and a meta head confocal microscope (Zeiss), Size bars are equal to 20µm. These images are representative of three independent experiments.

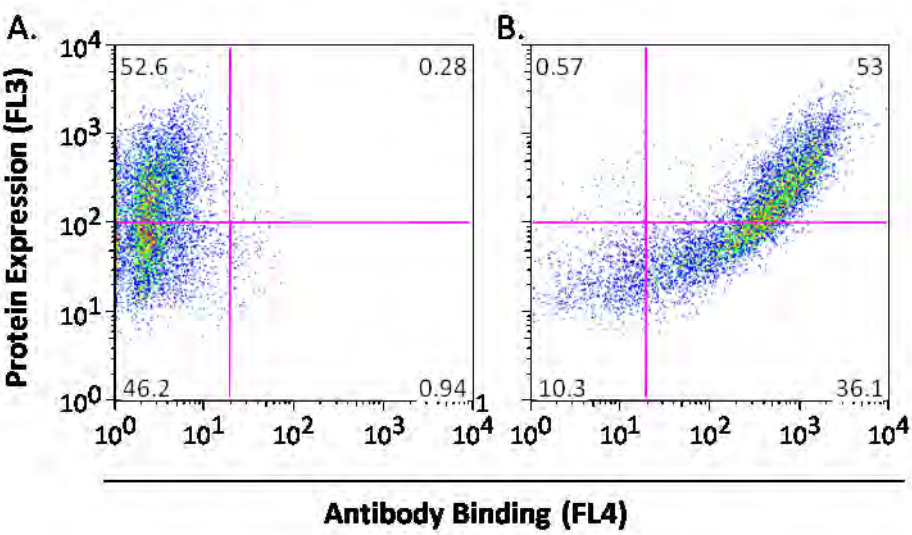


C.

| | Anti-CD81 (%binding) | | | | |
|---|---|---|---|---|---|
| | 2s20 | 2s155 | 1s337 | 1s135 | 2s290 |
| WT | 98 | 96 | 97 | 94 | 98 |
| K148A | 98 | 83 | 84 | 88 | 86 |
| T149A | 99 | 97 | 86 | 83 | 86 |
| K148A T149A | 98 | 97 | 99 | 90 | 96 |
| E152A | 98 | 97 | 95 | 89 | 86 |
| T153A | 99 | 97 | 86 | 96 | 90 |
| E152AT153A | 99 | 93 | 96 | 94 | 94 |
| K201A | 97 | 97 | 97 | 95 | 96 |

**Figure 5.12: Antigenicity of CD81 mutants.** HepG2 cells were transduced to express the panel of DsRED-CD81 mutants. The cells were incubated with anti-CD81 antibody 2s20 at a concentration 67µM. A) Shows the FACS plot of the DsRED-CD81 wild type incubated with Alexafluor 633 anti-mouse IgG. B) Shows the same cells stained with the anti-CD81. C) The graph shows the percentage of antibody binding to cells expressing DsRED-CD81. This data is representative of three independent experiments.

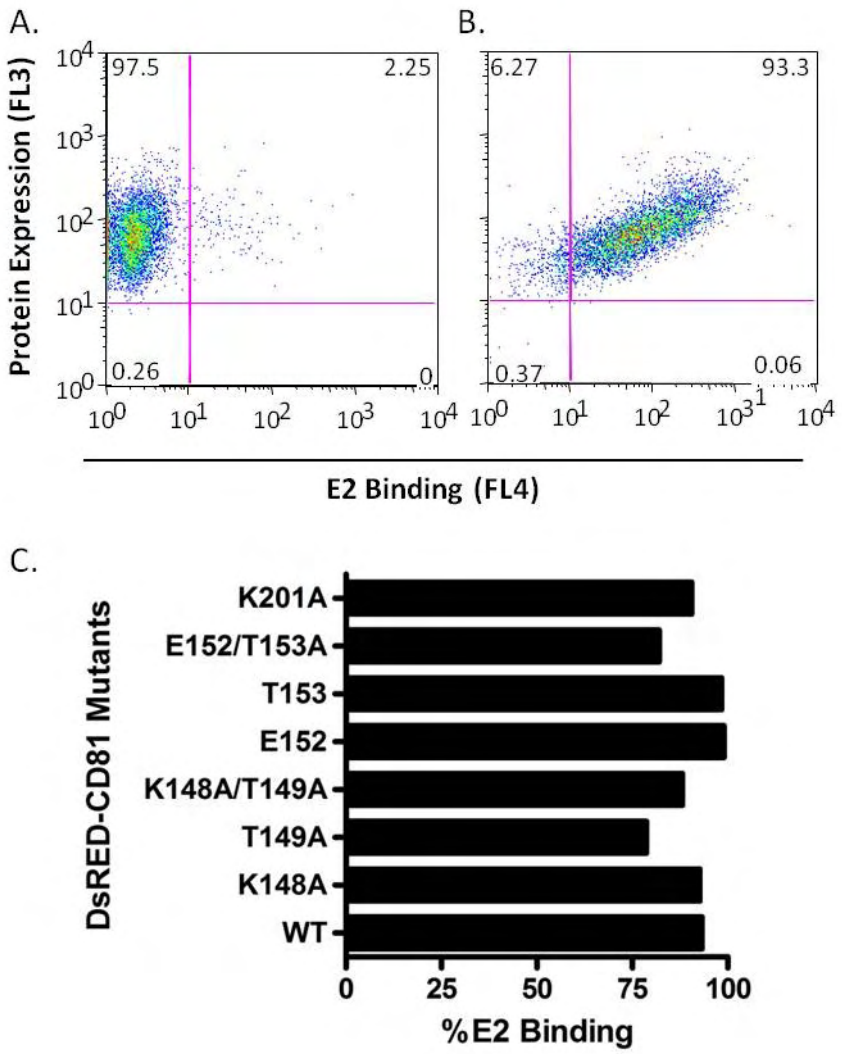


**Figure 5.13: Binding of HCV E2 protein to CD81 mutants.** CHO cells were transduced to express the panel of DsRED-CD81 mutants, which were incubated with HCV E2, where E2 binding was realised using 10ug/ml of anti-10/76B using an Alexaflour 633 Goat anti-Rat (invitrogen), at a 1:1000 dilution, secondary antibody. A) Shows the FACS plot of the DsRED-CD81 wild type. B) Shows the same cells incubated with the HCV E2 and stained with the anti-10/76B and Alexaflour 633 Goat anti-Rat. C) The graph shows the percentage of H77 sE2 binding to CHO cells, which is the percentage of cells positive for CD81 protein expression and E2 binding, with thresholds being set by naive CHO cells. This data is representative of two independent experiments.

**5.10 Receptor activity of mutant CD81 proteins.**

Having shown that CD81 mutations have minimal effect on protein localisation, antigenicity and interaction with HCV E2 protein we tested their receptor activity and ability to allow HCVpp infection of HepG2 cells (figure 5.14). The CD81 wild type, K148A and K148A/T149A CD81 proteins supported comparable levels of HCVpp infection with RLU levels of 13,010 ± 974.1, 9,886.6 ± 4917.4 and 11,273.3 ± 6004.4, respectively. In contrast, the remaining mutants showed negligible levels of HCVpp entry with RLU levels ranging from 683.3 to 3673.3, which is not significantly different from the mean RLU value of 540 for the parental HepG2 cells. The MLVpp entry levels into the cells were of a similar level across all the CD81 mutants. These results demonstrate that threonines at position 149 and 153, glutamic acid at residue 152 and lysine residue at position 201 are all essential for the receptor activity of CD81.

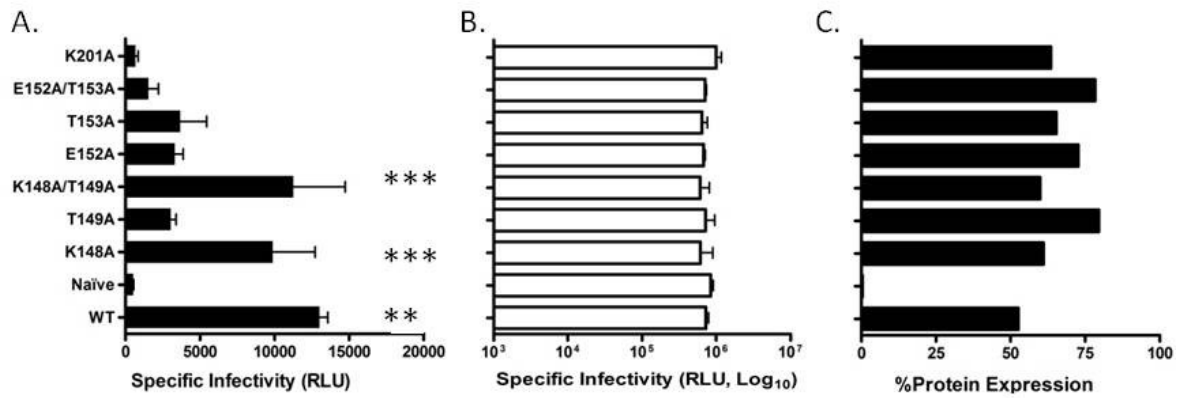


**Figure 5.14: The effect of CD81 EC2 mutations on viral receptor activity**. HepG2 cells were transduced to express DsRED-CD81 mutants and evaluated for their ability to support HCVpp and MLVpp infection. Data is represented as specific infectivity (Relative Light Units, RLU) and represents the mean plus the standard error of three replicates. A) shows the specific infectivity of HCVpp. B) shows the specific infective of MLV. C) shows the percentage of cells expressing CD81 as determined by FACS analysis. A One way Analysis of Variance with a Bonferroni's Multiple Comparison Test was used to determine the degree of significant difference from the naive 293-T negative control (**p<0.01, ***p<0.001)This data is representative of two independent experiments.

### 5.11 Association of CD81 mutants with Claudin1

Having identified receptor inactive CD81 mutants, which retained antigenicity and E2 binding, we sought to investigate their association with Claudin1 (figure 5.15a). In addition, we tested their ability to form homodimers (figure 5.15b), as this has been shown to be important for viral entry (152). For wild type Claudin1-CD81 association the $R^2$ was shown to be 0.29 (IQR 0.23 – 0.38) and FIR value of 0.67 (IQR 0.54 – 0.89) and a %FRET of 33.8 ± 4.45.

These values were not significantly different from the values seen with the receptor active mutants K148A and K148A/T149A, with $R^2$ of 0.21 (IQR 0.073 – 0.37) and 0.19 (IQR 0.043 – 0.31), FIR values of 0.54 (IQR 0.51 – 0.85) and 0.55 (IQR 0.28 – 0.69) and %FRET values of 19.74% ± 17.84 and 21.31% ± 15.22. In contrast the receptor inactive mutants showed reduced levels of association, with $R^2$ values ranging from 0.07 to 0.14. For those cells which had a sufficiently high enough level of association, the FIR values were not significantly different from the wild type control with values ranging from 0.43 to 0.91. Although some cells showed a FIR value similar to wild type CD81, the overall %FRET values observed for the receptor inactive mutants was significantly lower than wild type and within the region observed for non-specific protein associations (3.54% to 10.52%). When CD81 mutants were assessed for their ability to form homodimers, only the T149A mutant demonstrated any reduction in self-dimerization. CD81 produced an $R^2$ of 0.39 (IQR 0.2 – 0.57), FIR value of 0.7 (IQR 0.4 – 0.99) and %FRET of 34.11% ± 4.9 with the T149A mutant producing values of 0.18 (IQR 0.067 – 0.47), 0.65 (IQR 0.57 – 1.02) and 16.29% ± 17.66, respectively. Although these values are not significantly reduced the associations were only seen in a subset of cells.

We used the mammalian two-hybrid system to independently confirm our FRET imaging results (figure 5.16). The overall pattern for Claudin1-CD81 mutant association was

repeated, where wild type CD81 produced a mean RLU of $1.6x10^8 \pm 1.15x10^7$ with receptor active K148A and K148A/T149A mutants producing mean RLU levels of $1.6x10^8 \pm 5.4x10^6$ and $5x10^7 \pm 2.07x10^6$, significantly above the negative control of $4.6x10^6 \pm 1.98x10^5$. The remaining receptor inactive mutants produced low RLU levels of between 2.05 and $9.93x10^6$ which were not significantly above the negative control. Overall, the results of the CD81-CD81 mutant interaction again mirrored the FIR and FRET analysis, with T149A being similar to the negative control, with mean RLU levels of $5.35x10^5 \pm 2.74x10^4$ and $4.04x10^5 \pm 1.95x10^4$, respectively. These results clearly show that receptor active CD81 mutants associate with Claudin1 and can still form homodimers, whereas receptor inactive mutants show no association with Claudin1 but, with the exception of the T149A mutant, maintained their ability to form homodimers.

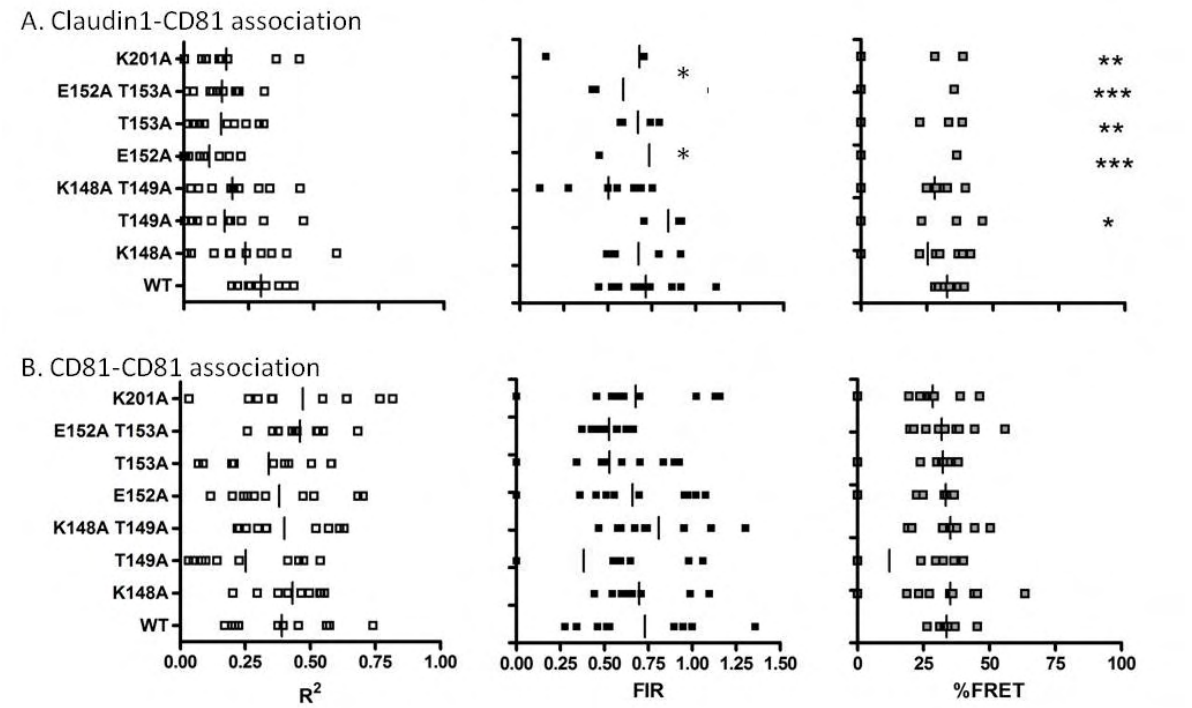


**Figure 5.15: Effect of CD81 EC2 mutations on Claudin1 association and homodimerisation**. HepG2 cells were transduced to express fluorescent-tagged wild-type and mutant forms of DsRED-CD81 and AcGFP-Claudin1 (A) or AcGFP-CD81 (B), and the degree of association between fluorophore-tagged proteins assessed by FIR and FRET analysis. Median FIR and FRET values from ten individual cells are presented (*p<0.05, **p<0.01, ***p<0.001). This data is representative of two independent experiments.

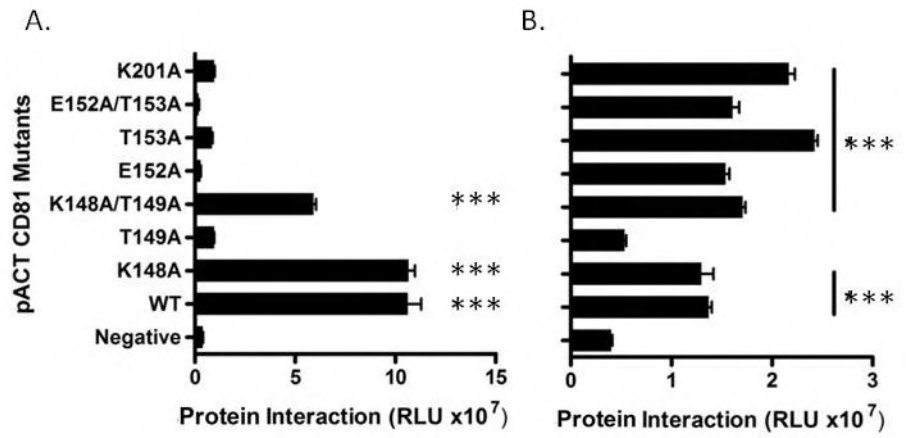


**Figure 5.16: Mammalian two-hybrid analysis of CD81 EC2 mutations on Claudin1 association and homodimersiation.** 293-T cells were transfected to express the pG5luc and the pACT-CD81 mutants with A) pBind-Claudin1 or B) pBind-CD81, pACT-MyoD was used as a negative control for non-specific interactions. An interaction of the proteins are determined by showing a luciferase level significantly above the negative controls using a One way Analysis of Variance with a Bonferroni's Multiple Comparison Test to determine the degree of difference from the negative control (***$p<0.001$). This data is representative of two independent experiments.

## 5.12 Discussion

Previous reports demonstrated that the receptor activity of Claudin1 and Claudin7 could be reversed by exchanging two residues within EC1, at amino acid position 32 and 48 (110). However, the authors did not provide a mechanism for the mutant phenotype. Further mutational analysis by Cukierman et al highlighted a highly conserved motif W30-GLW51-C54-C64 in Claudin1, that was essential for viral receptor activity and in the formation of cell-to-cell contacts (183). Since HCV can enter 293T cells transduced to express Claudin1 that do not form tight junctions, we conclude that a cells ability to form tight junctions is not a defining feature required for virus infection. We hypothesised that the mutations perturb Claudin1 association with CD81. We therefore studied the effect of the mutations on Claudin1 localisation, antigencity and ability to interact with CD81. Although the I32M mutation showed pools of intracellular staining and a more punctuate appearance it retained antibody binding and surface expression (Figure 5.1 and 5.2, respectively). This result for the anti-Claudin1 R+D monoclonal contradicts previous reports but unfortunately there is not enough information within the publication to assess these differences (114). The E48K and I32M/E48K double mutations showed a more marked effect on protein localisation and antibody binding. Given the effect of the double mutation on Claudin1 location and antibody binding we are unable to ascribe the mechanism of receptor inactivity to a loss in Claudin-CD81 interaction. The Claudin7 mutants demonstrate that receptor activity is increased by the M32I and K48E single mutation but the double mutation is required to produce a Claudin1 like staining pattern in 293-T cells and an ability, albeit at a low level, to bind the polyclonal anti-Claudin1 and two of the monoclonal anti-Claudin1 antibodies (7D3 and 8A9).

We sought to model the interactive face between the two proteins using a bioinformatics approach. The interaction for the wild type proteins was assessed and the potential alterations to the protein caused by the Evans mutants to positions 32 and 48 analysed. The model predicted that the Claudin1 loop is unstructured with a coiled coil appearance. The regions predicted to interact with CD81 are between residues 33-35 and 63-66. The receptor inactive mutations were predicted to cause a marked change in the orientation of the loop, introducing a α-helical region into the structure. This change predicted a loss of the interaction with CD81 which matches both the FIR and FRET analysis as well as the mammalian two-hybrid system. To further validate this model we compared the predicted results for twelve Claudin1 mutants reported by Cukierman et al against our experimental results measuring Claudin1-CD81 interaction. Our model was able to accurately predict which Claudin1 mutants would interact with CD81. However, receptor inactive Claudin1 mutants L50A, C54A and C64A could still interact with CD81, illustrating that a simple interaction with CD81 is not sufficient to explain Claudin1 receptor activity and the protein interaction may have to occur in a specific orientation. Indeed, the model predicts that these mutants interact with alternative CD81 residues compared to the wild type protein. If the orientation of the interaction has altered this could lead to a loss of CD81-HCV E2 interaction or the association with other accessory proteins required for entry. Further investigations of how these mutations render Claudin1 receptor inactive could help to further define the role of these proteins in viral entry.

Having validated the model we performed site-directed mutagenesis on CD81 residues predicted to interact with Claudin1 (residues K148, T149, E152, T153 and K201). We were able to demonstrate that, with the exception of K148, these residues are all essential for

receptor activity. Unlike the Claudin1 mutants, there was no effect on the protein's localisation or antibody binding. We were able to demonstrate that these mutants could still interact with HCV E2. Due to the highly structured nature of CD81, which has multiple α-helical regions as well as disulphide bridges, the mutations are not predicted to have a significant effect on protein 3D structure. Zhang et al demonstrated that mutants F186, E188 and D196, originally identified to prevent sE2 binding (262), could still allow HCVpp entry (149). A subsequent report identified that CD81 residues K171, I181, I182 and F186 were essential for both HCV E2 binding and virus infection (263), highlighting different regions of CD81 that engage HCV and interact with Claudin1.

One aspect of our results which is interesting is the double mutation of positions 148 and 149. As a single mutant the K148A is receptor active, whilst the T149A is receptor inactive. However the double mutation in this position produces a receptor active mutant, meaning that the K148A mutation is "rescuing" the receptor activity of the T149A mutant. The reason for this rescue is at this point unclear. The experimental data show a clear requirement for each residue for HCV entry to occur. The model predicted that K148 and T149 residues interact with different residues of Claudin1, and the loss of either single residue will negate protein-protein interaction. This could indicate that the overall strength of the interaction is reliant on each residue and the loss of any single interaction reduces the ability of the two proteins to overcome separating forces. The T149 residue is predicted to interact with the 63-66 region of the Claudin1 EC1, whereas K148 is predicted to interact with the 33-35 regions (specifically Y33). These results suggest that the 33-35 region is not essential for the Claudin1-CD81 complex as the K148A is still receptor active as are mutations of Y33 and Y35, reported in (183).

The results also indicate that the K201 residue is not essential for CD81 dimersiation. As other residues are implicated in the dimersiation of CD81 the mutation of the K201 residue may cause an alteration in the orientation of the dimer. As the K201 mutant does not interact with Claudin1 it may indicate that a specific orientation of the CD81 loops is essential. The K201 residue of the CD81 interacting with Claudin1 is predicted to interact with the T149 residue of the second CD81 of the CD81-CD81 dimer. As the T149 is also predicted to interact with the C64 residue of Claudin1 the residue appears to be central to the Claudin1-CD81 and CD81-CD81 complex formation

Our mutational analysis was directed by the bioinformatic model which was able to predict residues essential for Claudin1 binding. The model also predicts that the complex forms in an orientation that does not occlude the putative E2 binding site on CD81. Drummer et al have predicted that the binding site for E2 on the CD81 consists of L162, I182, A184 and F186 (258). Although Claudin1 is not required for the binding of E2 to CD81 it is not known whether its presence in the complex may increase the strength of the interaction. An interaction between the virus and Claudin1 has not been clearly demonstrated, although this could occur after the virus interacts with CD81. The dimerization of CD81 is also not required for E2 binding but it has been previously shown to improve the affinity of the binding of both E2 and the E1-E2 heterodimer (153). Nakajima et al used SPR to show that CD81 LEL fused to glutathione-S-transferase, which tends to form dimers and multimers, interacted with a higher avidity and affinity to the HCV E1-E2 than a CD81 LEL fused to MBP, which has a lower propensity to form multimers (153). Whether the Envelope proteins are interacting with multiple CD81 proteins or simply releasing from one CD81 and binding to the other CD81 in the dimer is unknown. Overall the data suggest the virus is interacting

with the Claudin1-CD81 receptors that are part of a larger multimeric structure. The associations may not be essential for virus binding, although the complex may increase the avidity and affinity, suggesting the interaction of Claudin1 with CD81 is essential for other aspects of the entry process.

# Chapter 6:

# Discussion and Conclusions

## 6.1 The role of Claudin1 in HCV entry

The entry process of HCV is multi-stepped culminating in a pH and Clathrin dependent internalisation of the virus particle (223-224). It has been shown that the expression of CD81, SR-BI, Claudin1 and Occludin within cells are essential for entry and these proteins constitute the main co-receptors for viral entry (112, 115). Although it is known that the virus encoded glycoproteins directly interact with CD81 (88, 91, 93, 105-106) and SR-BI (107-109), the role and function of the tight junction proteins Claudin1 and Occludin in the viral entry process are poorly understood. CD81 has been reported to associate with Claudin1 (125, 183-184), with our group demonstrating that the receptor inactive Claudin4 molecule showed no interaction with CD81 (184).

In this thesis we provide further evidence that only receptor active Claudin proteins associate with CD81. Treating cells with antibodies specific for CD81 or Claudin1 reduced Claudin1-CD81 association and viral entry. As these antibodies were directed to the EC1 of Claudin1 and the EC2 of CD81 we hypothesised that these regions may be involved in the complex formation. We were able to demonstrate that these regions were responsible for the complex formation using recombinant forms of Claudin1 EC1 and CD81 EC2 in a SPR based assay.

To further define the protein-protein interface and extracellular loop residues responsible for the interaction we evaluated the ability of a previously published panel of Claudin1 mutants to interact with CD81 to inform a bioinfomatic model of the receptor complex. The model predicted that association of T149, E152 and T153 CD81 EC2 residues with the 62-66 region of Claudin1. A further interaction between CD81 K148 residue and Claudin1 region Y33-Y35 is also predicted. Using a site directed mutagenesis approach we were able to

validate the role of T149, E152 and T153 CD81 residues in association with Claudin1. The K148 residue was shown to be non-essential and although it may interact with the Claudin1 loop, the strength of the interaction may not be sufficient to support a complex. In contrast mutation of T149, E152 and T153 residues lead to a reduction in HCV entry without affecting the E2 binding, which further indicates the requirement of the Claudin1-CD81 complex in the entry process. A schematic representation of the Claudin1-CD81 complex is shown in figure 6.1 with the essential residues indicated.

Our laboratory has performed further analysis on the dynamics of the Claudin1-CD81 complex using single particle tracking (SPT) and fluorescence recovery after photobleaching methodologies. The results of SPT demonstrated that the two proteins diffuse separately before coming together and co-diffuse as a complex. In contrast, SR-BI showed no co-diffusion with CD81, suggesting that these proteins do not form a complex. These data sets highlight the presence of CD81 and Claudin1 existing separately and as a complex which raises the question of whether the virus binds to the CD81 before or after Claudin1 association. The binding of sE2 to CD81-EC2 has been previously shown by Elisa and surface Plasmon resonance with the latter technique also showing recombinant E1/E2 as well as HCVpp interaction(s) with CD81-EC2 (153, 264-266). These results suggest that Claudin1 is not required for the virus to interact with CD81 but we have no evidence to show whether the virus preferentially binds to a particular form of CD81, either alone or in complex with Claudin1.

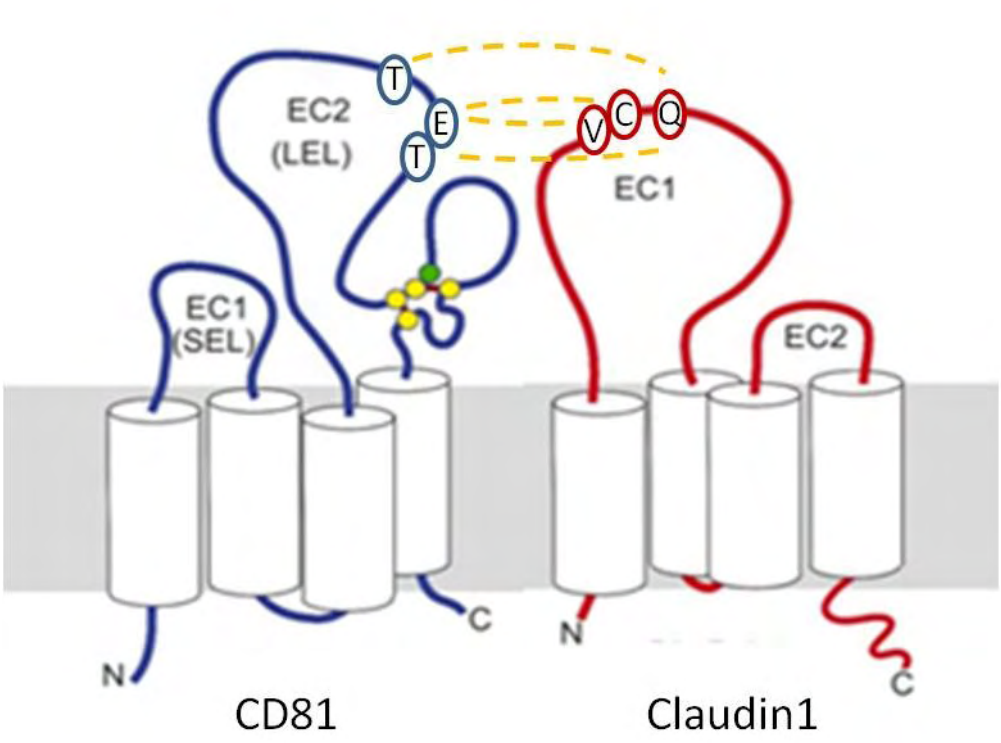


**Figure 6.1 Schematic representation of the Claudin1-CD81 complex.** The residues responsible for the formation of the Claudin1-CD81 complex are shown for both the CD81 and Claudin1 with the orange dotted line indicating which residues are associating. Mutation of the CD81 residues shown lead to a loss of Claudin1 interaction and HCV entry whilst maintain conformational antibody and sE2 binding.

Extensive work by Michelle Farquhar in our laboratory has recently demonstrated that ligation of CD81 and Claudin1 with receptor specific antibodies, HCV sE2 or HCV particles (HCVcc and HCVpp) promotes receptor internalization via a clathrin and dynamin dependent process. It has been previously shown that the engagement of anti-CD81 antibodies could induce internalisation of CD81 (267). Our data is consistent with work that has reported HCV enters the cells via clathrin mediated endocytosis (224, 268). It has been previously reported that Claudin1 and CD81 co-localise with early endosomes antigen-1, a marker of early endosomes, positive vesicles (112). Using fluorescent labelled markers of different endosomal vesicles we were able to demonstrate that the majority of CD81 (61%) co-localised with an early endosomal marker Rab5, with the remainder localising with the early and recycling marker rab4 and the recycling marker rab11. We were also able to show evidence that internalisation leads to the degradation pathway as half of the internalised CD81 (52%) associated with lysosomal markers. It must be noted that the data is based on static images and therefore the movements and fates of the various vesicles still needs further investigation. Many viruses enter cells via an endocytic pathway, with the acidification of the endosome prior to lysosomal fusion acting to prime the fusion machinery of the virus. The closely related flaviviruses Dengue and west Nile virus have both been shown to enter cells via clathrin mediated endocytosis with Rab5 being essential in both entry processes, indicating at least a transition through the early endosome (269-271). Van der Schaar et al and Zaitsva et al both showed, in addition to the requirement of Rab5, that Dengue virus also requires Rab7, suggesting that fusion can occur in late endosomes (269-270). HCV infection has been reported to be dependent on Rab5 as cells expressing dominant negative mutants of Rab5 were refractory to entry. In addition Rab7 was shown to be not required for entry suggesting that fusion may occur in early endosomes (268).

Several members of the tetraspanin family have been shown to endocytose into cells, via various routes, due to the presence of the endocytic motif YXXØ. Not only does CD81 lack this motif, removal of the N- and C-termini have minimal effect(s) on the proteins ability to internalise or to confer HCV infection. Overall these results suggest that Claudin1 may promote CD81 internalisation within the early endosomes upon certain stimuli, in this case antibody engagement or viral interaction.

**6.2 The analogy to Coxsackie B virus Entry**

A mechanism for the entry process of HCV has been proposed based on the model of CVB entry (figure 6.2). Although parallels between the viruses receptor usage can be drawn the evidence to define the entry process of HCV is lacking. Before discussing the possible entry process of HCV it is important to review the CVB model of entry. As described earlier (section *1.5 Tight Junction Proteins and viral entry)* the receptors for CVB entry are DAF and tight junction proteins CAR and Occludin. Virus entry into polarised Caco-2 cells is thought to occur in a stepwise process which starts with the interaction with DAF. The DAF-CVB complex then relocates to the tight junction where the virus interacts with CAR (208). The interaction with CAR is then thought to cause a conformational change in the virus which enters the cell with Occludin, whilst CAR remains at the plasma membrane. The role of Occludin is not presently known but the authors suggest that Occludin association with Caveolin-1 may be important for the recruitment of Caveolin-1 to the tight junction (209).

Reports indicate that the entry of the CVB differs depending on the polarisation state of the cell. In non-polarised Hela cells DAF-independent and dependent viral strains, CVB-Nancy

and CVB-RD strains respectively, require Dynamin to enter cells but their infection is independent of Caveolin, Clathrin and endosomal acidification (210). The movement of CAR was also shown to be different as the receptor is internalised into endosomes with the virus in non-polarised cells (210).

Many review articles depict the entry process of HCV as a stepwise association with co-receptors which ends in the internalisation of the virus (figure 6.2) (reviewed (272-274). The evidence for the proposed model of entry was published by Brazzoli et al who reported images that appear to demonstrate the relocation of the HCV E2 and CD81 proteins to cell-cell contact areas, which they refer to as tight junctions, in a CVB like pathway (267). However, the Huh-7 cell line type used by Brazzoli et al have been shown not to fully polarise or form mature tight junctions (179), without functional tight junctions and a polarised phenotype it seems difficult to draw solid conclusion about the movement of viral particles to cell contacts. The conclusions that HCV E2 engagement causes a redistribution to tight junctions is open to question. Recently single particle trafficking of DiD labelled HCV particles suggested that internalisation can occur within 10 minutes of attachment (275). We were also able to demonstrate that $t_{50\%}$ for internalisation of virus bound to the cell surface was between 12mins and 22mins, as indicated by the escape from proteinase K degradation and anti-E2 C1 Mab neutralisation respectively (276). The images in the Brazzoli et al publication are static images taken at 60mins which would suggest they have missed the majority of the internalisation event (267).

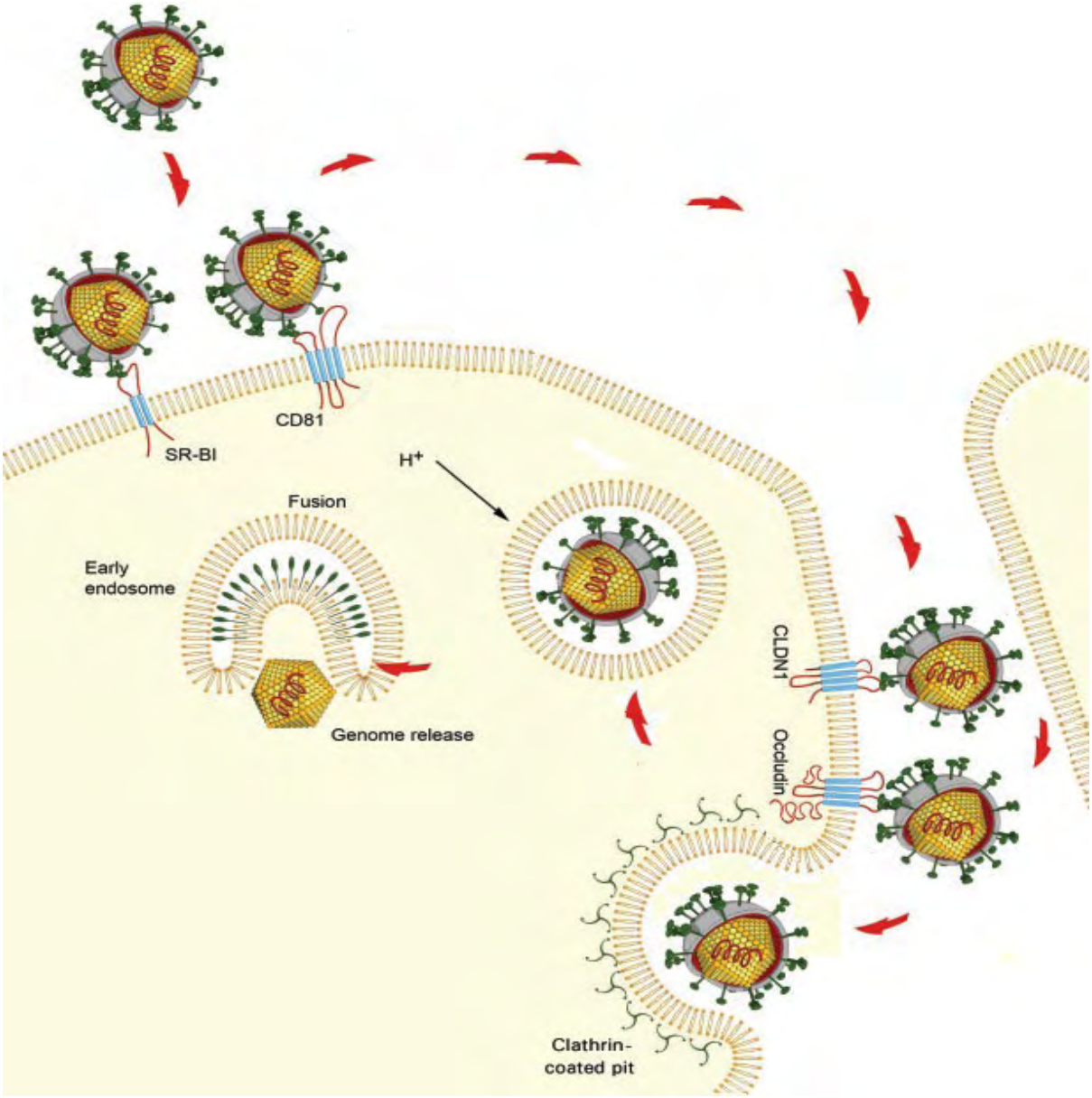


**Figure 6.2: Schematic representation of the proposed stepwise entry process of HCV based on the Coxsackie B virus entry**. The theory states the interaction with SR-BI, then CD81 which translocates with the virus to the tight junction. At the tight junction the virus interacts with Claudin1 then Occludin before internalising within Clathrin coated pits. The image is modified version taken from (273-274).

The sequential nature of HCV entry has been suggested due to the escape times of anti-receptor antibodies. Catanese et al showed that anti-SR-BI Mab C167 could only inhibit entry when the cells were pre-incubated with the Mab (277). Evans et al reported that anti-CD81 Mab JS81 could neutralise infection up to 18mins post viral binding. They also demonstrated using a Claudin1 protein containing an FLAG epitope within the EC1 that neutralisation by an anti-FLAG could occur up 78 mins post binding (110). Taken together these times would indicate a sequential function of the receptor proteins. In contrast other publications have demonstrated using alternative antibodies different kinetics for viral neutralisation. Zeisel et al reported with Rat anti-SR-BI serum that the entry could be neutralised up to 60mins post binding with similar kinetics to an anti-CD81 Mab (278). Krieger et al have also shown that a Rat anti-Claudin1 serum is able to inhibit virus up to 33mins post binding, which is half the time showed by Evans et al, with their anti-CD81 JS81 Mab recording a similar time of 30mins (182). In addition to these viral escape times we have demonstrated that the two commercial anti-CD81 Mabs (1.3.3.22 and JS81) and two in house Mabs (2s66 and 2s131) have viral escape times of 37, 40, 51 and 59 mins, respectively. We demonstrated that the ability of the mAb to inhibit infection at late times post infection was dependent on CD81 epitope recognition and not affinity. Due to the wide variation in viral escape times between the different antibodies care should be taken in concluding whether the receptors act in a sequential fashion. Furthermore, endocytosis of the virus has been determined by single particle tracking and the escape from proteinase K degradation, of 10mins and 12mins respectively, the antibodies appear to have the ability to inhibit the entry of internalised viral particles.

The issue of cell type and polarity are other aspects that lead us to move away from a CVB like entry process for HCV. The epithelial polarity, which CVB is presented with, is very different from that of hepatocyte polarity where the cells have an apical surface exposed to the lumen, tight junctions which are located close to the apical surface (introduction figure 1.4) (170, 195). The hepatocyte polarity is somewhat different with tight junctions enclosing the apical surface to form the bile canliculi with at least two basal surfaces exposed to the lumen (introduction figure 1.4) (216). Recent data demonstrates that tight junction associated proteins in polarised HepG2 cells are not accessible to anti-Claudin1 antibodies, whereas antibodies can bind basolateral pools of Claudin1 (Chris Mee, unpublished data). We have reported that polarised HepG2 cells are less susceptible to HCV infection. Either allowing the cells to polarise over time or promoting polarity, using PKA inhibitors or human oncostatin M, decreases HCVpp entry. Importantly, HCV still infects polarized HepG2 cells in an SR-BI, CD81 and Claudin1 dependent manner (Mee, in preparation). Reducing polarity with phorbol ester, a PKA activator, or vascular endothelial growth factor increased HCV entry (179-180). Since HCV enters the liver via the sinusoidal blood, the virus will encounter receptors expressed on the basal surface of the hepatocyte. Figure 6.3 shows a schematic of the environment that the virus is presented with in a polarised liver. We have been able to show, by staining liver sections for SR-BI, CD81, Claudin1, that all three receptors are present at the basal surface of hepatocytes (179, 256). In contrast, Occludin is only detectable at the apical tight junctions in vitro in polarized HepG2 and WIFB9 cells and in vivo in human liver tissue (179). In contrast, expression of a fluorophore labelled Occludin shows staining around the basal surface of a polarised HepG2 cells (figure 1.5), although this could be due to the over expression of the protein it could also indicate the levels of protein at the basal surface may be below the detection threshold for the available anti-occludin.

The polarisation of HepG2 cells was shown to have a notable change in the distribution of Claudin1 leading to a reduction of basal forms of the protein, which appear to be redistributed to the apical located tight junction (179). The data shown earlier in figure 4.1 indicates that tight junction pools of Claudin1 do not associate with CD81 in HepG2 cells. As we feel we have very good data implicating the association of Claudin1 with CD81 is essential for entry, we would conclude the tight junctions represent a non-permissive area for viral entry (179-180, 184). The location of Claudin1–CD81 complexes at the basolateral surface of polarized hepatoma cells supports a model where virus engagement of Claudin1–CD81 at the basal membrane may initiate the particle internalization process.

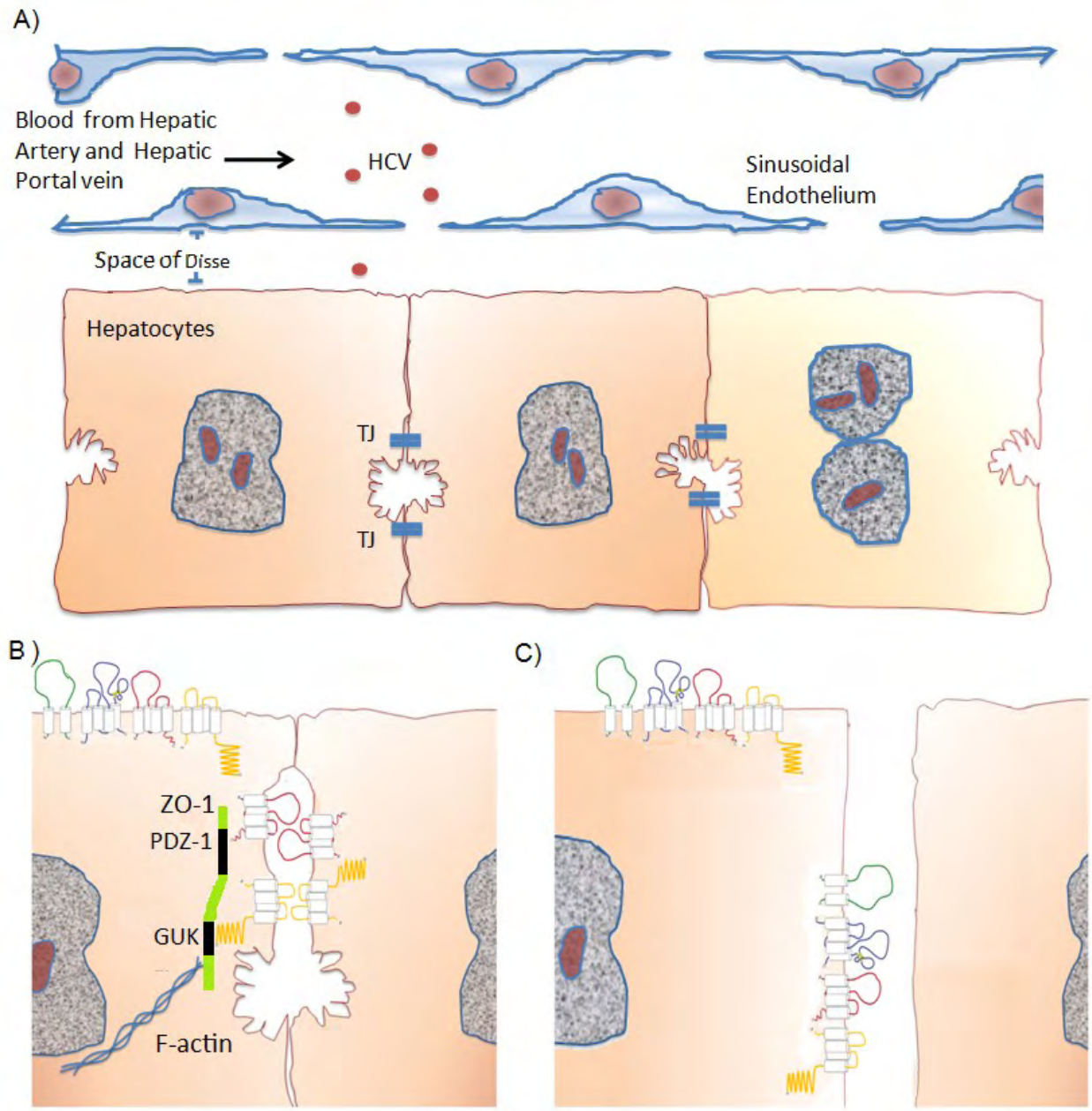


**Figure 6.3: Schematic representation of the hepatic environment.** HCV enters the liver in the blood carried by the hepatic artery. (A) The fenestrated sinusoidal endothelial layer which the virus has to traverse to gain access to its primary target cell, the hepatocyte. (B) In the case of polarized hepatocytes, although all receptors are detectable at the basal surface, the receptor proteins associated with the tight junctions may be inaccessible due to the closing of the space between neighbouring cells. (C) Depolarization of the hepatocytes, due to an underlying condition or to the actions of VEGF, PKC inhibition, etc., alters the presentation of the putative entry factors. In this state all of the receptor proteins will be available to allow viral engagement.

### 6.3 Conclusions and closing remarks

We feel our results demonstrate a role for CD81-Claudin1 complexes in HCV entry. We propose a role for Claudin1 in regulating CD81 endocytosis. Claudin1 appears to enable the internalisation of CD81, which itself lacks endocytic markers. Not only do the results provide a clearer picture of the function of the proteins in virus entry but highlight potential targets for therapeutic intervention. The modelling data, which we were able to validate, identify specific residues of both CD81 and Claudin1 that are essential for the interaction of the two proteins. The first third of the Claudin1 EC1, which was shown to be essential for entry (110, 183), appears to interact with T149, E152 and T153 of CD81. As the structure for CD81 is known, the design of small interfering molecules targeting the specific residues is very much achievable (120).

Ultimately the knowledge gained about the viral life cycle hopefully should lead to the creation of antiviral treatments. At present a combination therapy of pegylated Interferon α-2a and Ribavirin are used to treat for HCV infection. Unfortunately the rates of sustained virological response of the dual therapy is 46% for HCV genotype 1 infected individuals, 76% for those infected with genotypes 2 or 3 and 77% genotype 4 infections (80). Due to these low response rates, the toxicity and cost of treatment, new therapies are urgently required. The FDA has recently approved the use of the protease inhibitors Boceprevir (Merck) & Telaprevir (Vertex) for the treatment of HCV, with other antiviral compounds targeting the viral lifecycle at various stages of development. The ability of the virus to quickly develop resistance is a major concern for any potential therapies. The virus is found within individuals as a quasispecies, which develops over the course of their infection through neutral and adaptive evolution (81-82). The targeting of the CD81-Claudin1 complex may be a promising target due to the essential requirement for viral entry and it represents a stable

target. A small compound produced by iThreX targeting SR-BI has cross genotype antiviral activity and demonstrates the validity of targeting host proteins as a viable therapeutic approach (279-280). Without the knowledge of the biological relevance and function of the Claudin1-CD81 complex the long term effects of any targeted disruption is unknown. It has been demonstrated that anti-Claudin1 antibodies which inhibit the interaction and viral entry to above 90%, had no toxic effects in cell culture (254). If some toxicity is shown within individuals there is still the possibility of targeting the complex shortly after liver transplantation. HCV is now the most common indicator of liver transplant in the US with re-infection of the liver occurring with each case after transplantation leading to a more rapid and aggressive disease progression (281-282). The use of passive anti-HBV surface antigen (anti-HBVs) immunotherapy has been used with success to prevent the re-infection after liver transplantation (283). If the disruption of the CD81-Claudin1 complex has some long term toxic effects the short term use of anti-Claudin1 antibodies prior and shortly after transplant could serve to prevent the re-infection of the liver. In collaboration with the Baumert group we have been able to demonstrate that anti-Claudin1 antibodies inhibit HCV entry, with the mechanism appearing to be the disruption of the Claudin1-CD81 complexes (253-254). Overall the Claudin1-CD81 complex is important for the entry of HCV and could serve as an anti-viral target. The techniques utilised to show the CD81-Claudin1 interaction such as the FIR and FRET analysis and the SPR could easily be developed to enable screening of new drugs to perturb the complex. As stated earlier the biological function of the CD81-Claudin1 complex is unknown and the effects of disrupting the complex is unknown. More research is required to verify the complex is a valid target for anti-viral therapy.

# Chapter 7:

# References

1. Bayer ME, Blumberg BS, Werner B. Particles associated with Australia antigen in the sera of patients with leukaemia, Down's Syndrome and hepatitis. Nature. 1968 Jun 15;218(5146):1057-9.

2. Feinstone SM, Kapikian AZ, Purceli RH. Hepatitis A: detection by immune electron microscopy of a viruslike antigen associated with acute illness. Science. 1973 Dec 7;182(116):1026-8.

3. Lemon SM. Type A viral hepatitis: epidemiology, diagnosis, and prevention. Clin Chem. 1997 Aug;43(8 Pt 2):1494-9.

4. Liang TJ. Hepatitis B: the virus and disease. Hepatology. 2009 May;49(5 Suppl):S13-21.

5. Feinstone SM, Kapikian AZ, Purcell RH, Alter HJ, Holland PV. Transfusion-associated hepatitis not due to viral hepatitis type A or B. N Engl J Med. 1975 Apr 10;292(15):767-70.

6. Alter HJ, Purcell RH, Holland PV, Popper H. Transmissible agent in non-A, non-B hepatitis. Lancet. 1978 Mar 4;1(8062):459-63.

7. Hollinger FB, Gitnick GL, Aach RD, Szmuness W, Mosley JW, Stevens CE, et al. Non-A, non-B hepatitis transmission in chimpanzees: a project of the transfusion-transmitted viruses study group. Intervirology. 1978;10(1):60-8.

8. Feinstone SM, Mihalik KB, Kamimura T, Alter HJ, London WT, Purcell RH. Inactivation of hepatitis B virus and non-A, non-B hepatitis by chloroform. Infect Immun. 1983 Aug;41(2):816-21.

9. Bradley DW, McCaustland KA, Cook EH, Schable CA, Ebert JW, Maynard JE. Posttransfusion non-A, non-B hepatitis in chimpanzees. Physicochemical evidence that the tubule-forming agent is a small, enveloped virus. Gastroenterology. 1985 Mar;88(3):773-9.

10. Bergelson JM, Cunningham JA, Droguett G, Kurt-Jones EA, Krithivas A, Hong JS, et al. Isolation of a common receptor for Coxsackie B viruses and adenoviruses 2 and 5. Science. 1997 Feb 28;275(5304):1320-3.

11. Choo QL, Kuo G, Weiner AJ, Overby LR, Bradley DW, Houghton M. Isolation of a cDNA clone derived from a blood-borne non-A, non-B viral hepatitis genome. Science. 1989 Apr 21;244(4902):359-62.

12. Choo QL, Weiner AJ, Overby LR, Kuo G, Houghton M, Bradley DW. Hepatitis C virus: the major causative agent of viral non-A, non-B hepatitis. Br Med Bull. 1990 Apr;46(2):423-41.

13. Kuo G, Choo QL, Alter HJ, Gitnick GL, Redeker AG, Purcell RH, et al. An assay for circulating antibodies to a major etiologic virus of human non-A, non-B hepatitis. Science. 1989 Apr 21;244(4902):362-4.

14. Shepard CW, Finelli L, Alter MJ. Global epidemiology of hepatitis C virus infection. Lancet Infect Dis. 2005 Sep;5(9):558-67.

15. Ray Kim W. Global epidemiology and burden of hepatitis C. Microbes Infect. 2002 Oct;4(12):1219-25.

16. Hoofnagle JH. Course and outcome of hepatitis C. Hepatology. 2002 Nov;36(5 Suppl 1):S21-9.

17. Marrero CR, Marrero JA. Viral hepatitis and hepatocellular carcinoma. Arch Med Res. 2007 Aug;38(6):612-20.

18. Galossi A, Guarisco R, Bellis L, Puoti C. Extrahepatic manifestations of chronic HCV infection. J Gastrointestin Liver Dis. 2007 Mar;16(1):65-73.

19. Brown EA, Zhang H, Ping LH, Lemon SM. Secondary structure of the 5' nontranslated regions of hepatitis C virus and pestivirus genomic RNAs. Nucleic Acids Res. 1992 Oct 11;20(19):5041-5.

20. Pestova TV, Shatsky IN, Fletcher SP, Jackson RJ, Hellen CU. A prokaryotic-like mode of cytoplasmic eukaryotic ribosome binding to the initiation codon during internal translation initiation of hepatitis C and classical swine fever virus RNAs. Genes Dev. 1998 Jan 1;12(1):67-83.

21. McLauchlan J. Properties of the hepatitis C virus core protein: a structural protein that modulates cellular processes. J Viral Hepat. 2000 Jan;7(1):2-14.

22. Takahashi K, Kishimoto S, Yoshizawa H, Okamoto H, Yoshikawa A, Mishiro S. p26 protein and 33-nm particle associated with nucleocapsid of hepatitis C virus recovered from the circulation of infected hosts. Virology. 1992 Nov;191(1):431-4.

23. Klein KC, Polyak SJ, Lingappa JR. Unique features of hepatitis C virus capsid formation revealed by de novo cell-free assembly. J Virol. 2004 Sep;78(17):9257-69.

24. Kunkel M, Lorinczi M, Rijnbrand R, Lemon SM, Watowich SJ. Self-assembly of nucleocapsid-like particles from recombinant hepatitis C virus core protein. J Virol. 2001 Mar;75(5):2119-29.

25. McLauchlan J, Lemberg MK, Hope G, Martoglio B. Intramembrane proteolysis promotes trafficking of hepatitis C virus core protein to lipid droplets. EMBO J. 2002 Aug 1;21(15):3980-8.

26. Moradpour D, Penin F, Rice CM. Replication of hepatitis C virus. Nat Rev Microbiol. 2007 Jun;5(6):453-63.

27. McLauchlan J. Lipid droplets and hepatitis C virus infection. Biochim Biophys Acta. 2009 Jun;1791(6):552-9.

28. Boulant S, Douglas MW, Moody L, Budkowska A, Targett-Adams P, McLauchlan J. Hepatitis C virus core protein induces lipid droplet redistribution in a microtubule- and dynein-dependent manner. Traffic. 2008 Aug;9(8):1268-82.

29. Boulant S, Targett-Adams P, McLauchlan J. Disrupting the association of hepatitis C virus core protein with lipid droplets correlates with a loss in production of infectious virus. J Gen Virol. 2007 Aug;88(Pt 8):2204-13.

30. Boulant S, Montserret R, Hope RG, Ratinier M, Targett-Adams P, Lavergne JP, et al. Structural determinants that target the hepatitis C virus core protein to lipid droplets. J Biol Chem. 2006 Aug 4;281(31):22236-47.

31. Goffard A, Dubuisson J. Glycosylation of hepatitis C virus envelope proteins. Biochimie. 2003 Mar-Apr;85(3-4):295-301.

32. Merola M, Brazzoli M, Cocchiarella F, Heile JM, Helenius A, Weiner AJ, et al. Folding of hepatitis C virus E1 glycoprotein in a cell-free system. J Virol. 2001 Nov;75(22):11205-17.

33. Lavie M, Goffard A, Dubuisson J. Assembly of a functional HCV glycoprotein heterodimer. Curr Issues Mol Biol. 2007 Jul;9(2):71-86.

34. Brazzoli M, Helenius A, Foung SK, Houghton M, Abrignani S, Merola M. Folding and dimerization of hepatitis C virus E1 and E2 glycoproteins in stably transfected CHO cells. Virology. 2005 Feb 5;332(1):438-53.

35. Gonzalez ME, Carrasco L. Viroporins. FEBS Lett. 2003 Sep 18;552(1):28-34.

36. Griffin SD, Beales LP, Clarke DS, Worsfold O, Evans SD, Jaeger J, et al. The p7 protein of hepatitis C virus forms an ion channel that is blocked by the antiviral drug, Amantadine. FEBS Lett. 2003 Jan 30;535(1-3):34-8.

37. Sakai A, Claire MS, Faulk K, Govindarajan S, Emerson SU, Purcell RH, et al. The p7 polypeptide of hepatitis C virus is critical for infectivity and contains functionally important genotype-specific sequences. Proc Natl Acad Sci U S A. 2003 Sep 30;100(20):11646-51.

38. Griffin S, Stgelais C, Owsianka AM, Patel AH, Rowlands D, Harris M. Genotype-dependent sensitivity of hepatitis C virus to inhibitors of the p7 ion channel. Hepatology. 2008 Dec;48(6):1779-90.

39. Jones CT, Murray CL, Eastman DK, Tassello J, Rice CM. Hepatitis C virus p7 and NS2 proteins are essential for production of infectious virus. J Virol. 2007 Aug;81(16):8374-83.

40. Steinmann E, Penin F, Kallis S, Patel AH, Bartenschlager R, Pietschmann T. Hepatitis C virus p7 protein is crucial for assembly and release of infectious virions. PLoS Pathog. 2007 Jul;3(7):e103.

41. Steinmann E, Whitfield T, Kallis S, Dwek RA, Zitzmann N, Pietschmann T, et al. Antiviral effects of amantadine and iminosugar derivatives against hepatitis C virus. Hepatology. 2007 Aug;46(2):330-8.

42. Pietschmann T, Kaul A, Koutsoudakis G, Shavinskaya A, Kallis S, Steinmann E, et al. Construction and characterization of infectious intragenotypic and intergenotypic hepatitis C virus chimeras. Proc Natl Acad Sci U S A. 2006 May 9;103(19):7408-13.

43. Khromykh AA, Westaway EG. Subgenomic replicons of the flavivirus Kunjin: construction and applications. J Virol. 1997 Feb;71(2):1497-505.

44. Grakoui A, McCourt DW, Wychowski C, Feinstone SM, Rice CM. A second hepatitis C virus-encoded proteinase. Proc Natl Acad Sci U S A. 1993 Nov 15;90(22):10583-7.

45. Popescu CI, Callens N, Trinel D, Roingeard P, Moradpour D, Descamps V, et al. NS2 protein of hepatitis C virus interacts with structural and non-structural proteins towards virus assembly. PLoS Pathog. 2011;7(2):e1001278.

46. Dentzer TG, Lorenz IC, Evans MJ, Rice CM. Determinants of the hepatitis C virus nonstructural protein 2 protease domain required for production of infectious virus. J Virol. 2009 Dec;83(24):12702-13.

47. Phan T, Beran RK, Peters C, Lorenz IC, Lindenbach BD. Hepatitis C virus NS2 protein contributes to virus particle assembly via opposing epistatic interactions with the E1-E2 glycoprotein and NS3-NS4A enzyme complexes. J Virol. 2009 Sep;83(17):8379-95.

48. Gallinari P, Brennan D, Nardi C, Brunetti M, Tomei L, Steinkuhler C, et al. Multiple enzymatic activities associated with recombinant NS3 protein of hepatitis C virus. J Virol. 1998 Aug;72(8):6758-69.

49. Wolk B, Sansonno D, Krausslich HG, Dammacco F, Rice CM, Blum HE, et al. Subcellular localization, stability, and trans-cleavage competence of the hepatitis C virus

NS3-NS4A complex expressed in tetracycline-regulated cell lines. J Virol. 2000 Mar;74(5):2293-304.

50. Romano KP, Laine JM, Deveau LM, Cao H, Massi F, Schiffer CA. Molecular mechanisms of viral and host-cell substrate recognition by HCV NS3/4A protease. J Virol. 2011 Apr 20.

51. Bartenschlager R, Ahlborn-Laake L, Mous J, Jacobsen H. Nonstructural protein 3 of the hepatitis C virus encodes a serine-type proteinase required for cleavage at the NS3/4 and NS4/5 junctions. J Virol. 1993 Jul;67(7):3835-44.

52. Serebrov V, Pyle AM. Periodic cycles of RNA unwinding and pausing by hepatitis C virus NS3 helicase. Nature. 2004 Jul 22;430(6998):476-80.

53. Levin MK, Gurjar M, Patel SS. A Brownian motor mechanism of translocation and strand separation by hepatitis C virus helicase. Nat Struct Mol Biol. 2005 May;12(5):429-35.

54. Seth RB, Sun L, Chen ZJ. Antiviral innate immunity pathways. Cell Res. 2006 Feb;16(2):141-7.

55. Li XD, Sun L, Seth RB, Pineda G, Chen ZJ. Hepatitis C virus protease NS3/4A cleaves mitochondrial antiviral signaling protein off the mitochondria to evade innate immunity. Proc Natl Acad Sci U S A. 2005 Dec 6;102(49):17717-22.

56. Sen GC, Sarkar SN. Hitching RIG to action. Nat Immunol. 2005 Nov;6(11):1074-6.

57. Meylan E, Curran J, Hofmann K, Moradpour D, Binder M, Bartenschlager R, et al. Cardif is an adaptor protein in the RIG-I antiviral pathway and is targeted by hepatitis C virus. Nature. 2005 Oct 20;437(7062):1167-72.

58. Li K, Foy E, Ferreon JC, Nakamura M, Ferreon AC, Ikeda M, et al. Immune evasion by hepatitis C virus NS3/4A protease-mediated cleavage of the Toll-like receptor 3 adaptor protein TRIF. Proc Natl Acad Sci U S A. 2005 Feb 22;102(8):2992-7.

59. Egger D, Wolk B, Gosert R, Bianchi L, Blum HE, Moradpour D, et al. Expression of hepatitis C virus proteins induces distinct membrane alterations including a candidate viral replication complex. J Virol. 2002 Jun;76(12):5974-84.

60. Gosert R, Egger D, Lohmann V, Bartenschlager R, Blum HE, Bienz K, et al. Identification of the hepatitis C virus RNA replication complex in Huh-7 cells harboring subgenomic replicons. J Virol. 2003 May;77(9):5487-92.

61. Gouttenoire J, Penin F, Moradpour D. Hepatitis C virus nonstructural protein 4B: a journey into unexplored territory. Rev Med Virol. 2010 Mar;20(2):117-29.

62. Einav S, Elazar M, Danieli T, Glenn JS. A nucleotide binding motif in hepatitis C virus (HCV) NS4B mediates HCV RNA replication. J Virol. 2004 Oct;78(20):11288-95.

63. Jones DM, Patel AH, Targett-Adams P, McLauchlan J. The hepatitis C virus NS4B protein can trans-complement viral RNA replication and modulates production of infectious virus. J Virol. 2009 Mar;83(5):2163-77.

64. Yamashita T, Kaneko S, Shirota Y, Qin W, Nomura T, Kobayashi K, et al. RNA-dependent RNA polymerase activity of the soluble recombinant hepatitis C virus NS5B protein truncated at the C-terminal region. J Biol Chem. 1998 Jun 19;273(25):15479-86.

65. Lohmann V, Korner F, Herian U, Bartenschlager R. Biochemical properties of hepatitis C virus NS5B RNA-dependent RNA polymerase and identification of amino acid sequence motifs essential for enzymatic activity. J Virol. 1997 Nov;71(11):8416-28.

66. Behrens SE, Tomei L, De Francesco R. Identification and properties of the RNA-dependent RNA polymerase of hepatitis C virus. EMBO J. 1996 Jan 2;15(1):12-22.

67. Ago H, Adachi T, Yoshida A, Yamamoto M, Habuka N, Yatsunami K, et al. Crystal structure of the RNA-dependent RNA polymerase of hepatitis C virus. Structure. 1999 Nov 15;7(11):1417-26.

68. Bressanelli S, Tomei L, Roussel A, Incitti I, Vitale RL, Mathieu M, et al. Crystal structure of the RNA-dependent RNA polymerase of hepatitis C virus. Proc Natl Acad Sci U S A. 1999 Nov 9;96(23):13034-9.

69. Lesburg CA, Cable MB, Ferrari E, Hong Z, Mannarino AF, Weber PC. Crystal structure of the RNA-dependent RNA polymerase from hepatitis C virus reveals a fully encircled active site. Nat Struct Biol. 1999 Oct;6(10):937-43.

70. Appel N, Schaller T, Penin F, Bartenschlager R. From structure to function: new insights into hepatitis C virus RNA replication. J Biol Chem. 2006 Apr 14;281(15):9833-6.

71. Pawlotsky JM. Hepatitis C virus (HCV) NS5A protein: role in HCV replication and resistance to interferon-alpha. J Viral Hepat. 1999 Jul;6 Suppl 1:47-8.

72. Pan Y, Wei W, Kang L, Wang Z, Fang J, Zhu Y, et al. NS5A protein of HCV enhances HBV replication and resistance to interferon response. Biochem Biophys Res Commun. 2007 Jul 20;359(1):70-5.

73. Palomares-Jerez MF, Guillen J, Villalain J. Interaction of the N-terminal segment of HCV protein NS5A with model membranes. Biochim Biophys Acta. 2010 Jun;1798(6):1212-24.

74. Gale MJ, Jr., Korth MJ, Tang NM, Tan SL, Hopkins DA, Dever TE, et al. Evidence that hepatitis C virus resistance to interferon is mediated through repression of the PKR protein kinase by the nonstructural 5A protein. Virology. 1997 Apr 14;230(2):217-27.

75. Samuel CE. Antiviral actions of interferons. Clin Microbiol Rev. 2001 Oct;14(4):778-809, table of contents.

76. Qadri I, Iwahashi M, Simon F. Hepatitis C virus NS5A protein binds TBP and p53, inhibiting their DNA binding and p53 interactions with TBP and ERCC3. Biochim Biophys Acta. 2002 Oct 21;1592(2):193-204.

77. Tan SL, Nakao H, He Y, Vijaysri S, Neddermann P, Jacobs BL, et al. NS5A, a nonstructural protein of hepatitis C virus, binds growth factor receptor-bound protein 2 adaptor protein in a Src homology 3 domain/ligand-dependent manner and perturbs mitogenic signaling. Proc Natl Acad Sci U S A. 1999 May 11;96(10):5533-8.

78. Burckstummer T, Kriegs M, Lupberger J, Pauli EK, Schmittel S, Hildt E. Raf-1 kinase associates with Hepatitis C virus NS5A and regulates viral replication. FEBS Lett. 2006 Jan 23;580(2):575-80.

79. Street A, Macdonald A, Crowder K, Harris M. The Hepatitis C virus NS5A protein activates a phosphoinositide 3-kinase-dependent survival signaling cascade. J Biol Chem. 2004 Mar 26;279(13):12232-41.

80. Fried MW, Shiffman ML, Reddy KR, Smith C, Marinos G, Goncales FL, Jr., et al. Peginterferon alfa-2a plus ribavirin for chronic hepatitis C virus infection. N Engl J Med. 2002 Sep 26;347(13):975-82.

81. Martell M, Esteban JI, Quer J, Genesca J, Weiner A, Esteban R, et al. Hepatitis C virus (HCV) circulates as a population of different but closely related genomes: quasispecies nature of HCV genome distribution. J Virol. 1992 May;66(5):3225-9.

82. Simmonds P. Genetic diversity and evolution of hepatitis C virus--15 years on. J Gen Virol. 2004 Nov;85(Pt 11):3173-88.

83. Selby MJ, Glazer E, Masiarz F, Houghton M. Complex processing and protein:protein interactions in the E2:NS2 region of HCV. Virology. 1994 Oct;204(1):114-22.

84. Whidby J, Mateu G, Scarborough H, Demeler B, Grakoui A, Marcotrigiano J. Blocking hepatitis C virus infection with a recombinant form of envelope protein 2 ectodomain. J Virol. 2009 Aug 26.

85. Deleersnyder V, Pillez A, Wychowski C, Blight K, Xu J, Hahn YS, et al. Formation of native hepatitis C virus glycoprotein complexes. J Virol. 1997 Jan;71(1):697-704.

86. Op De Beeck A, Voisset C, Bartosch B, Ciczora Y, Cocquerel L, Keck Z, et al. Characterization of functional hepatitis C virus envelope glycoproteins. J Virol. 2004 Mar;78(6):2994-3002.

87. Flint M, Dubuisson J, Maidens C, Harrop R, Guile GR, Borrow P, et al. Functional characterization of intracellular and secreted forms of a truncated hepatitis C virus E2 glycoprotein. J Virol. 2000 Jan;74(2):702-9.

88. Flint M, von Hahn T, Zhang J, Farquhar M, Jones CT, Balfe P, et al. Diverse CD81 proteins support hepatitis C virus infection. J Virol. 2006 Nov;80(22):11331-42.

89. Bartosch B, Dubuisson J, Cosset FL. Infectious hepatitis C virus pseudo-particles containing functional E1-E2 envelope protein complexes. J Exp Med. 2003 Mar 3;197(5):633-42.

90. Drummer HE, Maerz A, Poumbourios P. Cell surface expression of functional hepatitis C virus E1 and E2 glycoproteins. FEBS Lett. 2003 Jul 10;546(2-3):385-90.

91. Hsu M, Zhang J, Flint M, Logvinoff C, Cheng-Mayer C, Rice CM, et al. Hepatitis C virus glycoproteins mediate pH-dependent cell entry of pseudotyped retroviral particles. Proc Natl Acad Sci U S A. 2003 Jun 10;100(12):7271-6.

92. von Hahn T, Rice CM. Hepatitis C virus entry. J Biol Chem. 2008 Feb 15;283(7):3689-93.

93. Bartosch B, Vitelli A, Granier C, Goujon C, Dubuisson J, Pascale S, et al. Cell entry of hepatitis C virus requires a set of co-receptors that include the CD81 tetraspanin and the SR-B1 scavenger receptor. J Biol Chem. 2003 Oct 24;278(43):41624-30.

94. Lindenbach BD, Evans MJ, Syder AJ, Wolk B, Tellinghuisen TL, Liu CC, et al. Complete replication of hepatitis C virus in cell culture. Science. 2005 Jul 22;309(5734):623-6.

95. Wakita T, Pietschmann T, Kato T, Date T, Miyamoto M, Zhao Z, et al. Production of infectious hepatitis C virus in tissue culture from a cloned viral genome. Nat Med. 2005 Jul;11(7):791-6.

96. Zhong J, Gastaminza P, Chung J, Stamataki Z, Isogawa M, Cheng G, et al. Persistent hepatitis C virus infection in vitro: coevolution of virus and host. J Virol. 2006 Nov;80(22):11082-93.

97. Gottwein JM, Scheel TK, Hoegh AM, Lademann JB, Eugen-Olsen J, Lisby G, et al. Robust hepatitis C genotype 3a cell culture releasing adapted intergenotypic 3a/2a (S52/JFH1) viruses. Gastroenterology. 2007 Nov;133(5):1614-26.

98. Lindenbach BD, Meuleman P, Ploss A, Vanwolleghem T, Syder AJ, McKeating JA, et al. Cell culture-grown hepatitis C virus is infectious in vivo and can be recultured in vitro. Proc Natl Acad Sci U S A. 2006 Mar 7;103(10):3805-9.

99. Scheel TK, Gottwein JM, Jensen TB, Prentoe JC, Hoegh AM, Alter HJ, et al. Development of JFH1-based cell culture systems for hepatitis C virus genotype 4a and evidence for cross-genotype neutralization. Proc Natl Acad Sci U S A. 2008 Jan 22;105(3):997-1002.

100. Pokrovskii MV, Bush CO, Beran RK, Robinson MF, Cheng G, Tirunagari N, et al. Novel mutations in a tissue culture-adapted hepatitis C virus strain improve infectious-virus stability and markedly enhance infection kinetics. J Virol. 2011 Apr;85(8):3978-85.

101. Molina S, Castet V, Pichard-Garcia L, Wychowski C, Meurs E, Pascussi JM, et al. Serum-derived hepatitis C virus infection of primary human hepatocytes is tetraspanin CD81 dependent. J Virol. 2008 Jan;82(1):569-74.

102. Barth H, Schafer C, Adah MI, Zhang F, Linhardt RJ, Toyoda H, et al. Cellular binding of hepatitis C virus envelope glycoprotein E2 requires cell surface heparan sulfate. J Biol Chem. 2003 Oct 17;278(42):41003-12.

103. Mandl CW, Kroschewski H, Allison SL, Kofler R, Holzmann H, Meixner T, et al. Adaptation of tick-borne encephalitis virus to BHK-21 cells results in the formation of multiple heparan sulfate binding sites in the envelope protein and attenuation in vivo. J Virol. 2001 Jun;75(12):5627-37.

104. Hulst MM, van Gennip HG, Moormann RJ. Passage of classical swine fever virus in cultured swine kidney cells selects virus variants that bind to heparan sulfate due to a single amino acid change in envelope protein E(rns). J Virol. 2000 Oct;74(20):9553-61.

105. Cormier EG, Tsamis F, Kajumo F, Durso RJ, Gardner JP, Dragic T. CD81 is an entry coreceptor for hepatitis C virus. Proc Natl Acad Sci U S A. 2004 May 11;101(19):7270-4.

106. Pileri P, Uematsu Y, Campagnoli S, Galli G, Falugi F, Petracca R, et al. Binding of hepatitis C virus to CD81. Science. 1998 Oct 30;282(5390):938-41.

107. Barth H, Schnober EK, Neumann-Haefelin C, Thumann C, Zeisel MB, Diepolder HM, et al. Scavenger receptor class B is required for hepatitis C virus uptake and cross-presentation by human dendritic cells. J Virol. 2008 Apr;82(7):3466-79.

108. Grove J, Huby T, Stamataki Z, Vanwolleghem T, Meuleman P, Farquhar M, et al. Scavenger receptor BI and BII expression levels modulate hepatitis C virus infectivity. J Virol. 2007 Apr;81(7):3162-9.

109. Scarselli E, Ansuini H, Cerino R, Roccasecca RM, Acali S, Filocamo G, et al. The human scavenger receptor class B type I is a novel candidate receptor for the hepatitis C virus. EMBO J. 2002 Oct 1;21(19):5017-25.

110. Evans MJ, von Hahn T, Tscherne DM, Syder AJ, Panis M, Wolk B, et al. Claudin-1 is a hepatitis C virus co-receptor required for a late step in entry. Nature. 2007 Apr 12;446(7137):801-5.

111. Meertens L, Bertaux C, Cukierman L, Cormier E, Lavillette D, Cosset FL, et al. The tight junction proteins claudin-1, -6, and -9 are entry cofactors for hepatitis C virus. J Virol. 2008 Apr;82(7):3555-60.

112. Yang W, Qiu C, Biswas N, Jin J, Watkins SC, Montelaro RC, et al. Correlation of the tight junction-like distribution of Claudin-1 to the cellular tropism of hepatitis C virus. J Biol Chem. 2008 Mar 28;283(13):8643-53.

113. Zheng A, Yuan F, Li Y, Zhu F, Hou P, Li J, et al. Claudin-6 and claudin-9 function as additional coreceptors for hepatitis C virus. J Virol. 2007 Nov;81(22):12465-71.

114. Liu S, Yang W, Shen L, Turner JR, Coyne CB, Wang T. Tight junction proteins claudin-1 and occludin control hepatitis C virus entry and are downregulated during infection to prevent superinfection. J Virol. 2009 Feb;83(4):2011-4.

115. Ploss A, Evans MJ, Gaysinskaya VA, Panis M, You H, de Jong YP, et al. Human occludin is a hepatitis C virus entry factor required for infection of mouse cells. Nature. 2009 Feb 12;457(7231):882-6.

116. Huang S, Yuan S, Dong M, Su J, Yu C, Shen Y, et al. The phylogenetic analysis of tetraspanins projects the evolution of cell-cell interactions from unicellular to multicellular organisms. Genomics. 2005 Dec;86(6):674-84.

117. Hemler ME. Tetraspanin proteins mediate cellular penetration, invasion, and fusion events and define a novel type of membrane microdomain. Annu Rev Cell Dev Biol. 2003;19:397-422.

118. Boucheix C, Duc GH, Jasmin C, Rubinstein E. Tetraspanins and malignancy. Expert Rev Mol Med. 2001 Jan 31;2001:1-17.

119. Boucheix C, Rubinstein E. Tetraspanins. Cell Mol Life Sci. 2001 Aug;58(9):1189-205.

120. Kitadokoro K, Bordo D, Galli G, Petracca R, Falugi F, Abrignani S, et al. CD81 extracellular domain 3D structure: insight into the tetraspanin superfamily structural motifs. EMBO J. 2001 Jan 15;20(1-2):12-8.

121. Seigneuret M, Delaguillaumie A, Lagaudriere-Gesbert C, Conjeaud H. Structure of the tetraspanin main extracellular domain. A partially conserved fold with a structurally variable domain insertion. J Biol Chem. 2001 Oct 26;276(43):40055-64.

122. Hemler ME. Tetraspanin functions and associated microdomains. Nat Rev Mol Cell Biol. 2005 Oct;6(10):801-11.

123. Rubinstein E, Le Naour F, Lagaudriere-Gesbert C, Billard M, Conjeaud H, Boucheix C. CD9, CD63, CD81, and CD82 are components of a surface tetraspan network connected to HLA-DR and VLA integrins. Eur J Immunol. 1996 Nov;26(11):2657-65.

124. Kovalenko OV, Yang X, Kolesnikova TV, Hemler ME. Evidence for specific tetraspanin homodimers: inhibition of palmitoylation makes cysteine residues available for cross-linking. Biochem J. 2004 Jan 15;377(Pt 2):407-17.

125. Kovalenko OV, Yang XH, Hemler ME. A novel cysteine cross-linking method reveals a direct association between claudin-1 and tetraspanin CD9. Mol Cell Proteomics. 2007 Nov;6(11):1855-67.

126. Charrin S, le Naour F, Silvie O, Milhiet PE, Boucheix C, Rubinstein E. Lateral organization of membrane proteins: tetraspanins spin their web. Biochem J. 2009 Jun 1;420(2):133-54.

127. Levy S, Shoham T. The tetraspanin web modulates immune-signalling complexes. Nat Rev Immunol. 2005 Feb;5(2):136-48.

128. Tsitsikov EN, Gutierrez-Ramos JC, Geha RS. Impaired CD19 expression and signaling, enhanced antibody response to type II T independent antigen and reduction of B-1 cells in CD81-deficient mice. Proc Natl Acad Sci U S A. 1997 Sep 30;94(20):10844-9.

129. Miyazaki T, Muller U, Campbell KS. Normal development but differentially altered proliferative responses of lymphocytes in mice lacking CD81. EMBO J. 1997 Jul 16;16(14):4217-25.

130. Maecker HT, Levy S. Normal lymphocyte development but delayed humoral immune response in CD81-null mice. J Exp Med. 1997 Apr 21;185(8):1505-10.

131. Yamada M, Sumida Y, Fujibayashi A, Fukaguchi K, Sanzen N, Nishiuchi R, et al. The tetraspanin CD151 regulates cell morphology and intracellular signaling on laminin-511. FEBS J. 2008 Jul;275(13):3335-51.

132. Karamatic Crew V, Burton N, Kagan A, Green CA, Levene C, Flinter F, et al. CD151, the first member of the tetraspanin (TM4) superfamily detected on erythrocytes, is essential for the correct assembly of human basement membranes in kidney and skin. Blood. 2004 Oct 15;104(8):2217-23.

133. Kagan A, Feld S, Chemke J, Bar-Khayim Y. Occurrence of hereditary nephritis, pretibial epidermolysis bullosa and beta-thalassemia minor in two siblings with end-stage renal disease. Nephron. 1988;49(4):331-2.

134. Lau LM, Wee JL, Wright MD, Moseley GW, Hogarth PM, Ashman LK, et al. The tetraspanin superfamily member CD151 regulates outside-in integrin alphaIIbbeta3 signaling and platelet function. Blood. 2004 Oct 15;104(8):2368-75.

135. Wright MD, Geary SM, Fitter S, Moseley GW, Lau LM, Sheng KC, et al. Characterization of mice lacking the tetraspanin superfamily member CD151. Mol Cell Biol. 2004 Jul;24(13):5978-88.

136. Le Naour F, Rubinstein E, Jasmin C, Prenant M, Boucheix C. Severely reduced female fertility in CD9-deficient mice. Science. 2000 Jan 14;287(5451):319-21.

137. Miyado K, Yamada G, Yamada S, Hasuwa H, Nakamura Y, Ryu F, et al. Requirement of CD9 on the egg plasma membrane for fertilization. Science. 2000 Jan 14;287(5451):321-4.

138. Kaji K, Oda S, Shikano T, Ohnuki T, Uematsu Y, Sakagami J, et al. The gamete fusion process is defective in eggs of Cd9-deficient mice. Nat Genet. 2000 Mar;24(3):279-82.

139. Ishibashi T, Ding L, Ikenaka K, Inoue Y, Miyado K, Mekada E, et al. Tetraspanin protein CD9 is a novel paranodal component regulating paranodal junctional formation. J Neurosci. 2004 Jan 7;24(1):96-102.

140. Wang L, Liu L, Che Y, Jiang L, Dong C, Zhang Y, et al. Egress of HSV-1 capsid requires the interaction of VP26 and a cellular tetraspanin membrane protein. Virol J. 2010;7:156.

141. Spoden G, Freitag K, Husmann M, Boller K, Sapp M, Lambert C, et al. Clathrin- and caveolin-independent entry of human papillomavirus type 16--involvement of tetraspanin-enriched microdomains (TEMs). PLoS One. 2008;3(10):e3313.

142. Thali M. Tetraspanin functions during HIV-1 and influenza virus replication. Biochem Soc Trans. 2011 Apr 1;39(2):529-31.

143. Garcia E, Nikolic DS, Piguet V. HIV-1 replication in dendritic cells occurs through a tetraspanin-containing compartment enriched in AP-3. Traffic. 2008 Feb;9(2):200-14.

144. Meroni L, Milazzo L, Menzaghi B, Mazzucchelli R, Mologni D, Morelli P, et al. Altered expression of the tetraspanin CD81 on B and T lymphocytes during HIV-1 infection. Clin Exp Immunol. 2007 Jan;147(1):53-9.

145. Nydegger S, Khurana S, Krementsov DN, Foti M, Thali M. Mapping of tetraspanin-enriched microdomains that can function as gateways for HIV-1. J Cell Biol. 2006 Jun 5;173(5):795-807.

146. Garcia E, Pion M, Pelchen-Matthews A, Collinson L, Arrighi JF, Blot G, et al. HIV-1 trafficking to the dendritic cell-T-cell infectious synapse uses a pathway of tetraspanin sorting to the immunological synapse. Traffic. 2005 Jun;6(6):488-501.

147. Lavillette D, Tarr AW, Voisset C, Donot P, Bartosch B, Bain C, et al. Characterization of host-range and cell entry properties of the major genotypes and subtypes of hepatitis C virus. Hepatology. 2005 Feb;41(2):265-74.

148. Zhong J, Gastaminza P, Cheng G, Kapadia S, Kato T, Burton DR, et al. Robust hepatitis C virus infection in vitro. Proc Natl Acad Sci U S A. 2005 Jun 28;102(26):9294-9.

149. Zhang J, Randall G, Higginbottom A, Monk P, Rice CM, McKeating JA. CD81 is required for hepatitis C virus glycoprotein-mediated viral infection. J Virol. 2004 Feb;78(3):1448-55.

150. McKeating JA, Zhang LQ, Logvinoff C, Flint M, Zhang J, Yu J, et al. Diverse hepatitis C virus glycoproteins mediate viral infection in a CD81-dependent manner. J Virol. 2004 Aug;78(16):8496-505.

151. Jamshad M, Rajesh S, Stamataki Z, McKeating JA, Dafforn T, Overduin M, et al. Structural characterization of recombinant human CD81 produced in Pichia pastoris. Protein Expr Purif. 2008 Feb;57(2):206-16.

152. Drummer HE, Wilson KA, Poumbourios P. Determinants of CD81 dimerization and interaction with hepatitis C virus glycoprotein E2. Biochem Biophys Res Commun. 2005 Mar 4;328(1):251-7.

153. Nakajima H, Cocquerel L, Kiyokawa N, Fujimoto J, Levy S. Kinetics of HCV envelope proteins' interaction with CD81 large extracellular loop. Biochem Biophys Res Commun. 2005 Mar 25;328(4):1091-100.

154. Triyatni M, Vergalla J, Davis AR, Hadlock KG, Foung SK, Liang TJ. Structural features of envelope proteins on hepatitis C virus-like particles as determined by anti-envelope monoclonal antibodies and CD81 binding. Virology. 2002 Jun 20;298(1):124-32.

155. Yagnik AT, Lahm A, Meola A, Roccasecca RM, Ercole BB, Nicosia A, et al. A model for the hepatitis C virus envelope glycoprotein E2. Proteins. 2000 Aug 15;40(3):355-66.

156. Calvo D, Vega MA. Identification, primary structure, and distribution of CLA-1, a novel member of the CD36/LIMPII gene family. J Biol Chem. 1993 Sep 5;268(25):18929-35.

157. Krieger M. Charting the fate of the "good cholesterol": identification and characterization of the high-density lipoprotein receptor SR-BI. Annu Rev Biochem. 1999;68:523-58.

158. Brown MS, Goldstein JL. Lipoprotein metabolism in the macrophage: implications for cholesterol deposition in atherosclerosis. Annu Rev Biochem. 1983;52:223-61.

159. Krieger M. The other side of scavenger receptors: pattern recognition for host defense. Curr Opin Lipidol. 1997 Oct;8(5):275-80.

160. Krieger M, Herz J. Structures and functions of multiligand lipoprotein receptors: macrophage scavenger receptors and LDL receptor-related protein (LRP). Annu Rev Biochem. 1994;63:601-37.

161. Fidge NH. High density lipoprotein receptors, binding proteins, and ligands. J Lipid Res. 1999 Feb;40(2):187-201.

162. von Hahn T, Lindenbach BD, Boullier A, Quehenberger O, Paulson M, Rice CM, et al. Oxidized low-density lipoprotein inhibits hepatitis C virus cell entry in human hepatoma cells. Hepatology. 2006 May;43(5):932-42.

163. Lavie M, Voisset C, Vu-Dac N, Zurawski V, Duverlie G, Wychowski C, et al. Serum amyloid A has antiviral activity against hepatitis C virus by inhibiting virus entry in a cell culture system. Hepatology. 2006 Dec;44(6):1626-34.

164. Cai Z, Cai L, Jiang J, Chang KS, van der Westhuyzen DR, Luo G. Human serum amyloid A protein inhibits hepatitis C virus entry into cells. J Virol. 2007 Jun;81(11):6128-33.

165. Voisset C, Op de Beeck A, Horellou P, Dreux M, Gustot T, Duverlie G, et al. High-density lipoproteins reduce the neutralizing effect of hepatitis C virus (HCV)-infected patient antibodies by promoting HCV entry. J Gen Virol. 2006 Sep;87(Pt 9):2577-81.

166. Voisset C, Callens N, Blanchard E, Op De Beeck A, Dubuisson J, Vu-Dac N. High density lipoproteins facilitate hepatitis C virus entry through the scavenger receptor class B type I. J Biol Chem. 2005 Mar 4;280(9):7793-9.

167. Bartosch B, Verney G, Dreux M, Donot P, Morice Y, Penin F, et al. An interplay between hypervariable region 1 of the hepatitis C virus E2 glycoprotein, the scavenger receptor BI, and high-density lipoprotein promotes both enhancement of infection and protection against neutralizing antibodies. J Virol. 2005 Jul;79(13):8217-29.

168. Grove J, Nielsen S, Zhong J, Bassendine MF, Drummer HE, Balfe P, et al. Identification of a residue in hepatitis C virus E2 glycoprotein that determines scavenger receptor BI and CD81 receptor dependency and sensitivity to neutralizing antibodies. J Virol. 2008 Dec;82(24):12020-9.

169. Dreux M, Dao Thi VL, Fresquet J, Guerin M, Julia Z, Verney G, et al. Receptor complementation and mutagenesis reveal SR-BI as an essential HCV entry factor and functionally imply its intra- and extra-cellular domains. PLoS Pathog. 2009 Feb;5(2):e1000310.

170. Furuse M, Tsukita S. Claudins in occluding junctions of humans and flies. Trends Cell Biol. 2006 Apr;16(4):181-8.

171. Furuse M, Sasaki H, Tsukita S. Manner of interaction of heterogeneous claudin species within and between tight junction strands. J Cell Biol. 1999 Nov 15;147(4):891-903.

172. Krause G, Winkler L, Mueller SL, Haseloff RF, Piontek J, Blasig IE. Structure and function of claudins. Biochim Biophys Acta. 2008 Mar;1778(3):631-45.

173. Turksen K, Troy TC. Claudin-6: a novel tight junction molecule is developmentally regulated in mouse embryonic epithelium. Dev Dyn. 2001 Oct;222(2):292-300.

174. Umeda K, Ikenouchi J, Katahira-Tayama S, Furuse K, Sasaki H, Nakayama M, et al. ZO-1 and ZO-2 independently determine where claudins are polymerized in tight-junction strand formation. Cell. 2006 Aug 25;126(4):741-54.

175. Sasaki H, Matsui C, Furuse K, Mimori-Kiyosue Y, Furuse M, Tsukita S. Dynamic behavior of paired claudin strands within apposing plasma membranes. Proc Natl Acad Sci U S A. 2003 Apr 1;100(7):3971-6.

176. Hamazaki Y, Itoh M, Sasaki H, Furuse M, Tsukita S. Multi-PDZ domain protein 1 (MUPP1) is concentrated at tight junctions through its possible interaction with claudin-1 and junctional adhesion molecule. J Biol Chem. 2002 Jan 4;277(1):455-61.

177. Itoh M, Furuse M, Morita K, Kubota K, Saitou M, Tsukita S. Direct binding of three tight junction-associated MAGUKs, ZO-1, ZO-2, and ZO-3, with the COOH termini of claudins. J Cell Biol. 1999 Dec 13;147(6):1351-63.

178. Roh MH, Liu CJ, Laurinec S, Margolis B. The carboxyl terminus of zona occludens-3 binds and recruits a mammalian homologue of discs lost to tight junctions. J Biol Chem. 2002 Jul 26;277(30):27501-9.

179. Mee CJ, Harris HJ, Farquhar MJ, Wilson G, Reynolds G, Davis C, et al. Polarization restricts hepatitis C virus entry into HepG2 hepatoma cells. J Virol. 2009 Jun;83(12):6211-21.

180. Mee CJ, Grove J, Harris HJ, Hu K, Balfe P, McKeating JA. Effect of cell polarization on hepatitis C virus entry. J Virol. 2008 Jan;82(1):461-70.

181. Kojima T, Murata M, Yamamoto T, Lan M, Imamura M, Son S, et al. Tight junction proteins and signal transduction pathways in hepatocytes. Histol Histopathol. 2009 Nov;24(11):1463-72.

182. Krieger SE, Zeisel MB, Davis C, Thumann C, Harris HJ, Schnober EK, et al. Inhibition of hepatitis C virus infection by anti-claudin-1 antibodies is mediated by neutralization of E2-CD81-claudin-1 associations. Hepatology. 2010 Apr;51(4):1144-57.

183. Cukierman L, Meertens L, Bertaux C, Kajumo F, Dragic T. Residues in a Highly Conserved Claudin-1 Motif Are Required for Hepatitis C Virus Entry and Mediate the Formation of Cell-Cell Contacts. J Virol. 2009 Mar 18.

184. Harris HJ, Farquhar MJ, Mee CJ, Davis C, Reynolds GM, Jennings A, et al. CD81 and claudin 1 coreceptor association: role in hepatitis C virus entry. J Virol. 2008 May;82(10):5007-20.

185. Furuse M, Hirase T, Itoh M, Nagafuchi A, Yonemura S, Tsukita S. Occludin: a novel integral membrane protein localizing at tight junctions. J Cell Biol. 1993 Dec;123(6 Pt 2):1777-88.

186. Saitou M, Furuse M, Sasaki H, Schulzke JD, Fromm M, Takano H, et al. Complex phenotype of mice lacking occludin, a component of tight junction strands. Mol Biol Cell. 2000 Dec;11(12):4131-42.

187. Everett RS, Vanhook MK, Barozzi N, Toth I, Johnson LG. Specific modulation of airway epithelial tight junctions by apical application of an occludin peptide. Mol Pharmacol. 2006 Feb;69(2):492-500.

188. Tavelin S, Hashimoto K, Malkinson J, Lazorova L, Toth I, Artursson P. A new principle for tight junction modulation based on occludin peptides. Mol Pharmacol. 2003 Dec;64(6):1530-40.

189. Feldman GJ, Mullin JM, Ryan MP. Occludin: structure, function and regulation. Adv Drug Deliv Rev. 2005 Apr 25;57(6):883-917.

190. Haskins J, Gu L, Wittchen ES, Hibbard J, Stevenson BR. ZO-3, a novel member of the MAGUK protein family found at the tight junction, interacts with ZO-1 and occludin. J Cell Biol. 1998 Apr 6;141(1):199-208.

191. Paris L, Tonutti L, Vannini C, Bazzoni G. Structural organization of the tight junctions. Biochim Biophys Acta. 2008 Mar;1778(3):646-59.

192. Shen L, Weber CR, Turner JR. The tight junction protein complex undergoes rapid and continuous molecular remodeling at steady state. J Cell Biol. 2008 May 19;181(4):683-95.

193. Matsuda M, Kubo A, Furuse M, Tsukita S. A peculiar internalization of claudins, tight junction-specific adhesion molecules, during the intercellular movement of epithelial cells. J Cell Sci. 2004 Mar 1;117(Pt 7):1247-57.

194. Stamatovic SM, Keep RF, Wang MM, Jankovic I, Andjelkovic AV. Caveolae-mediated internalization of occludin and claudin-5 during CCL2-induced tight junction remodeling in brain endothelial cells. J Biol Chem. 2009 Jul 10;284(28):19053-66.

195. Guttman JA, Finlay BB. Tight junctions as targets of infectious agents. Biochim Biophys Acta. 2009 Apr;1788(4):832-41.

196. Van Itallie CM, Anderson JM. Claudins and epithelial paracellular transport. Annu Rev Physiol. 2006;68:403-29.

197. Lopez S, Arias CF. Multistep entry of rotavirus into cells: a Versaillesque dance. Trends Microbiol. 2004 Jun;12(6):271-8.

198. Stuart AD, Brown TD. Alpha2,6-linked sialic acid acts as a receptor for Feline calicivirus. J Gen Virol. 2007 Jan;88(Pt 1):177-86.

199. Coyne KP, Jones BR, Kipar A, Chantrey J, Porter CJ, Barber PJ, et al. Lethal outbreak of disease associated with feline calicivirus infection in cats. Vet Rec. 2006 Apr 22;158(16):544-50.

200. Pedersen NC, Elliott JB, Glasgow A, Poland A, Keel K. An isolated epizootic of hemorrhagic-like fever in cats caused by a novel and highly virulent strain of feline calicivirus. Vet Microbiol. 2000 May 11;73(4):281-300.

201. Maginnis MS, Mainou BA, Derdowski A, Johnson EM, Zent R, Dermody TS. NPXY motifs in the beta1 integrin cytoplasmic tail are required for functional reovirus entry. J Virol. 2008 Apr;82(7):3181-91.

202. Tomko RP, Xu R, Philipson L. HCAR and MCAR: the human and mouse cellular receptors for subgroup C adenoviruses and group B coxsackieviruses. Proc Natl Acad Sci U S A. 1997 Apr 1;94(7):3352-6.

203. Freimuth P, Springer K, Berard C, Hainfeld J, Bewley M, Flanagan J. Coxsackievirus and adenovirus receptor amino-terminal immunoglobulin V-related domain binds adenovirus type 2 and fiber knob from adenovirus type 12. J Virol. 1999 Feb;73(2):1392-8.

204. Kirby I, Davison E, Beavil AJ, Soh CP, Wickham TJ, Roelvink PW, et al. Identification of contact residues and definition of the CAR-binding site of adenovirus type 5 fiber protein. J Virol. 2000 Mar;74(6):2804-13.

205. Wickham TJ, Mathias P, Cheresh DA, Nemerow GR. Integrins alpha v beta 3 and alpha v beta 5 promote adenovirus internalization but not virus attachment. Cell. 1993 Apr 23;73(2):309-19.

206. Rentsendorj A, Xie J, MacVeigh M, Agadjanian H, Bass S, Kim DH, et al. Typical and atypical trafficking pathways of Ad5 penton base recombinant protein: implications for gene transfer. Gene Ther. 2006 May;13(10):821-36.

207. Rogee S, Grellier E, Bernard C, Loyens A, Beauvillain JC, D'Halluin J C, et al. Intracellular trafficking of a fiber-modified adenovirus using lipid raft/caveolae endocytosis. Mol Ther. 2007 Nov;15(11):1963-72.

208. Coyne CB, Bergelson JM. Virus-induced Abl and Fyn kinase signals permit coxsackievirus entry through epithelial tight junctions. Cell. 2006 Jan 13;124(1):119-31.

209. Coyne CB, Shen L, Turner JR, Bergelson JM. Coxsackievirus entry across epithelial tight junctions requires occludin and the small GTPases Rab34 and Rab5. Cell Host Microbe. 2007 Sep 13;2(3):181-92.

210. Patel KP, Coyne CB, Bergelson JM. Dynamin- and lipid raft-dependent entry of DAF-binding and non-DAF-binding Coxsackieviruses into non-polarized cells. J Virol. 2009 Aug 26.

211. Farquhar MJ, Harris HJ, Diskar M, Jones S, Mee CJ, Nielsen SU, et al. Protein kinase A-dependent step(s) in hepatitis C virus entry and infectivity. J Virol. 2008 Sep;82(17):8797-811.

212. Chiaradonna F, Balestrieri C, Gaglio D, Vanoni M. RAS and PKA pathways in cancer: new insight from transcriptional analysis. Front Biosci. 2008;13:5257-78.

213. Matter K, Balda MS. Signalling to and from tight junctions. Nat Rev Mol Cell Biol. 2003 Mar;4(3):225-36.

214. Ferrannini E, Gastaldelli A, Matsuda M, Miyazaki Y, Pettiti M, Glass L, et al. Influence of ethnicity and familial diabetes on glucose tolerance and insulin action: a physiological analysis. J Clin Endocrinol Metab. 2003 Jul;88(7):3251-7.

215. Aktories K, Barbieri JT. Bacterial cytotoxins: targeting eukaryotic switches. Nat Rev Microbiol. 2005 May;3(5):397-410.

216. Decaens C, Durand M, Grosse B, Cassio D. Which in vitro models could be best used to study hepatocyte polarity? Biol Cell. 2008 Jul;100(7):387-98.

217. Harris HJ, Davis C, Mullins JG, Hu K, Goodall M, Farquhar MJ, et al. Claudin association with CD81 defines hepatitis C virus entry. J Biol Chem. 2010 Jul 2;285(27):21092-102.

218. Fanning AS, Jameson BJ, Jesaitis LA, Anderson JM. The tight junction protein ZO-1 establishes a link between the transmembrane protein occludin and the actin cytoskeleton. J Biol Chem. 1998 Nov 6;273(45):29745-53.

219. Yancey PG, Rodrigueza WV, Kilsdonk EP, Stoudt GW, Johnson WJ, Phillips MC, et al. Cellular cholesterol efflux mediated by cyclodextrins. Demonstration Of kinetic pools and mechanism of efflux. J Biol Chem. 1996 Jul 5;271(27):16026-34.

220. Staruschenko A, Adams E, Booth RE, Stockand JD. Epithelial Na+ channel subunit stoichiometry. Biophys J. 2005 Jun;88(6):3966-75.

221. Zheng J, Zagotta WN. Stoichiometry and assembly of olfactory cyclic nucleotide-gated channels. Neuron. 2004 May 13;42(3):411-21.

222. Zal T, Gascoigne NR. Photobleaching-corrected FRET efficiency imaging of live cells. Biophys J. 2004 Jun;86(6):3923-39.

223. Tscherne DM, Jones CT, Evans MJ, Lindenbach BD, McKeating JA, Rice CM. Time- and temperature-dependent activation of hepatitis C virus for low-pH-triggered entry. J Virol. 2006 Feb;80(4):1734-41.

224. Blanchard E, Belouzard S, Goueslain L, Wakita T, Dubuisson J, Wychowski C, et al. Hepatitis C virus entry depends on clathrin-mediated endocytosis. J Virol. 2006 Jul;80(14):6964-72.

225. He L, Olson DP, Wu X, Karpova TS, McNally JG, Lipsky PE. A flow cytometric method to detect protein-protein interaction in living cells by directly visualizing donor fluorophore quenching during CFP-->YFP fluorescence resonance energy transfer (FRET). Cytometry A. 2003 Oct;55(2):71-85.

226. van Rheenen J, Langeslag M, Jalink K. Correcting confocal acquisition to optimize imaging of fluorescence resonance energy transfer by sensitized emission. Biophys J. 2004 Apr;86(4):2517-29.

227. Chen H, Puhl HL, 3rd, Koushik SV, Vogel SS, Ikeda SR. Measurement of FRET efficiency and ratio of donor to acceptor concentration in living cells. Biophys J. 2006 Sep 1;91(5):L39-41.

228. Rizzo MA, Springer G, Segawa K, Zipfel WR, Piston DW. Optimization of pairings and detection conditions for measurement of FRET between cyan and yellow fluorescent proteins. Microsc Microanal. 2006 Jun;12(3):238-54.

229. Berney C, Danuser G. FRET or no FRET: a quantitative comparison. Biophys J. 2003 Jun;84(6):3992-4010.

230. Ganesan S, Ameer-Beg SM, Ng TT, Vojnovic B, Wouters FS. A dark yellow fluorescent protein (YFP)-based Resonance Energy-Accepting Chromoprotein (REACh) for Forster resonance energy transfer with GFP. Proc Natl Acad Sci U S A. 2006 Mar 14;103(11):4089-94.

231. Ng T, Squire A, Hansra G, Bornancin F, Prevostel C, Hanby A, et al. Imaging protein kinase Calpha activation in cells. Science. 1999 Mar 26;283(5410):2085-9.

232. Mattheyses AL, Hoppe AD, Axelrod D. Polarized fluorescence resonance energy transfer microscopy. Biophys J. 2004 Oct;87(4):2787-97.

233. Piston DW, Kremers GJ. Fluorescent protein FRET: the good, the bad and the ugly. Trends Biochem Sci. 2007 Sep;32(9):407-14.

234. Frank M. MAL, a proteolipid in glycosphingolipid enriched domains: functional implications in myelin and beyond. Prog Neurobiol. 2000 Apr;60(6):531-44.

235. Zuckerman E. Expansion of CD5+ B-cell overexpressing CD81 in HCV infection: towards better understanding the link between HCV infection, B-cell activation and lymphoproliferation. J Hepatol. 2003 May;38(5):674-6.

236. Schreiber G, Haran G, Zhou HX. Fundamental aspects of protein-protein association kinetics. Chem Rev. 2009 Mar 11;109(3):839-60.

237. Ohlson S, Shoravi S, Fex T, Isaksson R. Screening for transient biological interactions as applied to albumin ligands: a new concept for drug discovery. Anal Biochem. 2006 Dec 1;359(1):120-3.

238. Crowley PB, Ubbink M. Close encounters of the transient kind: protein interactions in the photosynthetic redox chain investigated by NMR spectroscopy. Acc Chem Res. 2003 Oct;36(10):723-30.

239. Kitajiri SI, Furuse M, Morita K, Saishin-Kiuchi Y, Kido H, Ito J, et al. Expression patterns of claudins, tight junction adhesion molecules, in the inner ear. Hear Res. 2004 Jan;187(1-2):25-34.

240. Ip YC, Cheung ST, Lee YT, Ho JC, Fan ST. Inhibition of hepatocellular carcinoma invasion by suppression of claudin-10 in HLE cells. Mol Cancer Ther. 2007 Nov;6(11):2858-67.

241. Zhu Y, Brannstrom M, Janson PO, Sundfeldt K. Differences in expression patterns of the tight junction proteins,claudin 1, 3, 4 and 5, in human ovarian surface epithelium as compared to epithelia in inclusion cysts and epithelial ovarian tumours. Int J Cancer. 2006 Apr 15;118(8):1884-91.

242. Takala H, Saarnio J, Wiik H, Soini Y. Claudins 1, 3, 4, 5 and 7 in esophageal cancer: loss of claudin 3 and 4 expression is associated with metastatic behavior. APMIS. 2007 Jul;115(7):838-47.

243. Cheung ST, Leung KL, Ip YC, Chen X, Fong DY, Ng IO, et al. Claudin-10 expression level is associated with recurrence of primary hepatocellular carcinoma. Clin Cancer Res. 2005 Jan 15;11(2 Pt 1):551-6.

244. Muller HM, Pfaff E, Goeser T, Kallinowski B, Solbach C, Theilmann L. Peripheral blood leukocytes serve as a possible extrahepatic site for hepatitis C virus replication. J Gen Virol. 1993 Apr;74 ( Pt 4):669-76.

245. Morsica G, Tambussi G, Sitia G, Novati R, Lazzarin A, Lopalco L, et al. Replication of hepatitis C virus in B lymphocytes (CD19+). Blood. 1999 Aug 1;94(3):1138-9.

246. Kaiser P, Niederost B, Joos B, von Wyl V, Opravil M, Weber R, et al. Equal amounts of intracellular and virion-enclosed hepatitis C virus RNA are associated with peripheral-blood mononuclear cells in vivo. J Infect Dis. 2006 Dec 15;194(12):1713-23.

247. Blackard JT, Kemmer N, Sherman KE. Extrahepatic replication of HCV: insights into clinical manifestations and biological consequences. Hepatology. 2006 Jul;44(1):15-22.

248. Rocha-Perugini V, Lavie M, Delgrange D, Canton J, Pillez A, Potel J, et al. The association of CD81 with tetraspanin-enriched microdomains is not essential for Hepatitis C virus entry. BMC Microbiol. 2009;9:111.

249. Kapadia SB, Barth H, Baumert T, McKeating JA, Chisari FV. Initiation of hepatitis C virus infection is dependent on cholesterol and cooperativity between CD81 and scavenger receptor B type I. J Virol. 2007 Jan;81(1):374-83.

250. Espenel C, Margeat E, Dosset P, Arduise C, Le Grimellec C, Royer CA, et al. Single-molecule analysis of CD9 dynamics and partitioning reveals multiple modes of interaction in the tetraspanin web. J Cell Biol. 2008 Aug 25;182(4):765-76.

251. Charrin S, Le Naour F, Labas V, Billard M, Le Caer JP, Emile JF, et al. EWI-2 is a new component of the tetraspanin web in hepatocytes and lymphoid cells. Biochem J. 2003 Jul 15;373(Pt 2):409-21.

252. Timpe JM, McKeating JA. Hepatitis C virus entry: possible targets for therapy. Gut. 2008 Dec;57(12):1728-37.

253. Krieger SE, Zeisel MB, Davis C, Thumann C, Harris HJ, Schnober EK, et al. Inhibition of hepatitis C virus infection by anti-claudin-1 antibodies is mediated by neutralization of E2-CD81-Claudin-1 associations. Hepatology. 2009 Nov 30.

254. Fofana I, Krieger SE, Grunert F, Glauben S, Xiao F, Fafi-Kremer S, et al. Monoclonal anti-claudin 1 antibodies prevent hepatitis C virus infection of primary human hepatocytes. Gastroenterology. 2010 Sep;139(3):953-64, 64 e1-4.

255. Wang L, Boyer JL. The maintenance and generation of membrane polarity in hepatocytes. Hepatology. 2004 Apr;39(4):892-9.

256. Reynolds GM, Harris HJ, Jennings A, Hu K, Grove J, Lalor PF, et al. Hepatitis C virus receptor expression in normal and diseased liver tissue. Hepatology. 2008 Feb;47(2):418-27.

257. Koutsoudakis G, Herrmann E, Kallis S, Bartenschlager R, Pietschmann T. The level of CD81 cell surface expression is a key determinant for productive entry of hepatitis C virus into host cells. J Virol. 2007 Jan;81(2):588-98.

258. Drummer HE, Wilson KA, Poumbourios P. Identification of the hepatitis C virus E2 glycoprotein binding site on the large extracellular loop of CD81. J Virol. 2002 Nov;76(21):11143-7.

259. Fraedrich K, Muller B, Grassmann R. The HTLV-1 Tax protein binding domain of cyclin-dependent kinase 4 (CDK4) includes the regulatory PSTAIRE helix. Retrovirology. 2005;2:54.

260. de Jong AS, Schrama IW, Willems PH, Galama JM, Melchers WJ, van Kuppeveld FJ. Multimerization reactions of coxsackievirus proteins 2B, 2C and 2BC: a mammalian two-hybrid analysis. J Gen Virol. 2002 Apr;83(Pt 4):783-93.

261. Lwa SH, Chen WN. Hepatitis B virus X protein interacts with beta5 subunit of heterotrimeric guanine nucleotide binding protein. Virol J. 2005;2:76.

262. Higginbottom A, Quinn ER, Kuo CC, Flint M, Wilson LH, Bianchi E, et al. Identification of amino acid residues in CD81 critical for interaction with hepatitis C virus envelope glycoprotein E2. J Virol. 2000 Apr;74(8):3642-9.

263. Bertaux C, Dragic T. Different domains of CD81 mediate distinct stages of hepatitis C virus pseudoparticle entry. J Virol. 2006 May;80(10):4940-8.

264. Dreux M, Pietschmann T, Granier C, Voisset C, Ricard-Blum S, Mangeot PE, et al. High density lipoprotein inhibits hepatitis C virus-neutralizing antibodies by stimulating cell entry via activation of the scavenger receptor BI. J Biol Chem. 2006 Jul 7;281(27):18285-95.

265. Meola A, Sbardellati A, Bruni Ercole B, Cerretani M, Pezzanera M, Ceccacci A, et al. Binding of hepatitis C virus E2 glycoprotein to CD81 does not correlate with species permissiveness to infection. J Virol. 2000 Jul;74(13):5933-8.

266. Takayama H, Chelikani P, Reeves PJ, Zhang S, Khorana HG. High-level expression, single-step immunoaffinity purification and characterization of human tetraspanin membrane protein CD81. PLoS One. 2008;3(6):e2314.

267. Brazzoli M, Bianchi A, Filippini S, Weiner A, Zhu Q, Pizza M, et al. CD81 is a central regulator of cellular events required for hepatitis C virus infection of human hepatocytes. J Virol. 2008 Sep;82(17):8316-29.

268. Meertens L, Bertaux C, Dragic T. Hepatitis C virus entry requires a critical postinternalization step and delivery to early endosomes via clathrin-coated vesicles. J Virol. 2006 Dec;80(23):11571-8.

269. Zaitseva E, Yang ST, Melikov K, Pourmal S, Chernomordik LV. Dengue virus ensures its fusion in late endosomes using compartment-specific lipids. PLoS Pathog. 2010;6(10).

270. van der Schaar HM, Rust MJ, Chen C, van der Ende-Metselaar H, Wilschut J, Zhuang X, et al. Dissecting the cell entry pathway of dengue virus by single-particle tracking in living cells. PLoS Pathog. 2008 Dec;4(12):e1000244.

271. Krishnan MN, Sukumaran B, Pal U, Agaisse H, Murray JL, Hodge TW, et al. Rab 5 is required for the cellular entry of dengue and West Nile viruses. J Virol. 2007 May;81(9):4881-5.

272. Pietschmann T. Virology: Final entry key for hepatitis C. Nature. 2009 Feb 12;457(7231):797-8.

273. Burlone ME, Budkowska A. Hepatitis C virus cell entry: role of lipoproteins and cellular receptors. J Gen Virol. 2009 May;90(Pt 5):1055-70.

274. Budkowska A. Mechanism of cell infection with hepatitis C virus (HCV)--a new paradigm in virus-cell interaction. Pol J Microbiol. 2009;58(2):93-8.

275. Coller KE, Berger KL, Heaton NS, Cooper JD, Yoon R, Randall G. RNA interference and single particle tracking analysis of hepatitis C virus endocytosis. PLoS Pathog. 2009 Dec;5(12):e1000702.

276. Schwarz AK, Grove J, Hu K, Mee CJ, Balfe P, McKeating JA. Hepatoma cell density promotes claudin-1 and scavenger receptor BI expression and hepatitis C virus internalization. J Virol. 2009 Dec;83(23):12407-14.

277. Catanese MT, Graziani R, von Hahn T, Moreau M, Huby T, Paonessa G, et al. High-avidity monoclonal antibodies against the human scavenger class B type I receptor efficiently block hepatitis C virus infection in the presence of high-density lipoprotein. J Virol. 2007 Aug;81(15):8063-71.

278. Zeisel MB, Koutsoudakis G, Schnober EK, Haberstroh A, Blum HE, Cosset FL, et al. Scavenger receptor class B type I is a key host factor for hepatitis C virus infection required for an entry step closely linked to CD81. Hepatology. 2007 Dec;46(6):1722-31.

279. Brimacombe CL, Grove J, Meredith LW, Hu K, Syder AJ, Flores MV, et al. Neutralizing antibody-resistant hepatitis C virus cell-to-cell transmission. J Virol. 2011 Jan;85(1):596-605.

280. Syder AJ, Lee H, Zeisel MB, Grove J, Soulier E, Macdonald J, et al. Small molecule scavenger receptor BI antagonists are potent HCV entry inhibitors. J Hepatol. 2011 Jan;54(1):48-55.

281. Teixeira R, Menezes EG, Schiano TD. Therapeutic management of recurrent hepatitis C after liver transplantation. Liver Int. 2007 Apr;27(3):302-12.

282. Brown RS. Hepatitis C and liver transplantation. Nature. 2005 Aug 18;436(7053):973-8.

283. Samuel D, Bismuth A, Mathieu D, Arulnaden JL, Reynes M, Benhamou JP, et al. Passive immunoprophylaxis after liver transplantation in HBsAg-positive patients. Lancet. 1991 Apr 6;337(8745):813-5.